DAMOS
DISPOSAL AREA MONITORING SYSTEM

ANNUAL DATA REPORT

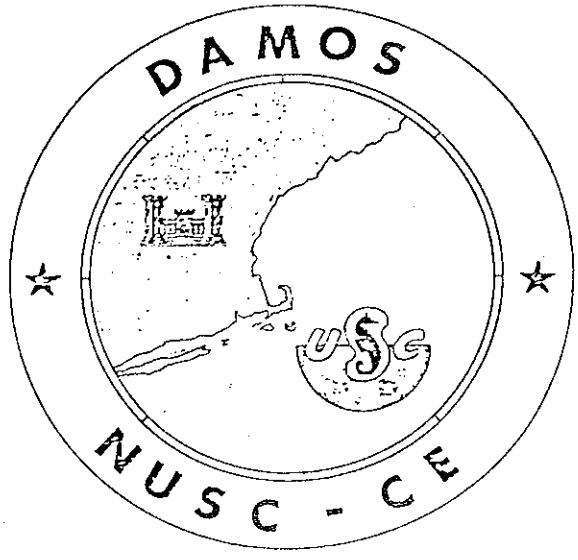

PROCEEDINGS OF SYMPOSIUM
14-15 MAY, 1979

VOL I
PHYSICAL MEASUREMENTS

NEW ENGLAND DIVISION
U.S. ARMY CORPS OF ENGINEERS
WALTHAM, MASSACHUSETTS

VOLUME I

PHYSICAL MEASUREMENTS

TABLE OF CONTENTS

LIST OF FIGURES

LIST OF TABLES

1.0

INTRODUCTION

ROBERT W. MORTON

1.0 INTRODUCTION

1.1 PROGRAM OBJECTIVES

The Disposal Area Monitoring System (DAMOS) is a comprehensive monitoring program, based on EPA guidelines, for measurement of physical, chemical, and biological impacts of dredge spoil disposal in coastal waters of New England. The fundamental concept behind the program, which has been conducted under the sponsorship of the New England Division of the U.S. Army Corps of Engineers, is a regional approach to monitoring of dredge spoil disposal sites. This allows standardization of data acquisition and analysis, thereby providing, for the first time in New England, a valid basis for comparison of data between sites and a consolidation of all environmental data in a common data base.

Prior to the initiation of the DAMOS program, funding for dredge spoil disposal site monitoring was provided to several different laboratories to study separate sites with specific project money. This situation produced a series of reports varying in content, quality, and completeness--often depending on the size of the dredging project and the particular strengths and weaknesses of the funding institutions. However, with the advent of the regional approach to monitoring and the consolidation of funding at one location, the development of more sophisticated data acquisition systems and the standardization of measurement techniques were possible while maintaining and improving the expertise available through subcontracts. It also allows the application of specific institutional strengths to regional investigations.

The DAMOS program is based on EPA criteria set forth in sections 228.9 through 228.13 of the Ocean Dumping Act (F.R. Jan. 11, 1977); however, these criteria have been used primarily as guidelines to accommodate the economic realities of a regional program and to permit flexibility in response to specific problems associated with disposal in the New England area. In practice, the criteria can be divided into two major monitoring studies: first, a physicochemical program to evaluate the stability of spoils in the disposal site, and second, a biochemical program to discover and evaluate any adverse impacts on biota, both within the disposal area and in the coastal environment

as a whole. Since these two study areas are closely related, the DAMOS project must be a multidisciplinary program with continuous interaction among scientists from various fields of study.

Dredge spoil disposal in the coastal environment is obviously a sensitive and controversial issue. However, results of the Dredged Material Research Program sponsored by the Corps of Engineers have shown that disposal can be accomplished with minimal damage to the environment if informed, prudent decisions are made relative to the disposal operations. The near-emergency conditions existing in some New England harbors continually emphasize the need for ocean disposal, primarily because of the large quantities of material to be removed.

To meet the emergency requirements in a responsible manner, management of disposal operations must be supported by meaningful, consistent data acquired through the most modern instrumentation systems. These data, the associated systems, and measurement techniques must always be available for scrutiny and criticism by government agencies, scientists, and the public at large. In particular, the instrumentation and measurement techniques employed to monitor the effects of disposal must be able to provide answers to the questions and reservations expressed by concerned environmental groups.

Consequently, a major emphasis in the DAMOS program has been, and will continue to be, centered on the presentation and open discussion of the approaches and techniques used to monitor environmental impact, the knowledge gained from these data, and the management decisions resulting from this knowledge. Dissemination of information has been accomplished through reports, public hearings, meetings with government agencies, presentations at professional conferences, and the annual DAMOS symposium. This program continues to be of extreme importance because it ensures that the effects of dredge spoil disposal are small, provides data for assessment of permit applications, aids in the management and operation of both large and small dredging projects, and distributes factual information to respond to questions raised by concerned environmental groups or to regulations imposed by other federal agencies.

The overall objectives of the DAMOS program are as follows:

- To monitor dredge spoil disposal sites in the New England area by empirical methods to ensure that no significant adverse environmental impacts result from disposal operations.
- To develop an understanding of the processes and mechanisms affecting dredge spoil in the marine environment.
- To develop an understanding of the interaction between dredge spoil and the biota of the disposal site.
- To utilize this knowledge to develop management techniques that will minimize the adverse effects of disposal.
- To distribute the results of the DAMOS program so as to provide better public understanding of the effects of dredge spoil disposal.

1.2 BACKGROUND

The DAMOS program was initiated by the New England Division of the U.S. Army Corps of Engineers during the summer of 1977 to provide a regional monitoring program for the entire New England area. Some of the major accomplishments of the program since that time have included:

- Development of comprehensive baseline environmental data including measurements of bathymetry, tidal and non-tidal currents, boundary layer dynamics, sediment chemistry, benthic macrofauna ecology, and ambient mussel chemistry at the following sites:

  Rockland, Maine
  Portland, Maine
  Isle of Shoals
  Boston Foul Ground
  Boston Lightship
  Cable and Anchor Reef
  Brenton Reef
  New London, Connecticut
  Cornfield Shoals
  New Haven, Connecticut
  Western Long Island Sound

- Techniques and instrumentation have been developed to provide specific data on the stability of dredge spoils in the marine environment. Spoil volumes have been calculated with a precision capable of defining changes with time due to erosion or additional disposal.
- A system for measuring the bottom boundary layer turbulence (BOLT) field has been designed, constructed, calibrated and tested. The BOLT system can measure the vertical current shear and Reynolds stress near the sediment-water interface where the conditions for erosion and transportation or containment of spoil material are defined. Evidence thus far indicates that severe coastal storms may be the most critical parameter affecting the movement of the spoil material.

- Factors controlling the fate of spoils at a site have been assessed at each location as related to the character of the disposal material.

- Bulk analyses of sediment chemistry have been used to classify spoil and natural sediments and to determine the spread of dredge spoil during a disposal project, thus measuring the effectiveness of capping operations at the central Long Island Sound disposal site.

- The benthic ecology of the disposal sites has been studied as a basis for future studies.

- Measurement of heavy metals in mussels as a valid monitor of the effects of spoil disposal has been demonstrated.

- Commercial fishermen have been involved in the DAMOS study through a direct and personal communications program.

- New techniques for future monitoring and management of disposal sites provide direction for future work and ensure that the Corps will continue in the forefront of environmental management.

Probably the most important contribution of the DAMOS program to date is its acquisition of background data to show what a disposal site is, how it changes, and how it can be "managed" as an important asset for the public good. New information is now available which allows the Corps to present a clearer picture of the effect of disposal sites on the environment. The data acquired through the DAMOS program have enhanced the public's confidence in the Corps' ability to manage disposal operations and thereby reduce the potential environmental impact of dredge spoil disposal.

1.3 SUMMARY OF SITE-SPECIFIC DATA

The disposal sites studied under the DAMOS program are shown in Fig. 1.1. Table 1.1 summarizes the pertinent physical characteristics of each site as determined through baseline studies. As discussed in previous reports, these disposal areas can be divided into two general types: one has relatively deep, exposed water with low tidal currents, and the other has comparatively shallow water with limited wave fetch but stronger tidal motion. These differences have led to differences in methods of studying the sites and interpretation of results, both physical and biological.

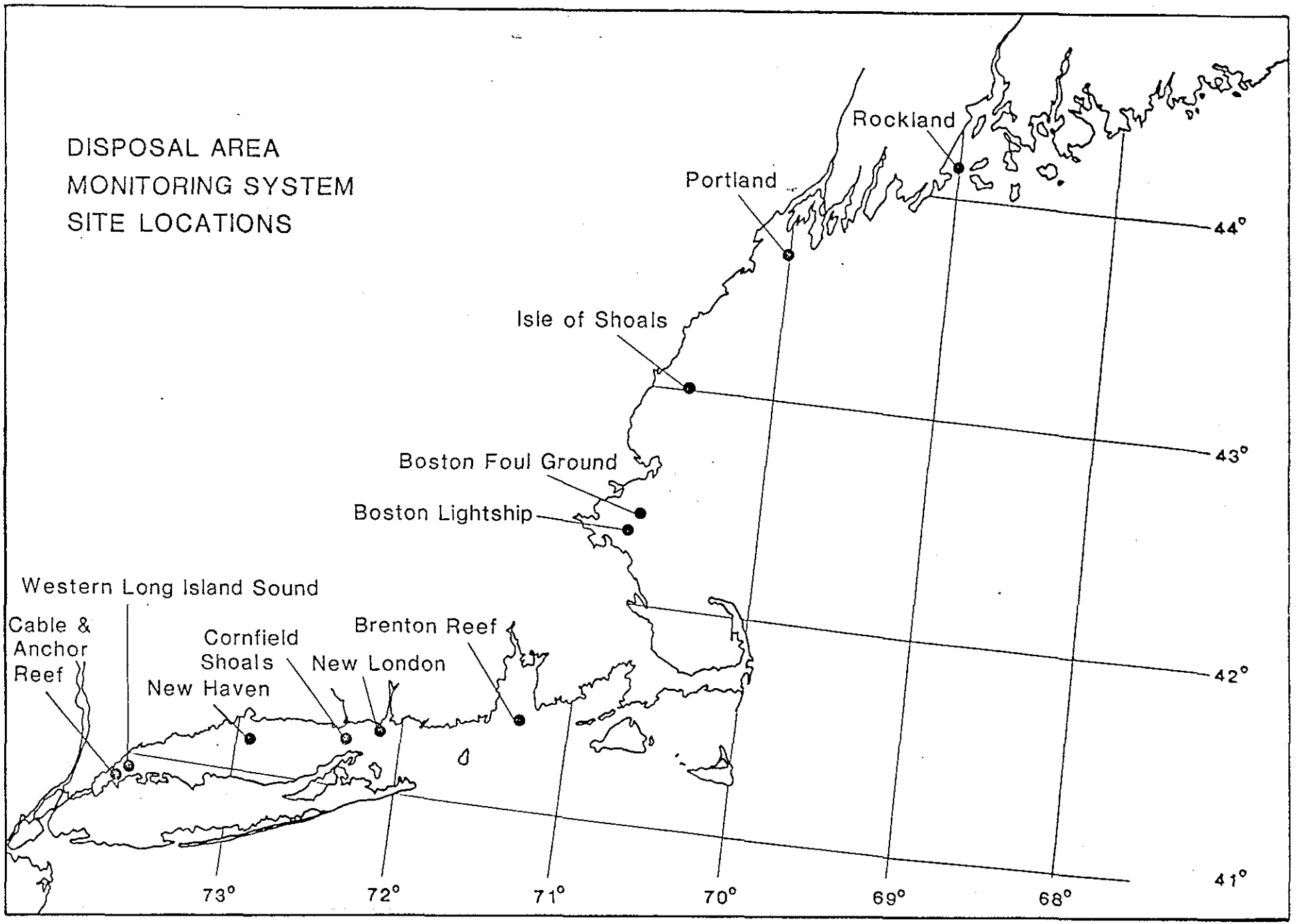
DISPOSAL AREA
MONITORING SYSTEM
SITE LOCATIONS
Rockland
Portland
Isle of Shoals
Boston Foul Ground
Boston Lightship
Western Long Island Sound
Cable &
Anchor
Reef
Cornfield
Shoals
New Haven
New London
Brenton Reef
44°
43°
42°
41°
73°
72°
71°
70°
69°
68°

FIGURE 1.1

Table 1.1 Characteristics of regional disposal sites studied under the DAMOS program

SITE	MUSSEL REFERENCE STATION	DEPTH(m)	ENERGY REGIME	ENERGY RANKING	SEDIMENT CHARACTER	HISTORY	SPOILS DISTRIBUTION	SPOILS CHARACTER
Rockland	Drunkard's Ledge	65-85	Currents	High	Silty clay	'74, Camden, Rockland	Scattered (mound reported)	Organic mud
Portland	Bulwark Shoal	60	Wave	Low	Rock outcrops, sand	New	-	-
Isle of Shoals	Smutty-nose	75	Wave	Low	Mud	New	-	-
Boston Foul Ground	Halfway Rock	90	Wave	Low	Mud	Continuous permit	Scattered	Black organic oily mud
Boston Lightship	Halfway Rock	60	Wave	Low	Mud	Continuous permit	Near buoy	Construction rocks
Brenton Reef	Ocean Drive	30	Wave	Low	Sand	'74, Providence	Mound	Organic mud covered with sand
New London	Latimer's Light	20	Currents	High	Sand	'77, New London	Two mounds	Variable silty sands
Cornfield Shoals	1.6 km NNW	55	Currents	High	Sand & Gravel	'77, North Cove	Scattered	Black oily silt
New Haven	3.2 km NW	20	Currents	Medium	Soft silty clay	'74, New Haven, Stamford-New Haven	Mound	Variable sands, silt, and clay
Western L.I. Sound	Eaton's Neck	30	Currents	Medium	Soft silty clay	New	-	-
Cable & Anchor Reef	Eaton's Neck	30	Currents	Medium	Soft silty clay	-	Two Mounds	-

1.3.1 Rockland

The Rockland disposal site (Fig. 1.2) is located approximately 5.5 km east of Rockland Harbor in the center of Penobscot Bay. This site ranges from 65 m in the southwest to 80 m deep in a valley at the northeast corner of the site (Fig. 1.3). Sediments consist of silty clays overlying a rocky glacial substratum that outcrops in the southwest corner of the area. The disposal site was last used in 1974, when spoils from Camden and Rockland were dumped in the northern half of the site. According to previous reports, a small mound was created in the valley: however, it is not evident at present. Spoils are present as an organic silt but are scattered around the general area of disposal.

The energy regime at the Rockland site is dominated by strong north-south tidal currents. Wave motion is probably negligible due to the short fetch and deep water at the site.

1.3.2 Portland

The determination of a suitable location for disposal of dredge spoil from Portland Harbor has been a major effort of the DAMOS program during the past two years. The first site suggested off Portland (Fig. 1.4) was investigated by Normandeau Associates prior to 1975. This area was located on hard, rocky bottom approximately 40 m deep, 1.8 km northwest of the Portland Lightship. Subsequent examination of the area based on new criteria for site selection indicated a more suitable location 1.8 km south of the site in Hue and Cry Gully, on the border between rock outcrops and silty clay deposits at much greater depths.

Portland fishermen stated that this site was an important fishing area and not suitable for a disposal site. Consequently, a new disposal site was proposed in the center of an old disposal area approximately 3.7 km north of the Portland Lightship. Surveys of this new site indicated that it consisted primarily of rock outcrops with some areas of sand. Detailed bathymetric and side-scan surveys of the area were conducted.

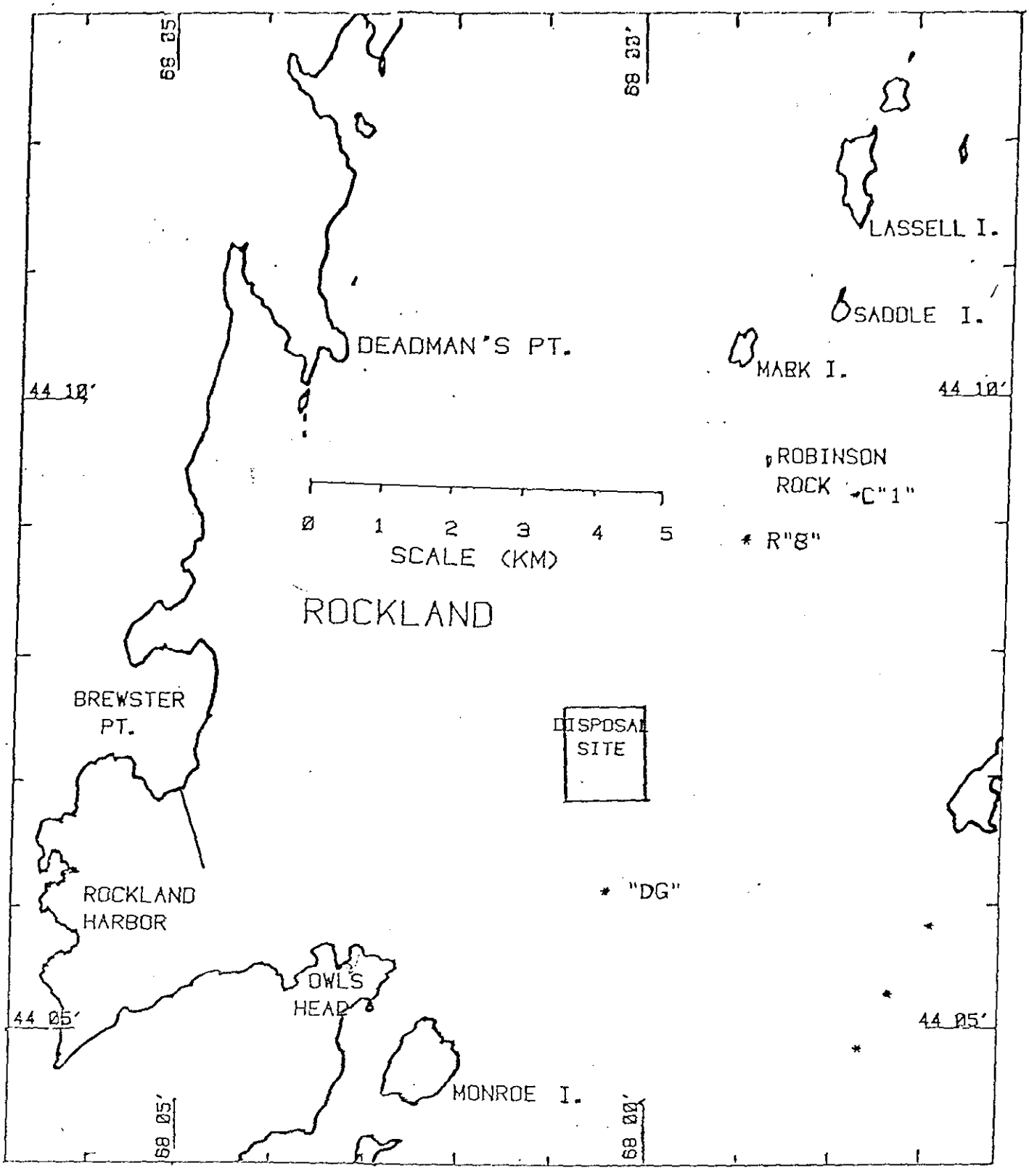
68 35'
68 33'
LASSELL I.
SADDLE I.
DEADMAN'S PT.
MARK I.
44 10'
44 10'
ROBINSON
ROCK
"C"1"
0 1 2 3 4 5
SCALE (KM)
R"8"
ROCKLAND
BREWSTER
PT.
DISPOSAL
SITE
ROCKLAND
HARBOR
"DG"
OWLS
HEAD
44 05'
44 05'
MONROE I.
68 05'
68 00'

FIGURE 1.2

Rockland, Maine
November 17, 1978

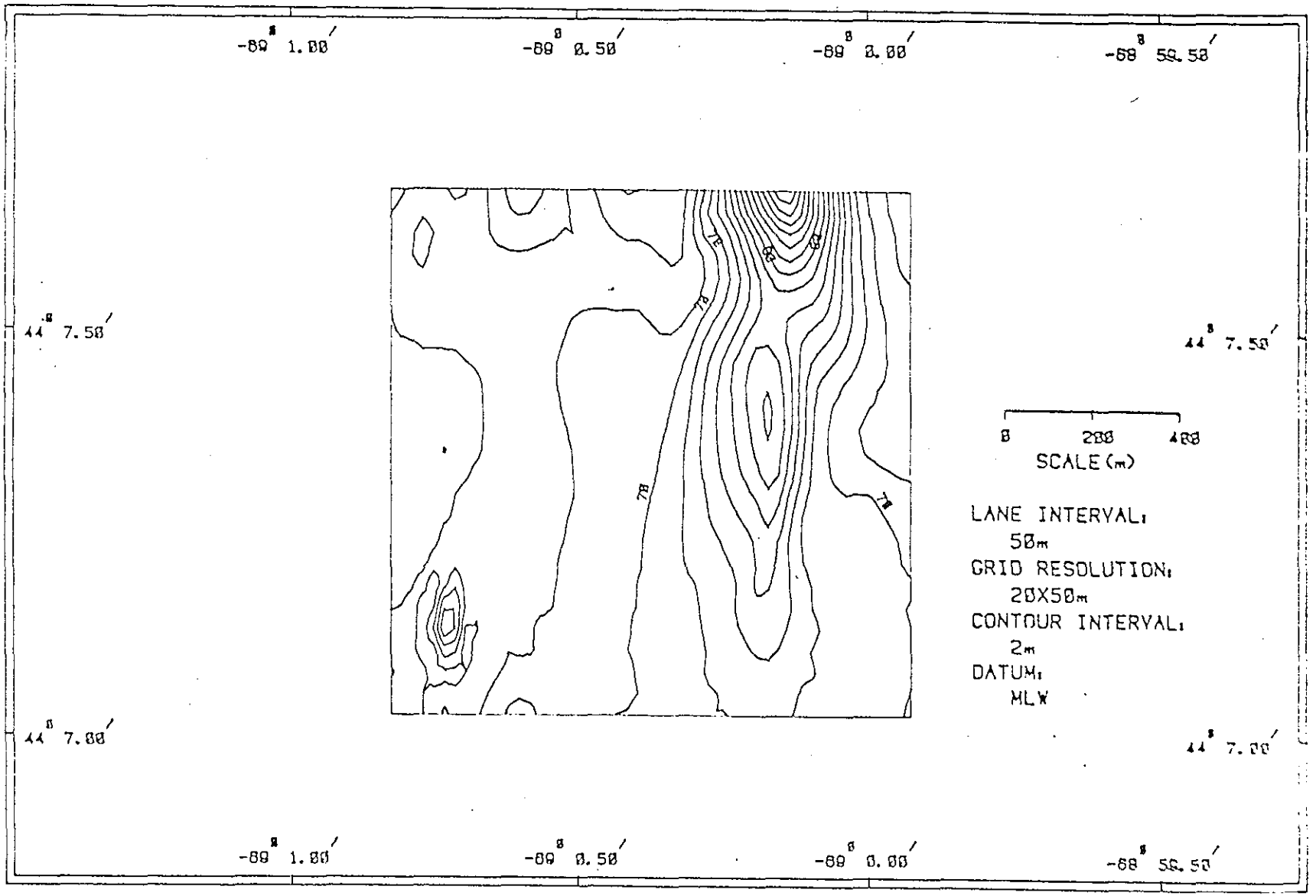

FIGURE 1.3

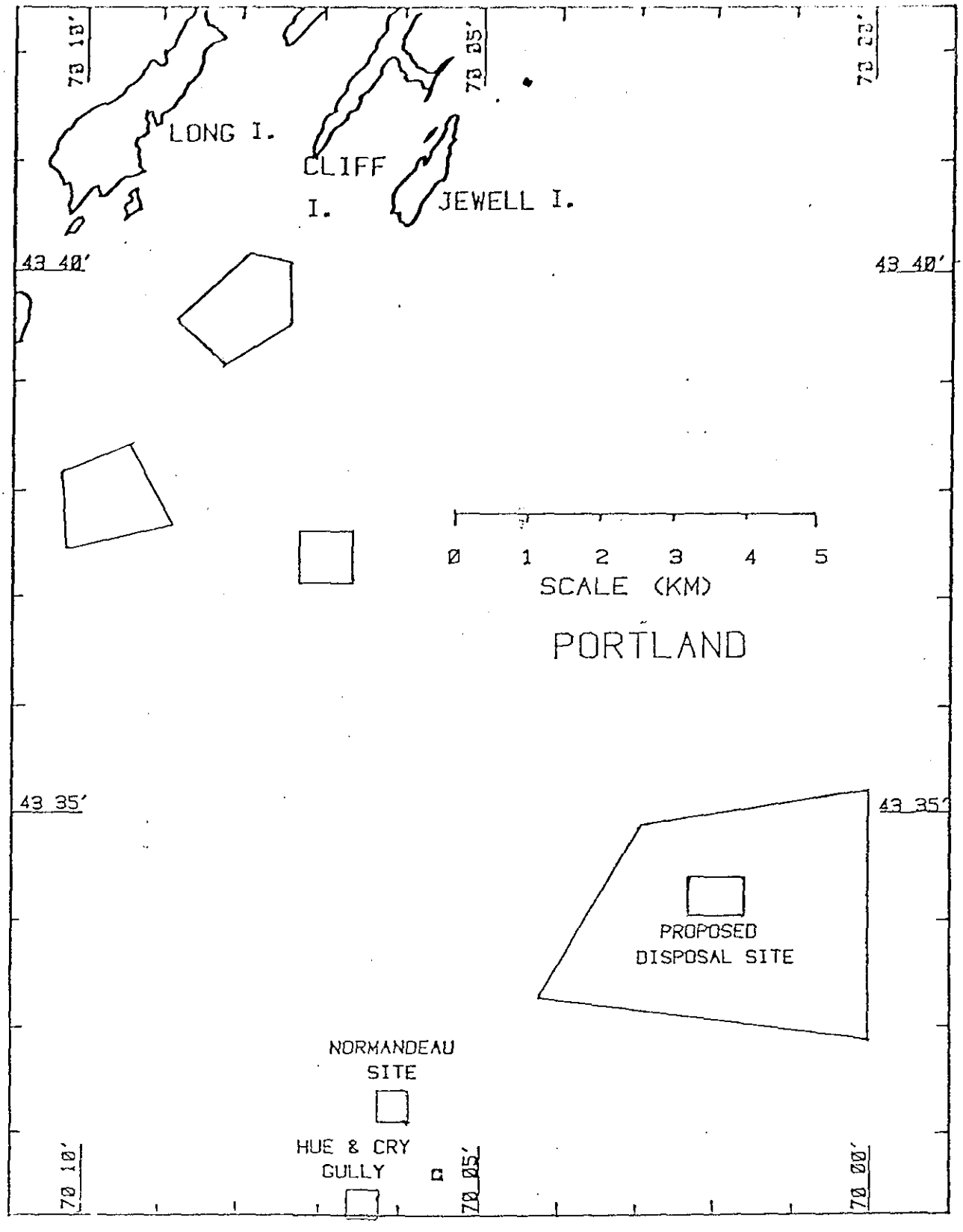
73 13'
73 35'
73 23'
LONG I.
CLIFF I.
JEWELL I.
43 40'
43 40'
0 1 2 3 4 5
SCALE (KM)
PORTLAND
43 35'
43 35'
PROPOSED
DISPOSAL SITE
NORMANDEAU
SITE
HUE & CRY
GULLY
70 10'
70 05'
70 00'

FIGURE 1.4

As a result of this work, five locations were presented to fishermen; a site at the center of the proposed area, at a depth of 60 m, was accepted as the most suitable location for disposal of Portland dredge material. This area is a flat, sandy plain at a depth of 60 m surrounded by rock outcrops (Fig. 1.5). Current measurements at this site have shown very weak tidal currents; however, wave action is possible, since there is essentially unlimited fetch to the south and southeast and strong gale force winds are common in winter. Dredging was scheduled to commence in September or October 1979.

1.3.3 Isle of Shoals

The Isle of Shoals disposal site, (Fig. 1.6) like the Portland site, is an old disposal site that has not been used in recent years except for the disposal of military ordnance. It is located approximately 3.7 km east of the Isle of Shoals at a depth of 75 m. The substrate is geologically similar to that of the Rockland area: a silty mud overlying glacial substrata, thus indicative of recent deposition. The most prominent feature is a flat, silty plain surrounded by rock outcrops. Fishermen indicated that the southwest corner of the plain would be an excellent point for disposal since it is not used extensively for fishing. Consequently, the bathymetry of the disposal site was surveyed (Fig. 1.7) concentrating on that location. This site has been proposed as a future disposal site for this region. Although current measurements have not been made at this site, conditions are probably similar to those at Portland, with low tidal energy and potentially high wave action.

1.3.4 Massachusetts Bay

Two regional disposal sites have been designated in Massachusetts Bay: The Boston Foul Ground and the Boston Lightship (Fig. 1.8). The Boston Foul Ground is located in 90 m of water immediately west of Stellwagon Bank (Fig. 1.9). The bottom in this area consists of fine silts with localized accumulations of spoil. Although no spoil mounds are present, there is a concentration of black, organic spoil material in a slight depression near the center of the area. Because there has been very little control of disposal operations within the foul ground area, spoils are scattered over the entire site.

Portland, Maine
November 20, 1978

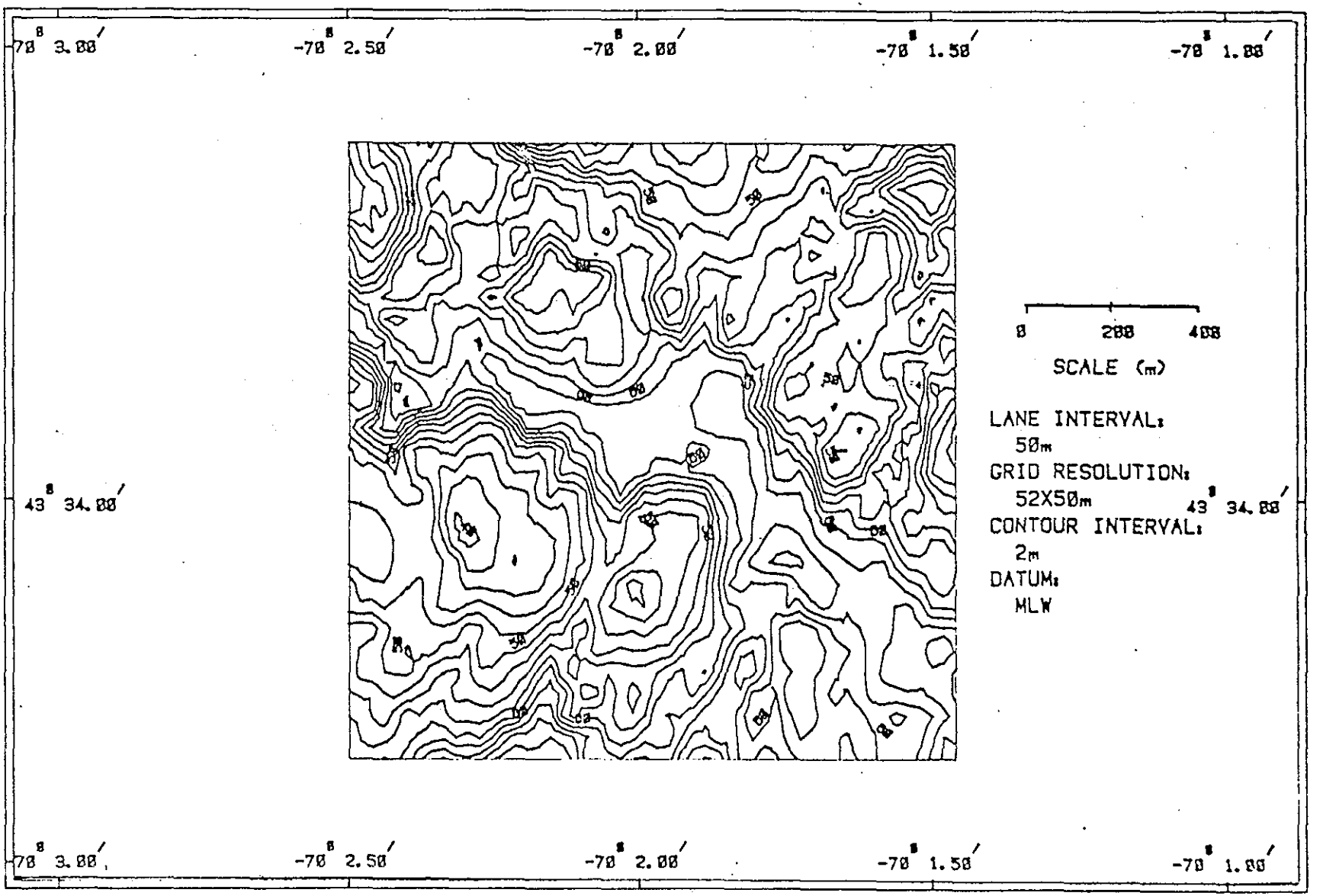

FIGURE 1.5

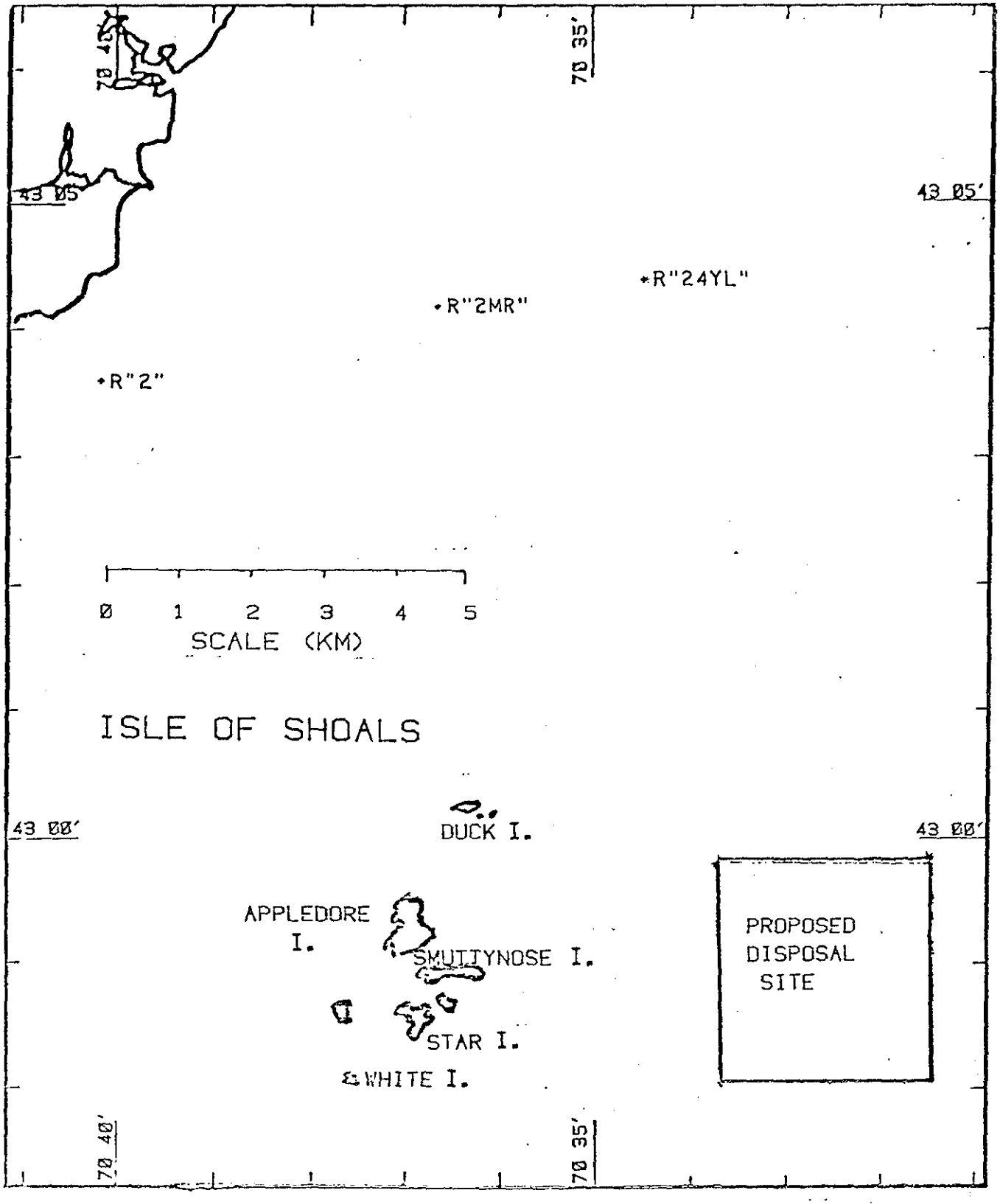
70 40'
70 35'
43 05'
43 05'
•R"24YL"
•R"2MR"
•R"2"
0 1 2 3 4 5
SCALE (KM)
ISLE OF SHOALS
43 00'
43 00'
DUCK I.
APPLEDORE I.
SMUTTYNOSE I.
STAR I.
WHITE I.
PROPOSED DISPOSAL SITE
70 40'
70 35'

FIGURE 1.6

ISLE OF SHOALS
DECEMBER 8, 1978

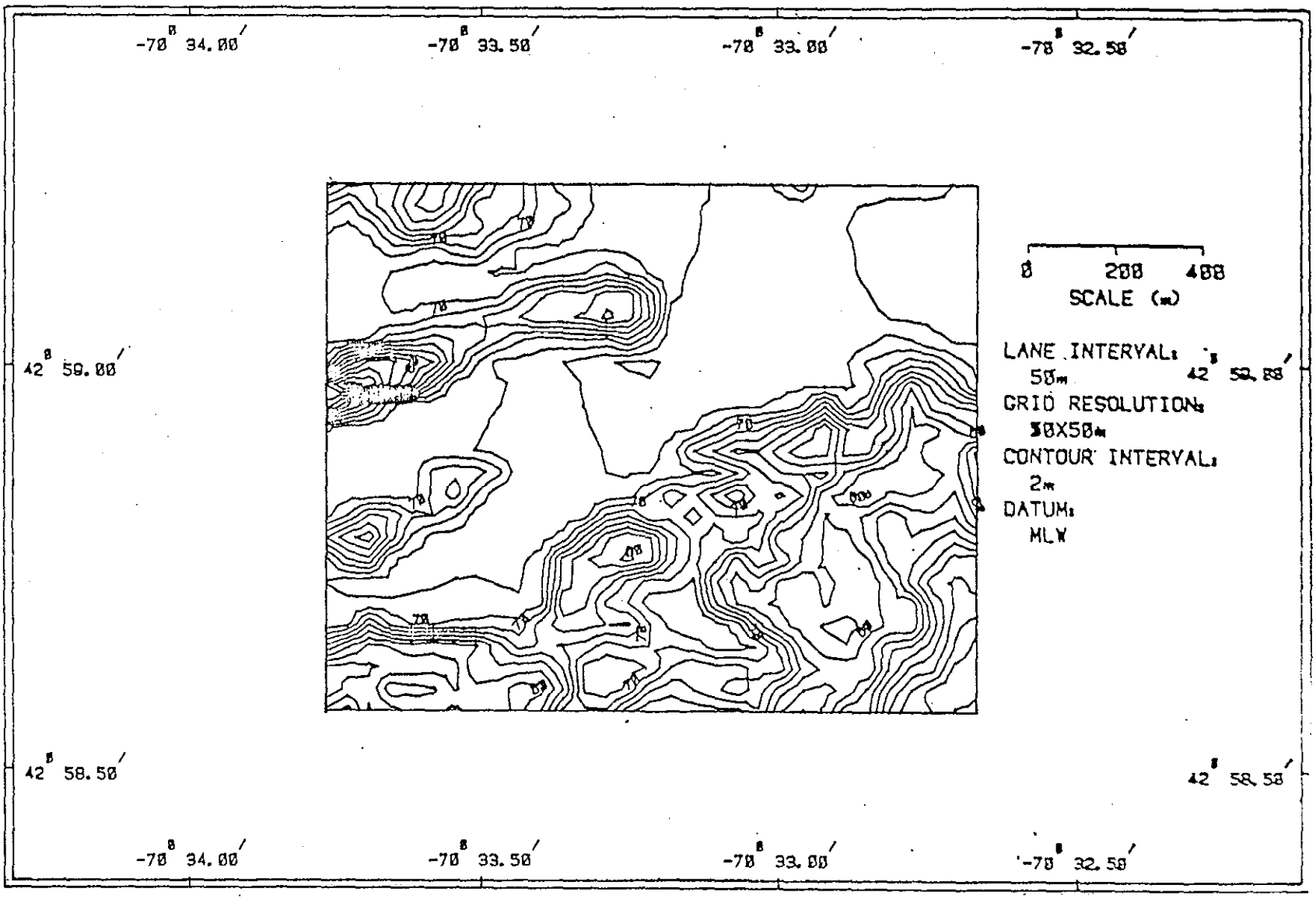

FIGURE 1.7

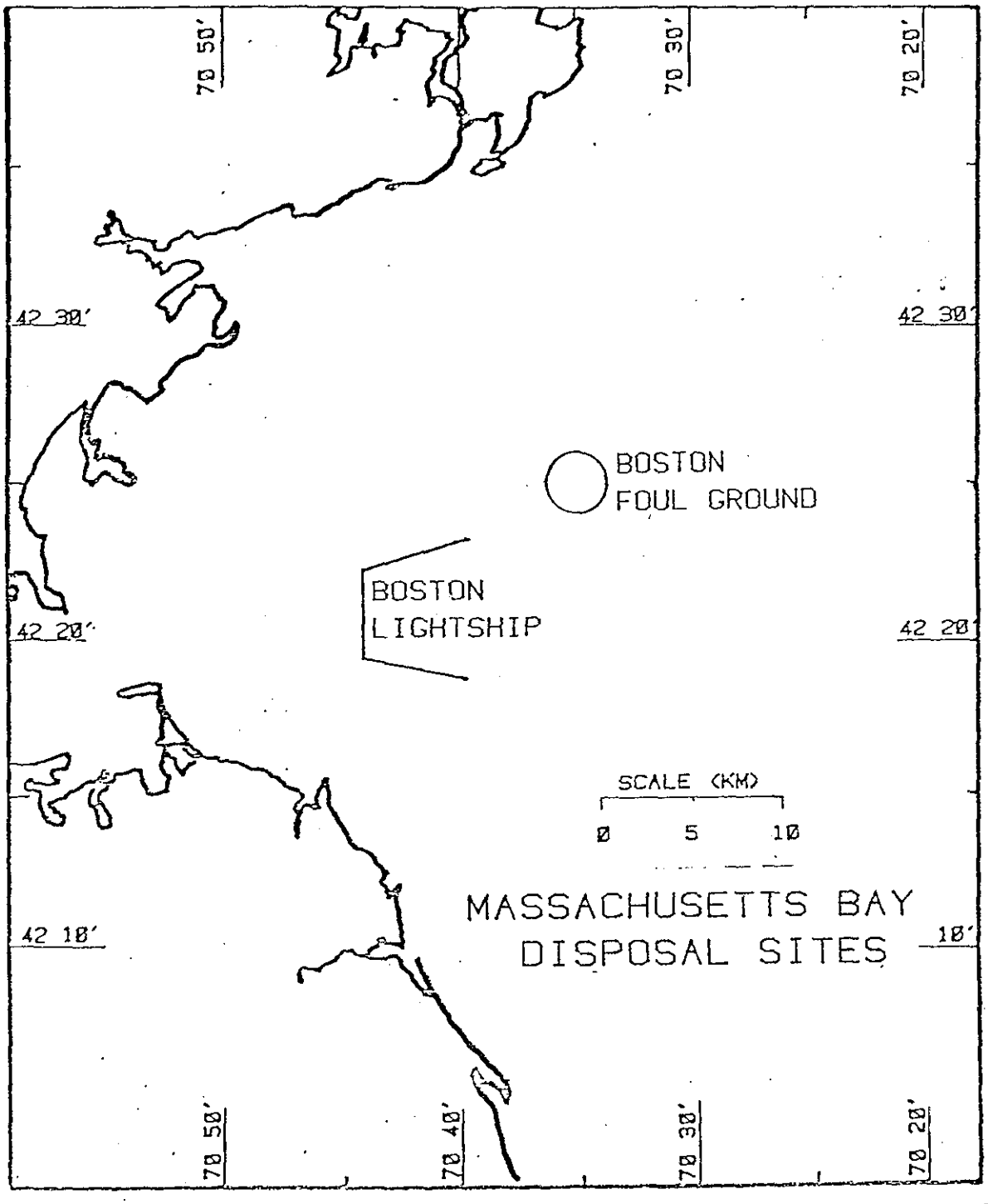
70 50'
70 30'
70 20'
42 30'
42 20'
42 10'
BOSTON
FOUL GROUND
BOSTON
LIGHTSHIP
SCALE (KM)
0 5 10
MASSACHUSETTS BAY
DISPOSAL SITES
70 50'
70 40'
70 30'
70 20'

FIGURE 1.8

Boston Foul Ground
January 16, 1978

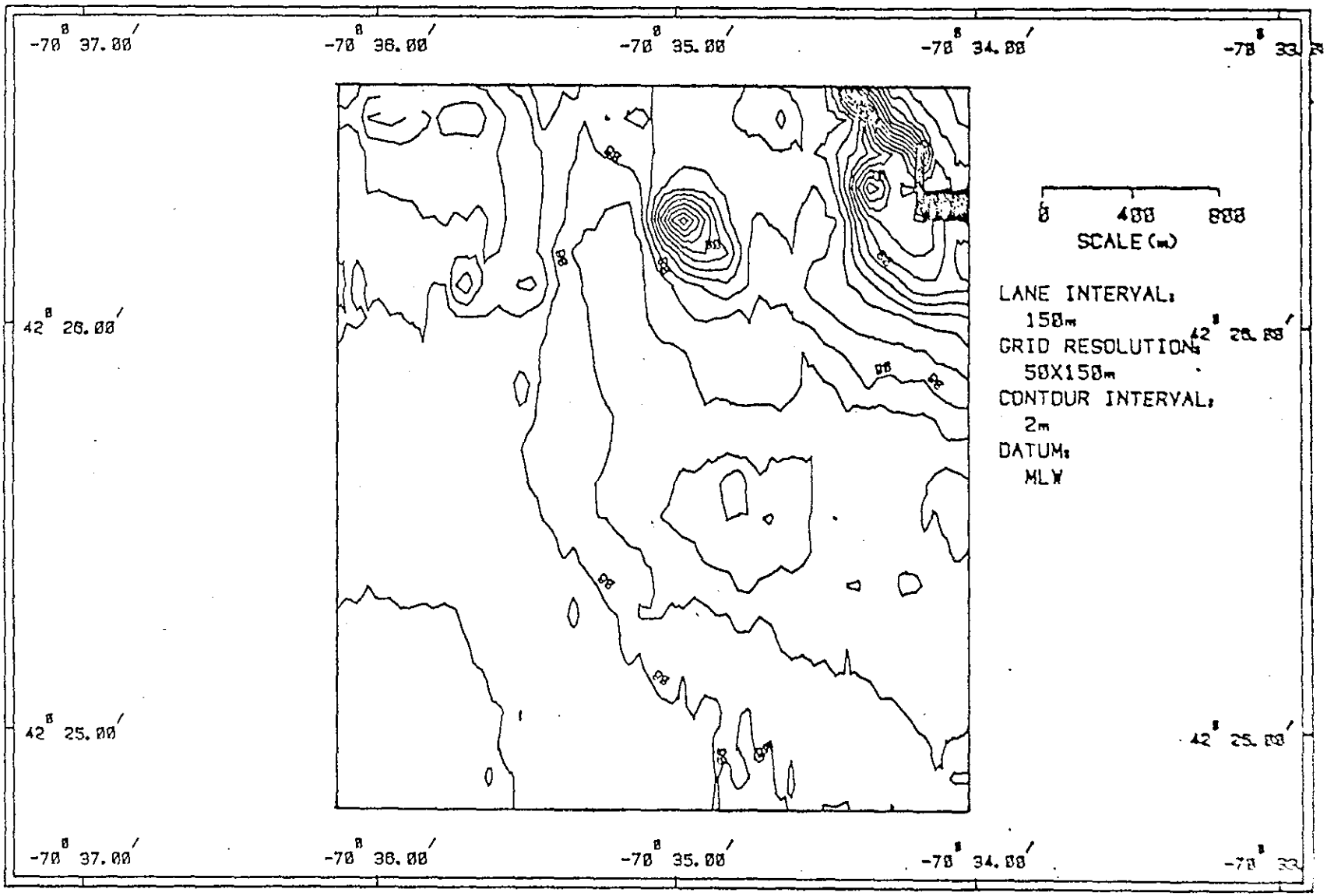

FIGURE 1.9

The Boston Lightship disposal site (Fig. 1.10) is located approximately 9 km south of the Foul Ground in an area 60 m deep. Southwest of the disposal point, the bottom shoals steeply toward Scituate; however, the actual disposal site is relatively flat. Clean construction material consisting of timbers, concrete slabs, and large rocks have been deposited at this site, and although no mound has been created, the spoils are readily detected by sampling near the disposal buoy.

Both the Boston Foul Ground and Lightship areas have extremely weak tidal currents but could be subjected to wave motion. However, the deep water encountered at these sites should reduce the frequency and severity of wave motion.

1.3.5 Brenton Reef

The Brenton Reef disposal site (Fig. 1.11) is located approximately 7.5 km south of Narragansett Bay in Rhode Island Sound. This area was last used in 1974 for disposal of material from the Providence River. During that operation, a disposal mound was formed with a minimum depth of 26 m on the ambient bottom at 30 m (Fig. 1.12).

This spoil mound consisted of fine-grained silts that have since been covered by sand. The origin of this sand layer may be either a lag deposit created by winnowing of fine spoils or a natural cap of material transported by wave action over the top of the disposal site.

The energy regime of this site is dominated by wave action. Currents of less than 20 cm/sec have been measured; however, the comparatively shallow depth of 30 m makes this site more susceptible to wave motion. Ripple marks on the adjacent bottom and in the sand cover over the spoil mound are indicative of such motion.

1.3.6 New London

The New London disposal site (Fig. 1.13) is located 3.7 km south of the Thames River in an area dominated by tidal currents. Although the mean depth

Boston Lightship
May 22, 1978

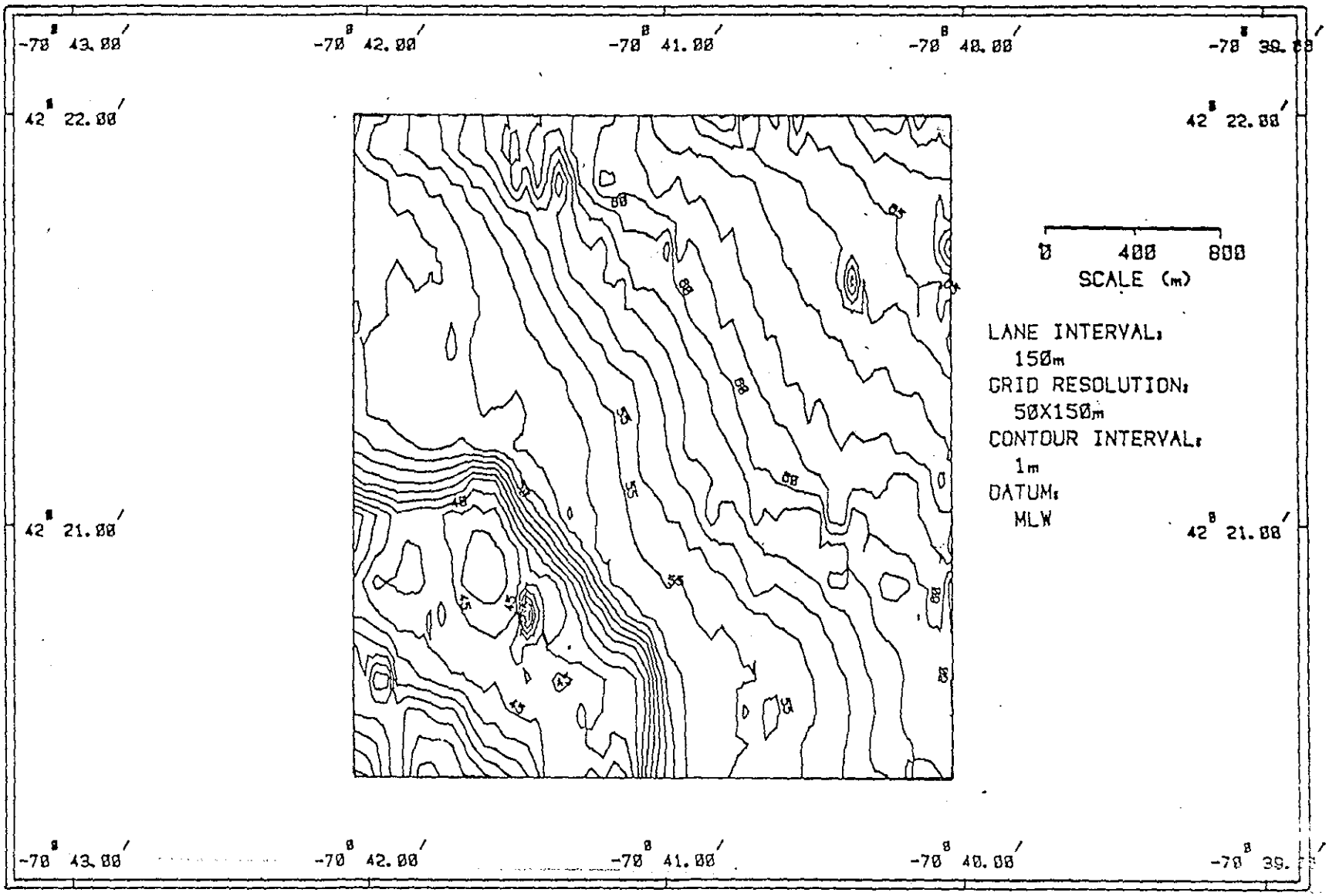

FIGURE 1.10

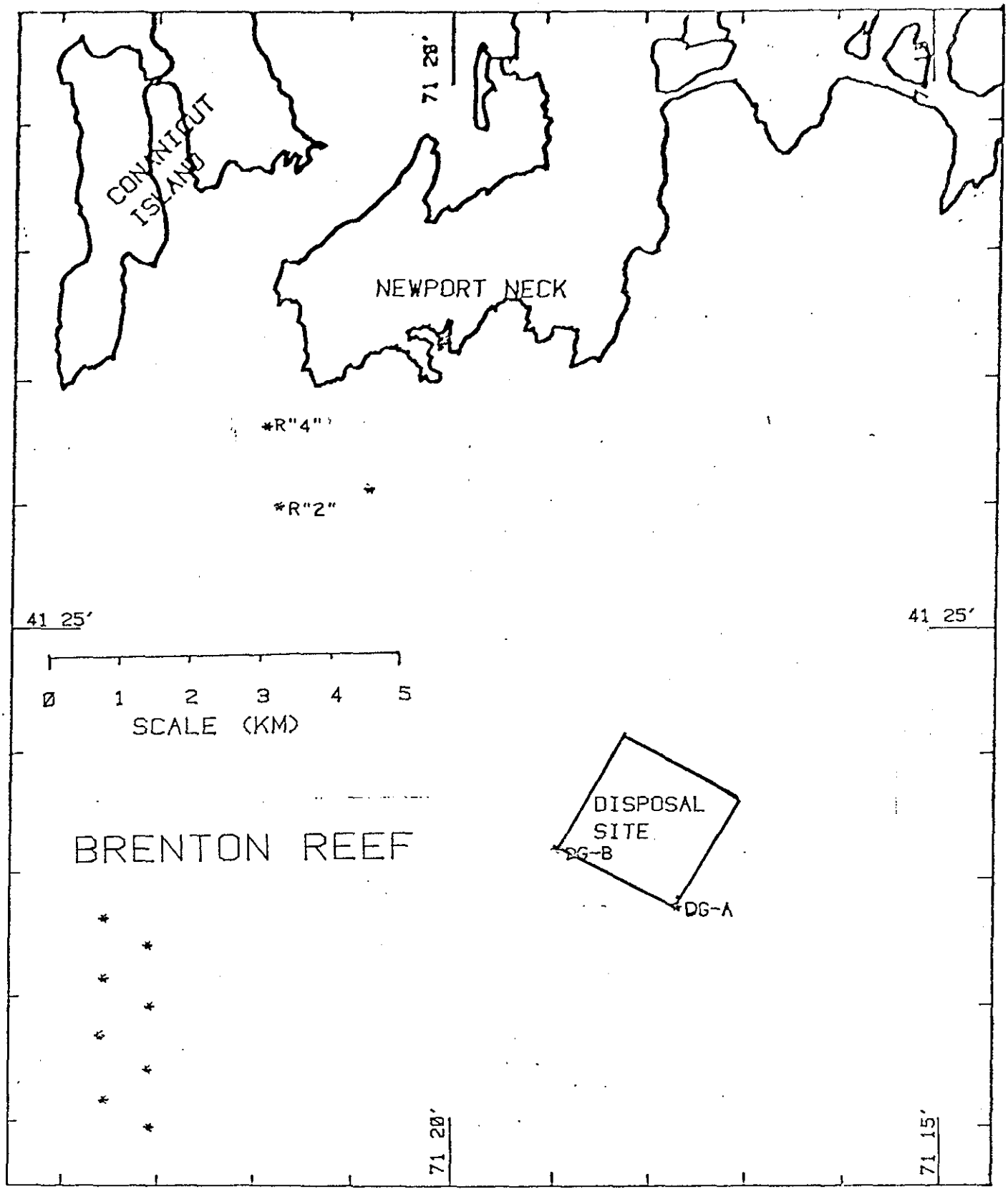
CONANICUT ISLAND
71 28'
NEWPORT NECK
*R"4"
*R"2"
41 25'
41 25'
Ø 1 2 3 4 5
SCALE (KM)
DISPOSAL SITE
DG-B
DG-A
BRENTON REEF
71 20'
71 15'

FIGURE 1.11

Brenton Reef
August 4, 1978

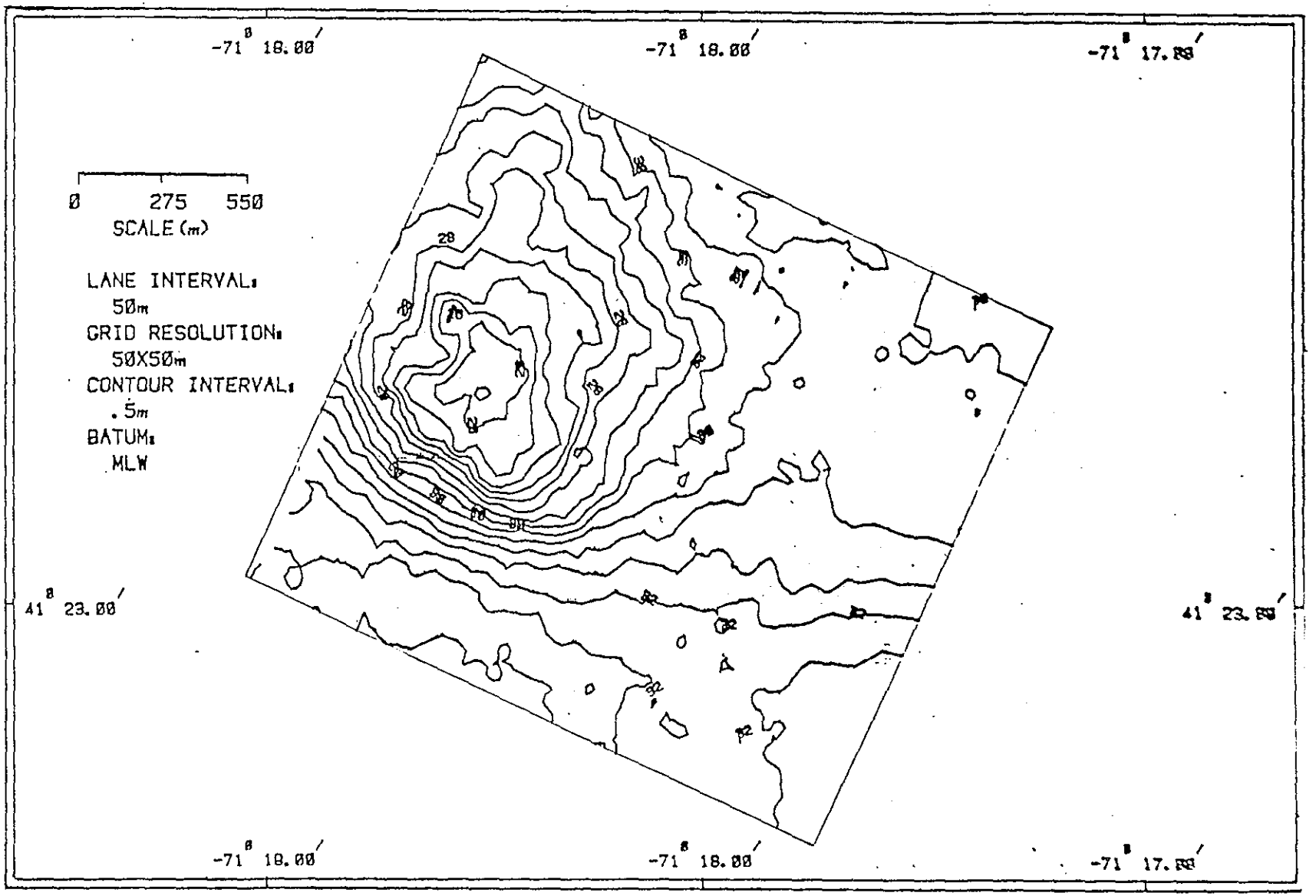

FIGURE 1.12

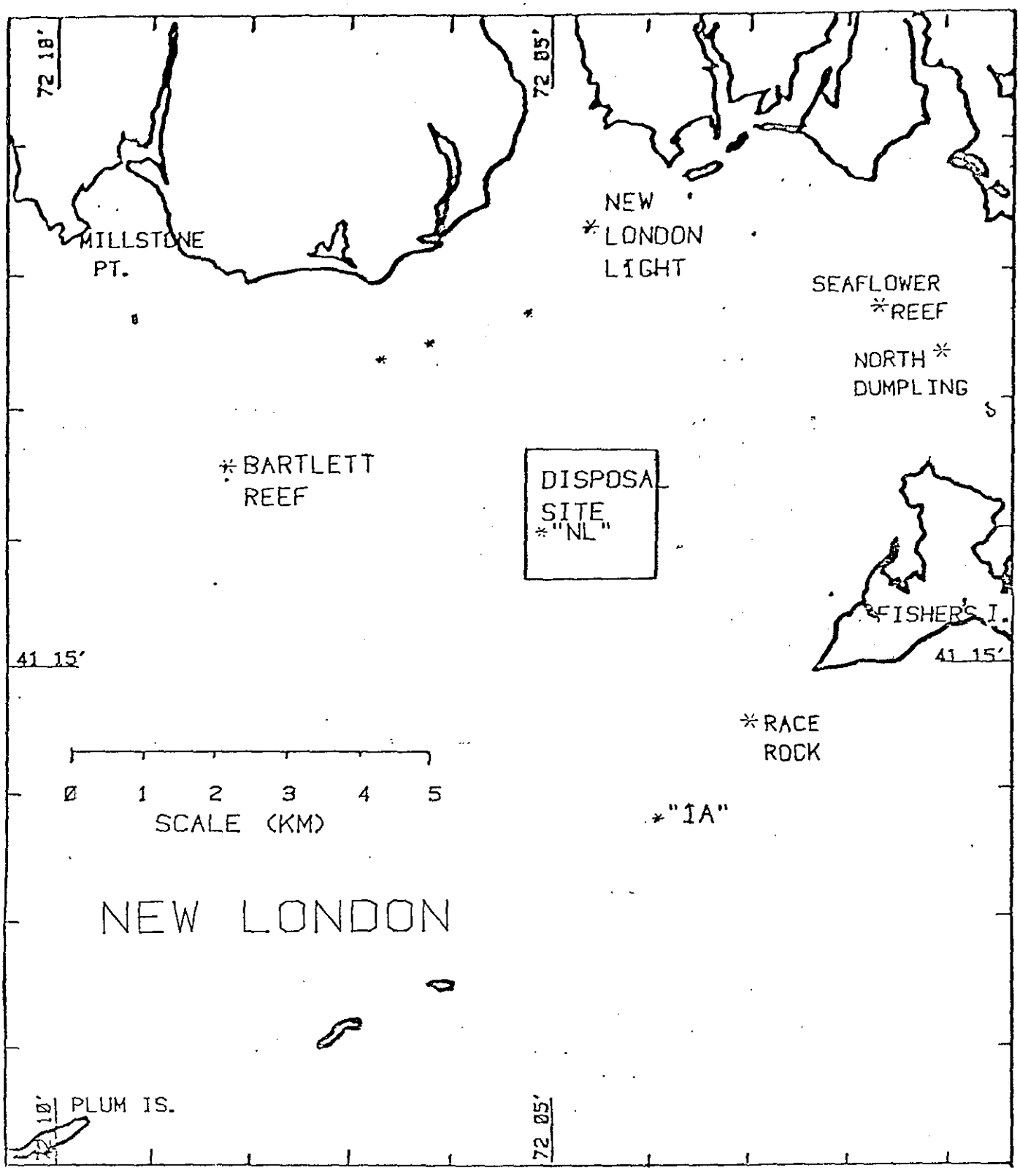
72 18'
72 05'
MILLSTONE PT.
NEW LONDON LIGHT
SEAFLOWER REEF
NORTH DUMPLING
BARTLETT REEF
DISPOSAL SITE "NL"
FISHER'S I.
41 15'
RACE ROCK
0 1 2 3 4 5
SCALE (KM)
"IA"
NEW LONDON
10'
PLUM IS.
72 05'

FIGURE 1.13

of the surrounding bottom is only 20 m, the lack of fetch reduces the potential for strong wave action and to date there have been no major problems with loss of dredge spoils from the disposal area. Bathymetric surveys of the New London site (Fig. 1.14) indicate the presence of a relict mound of spoil material in the northern part of the site, deposited prior to accurate disposal recording. However, this mound has maintained its shape and volume throughout the present study and indicates the stability of the area.

Additional disposal in recent years has created an elliptical mound oriented from southeast to northwest in the center of the disposal area. This mound, with minimum depth of 16 m, has also remained stable for the duration of the present study. The spoils in this mound are highly diverse, ranging from enriched muds to clean sands and coarse shelly deposits. As these different lithologies are randomly distributed both horizontally and vertically throughout the spoil mound, attempts to characterize the spoils thus require replicate samples taken from the entire mound.

Currents at the New London site reach 30-40 cm/sec near the bottom. Although there is evidence that some erosive processes are occurring on the disposal mound, these are generally restricted to the vicinity of topographic highs, and the net loss to the mound has been negligible. Spreading of the mound in the disposal site has not been detected; whatever material is lost from the surface of the site appears to be transported beyond the boundaries and dispersed so that it is essentially indistinguishable from natural sediment.

1.3.7 Cornfield Shoals

Farther west in Long Island Sound, the Cornfield Shoals disposal site is located 5.5 km south of the Connecticut River (Fig. 1.15). This site has a relatively smooth bottom with a gentle trough, oriented east-west and reaching a maximum depth of 55 m (Fig. 1.16). The energy regime at this site is the highest of all areas studied, and the bottom material, composed of sand and gravel reflects these conditions. Furthermore, clay and clay nodules from glacial lake deposits found in the site indicate scouring where recent deposition could not occur.

New London, Conn.
December 12, 1978

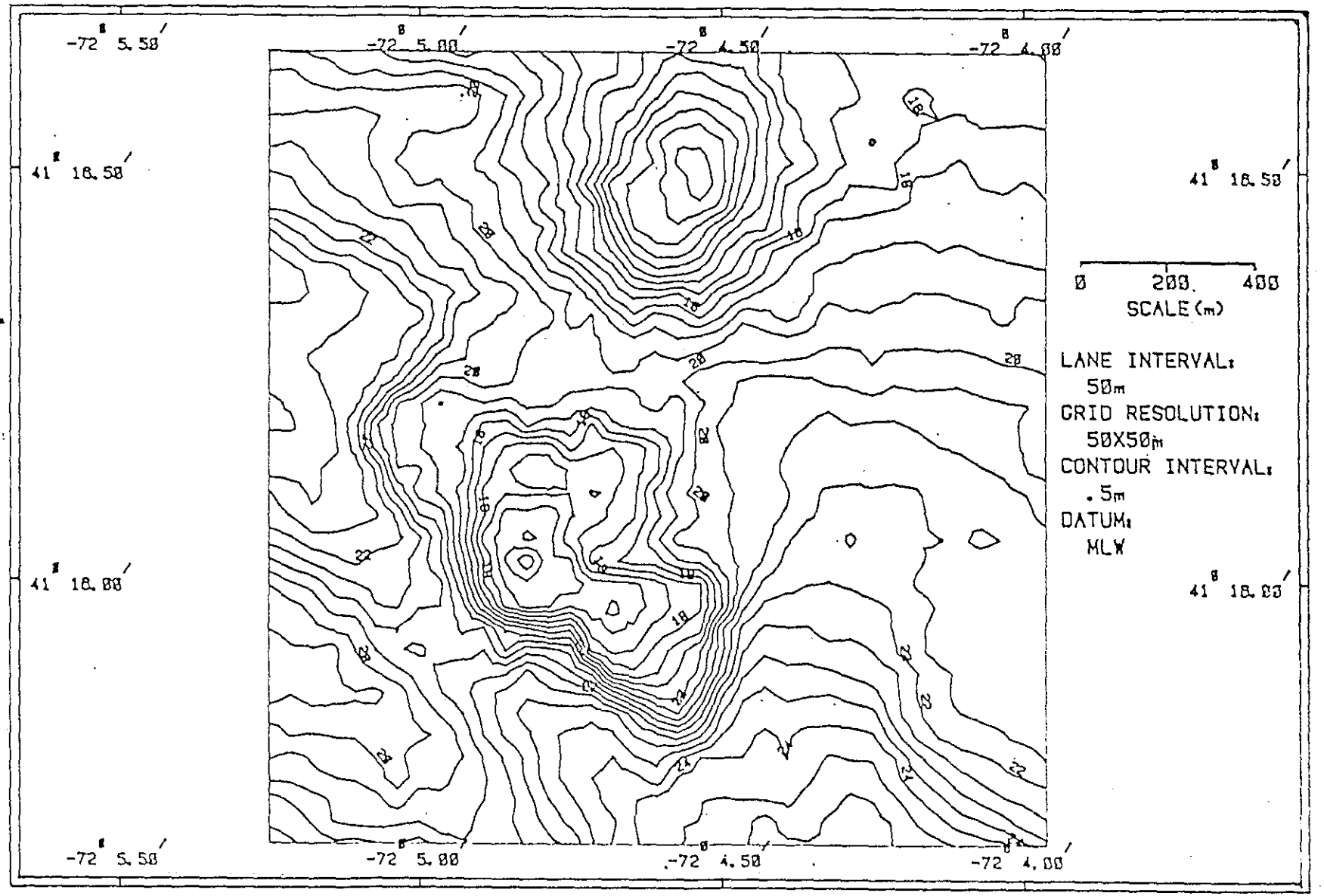

FIGURE 1 14

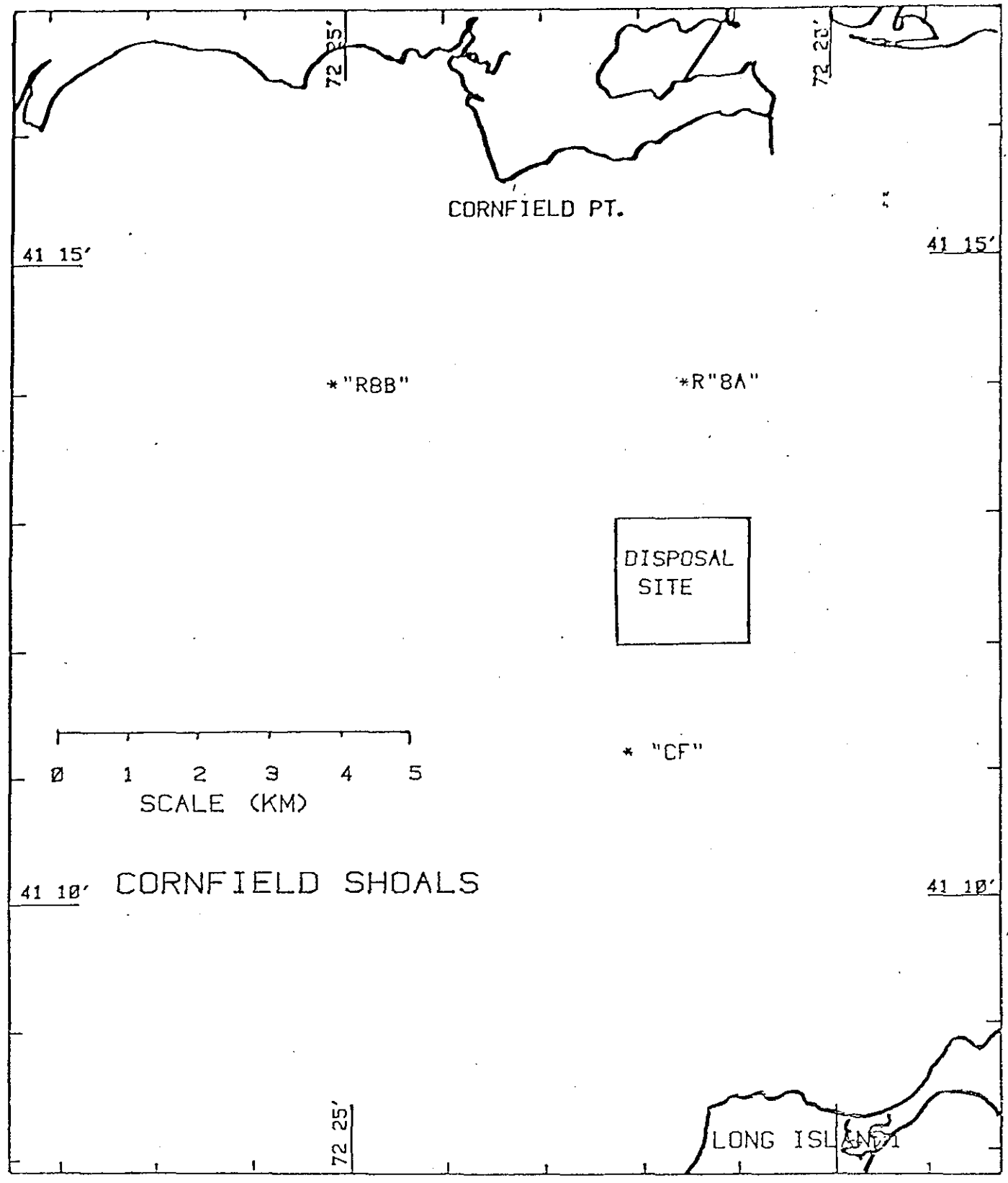
72 25'
72 23'
CORNFIELD PT.
41 15'
41 15'
*"R8B"
*R"8A"
DISPOSAL SITE
* "CF"
0 1 2 3 4 5
SCALE (KM)
41 10'
CORNFIELD SHOALS
41 10'
72 25'
LONG ISLAND

FIGURE 1.15

CORNFIELD SHOALS
JULY 30, 1978

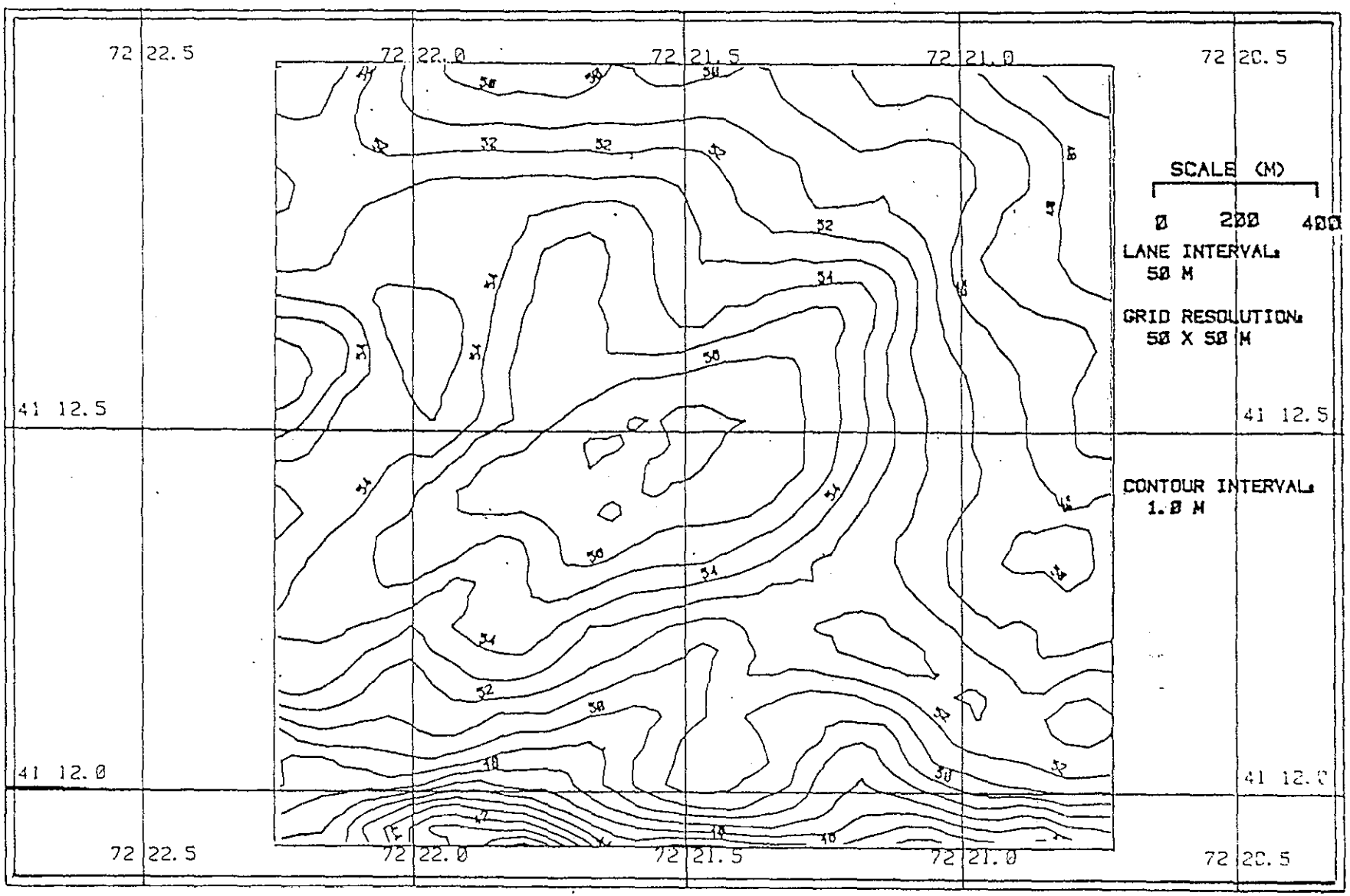

FIGURE 1.16

Although taut-wire mooring techniques have been used at this site to facilitate point dumping of spoils from North Cove in the Connecticut River, no spoil mound has formed. Occasional pockets of spoil material have been sampled. These patches of black, organic, silty spoils are easily distinguished from background material, and replicated samples from the same point on the sea surface, within navigational error, can be obtained. However, the areal extent of each pocket of spoil material is relatively small. The Cornfield Shoals site has been termed a dispersal, rather than a containment site, and this designation should be considered when issuing permits relative to this area.

1.3.8 Central Long Island Sound

The central Long Island Sound disposal site (Fig. 1.17) is currently the most active area in New England. This site received a substantial amount of spoil from New Haven Harbor during 1974, which formed a distinctive mound with a minimum depth of 15 m on an ambient bottom of 20 m (Fig. 1.18). This mound has remained essentially unchanged since the cessation of dredging, indicating the stability of this area.

The energy regime at this disposal site is dominated by tidal currents; however, they are not as strong as those in other areas of Long Island Sound. This lower energy is reflected in the natural sediments of the area, which consist of fine silts and clays with a surface layer of unconsolidated "fluff" that moves during periods of high current and settles out during slack water.

Since completion of the 1974 operation, additional spoils from permit dredging have been dumped at a new location approximately 1,000 m west of the original disposal point. These spoils have created a small mound.

This area was selected for disposal of Stamford and New Haven spoils currently being dredged because of the stability of the 1974 spoil mound, and because environmental measurements indicate that this site is a containment site. Two new disposal points have been designated 1,000 m north and south of the original spoil mound (Fig. 1.19). Both sites will receive about 40,000 m^3 of Stamford spoil which will then be capped with New Haven material: silt from the inner harbor on the southern site and sand from the vicinity of the breakwaters at the northern site. Point dumping and precise bathymetric surveys should result in greater control in disposal site management.

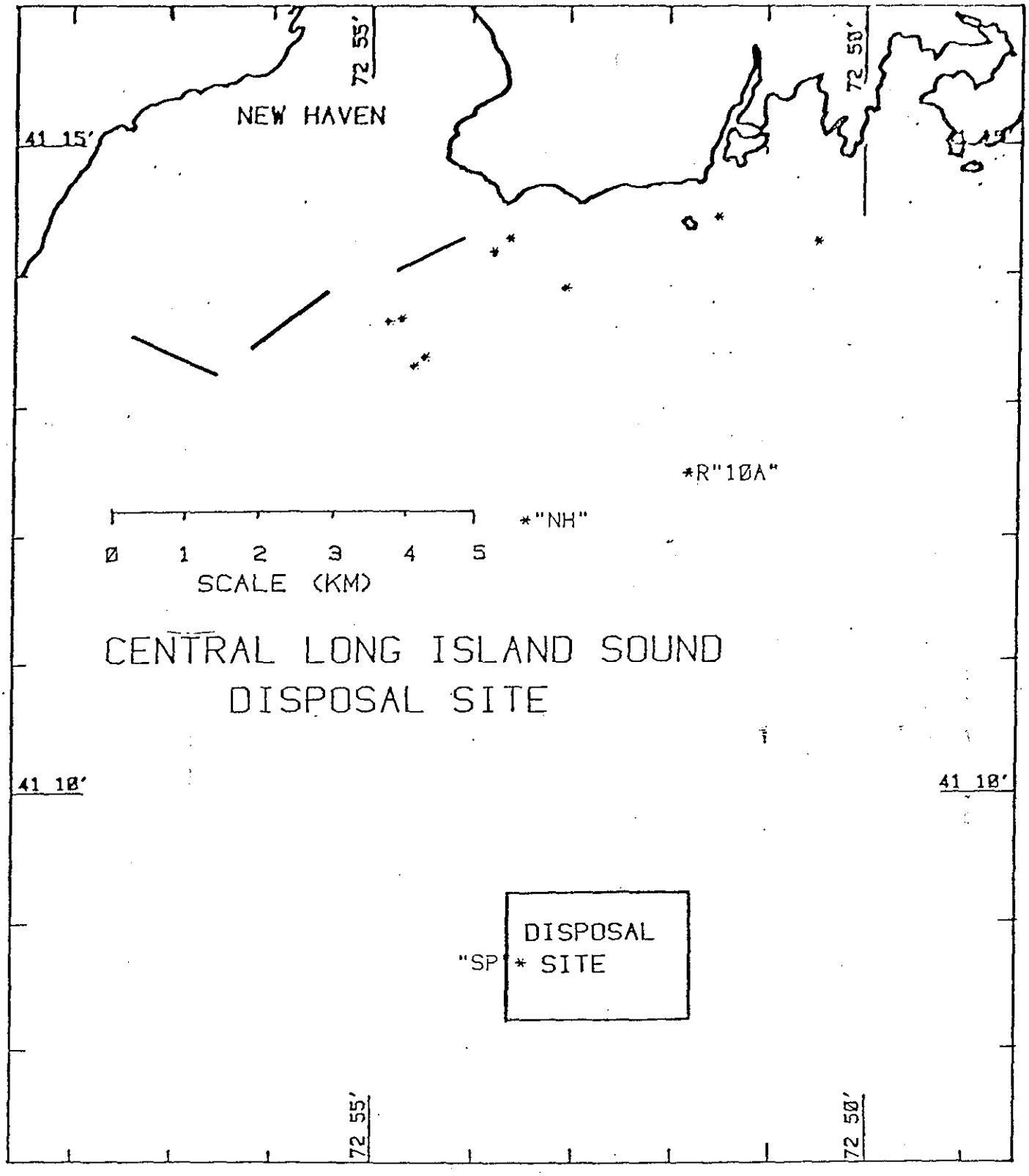
72 55'
NEW HAVEN
72 50'
41 15'
*R"10A"
*"NH"
0 1 2 3 4 5
SCALE (KM)
CENTRAL LONG ISLAND SOUND
DISPOSAL SITE
41 10'
41 10'
DISPOSAL
"SP" * SITE
72 55'
72 50'

FIGURE 1.17

Central Long Island Sound
Disposal Site
January 17, 1979

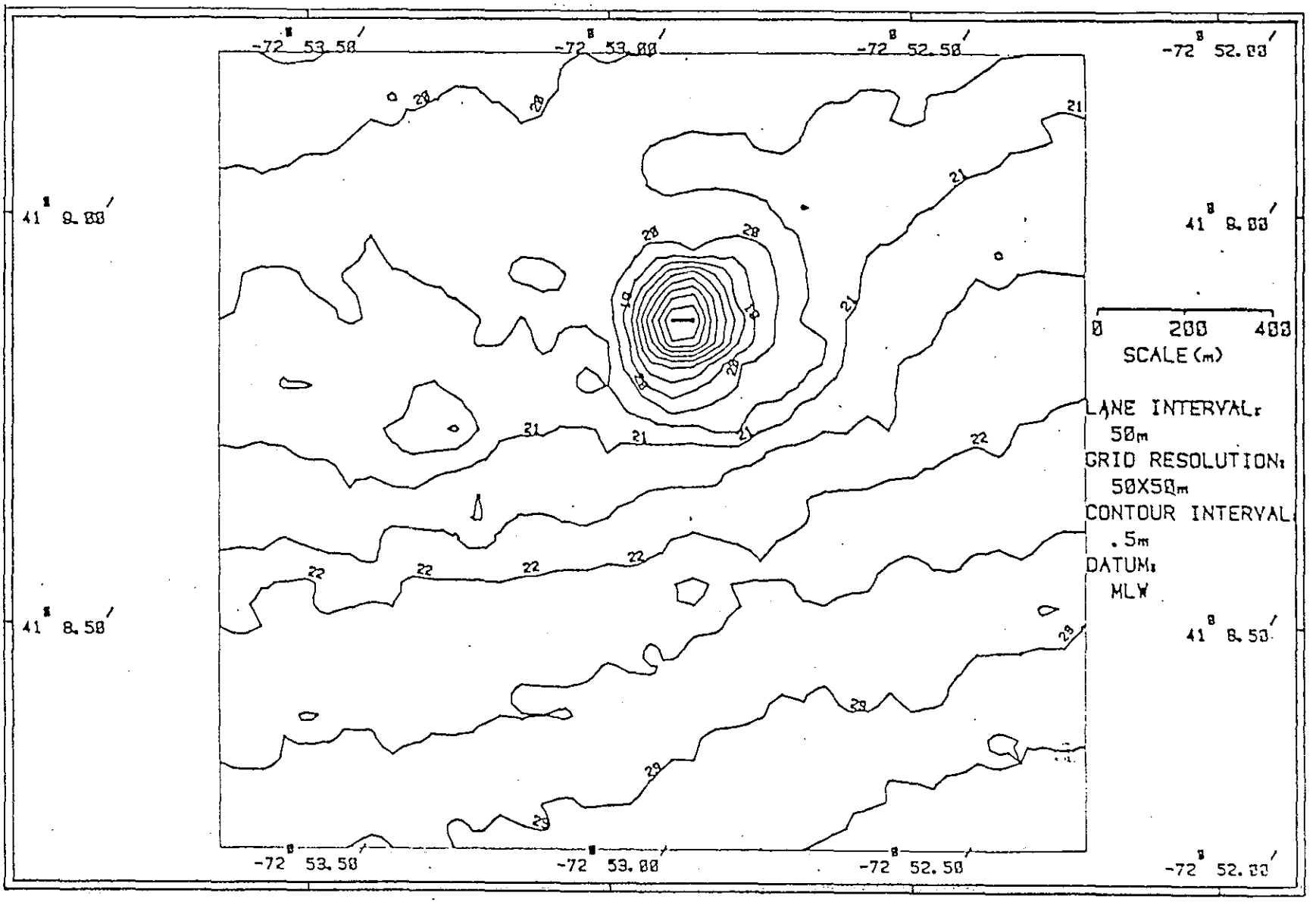

FIGURE 1.18

Central Long Island Sound
Disposal Area

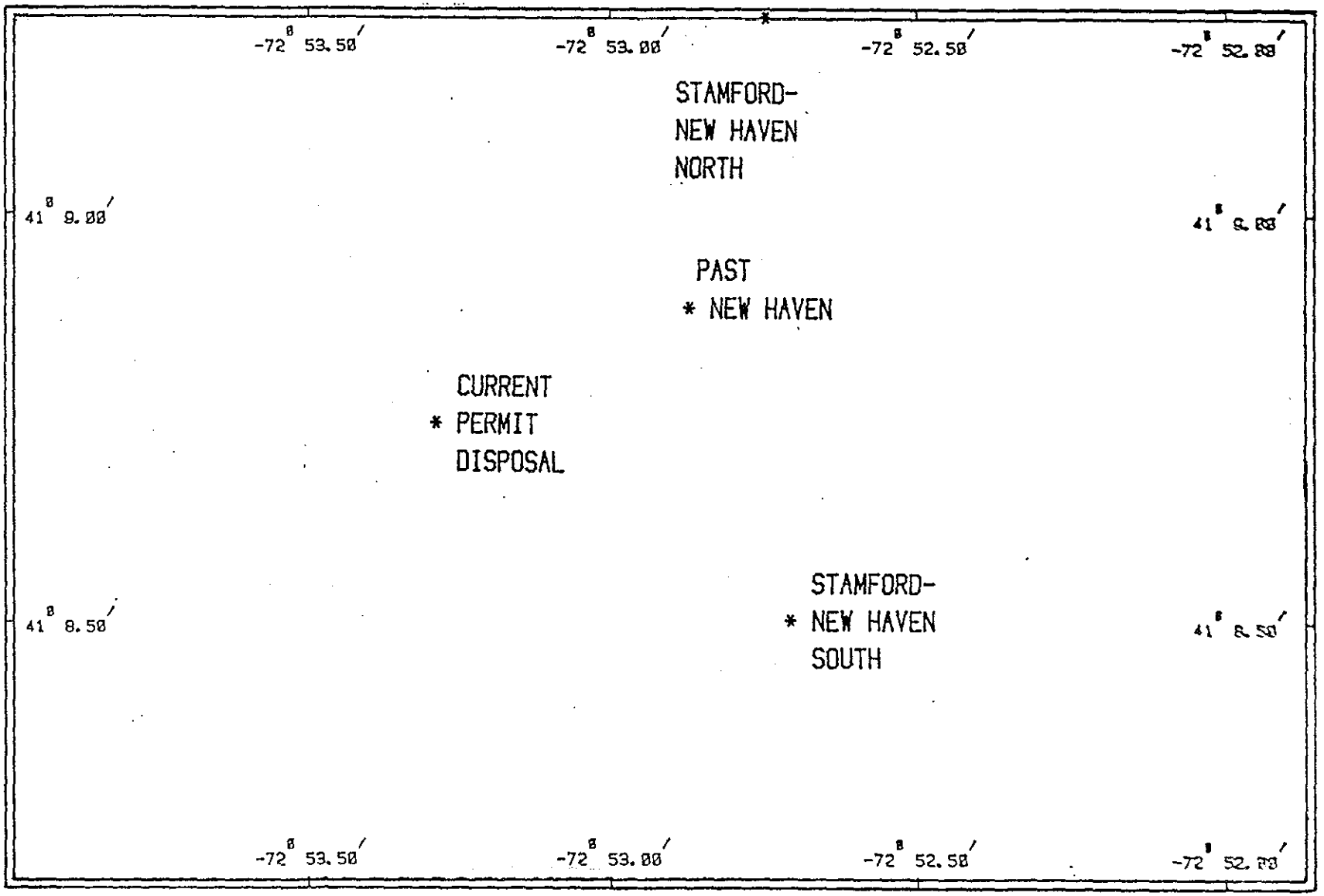

FIGURE 1.19

1.3.9 Western Long Island Sound

Although Stamford spoils are now being transported to the Central Long Island Sound disposal site, an active site in western Long Island Sound is needed. Significant amounts of material have been deposited at the Cable and Anchor Reef site (Fig. 1.20), previously known as the Eaton's Neck disposal site, during past operations (Fig. 1.21). However, as this site is now a prominent lobster fishery, future disposal in this area is not contemplated. Consequently, baseline surveys are being conducted to determine the best alternative location in terms of environmental parameters and fishing interests.

The states of Connecticut and New York suggested a potential site located approximately 5.5 km east of the Cable and Anchor Reef site which was studied in detail during 1978. The results of this study indicate an east-west-trending trough with a maximum depth of 46 m (Fig. 1.22). Currents in this trough were only slightly stronger than those at the central Long Island Sound site, and sediments consisting of fine silts were similar. Environmentally, this site would be suitable; however, the north slope of the trough is an extremely active lobstering ground which would be damaged, at least temporarily, by disposal operations.

A second disposal site, in an area of less fishing intensity was then proposed 3.7 km northwest of the original site. This area is located at the base of the slope forming the northern boundary of the deep basin in Long Island Sound. North of the proposed site the water is less than 20 m deep, whereas the proposed area is in water 26 m deep (Fig. 1.23). Sediments are fine silts, and currents are of the same magnitude as the other western Long Island Sound sites. When a specific use for this area arises, additional studies will be made; procedures for issuing permits must be developed before disposal can occur; however, at the present time this area is the most likely site to be designated as a regional site.

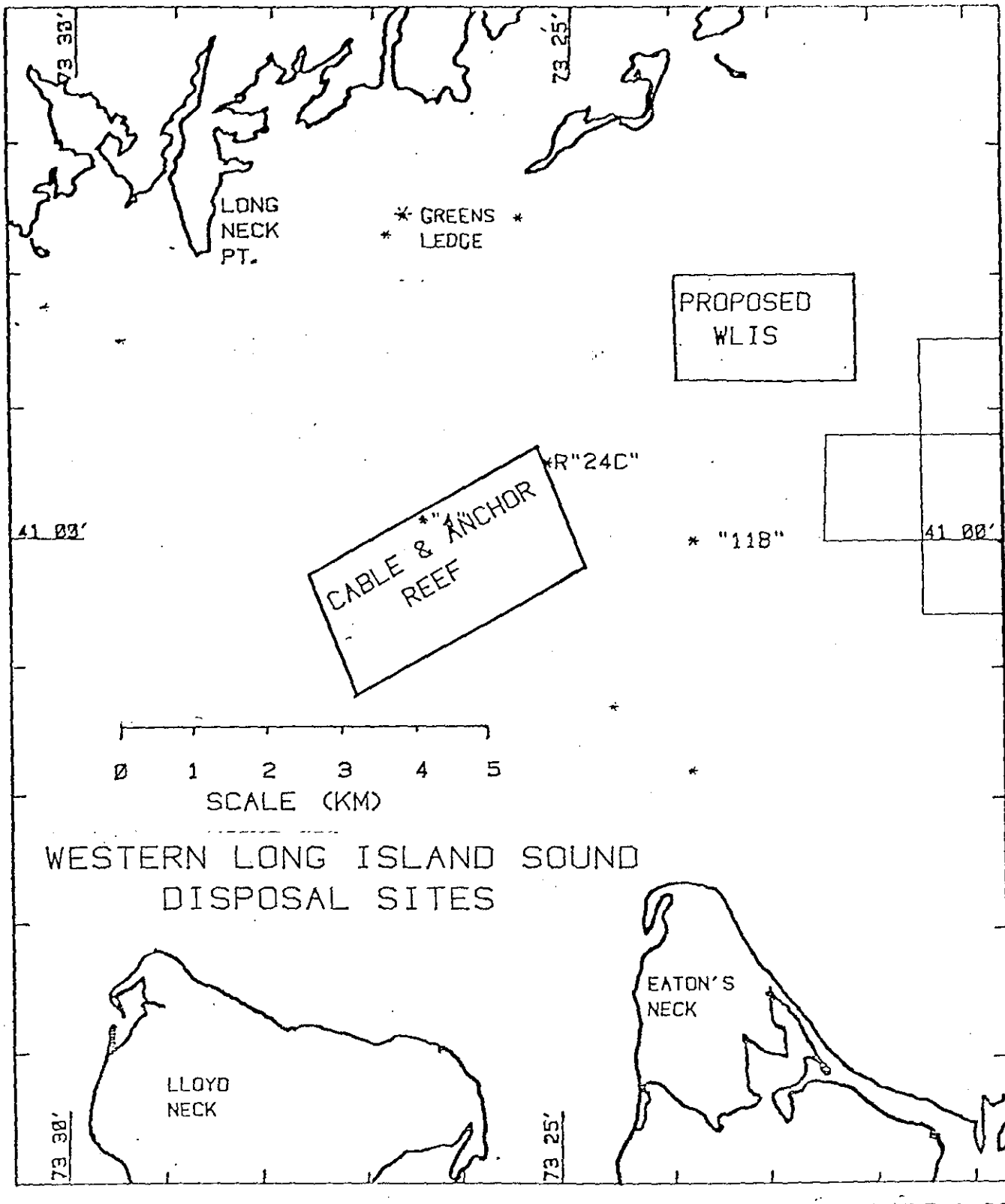
73 38'
73 25'
LONG NECK PT.
GREENS LEDGE
PROPOSED WLIS
"R"24C"
41 00'
CABLE & ANCHOR REEF
"118"
41 00'
0 1 2 3 4 5
SCALE (KM)
WESTERN LONG ISLAND SOUND
DISPOSAL SITES
LLOYD NECK
EATON'S NECK
73 30'
73 25'

FIGURE 1.20

Cable and Anchor Reef
July 26, 1978

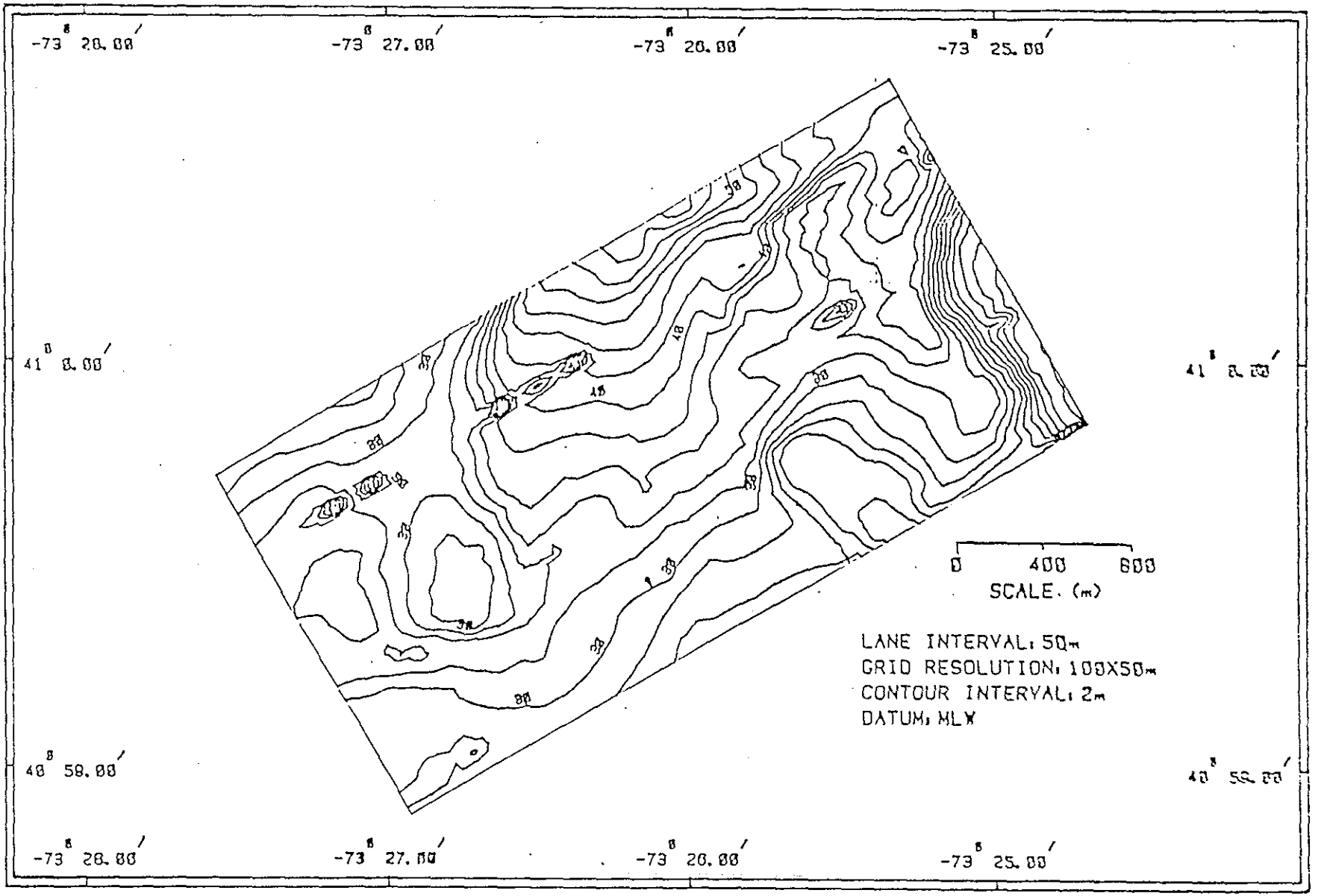

FIGURE 1.21

First Proposed
Western Long Island Sound
Disposal Site
July 25, 1979

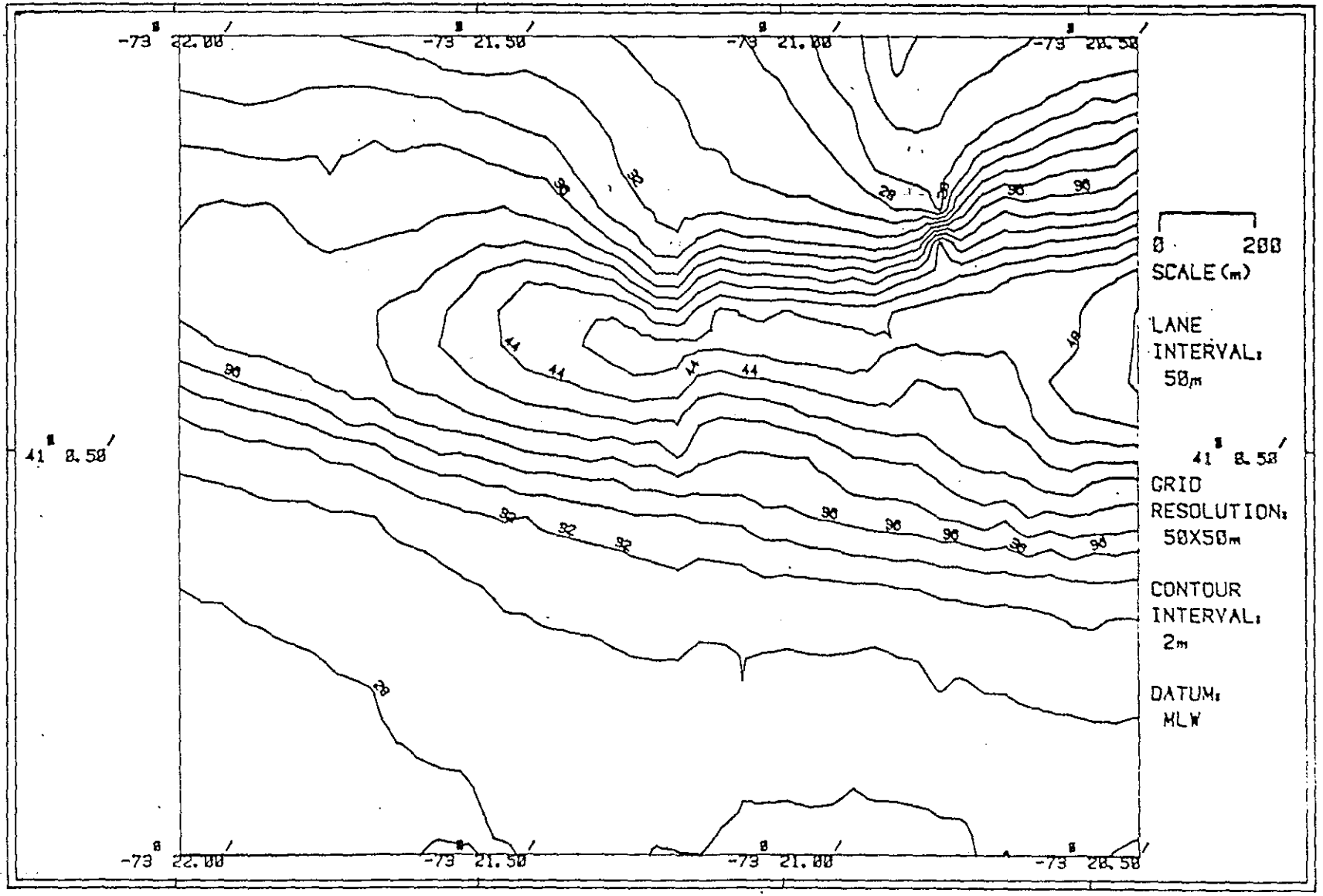

FIGURE 1.22

SECOND PROPOSED
WESTERN LONG ISLAND SOUND
DISPOSAL SITE
JANUARY 22, 1979

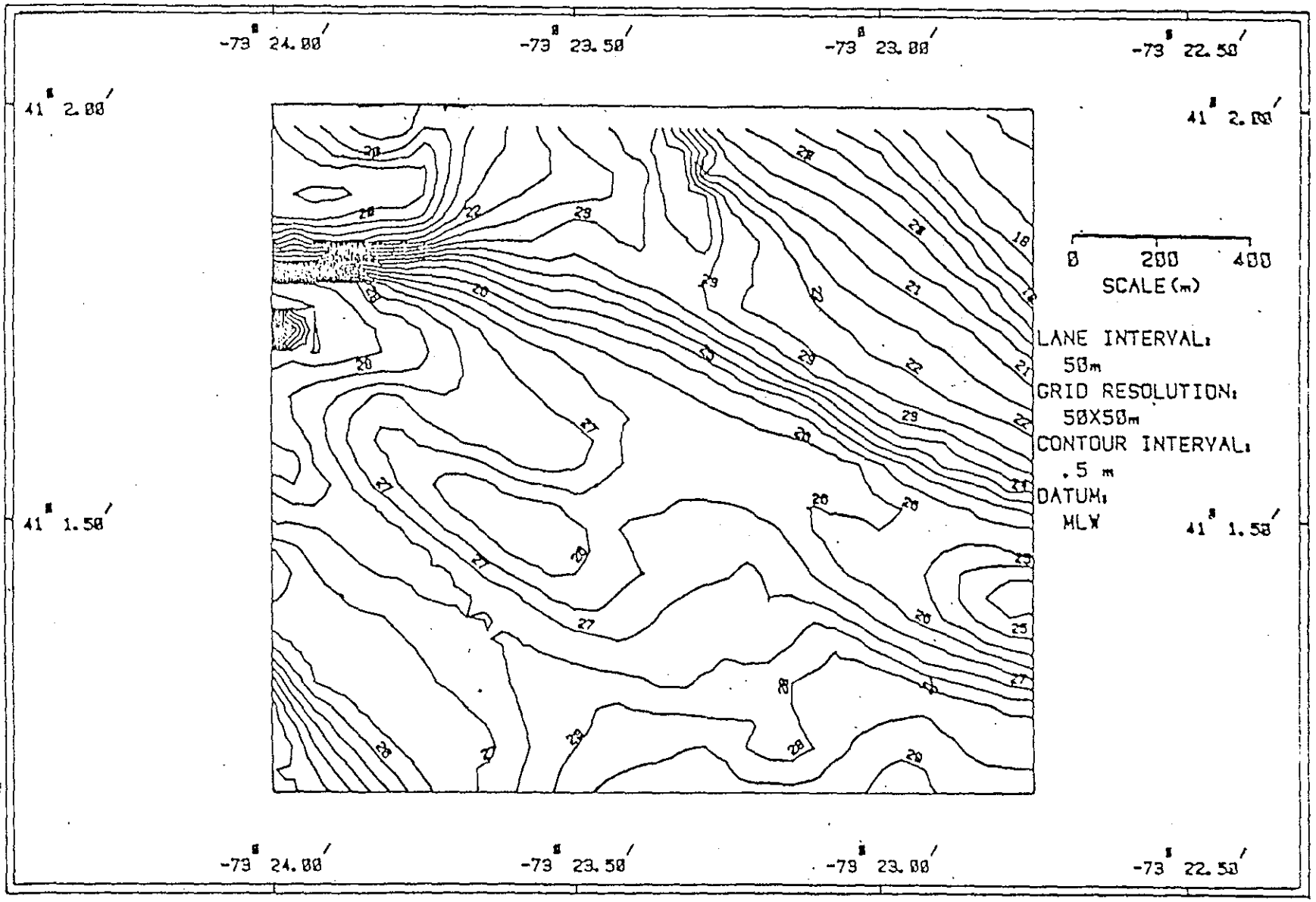

FIGURE 1.23

1.4 SUMMARY

Selections of disposal sites in the New England region have recently been based on the spoil containment potential of the designated areas. This emphasis on containment results from the following management criteria that are now being employed by the New England Division:

- Point dumping is used to build spoil mounds high enough to be monitored for spoil stability.
- Development of a spoil mound reduces the surface area of spoils exposed to the water column or benthic community; stability is required to maintain that condition.
- Dredging from the head to the mouth of estuaries and capping of enriched spoils with cleaner material requires a containment site to ensure that the cleaner material remains in place.

Containment is a relative term, since some loss of material is certain to occur through the interactions of the sediment, biota, and water on the surface of the spoil mound. However, with the exception of Cornfield Shoals, all disposal sites studied under the DAMOS program have been classified as containment sites. Further, these sites have been classified as high-, medium-, or low-energy areas, based on estimates of tidal current and wave motion. Although no significant movement of spoil has been observed in high-energy sites such as New London, the lower-energy sites would be favored for disposal.

Specific criteria have been established for site selection. These are based on EPA criteria but are specifically oriented toward disposal conditions in New England. These include:

- Disposal on previously used disposal sites to restrict the area affected by past and future disposal operations.
- Disposal on sites remote from fishing or shellfishing areas to reduce health hazards or damage to fishing equipment.
- Disposal on sites with maximum depth, minimum fetch, and minimum tidal currents to reduce the potential for spoil movement.

- Disposal of spoils in areas of similar lithology to minimize disruption of benthic communities and permit early recolonization.

The DAMOS program has determined the relative merits and disadvantages of the regional disposal sites used and proposed by the New England Division of the Corps of Engineers. With this information and with specific monitoring data to be presented in other portions of this document, management decisions can now be made to control the disposal of dredge spoil with much greater confidence and reliability than has previously been possible.

2.0

MEASUREMENT OF DREDGE SPOIL STABILITY THROUGH PRECISION BATHYMETRIC SURVEY TECHNIQUES

ROBERT W. MORTON

2.0 MEASUREMENT OF DREDGE SPOIL STABILITY THROUGH PRECISION BATHYMETRIC SURVEY TECHNIQUES

2.1 INTRODUCTION

In the New England area "containment" sites are generally designated for regional disposal operations because dredge spoils from New England harbors are usually enriched with heavy metals, and because many of the management procedures being used in the disposal of dredge spoils require that the spoils remain in place. In order to ensure that spoils are contained, it is essential that an accurate monitoring technique be developed capable of sensing small changes in spoil distribution. Under the DAMOS program, the monitoring of spoil stability is being accomplished through a combination of precision bathymetric surveying, diver observations, and remote sampling of sediment.

2.2 INSTRUMENTATION AND ANALYSIS

The precision bathymetric data acquisition system (Fig. 2.1) used on the DAMOS program consists of a microwave "Trisponder" navigation system, an EDO 4034A fathometer and an EDO 261-c Digitrak unit, all interfaced with a Hewlett Packard 9825A computer and 9827A digital plotter. This system has been used to survey all the disposal sites studied under the DAMOS program and has been shown to provide accurate and reliable data.

Application of this system to the measurement of dredge spoil stability is accomplished through repetition of precision bathymetric surveys and comparison of the resulting data to evaluate changes in the volume and distribution of spoils. The overall results of these surveys are then substantiated through diver observations of the spoil mound and sampling of the margins to determine the spread of material.

Analysis of bathymetric data is first accomplished through presentation of vertical profiles along transect lanes. Since the transects can be repeated with a positional accuracy of better than five meters, these profiles provide a means of evaluating small-scale changes in topography. Fig. 2.2 presents representative profiles across the New London spoil mound taken on

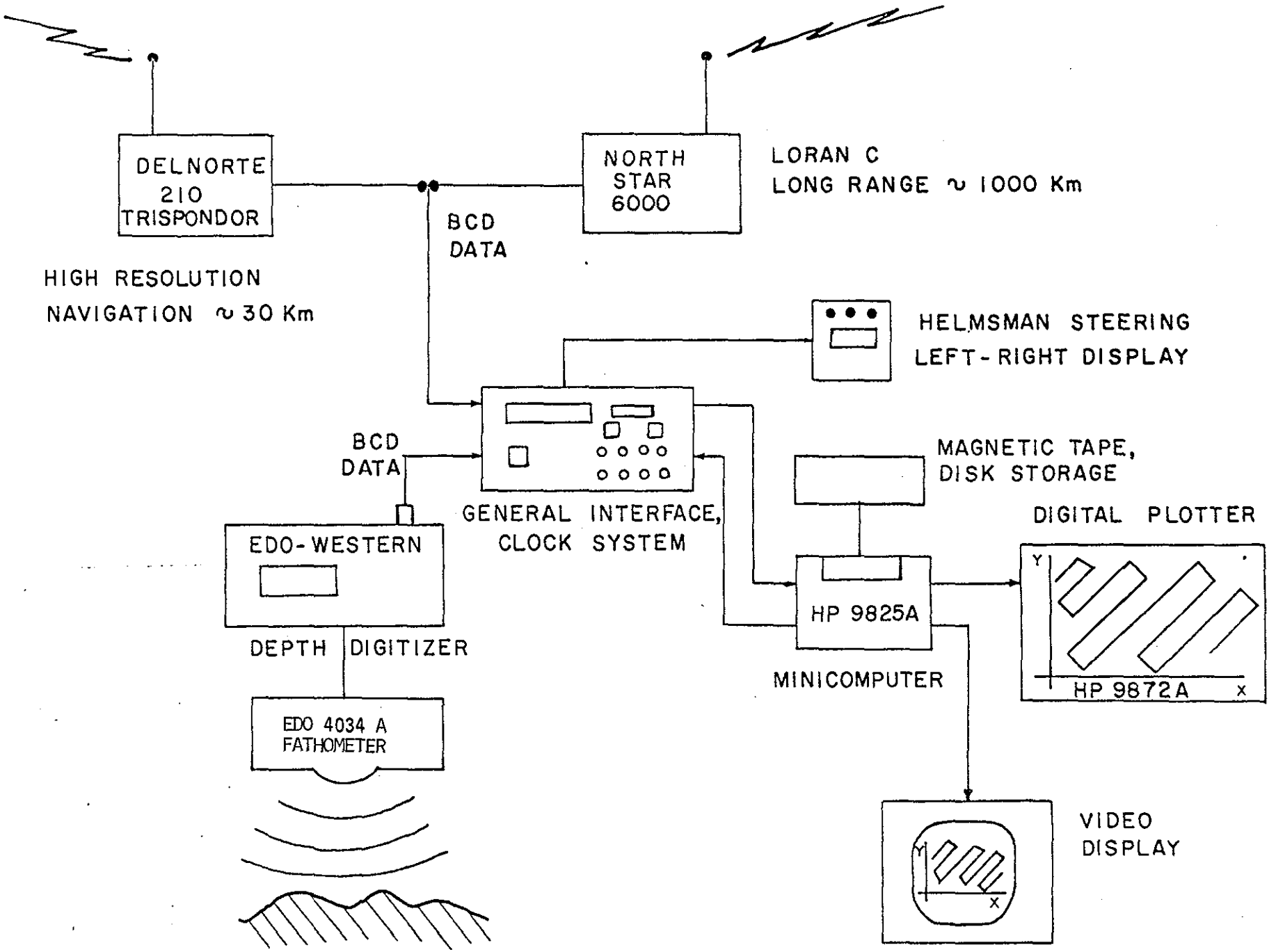

BATHYMETRIC DATA ACQUISITION SYSTEM

FIGURE 2.1

PRECISION OF BATHYMETRIC DATA ACQUISITION SYSTEM

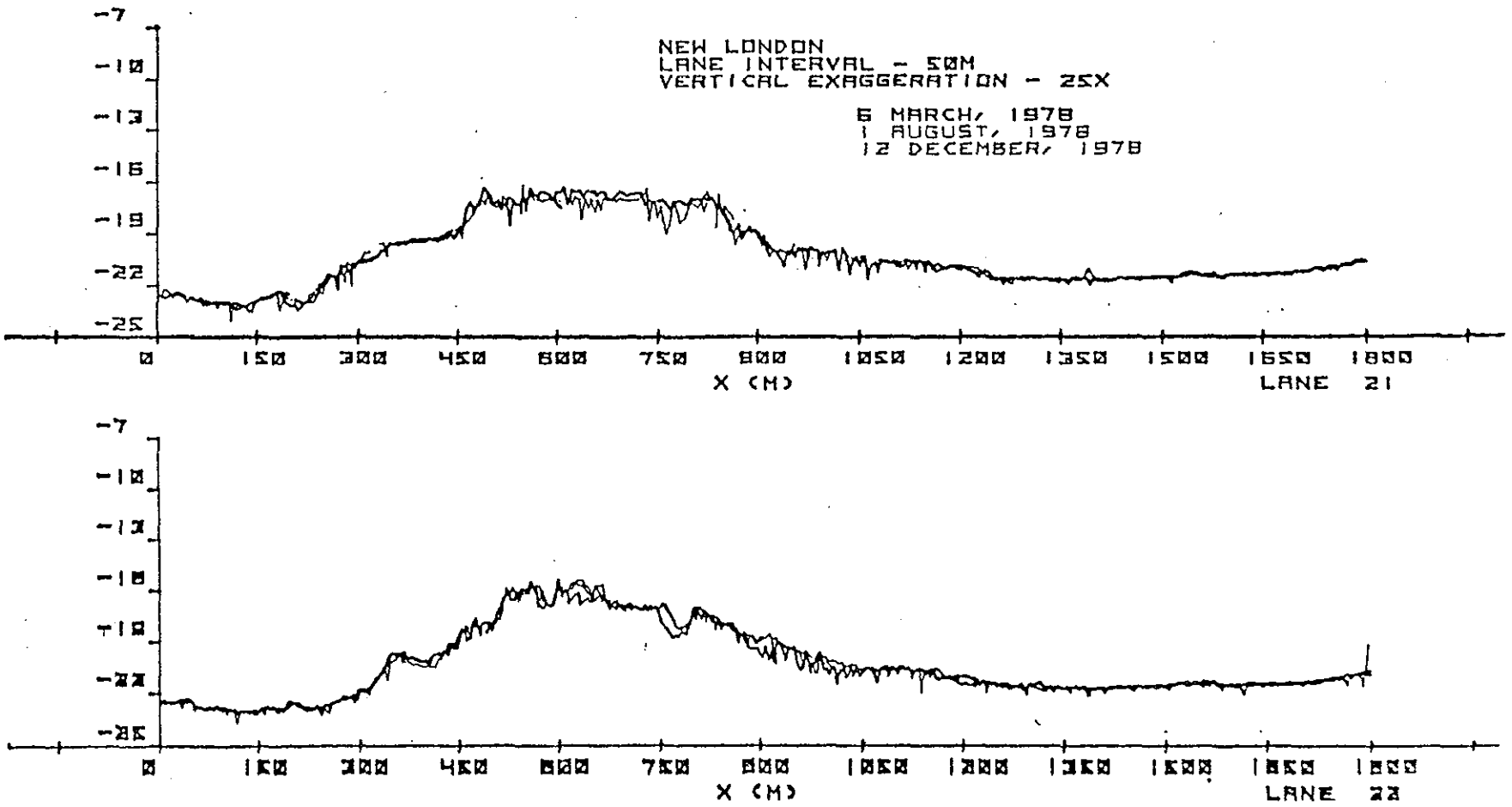

Figure 2.2

three successive cruises in March, August, and December 1978. All depths on these profiles have been corrected for sound velocity, draft, and tidal height. The stability of the spoil mound is readily apparent through the repeatability of the topographic features. Also the precision of the survey technique is verified by comparing depths observed during different surveys at significant distances from the disposal mound. The assumption of no deposition or depth changes on the margins of the disposal area is verified by these profiles. The repeated profiles of the disposal area margins thus provide a calibration technique through which successive surveys can be adjusted to best fit a baseline survey. This allows precise comparisons between profiles from different surveys.

After the vertical profiles have been analyzed, the data are inserted into an arbitrary grid pattern. Each grid block of the pattern is centered on a transect lane and has a height equal to the lane spacing and a width equal to one-half the spacing. Although it is possible to establish a finer grid pattern by sampling more frequently along the transects, this introduces a bias into the data since the resolution between lanes cannot be improved. All depth measurements falling within the area of the grid block are averaged, and a mean depth is assigned to each grid location. This matrix of depths is then used to develop contour charts, volume difference calculations, and difference contour charts.

The volume difference is calculated by subtracting the depth matrix of one survey grid from another on a point-by-point basis. However, to ensure that the volume calculation is as precise as possible, an additional correction factor is applied to eliminate errors resulting from inaccurate adjustment for sound velocity, draft, tide, or inherent system errors. To calculate this adjustment, we assume that the bottom is stable on the margins of the disposal area. We then adjust the sum of the differences between surveys for the first five and last five transects of the grid to zero through application of a correction factor for the first and last lanes. A linear interpolation for each lane is made between the first and last lane factors and is applied to the entire survey. Corrections of this type are generally less than 10 cm; however, they are important since small errors when averaged over the entire area of the survey can produce large-volume changes.

The first and last lane correction factors are also used in the contour difference program and are applied in the same manner to ensure precision between surveys. Contour intervals of 20 cm are used on these charts with consistent results.

2.3 DISCUSSION

The most notable application of this procedure has taken place at the Central Long Island Sound disposal site (Fig. 1.19) during the past few months. Disposal at this location is presently being conducted at two points in order to evaluate the effectiveness of "capping" procedures. Stamford spoils will be capped with New Haven material consisting of silt and clay from the inner harbor at the southern point and sand from the outer breakwater area at the northern point.

This capping procedure requires precision disposal of Stamford spoils to reduce the area necessary for complete coverage of the enriched spoils. Furthermore, accurate measurement of the resulting spoil distribution and subsequent capping material distribution is necessary to evaluate and monitor the coverage of Stamford material.

Earlier surveys at the Central Long Island Sound site and other DAMOS areas utilized a 50-meter grid spacing which was adequate for evaluation of major disposal operations. However, the volume of the Stamford spoil to be dumped at each site was less than 30,000 m^3 and a tighter grid was required to obtain useful data. A smaller survey grid consisting of 25 lanes, 600 meters long and 25 meters apart, was established for each site (Fig. 2.3). The disposal point was centered on each grid and marked using a taut-wire moored disposal buoy. Scow operators were instructed to dump spoils immediately south of each buoy.

Bathymetric surveys of both disposal sites for the Stamford-New Haven operation were made prior to the initiation of dumping to obtain baseline data. A second survey of the south site was made to evaluate the precision of the volume calculation technique. Contour charts of the south site (Figs. 2.4& 2.5) indicate that the bottom is essentially flat with a slight downward slope

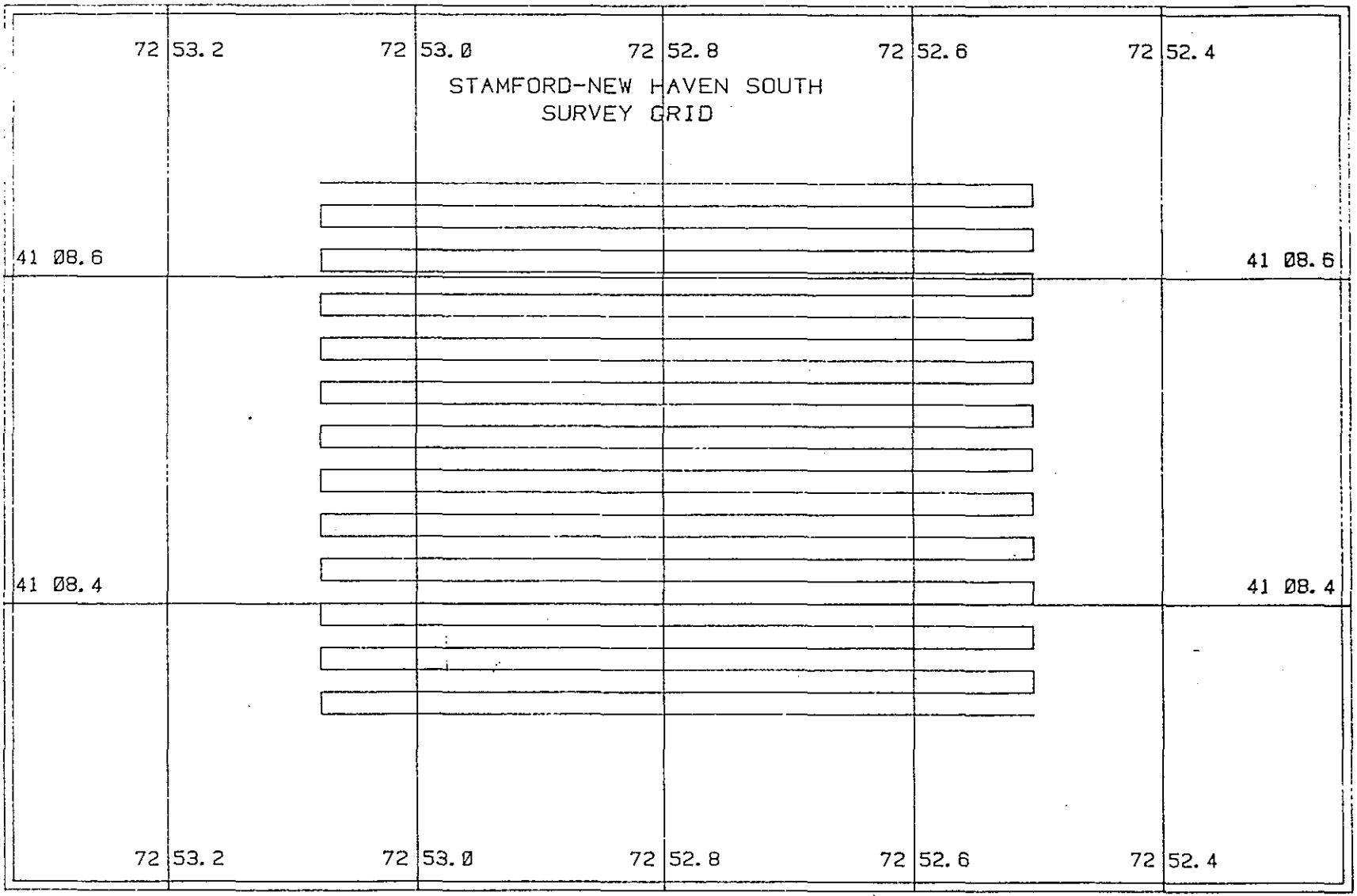
72 53.2
72 53.0
72 52.8
72 52.6
72 52.4
STAMFORD-NEW HAVEN SOUTH
SURVEY GRID
41 08.6
41 08.6
41 08.4
41 08.4
72 53.2
72 53.0
72 52.8
72 52.6
72 52.4

Figure 2.3

Stamford-New Haven Disposal Area
Southern Site
January 20, 1979

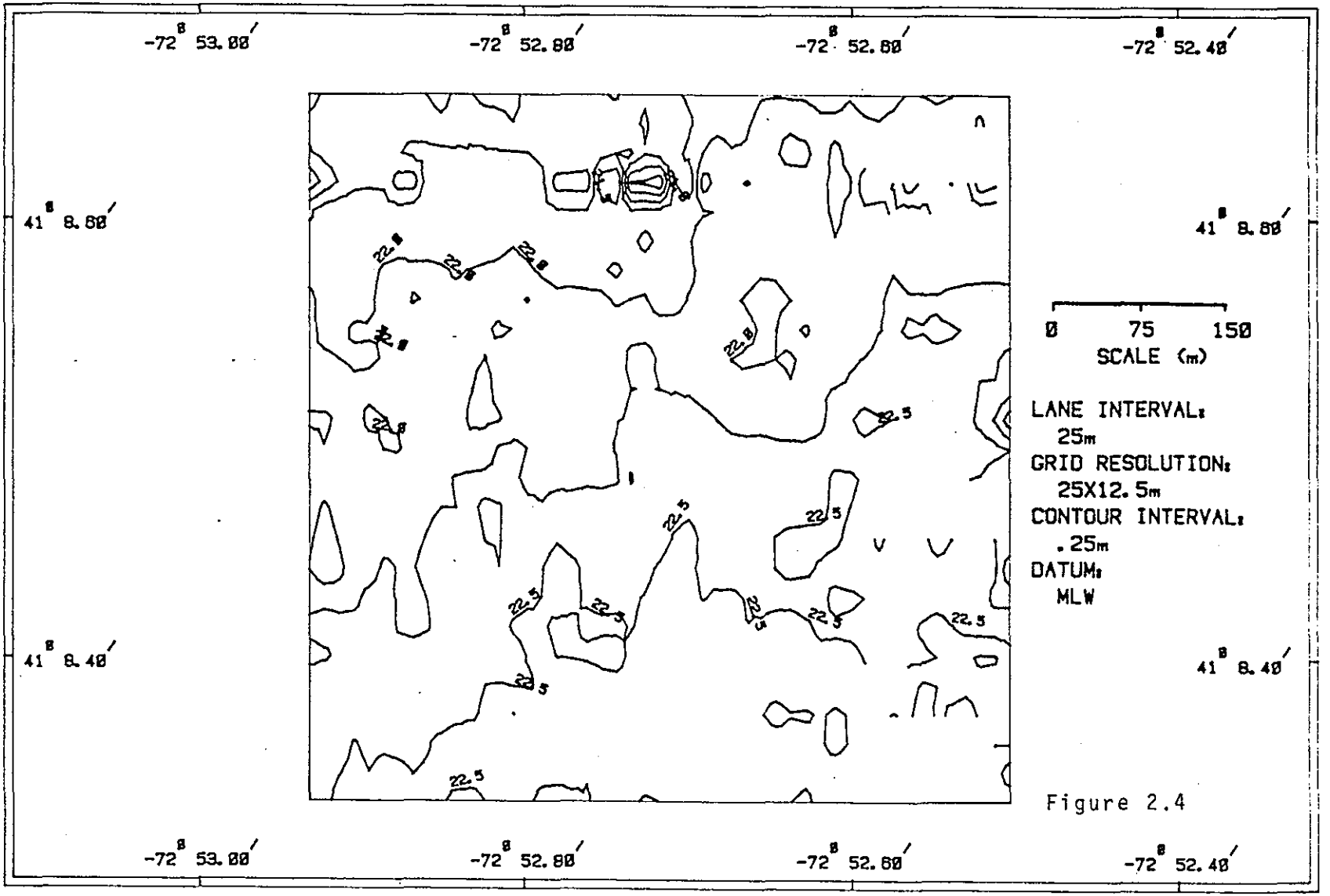

Figure 2.4

Stamford-New Haven Disposal Area
Southern Site
March 19, 1979

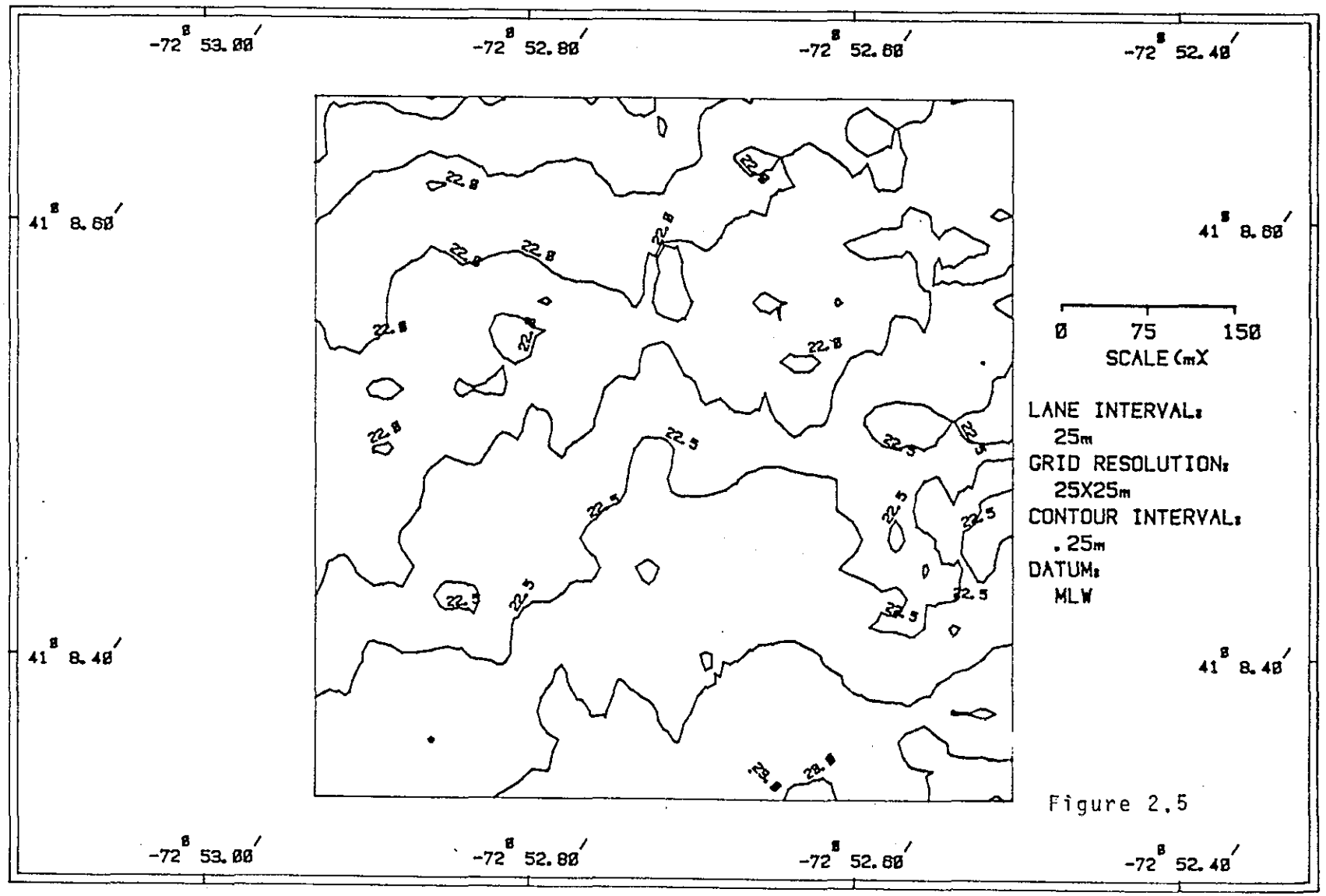

Figure 2.5

(1/400) to the south. The depth at the disposal point was 22.5 m. A similar condition exists at the north site (Fig. 2.6), where the bottom is slightly more shallow but is flat with a slight dip (1/600) to the south.

We applied the volume calculation technique to the surveys of the south site (Fig. 2.7). The volume difference resulting from survey error was less than 2,000 m^3. The contour difference chart (Fig. 2.8) indicated that these errors were random since there was no consistent pattern to the contour difference lines.

The random distribution of errors suggests that they result from imprecise navigation in retracing the transects rather than instrumental or correction errors. That both sites are essentially flat provides an excellent opportunity for evaluating the potential of this monitoring technique. We can make precise corrections, at sites with flat bottoms, based on the depth of the ambient bottom. In the regions with rough topography, slight changes in position can result in large changes in recorded depth. Consequently, the inherent precision of bathymetry must be less.

Disposal of Stamford material began in late March 1979 at the south site. As stated earlier, the capping procedure required that disposal of this material be restricted to as small an area as possible. To accomplish this objective, a taut-wire moored disposal buoy was placed at the center of each site and scows were dumped immediately south of the buoy. This technique worked extremely well since the tugs were generally able to steam with the scow alongside (except in rough water) and thus maneuver close to the buoy. During periods of rough weather, shortening the tow hawser provided sufficient control to dump within 25-50 meters south of the buoy.

One of these dumping operations was observed in late March during winds of 25-30 knots. The scow was on a short hawser, and the tug was able to make two passes on the buoy and dump material within 25 meters of the disposal point in both cases. This operation took place at slack water and therefore provided an opportunity to observe the distribution of spoils throughout the water column after dumping. A 200-Khz fathometer system was installed on a small boat stationed immediately astern of the scow. Approximately 30 seconds

Stamford- New Haven Disposal Site

Northern Site

March 22, 1979

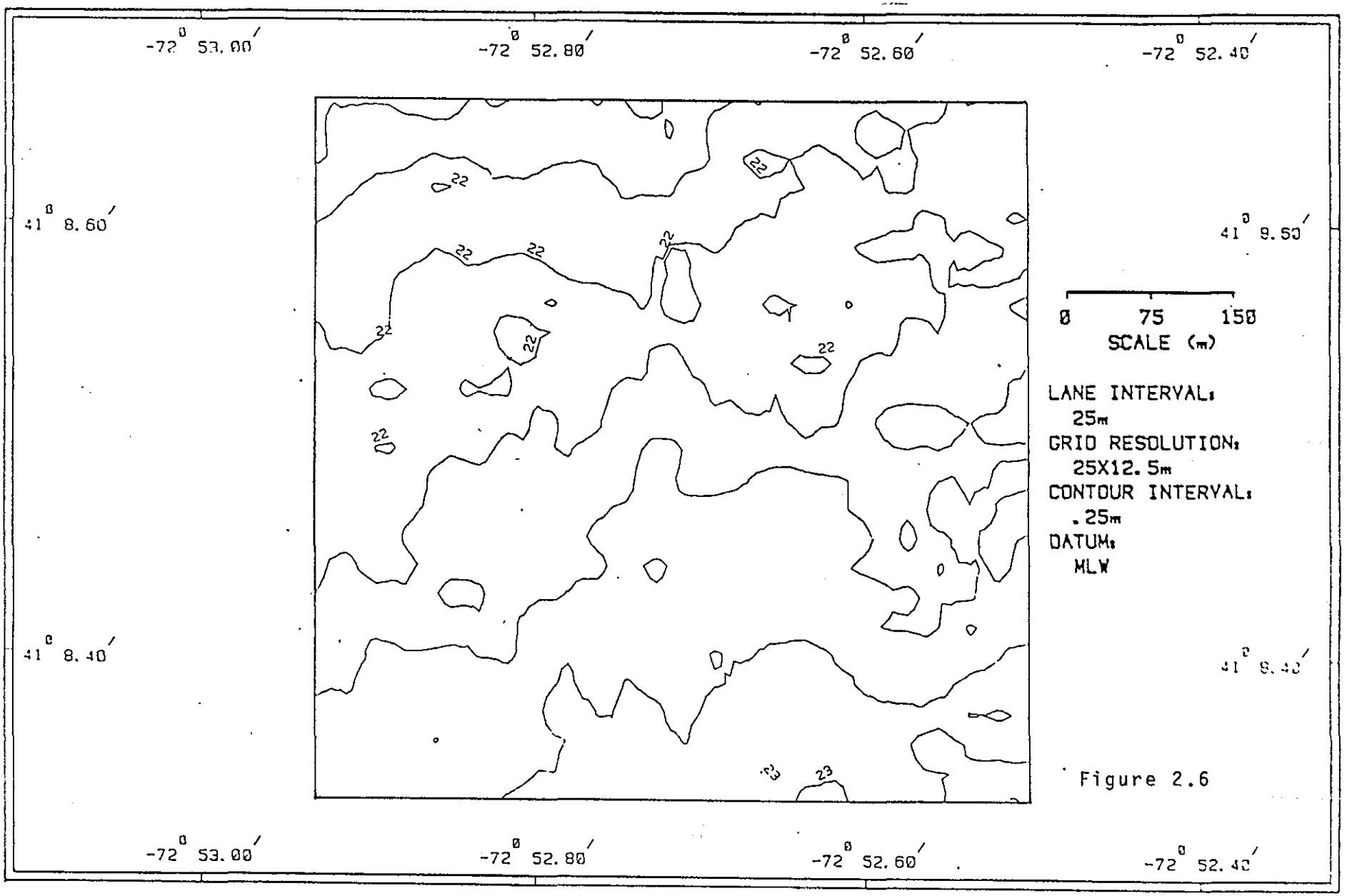

Figure 2.6

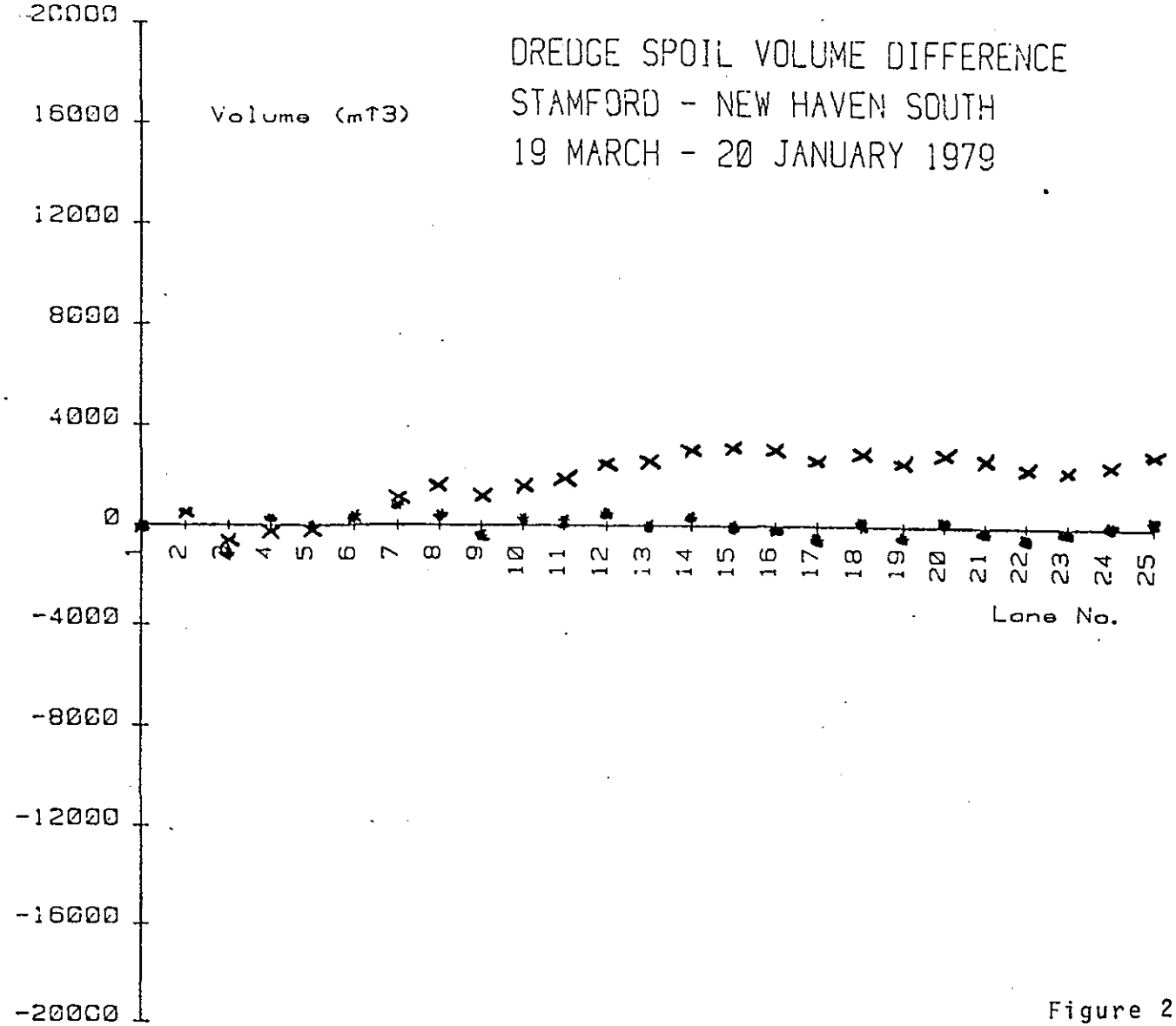
DREDGE SPOIL VOLUME DIFFERENCE
STAMFORD - NEW HAVEN SOUTH
19 MARCH - 20 JANUARY 1979
Volume (mT3)
20000
16000
12000
8000
4000
0
-4000
-8000
-12000
-16000
-20000
1
2
3
4
5
6
7
8
9
10
11
12
13
14
15
16
17
18
19
20
21
22
23
24
25
Lane No.

Figure 2.7

Stamford-New Haven Disposal Area
Southern Site
Contour Difference Chart
March - January, 1979

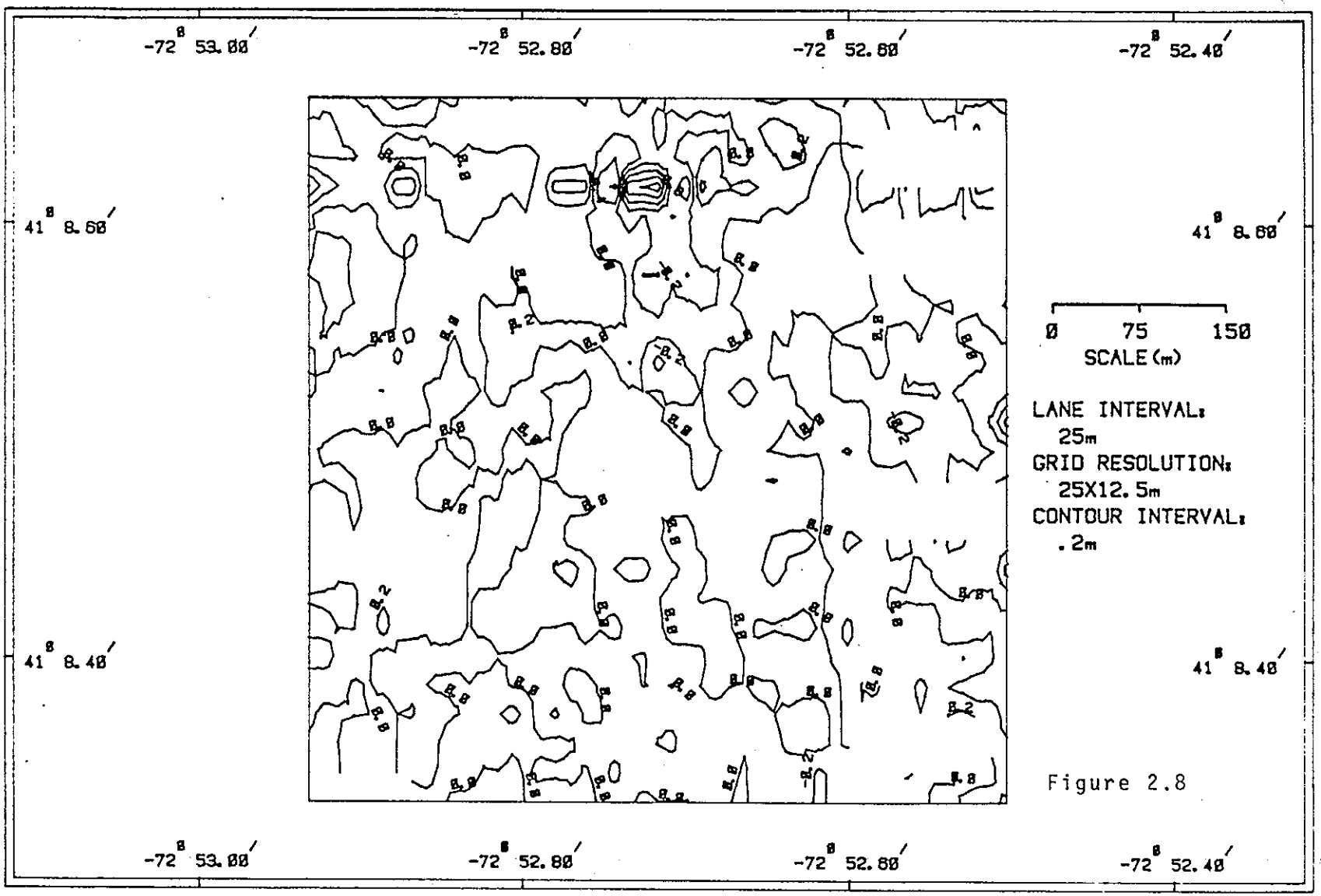

Figure 2.8

after opening of the scow doors, a turbidity cloud was detected that covered the entire water column. This turbidity lasted for four minutes; then the material began to settle, resulting in a persistent layer near the bottom that could be detected for seven minutes. From these observations it appears that most of the material falls directly to the bottom after disposal, leaving only a small amount of material in suspension. The turbid layer that develops near the bottom most likely settles to the bottom in a short time. Evidence to support this hypothesis of disposal dynamics has been gathered by divers, who are able to distinguish individual barge loads at the disposal point, and through remote sediment sampling where a gradation from coarse to fine material, similar to a turbidite deposit, can be observed at greater distances from the disposal point.

Disposal of Stamford material at the southern site continued through the first three weeks of April 1979, at which time the operation was shifted to the north site. A survey of the southern area was made on 24 April 1979 to determine the final distribution of Stamford spoils prior to capping with New Haven silt. The results of this survey are shown as a contour chart of the area in Fig. 2.9 The Stamford spoils are clearly shown as an elliptical mound in the center of the site with a minimum depth slightly greater than 20 meters. The east-west orientation of the mound is most likely a result of the orientation of the scows during the dumping operation. Since the tugs approach the site from the west, and since some time is required to empty the scow, the eastward momentum of the scow has extended the mound in that direction.

Figure 2.10 presents profiles from lanes 13-16, which cover the major part of the spoil mound. This can be compared to the initial baseline surveys of January and March 1979. The resulting topography of the spoil mound has amplitudes of 1-3 meters, indicative of the cohesiveness of the spoils and of the effect of individual scow loads maintaining their identity on the bottom after disposal. The easterly orientation of the dumping operation can be seen clearly on these profiles since the buoy is located at the 300-meter point and most of the spoils are found to the right of that position.

Stamford-New Haven Disposal Area
Southern Site
April 24, 1979

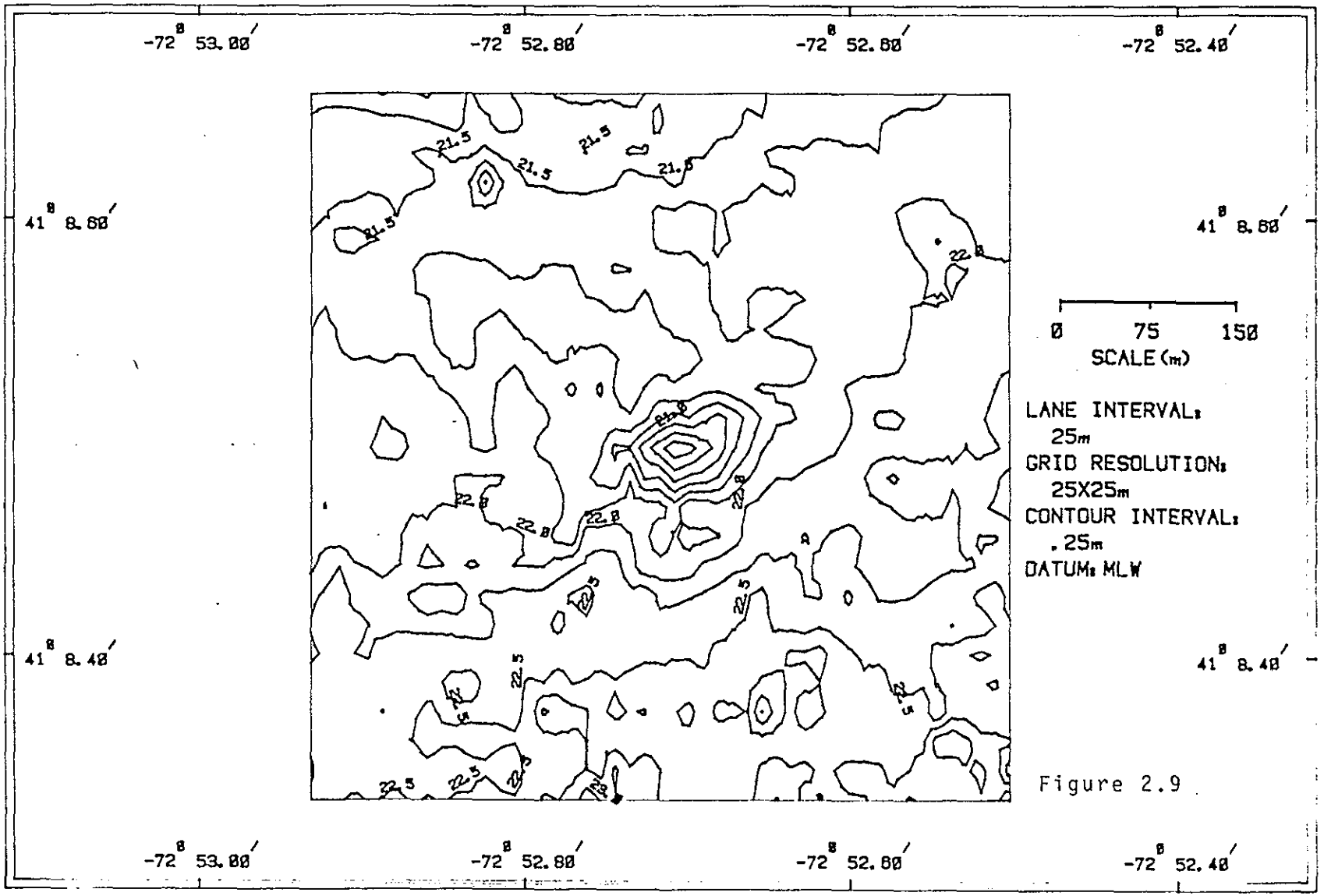

Figure 2.9

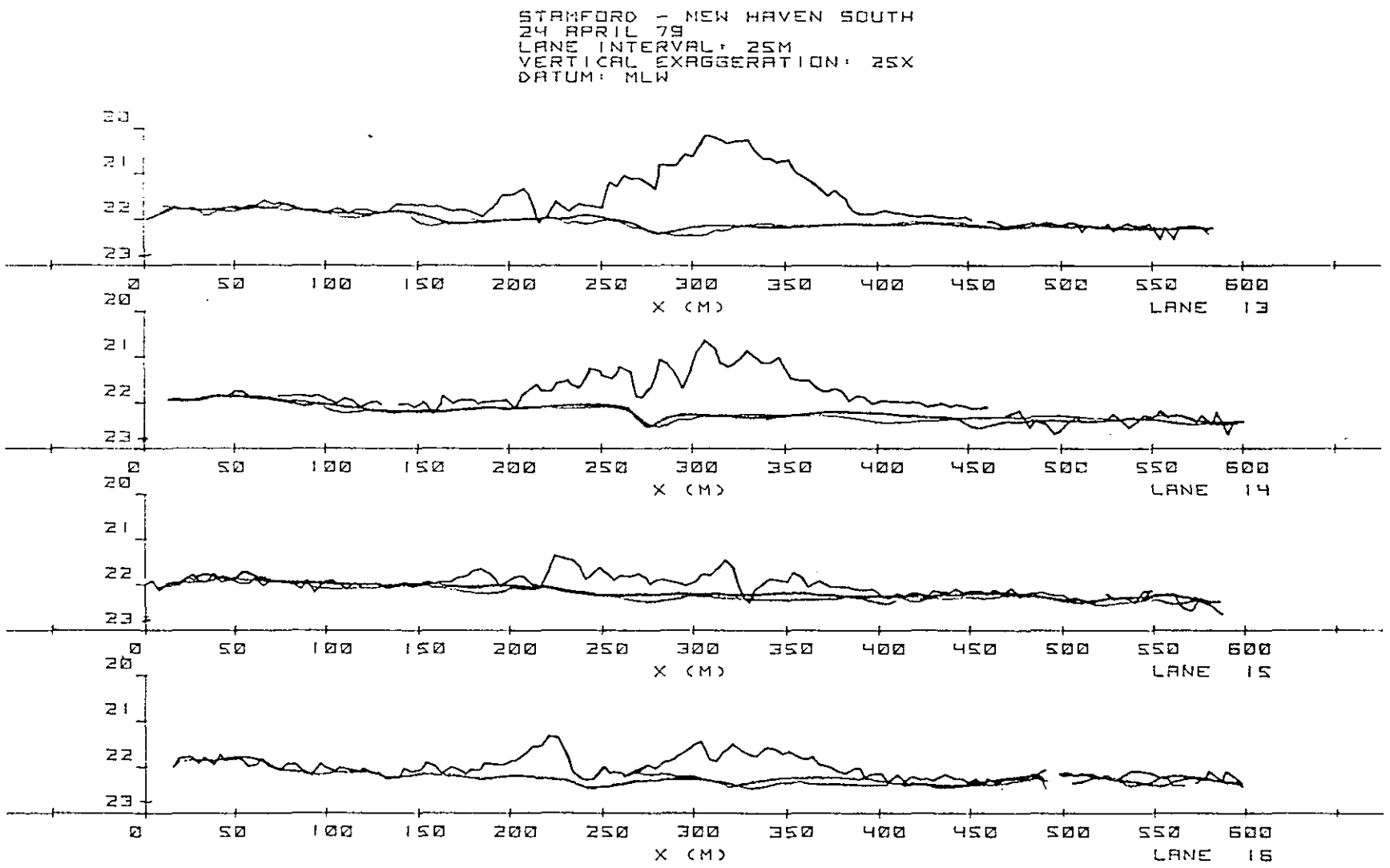
STAMFORD - NEW HAVEN SOUTH
24 APRIL 79
LANE INTERVAL: 25M
VERTICAL EXAGGERATION: 25X
DATUM: MLW
20
21
22
23
0 50 100 150 200 250 300 350 400 450 500 550 600
X (M)
LANE 13
LANE 14
LANE 15
LANE 16

Figure 2-10

The volume of Stamford spoils deposited at the site was calculated by subtracting the January and March survey depths from the April data. The changes in volume by lane and integrated over the entire survey area are presented in Figure 2.11. The resulting figure of 34250 m^3 accounts for 90% of the 38000 m^3 that were dumped at the site according to Corps of Engineers records. The contour difference chart (Fig. 2.12) emphasizes the compactness of the spoil mound and also shows the spread of fine material in a circular pattern around the disposal point.

This high percentage of material concentrated in a mound at the disposal point was not expected by many scientists because studies of earlier disposal at New Haven indicated that most of the spoils were widely spread over the flanks of the mound. The difference may result from the much tighter positioning of dumping, resulting from the taut-wire moor approach and from the cohesiveness of the spoils.

To evaluate the distribution of spoils more accurately, remote sampling of the margins of the mound was accomplished using a Smith-MacIntyre Grab Sampler at 50-meter intervals as controlled by the navigation system. Although this sampler cannot be considered the best sampler of undisturbed sediments, when used carefully, valid qualitative results can be obtained. At the Central Long Island Sount Disposal Site the natural sediment is a fine silt that generally has an oxidized layer approximately 2-5 cm thick at the surface. This layer provides an excellent horizon to distinguish between natural sediment and the black, reduced organic silt of the Stamford spoils deposited on the natural bottom.

Measurements of the spoil thickness above this layer were made in four directions beyond the limits of the spoil mound as identified on the bathymetric chart. The results of these measurements are presented in Figure 2.13. The most important finding of this study is the rapid reduction in spoil thickness over a very short distance. In all directions, the thickness of spoils changes from an entire grab of spoils (approximately 40 cm) to less than 5 cm in a distance less than 50 meters. At a 100-meter distance, the thickness is less than 1 cm. Since the precision of the bathymetric survey is on the order of 20 cm, we can certainly determine the margins of the mound

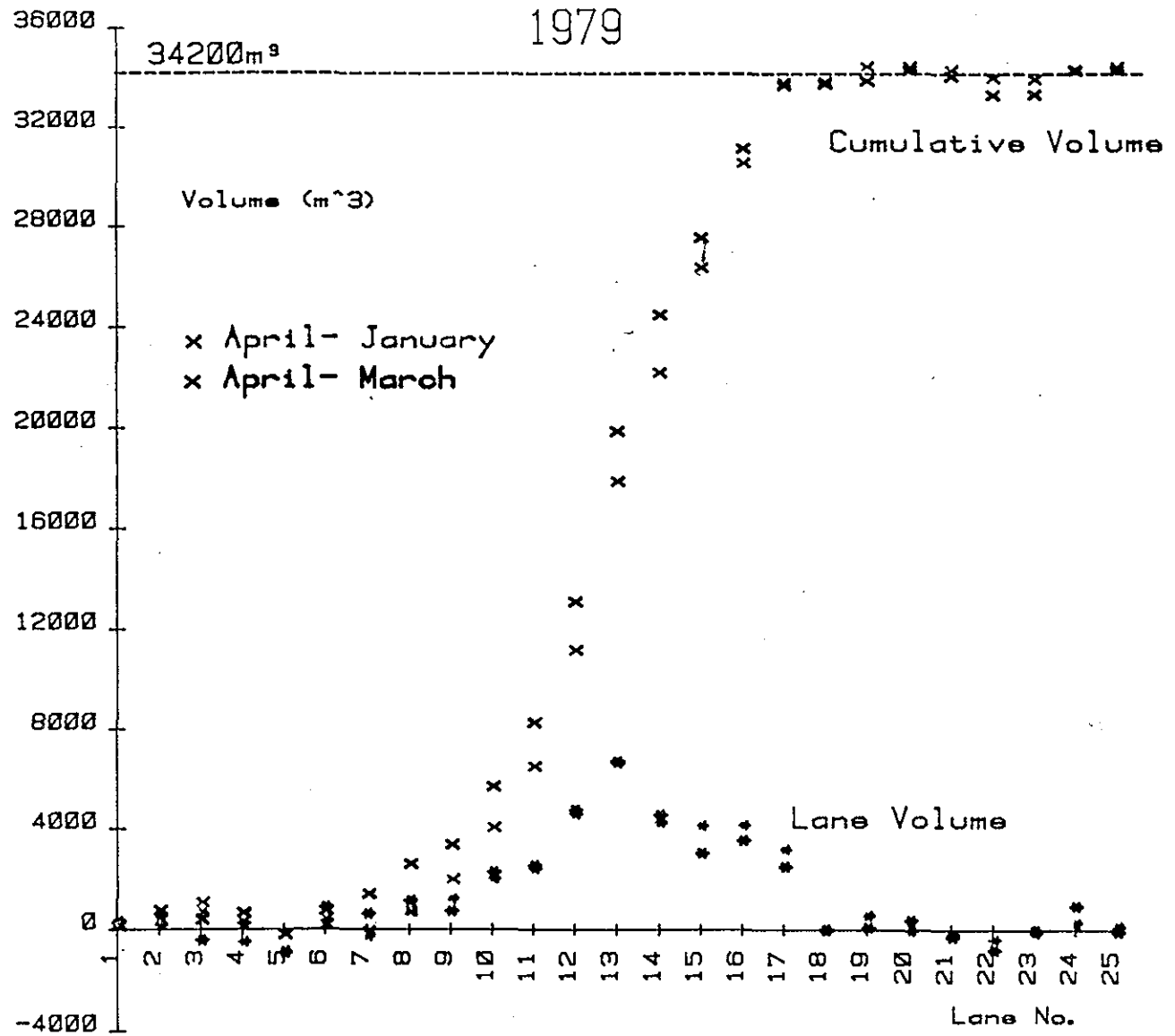
DREDGE SPOIL VOLUME
DETERMINATION
STAMFORD-NEW HAVEN DISPOSAL SITE
SOUTHERN SITE
1979
34200m³
Cumulative Volume
Volume (m^3)
× April- January
× April- March
Lane Volume
36000
32000
28000
24000
20000
16000
12000
8000
4000
0
-4000
1 2 3 4 5 6 7 8 9 10 11 12 13 14 15 16 17 18 19 20 21 22 23 24 25
Lane No.

Figure 2.11

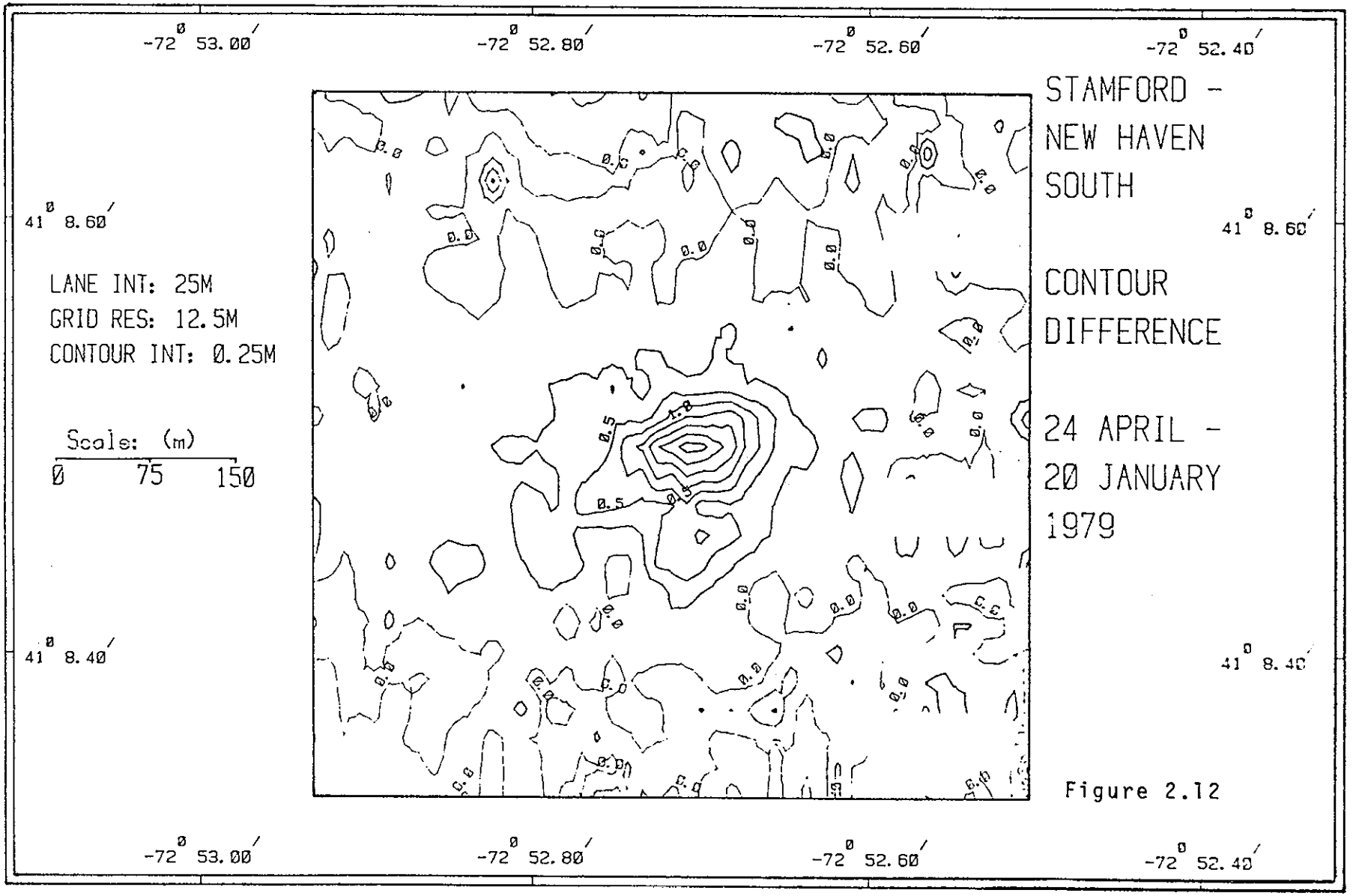
-72° 53.00′
-72° 52.80′
-72° 52.60′
-72° 52.40′
41° 8.60′
41° 8.40′
LANE INT: 25M
GRID RES: 12.5M
CONTOUR INT: 0.25M
Scale: (m)
0 75 150
STAMFORD - NEW HAVEN SOUTH
CONTOUR DIFFERENCE
24 APRIL - 20 JANUARY 1979

Figure 2.12

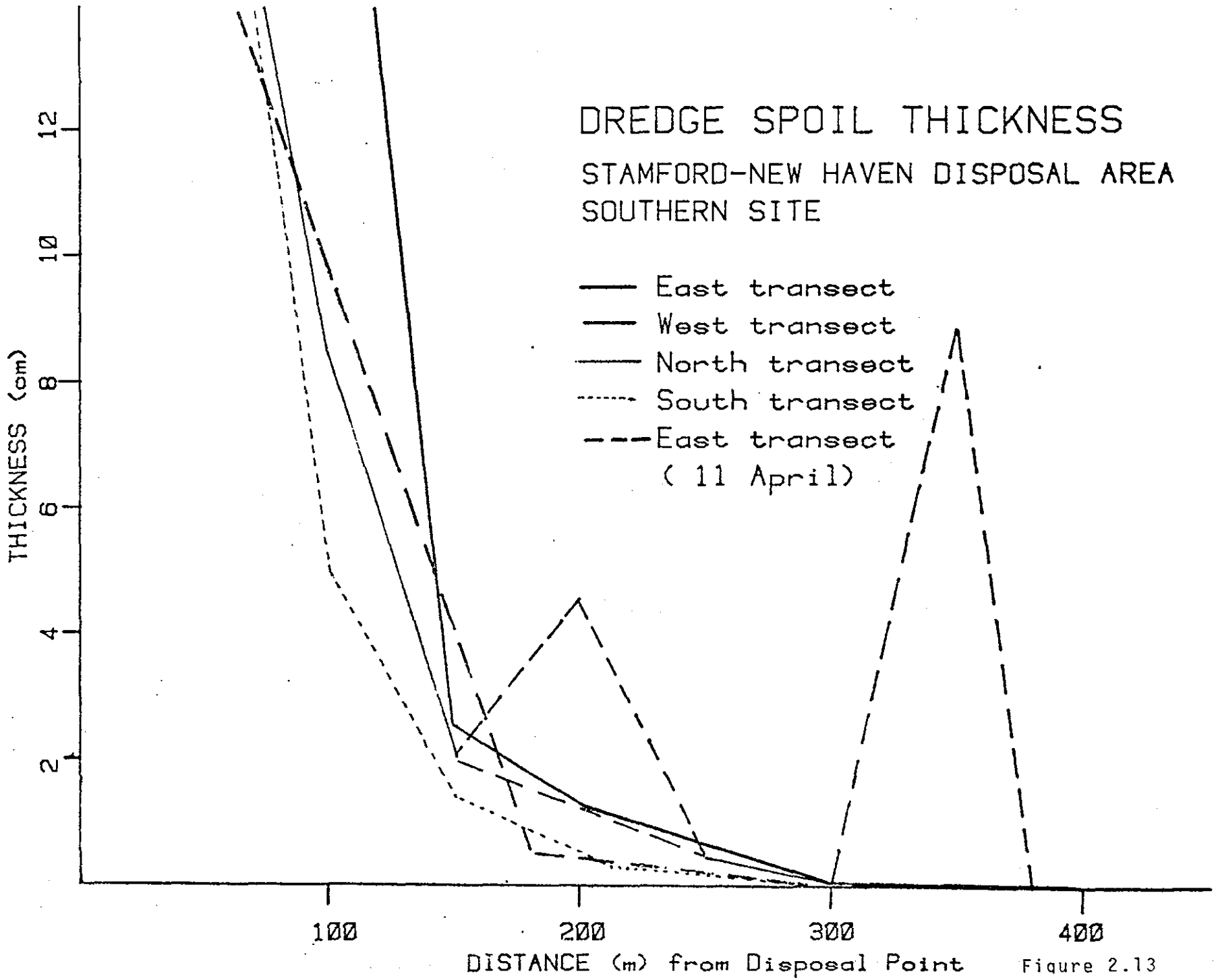
DREDGE SPOIL THICKNESS
STAMFORD-NEW HAVEN DISPOSAL AREA
SOUTHERN SITE
East transect
West transect
North transect
South transect
East transect
(11 April)
THICKNESS (cm)
2
4
6
8
10
12
100
200
300
400
DISTANCE (m) from Disposal Point

Figure 2.13

within 50 meters. The total volume of material in the flank area that could not be measured by the bathymetric technique was approximately 2,000 m^3, which is only slightly greater than the precision of the volume calculation. Adding this volume to that determined by bathymetry, we can account for 36250 m^3 or 95% of the material dumped at the site.

The bathymetric monitoring technique can also be applied at other locations to monitor disposal or to ensure stability after deposition. Although no baseline data are available prior to deposition of spoils at the New London disposal site, continued disposal can be monitored relative to existing conditions. Comparing the March 1978 survey (Fig. 2.14) which was made prior to Phase II dredging of the Thames River, with the August 1978 survey (Fig. 2.15), which was made after completion of the disposal operation, it is possible to determine the volume deposited during that time. Because of the size of the disposal mound and the large volume of material being handled, a 50-meter lane spacing was used at this site with a resulting loss of precision.

The volume difference calculation for this period is presented in Fig. 2.16 and indicates a buildup of material in the southern portion of the disposal area. This was in fact the case, since the disposal point was moved following Phase I dredging to keep the minimum depth of the spoil mound below wave base. The contour difference chart (Fig. 2.17) indicates the area of disposal was confined to the south and east of the initial mound. Continued monitoring of this site is planned for the future, as continued dredging of the Thames River is scheduled.

In summary, the measurement of spoil volume through repetitive precision bathymetric surveys appears to be a valid technique for management of disposal operations. Furthermore, the result of this technique applied to the Stamford-New Haven operation indicates excellent precision in the disposal of Stamford material which is necessary for capping with New Haven spoil.

New London, Conn.
March 6, 1978

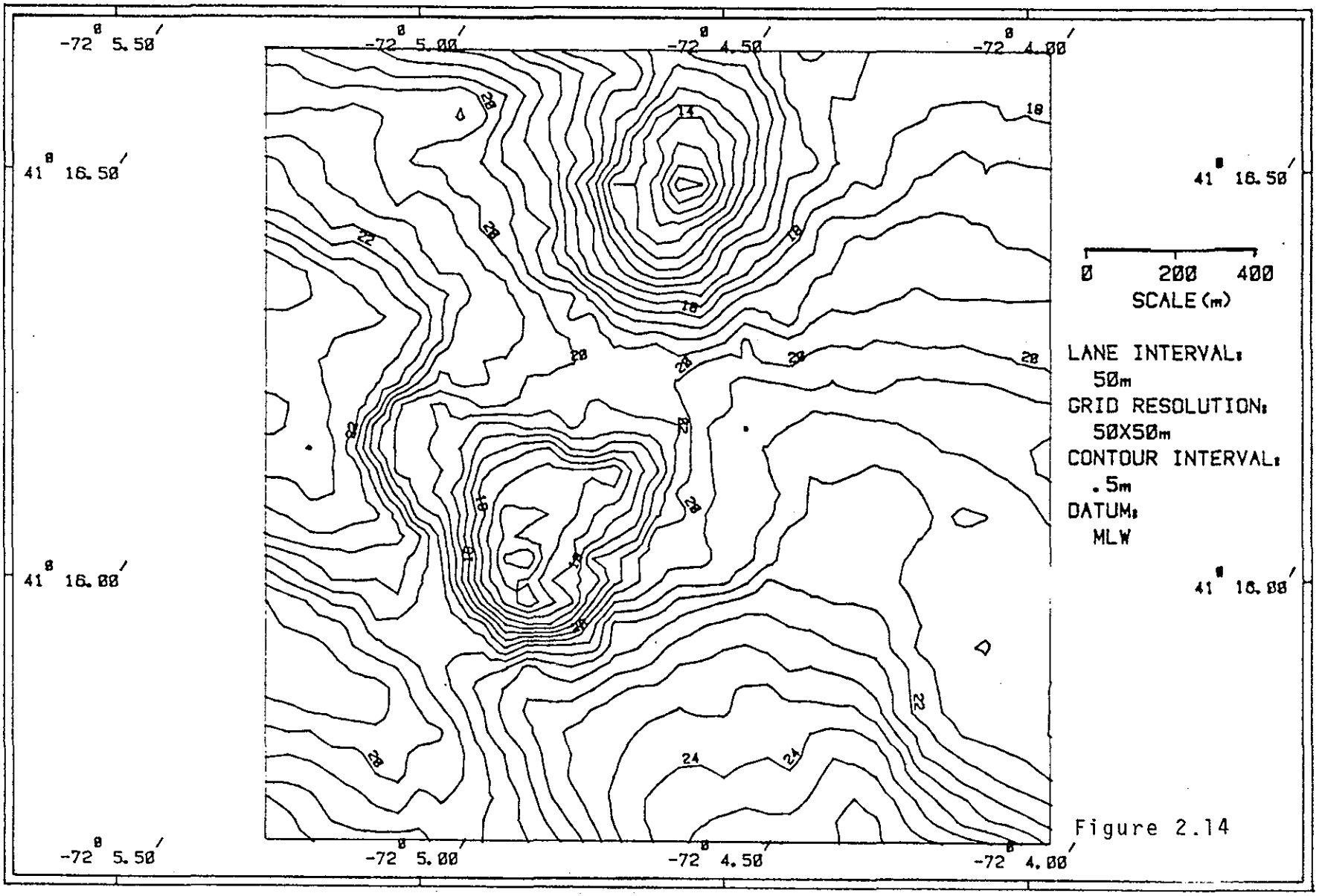

Figure 2.14

New London, Conn.
August 1, 1978

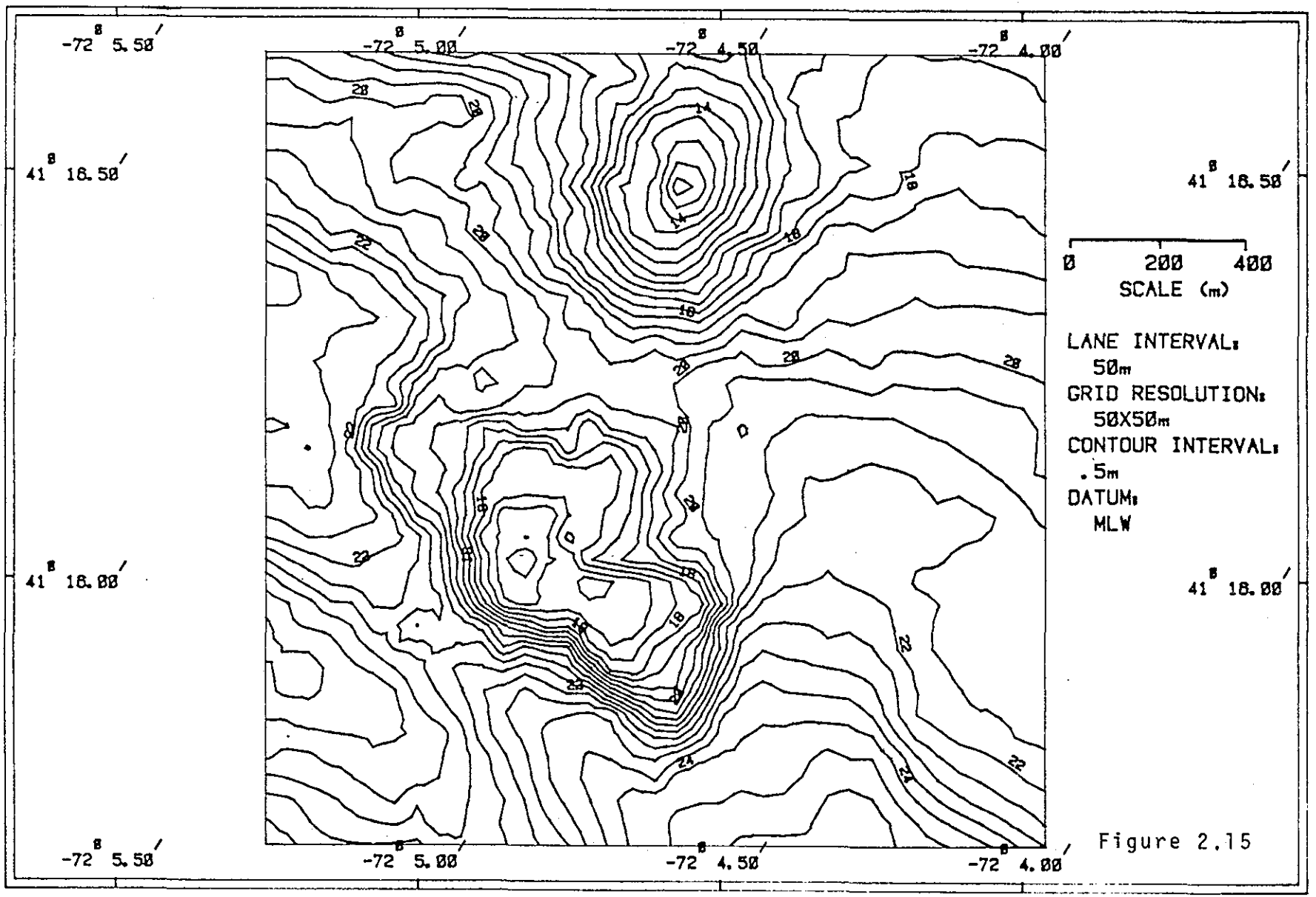

Figure 2.15

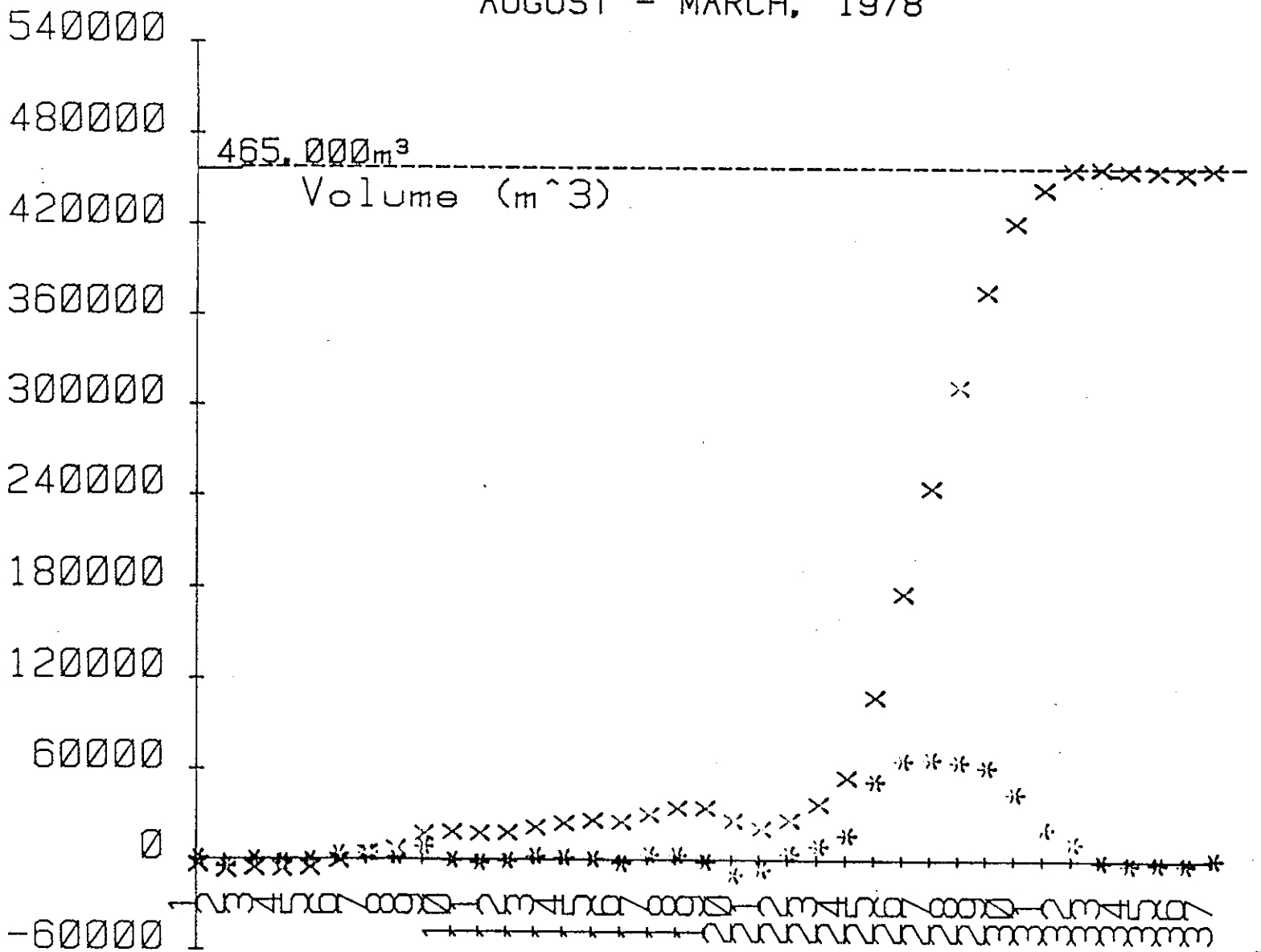
DREDGE SPOIL VOLUME
DETERMINATION
NEW LONDON DISPOSAL SITE
AUGUST - MARCH, 1978
540000
480000
465,000m³
Volume (m^3)
420000
360000
300000
240000
180000
120000
60000
0
-60000

Figure 2.16

New London Disposal Site
August-March, 1978

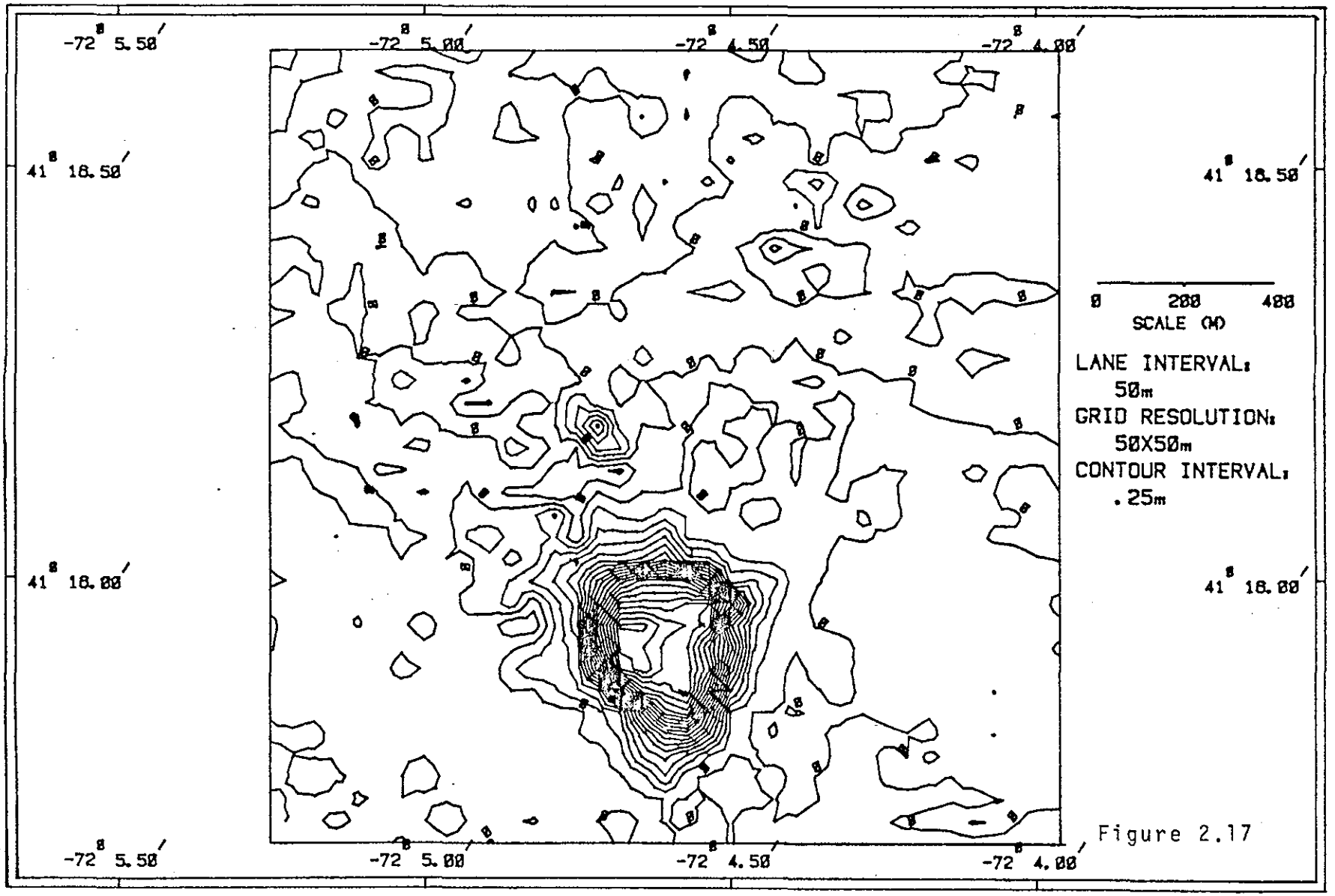

Figure 2.17

3.0

LONG TERM CURRENT MEASUREMENTS FOR THE DAMOS PROGRAM

GERALD S. COOK

3.0 LONG-TERM CURRENT MEASUREMENTS OF THE DAMOS PROGRAM

3.1 INTRODUCTION

Previous sections of this document have discussed the empirical methods used to monitor the stability of dredge spoil material using bathymetric techniques. Although these procedures can provide information on the long-term stability of existing deposits, prediction of stability at other locations requires that simultaneous measurements of the current regime be made to quantify the forces exerted on the spoils. Under the DAMOS program, this is being accomplished through the boundary layer turbulence project to evaluate stress on the spoils and through measurement of long-term currents to evaluate the current regime of the specific sites. This report presents the results of the current measurement program and is intended as a detailed overview which should provide input for decisions on disposal site management.

There are three major objectives of the current measurement program:

- To develop a long-term (seasonal) assessment of current velocity in the disposal areas.
- To provide an assessment of and classification for erosion potential of each site based on horizontal kinetic energy.
- To monitor current velocity during major storm conditions.

At the inception of the current measurement program, it was intended that current measurements be made continuously at each site for at least one complete year. The data actually obtained, however, were somewhat sporadic because of instrumentation difficulties both in the current meters and acoustic releasers. Nevertheless, sufficient data were obtained to permit an initial ranking of sites based on energy regimes. Additionally, continuous data will provide a means of determining the seasonal variability at each site in terms of the horizontal kinetic energy. Furthermore, specific storm events have been observed and their intensity relative to ambient conditions evaluated.

The disposal sites studied under the DAMOS program are shown in Fig. 1.1. The original program plan specified that one current meter would be installed at each disposal site, however, these specifications have since been modified so that meters are placed only at "priority" sites that are active or that may be active in the near future. No current meters were installed at the Rockland, Isle of Shoals, or Boston Lightship disposal sites. All other sites have had current measurements at least during part of the year.

3.1 INSTRUMENTATION

A relatively lightweight current meter mooring was developed for this program, as shown in Fig. 3.1. The mooring consists of a 43-cm diameter glass sphere attached by plastic-coated wire to an anchor via an acoustic release containing a rope cannister. The anchor is made of lead and is epoxy coated. It weighs approximately 100 kg. The current meter is attached to the plastic-coated wire approximately 1.5 m above the anchor. No surface marker is used with the mooring, since experience has shown that surface markers do not survive long in this coastal region.

The current meters used in the DAMOS program are ENDECO Type 174, ducted, impeller meters. Speed and direction data obtained by these meters are recorded internally on magnetic tape at a 5-minute sampling interval. The meters are neutrally buoyant and are attached to the taut wire via a flexible (rope) tether which is free to rotate about the vertical mooring wire. In general, these current meters have functioned well, but in a number of instances the directional information was partially or totally lost. In one verified instance, the current meter tether was tangled in the mooring wire so that directional information was lost and speed information was of questionable reliability. In another instance, direction was lost for the first few days of record, which was probably due to improper ballasting of the meter. (The ENDECO Type 174 has an internal leveling mechanism that is activated every 24 hours and that will eventually balance the current meter in a horizontal attitude). Another problem was improper magnetic tape alignment with the tape head in the Type 174 data reader, which resulted in sporadically high current values. However, these were salvaged after some adjustment by ENDECO. The specifications of the ENDECO Type 174 current meter are shown in Table 3.1.

DAMOS CURRENT METER MOORING

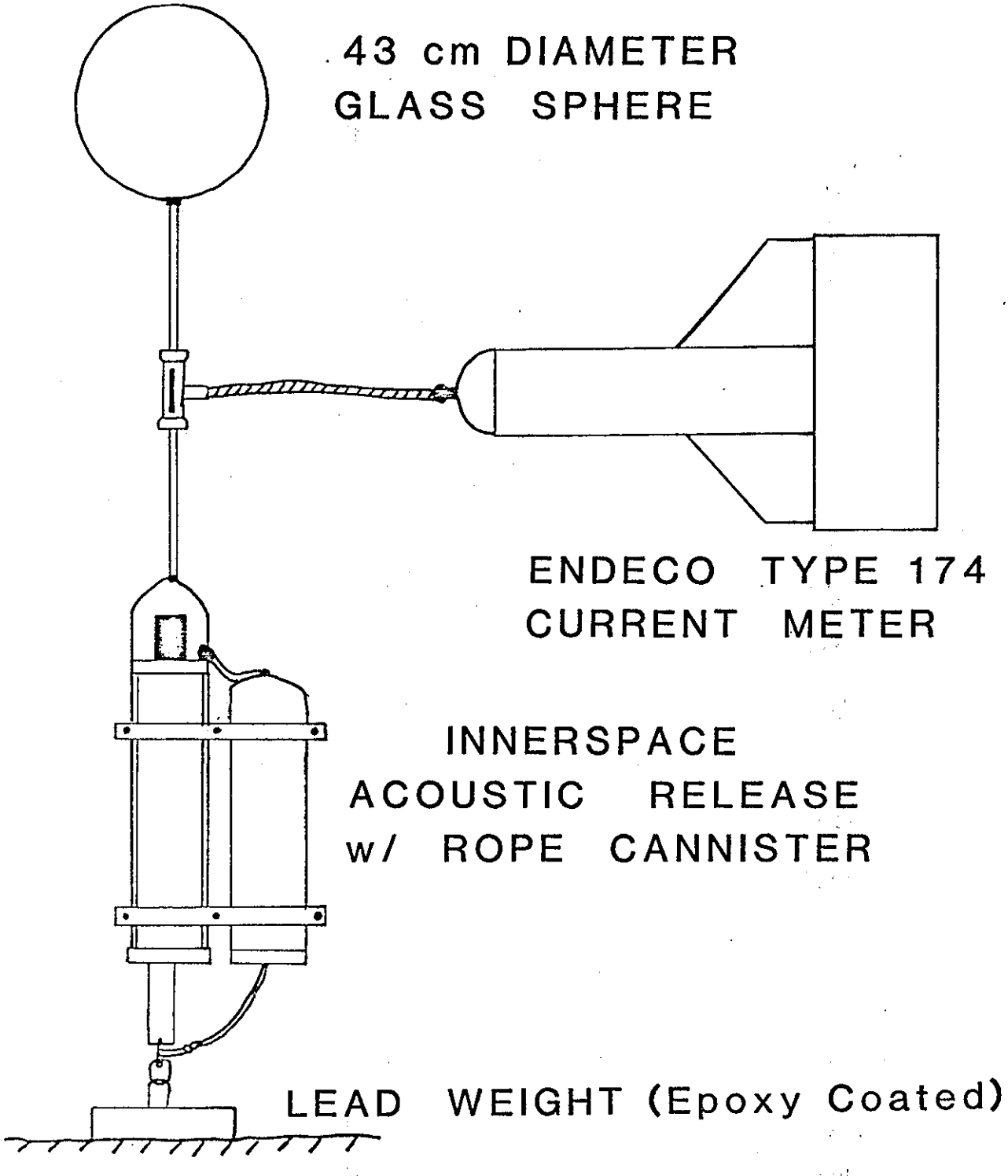

FIG. 3.1

Table 3.1 ENDECO TYPE 174 CURRENT METER SPECIFICATIONS

Speed range	0-68 cm/sec
	0-137 cm/sec
	0-274 cm/sec
Threshold	2.6 cm/sec
Resolution	0.4% full scale
Accuracy	± 3% full scale
Direction	0-360°
Resolution	± 1.4°
Accuracy	± 2% above 2.6 cm/sec ref calib.
Recording rate	1 sample/2,4,8 minutes
No. of samples	33K of speed & direction
Record period	40 days
	75 days
	110 days
Power	1.5V "D" Cells
Recording medium	8-track--90-min tape cartridge
Recording head	4-track

The Innerspace Technology Model 431 acoustic releases, used to moor the current meters and cages were originally specified to eliminate loss due to surface buoys. However, releaser problems required many hours at sea searching for and recovering moorings, using either divers or grapnel hooks. Cathodic corrosion, due to dissimilar metals on the mechanical release mechanism, prevented tripping in most instances, although the electronic-acoustic components of the releases functioned in all instances. Severe corrosion occurred at all sites, resulting in extremely high friction on the release bale, so that the 25 -30 kg of positive buoyancy exerted by the mooring configuration were insufficient to operate the mechanism, even though the release plunger had retracted. DAMOS personnel have worked closely with Innerspace Technology, to develop a modified release mechanism using sacrificial anodes to reduce corrosion and springs to ensure mechanical operation. The first of these modified units was installed in September 1978. The specifications for the acoustic releases are presented in Table 3.2.

In general, biological fouling of the current meters was not a severe problem except in Long Island Sound during the summer. The current meters were ordered without anti-fouling paint so there would be no source of heavy metals, however small. This precaution was taken to ensure that we did not contaminate the experimental mussels which were moored near the current meters. However, to limit the degradation of data by fouling, the meters have since been painted. It was generally agreed that the leaching of heavy metals from the anti-fouling paint would not have a significant effect on the mussels if the cages were positioned far (100 m) from the current meters. All other significant components of the mooring system were painted with epoxy paint to reduce exposure of metal to the water column.

3.2 DATA ANALYSIS

Current velocity data consist of speed and direction values averaged over 2-minute intervals (changed to 5 minutes after May-June 1979). These data are read from the magnetic tape by an ENDECO Type 273 data transmitter and analyzed using a Hewlett Packard 9825A computer and 9872A digital plotter. The analysis routine is shown in Figure 3.2.

Table 3.2 SPECIFICATIONS FOR SHIPBOARD CODE GENERATOR AND ACOUSTIC RELEASE

SHIPBOARD CODE GENERATOR

Transmit frequency	22 kHz
Output level	+ 80db ref 1 __ @ 1 yd
Transmit time	20 sec
Modulation	FM
Deviation	± I kHz
Low-frequency tone	150-175 Hz
Low-frequency tone group	697-941 Hz
Power supply	rechargeable

ACOUSTIC RELEASE

Receiver frequency	22 kHz
Receiver bandwidth	2 kHz
Low-frequency tone	150-175 Hz
High-frequency tone group	1209-1633 Hz
Low-frequency tone group	697-941 Hz
Decode time	2 sec
Battery life	3 mo & 10 releases
Depth capability	330 m
Load capability	200 kg
Weight in air	6 kg
Weight in water	25 kg
Size	63 cm high, 14 cm diameter

CURRENT VELOCITY DATA ANALYSIS

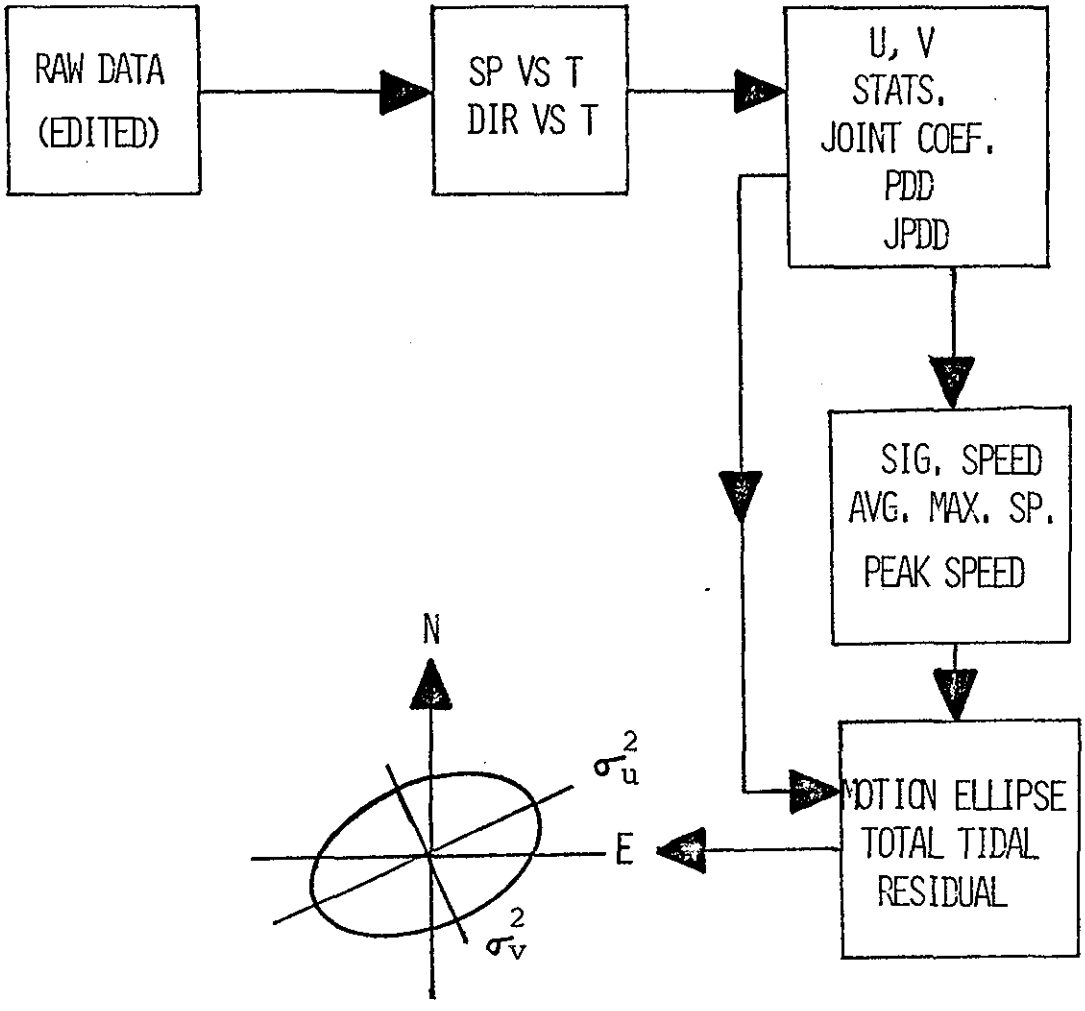

FIGURE 3.2

After the data have been edited, plots of speed and direction as functions of time are generated. Simultaneously, the speed and direction are resolved into (u,v) components (u = true East, v = true North) and the arithmetic averages, variances and covariance for the (u,v) components are calculated along with the correlation coefficients required for subsequent tidal analysis. Finally, probability density distributions are calculated for velocity vectors and for speed.

The variances and covariance for the (u,v) components (having their mean values removed) are used to define a rotated coordinate system. In the new coordinate system, the covariance is equal to zero and the standard deviations for the u and v directions are the semimajor and semiminor axes of a motion ellipse. This motion ellipse graphically represents the total fluctuating energy contained in the record. The horizontal kinetic energy is calculated as the sum of the variances for the velocity components in either the (u',v') or (u,v) directions. (The sum of the diagonal elements of the variance/covariance matrix is invariant under rotation of coordinates.) The bearing of the semimajor axis of the ellipse represents the predominant direction of the fluctuating velocity, and the length of the semiminor axis indicates the degree to which the motion is rectilinear or omnidirectional. Also calculated during analysis is the mean velocity which is plotted as a straight line segment terminated with an asterisk (*).

These motion ellipses provide an excellent technique for evaluating and comparing current records, since a separate ellipse can be generated to depict (a) the total observed motion, (b) the tidal component, and (c) residual (tides removed) motion. Each motion ellipse can be defined by its semimajor axis, its semiminor axis, and the direction of the semimajor axis. The length of the semimajor axis is equal to the standard deviation (σ_u) of the velocity component (u) along the direction of maximum energy, which is measured in degrees clockwise from north. The length of the semiminor axis is equal to the standard deviation (σ_v) of the velocity component (v) perpendicular to the direction of maximum energy.

An additional parameter of the current regime is the horizontal kinetic energy of the mean flow. It represents the energy of motion in the horizontal plane. This is expressed as $\frac{1}{2} \rho (u^2 + v^2)$, where ρ is the density of water. Since sites with lower horizontal kinetic energy would tend to be better containment locations, we use comparisons of horizontal kinetic energy to evaluate site suitability.

To evaluate the effect of tidal currents on the energy regime of each site, a tidal matrix is calculated consisting of correlations between the various pairs of sine and cosine functions for the five tidal components of interest (M_2,S_2,K_2,O_1,N_2) as well as the steady-state (zero-frequency) components. From this generated matrix we extract 11 amplitude coefficients which are used in calculating the variance and covariance of the tidal (u,v) components. Finally, a composite tidal ellipse is calculated by a coordinate rotation (similar to the one done for the total fluctuating motion) to bring the covariance to zero. Again, the semimajor and semiminor axes are equal to the standard deviations for the (u,v) components; the direction, however, represents the direction of ebb/flood, and the length of the semiminor axis indicates the degree of rectilinear or rotary tidal motion. The horizontal kinetic energy for the tide alone is calculated using the standard deviation (σ_u,σ_v) of the tidal components.

The tidal ellipse and the horizontal kinetic energy of the mean flow are indications of the normal current regime existing at a disposal site. The most significant factors affecting the containment or dispersal of spoil material, however, are the higher speeds associated with that regime. To examine these higher speeds the residual current is determined by subtracting the tide computed by least squares analysis from the observed data. Since the tide is statistically independent of the residual time series, the variance and covariance for the residual time series can be calculated from the difference between the corresponding values for the total time series and the tidal functions. These values indicate the extent to which the total motion is composed of tidal flow or other, essentially random motion. The horizontal kinetic energy of the residual motion quantifies the importance of random events. A motion ellipse for the residual current can then be determined that would generally have only small differences between the semimajor and semiminor axes if the motion is truly random.

Further analysis of extreme velocities encountered in the current data, oriented toward evaluating potential spoil movement, can be accomplished through definition of three quantities:

1. Significant speed.

   A quantity defined as the 10 percent highest speed or significant speed is calculated to characterize the maximum velocities. This speed is the arithmetic average, calculated from the probability density distribution of the highest 10 percent (or as close to 10 percent as allowed by the pdd) of the measured speeds. Although these values do not consider direction, virtually all of the components are along the direction of maximum motion.

2. Peak tidal velocity.

   The peak tidal speed is the maximum speed of tidal currents based on the computed tidal coefficients. The maximum would occur when all (five) time-varying components are simultaneously in phase. A more realistic "peak" could be calculated using the two dominant components (M_2 and N_2) only. These are in phase approximately every 27 days. The difference, however, between using five components and using two components, is small because the contributions from the remaining components are small for all locations analyzed.

3. Average maximum velocity.

   The average maximum speed represents typical maximum tidal speeds occurring on each flood or ebb. It is defined as the amplitude of a hypothetical sinusoidal tide having the same kinetic energy as the actual tide. Note that for all tidal calculations, the mean current is treated as a component.

The current velocity time series are also inspected for singular events, usually storm and wind generated anomalies that may significantly increase the stress exerted by the fluid motion on the spoils. These events are correlated with climatological wind data obtained for specific sites from the National Climatic Center in Asheville, North Carolina. The purpose of this effort is to provide a qualitative estimate of the effects of anomalous events on the bottom currents. When the Boundary Layer Turbulence (BOLT) system is employed under these circumstances, more quantitative information on bottom stress can be obtained.

3.3 RESULTS

Figure 3.3 summarizes the distribution of current measurements at the DAMOS sites during 1978. The dark bars indicate those data that have been analyzed thus far; the open bars indicate that raw data exist but have not yet been analyzed. The short vertical lines indicate a service period and replacement of current meters.

Typical segments of the current velocity records are shown in Fig. 3.4 for the Portland disposal area and Fig. 3.5 for the New Haven disposal area. In a general sense, these records are typical of the currents in the northern sites and southern sites, respectively. Note that the velocity scale on the New Haven record is twice that of the Portland data. In the Gulf of Maine, represented by the Portland data, the DAMOS sites are generally deeper and exhibit low average speeds. In Long Island Sound, represented by the New Haven data, the sites are shallower and exhibit higher speeds which are tidally driven.

The currents in Long Island Sound are clearly semidiurnal with very little randomness. On the other hand the currents in the Gulf of Maine exhibit a much higher degree of randomness but are nevertheless semidiurnal.

3.4 DISCUSSION

Total motion ellipses drawn to the same scale for six of the DAMOS sites, five in Long Island Sound and one in the Gulf of Maine, are shown in Fig. 3.6 This figure depicts the total horizontal kinetic energy at each site and the direction of maximum energy (the semimajor axis). In addition, the figure provides a visual 'integration' of the total kinetic energy (KE)of one site relative to another. Portland exhibits the lowest total horizontal kinetic energy while Cornfield Shoal and New London the exhibit the highest.

The small vector emanating from the center of the ellipses depicts the mean (non-tidal) current velocity over the period of the observations. The length of the vector and the lengths of semimajor and semiminor axes are scaled to the 10 cm/sec bar shown on the figure. Direction in degrees true is measured clockwise from north, which is the top of the figure.

DAMOS CURRENT MEASUREMENTS - 1978

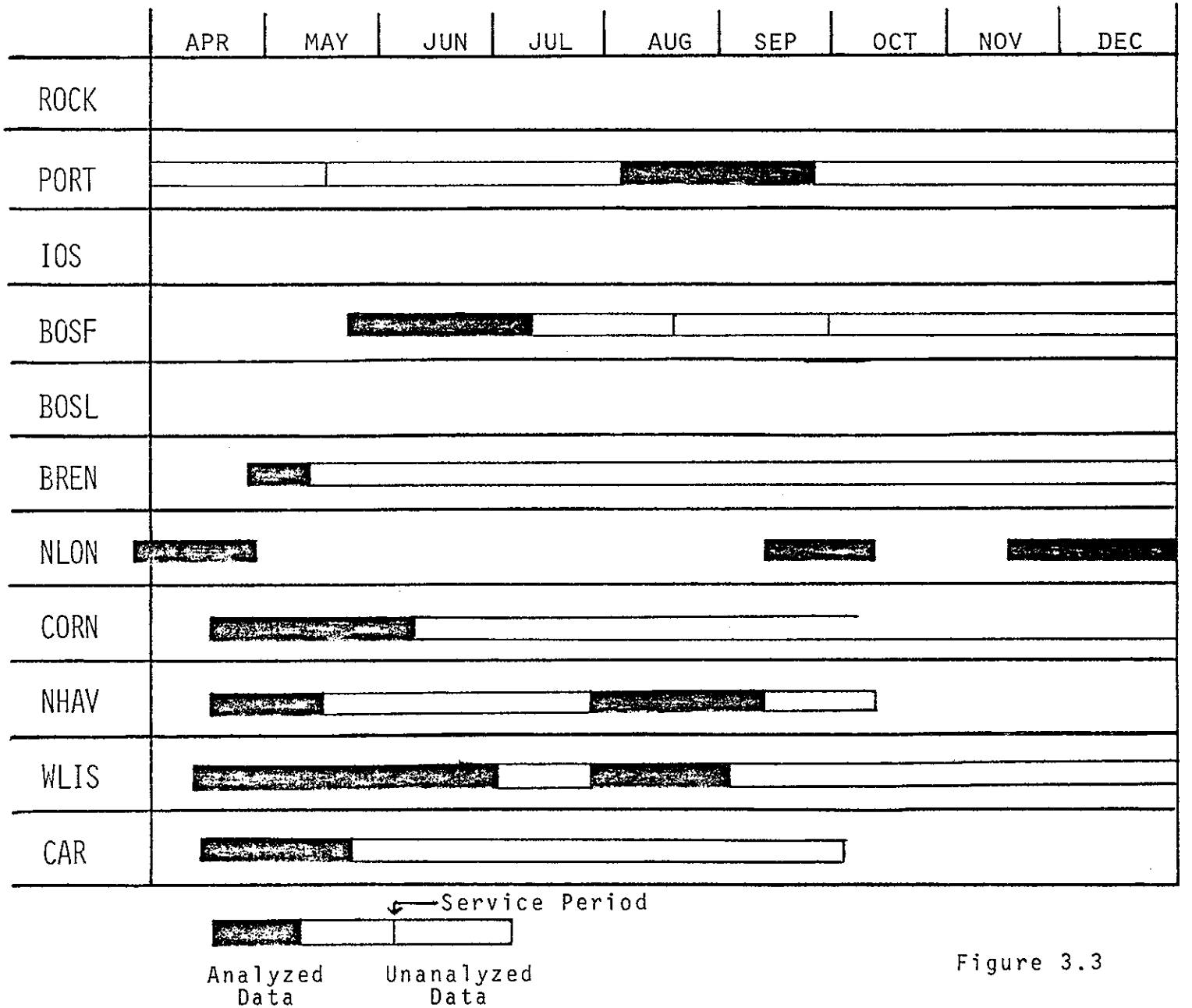

Figure 3.3

PORTLAND DISPOSAL SITE
CURRENT DATA

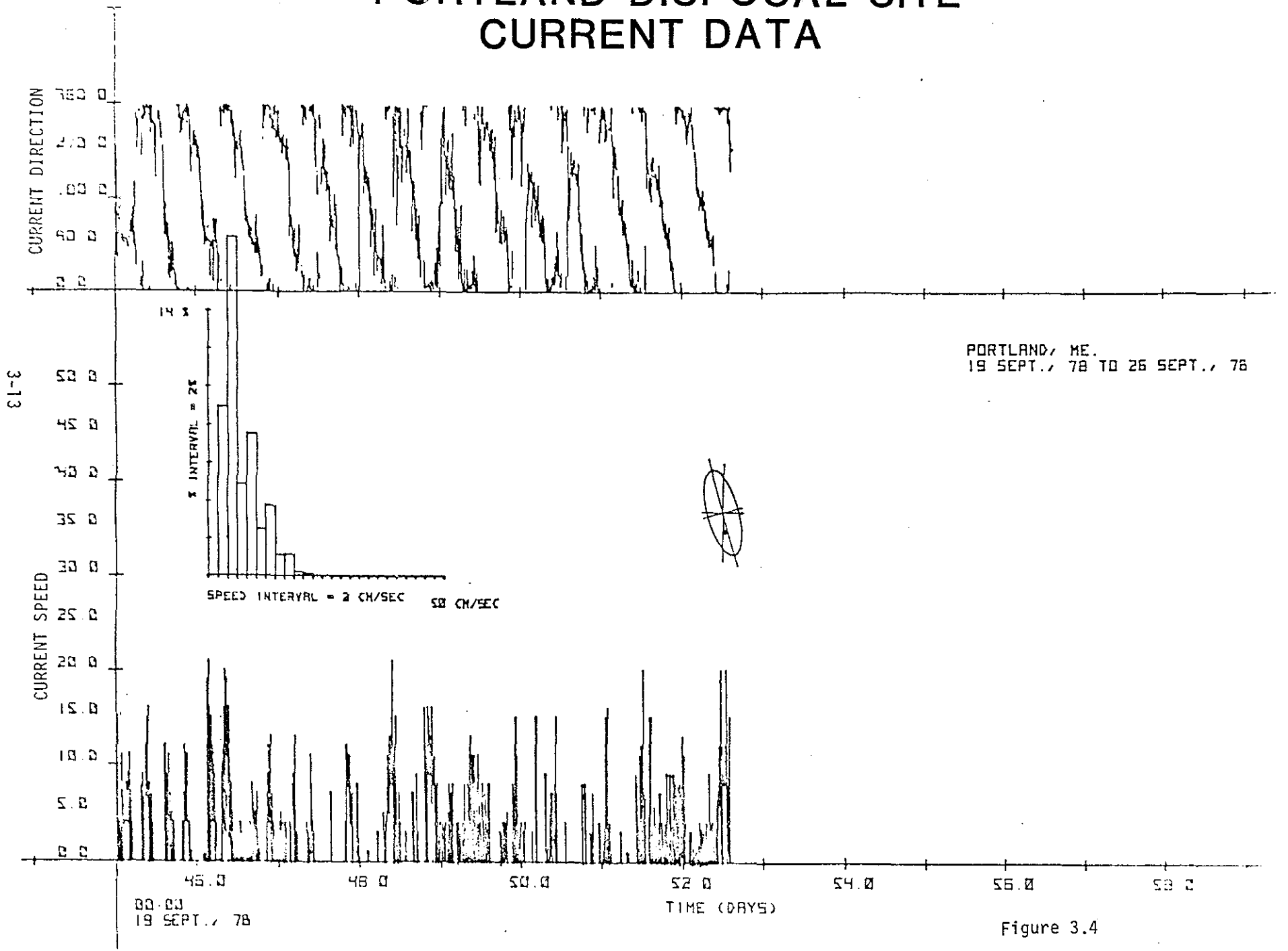

Figure 3.4

CENTRAL LONG ISLAND SOUND DISPOSAL SITE
CURRENT DATA

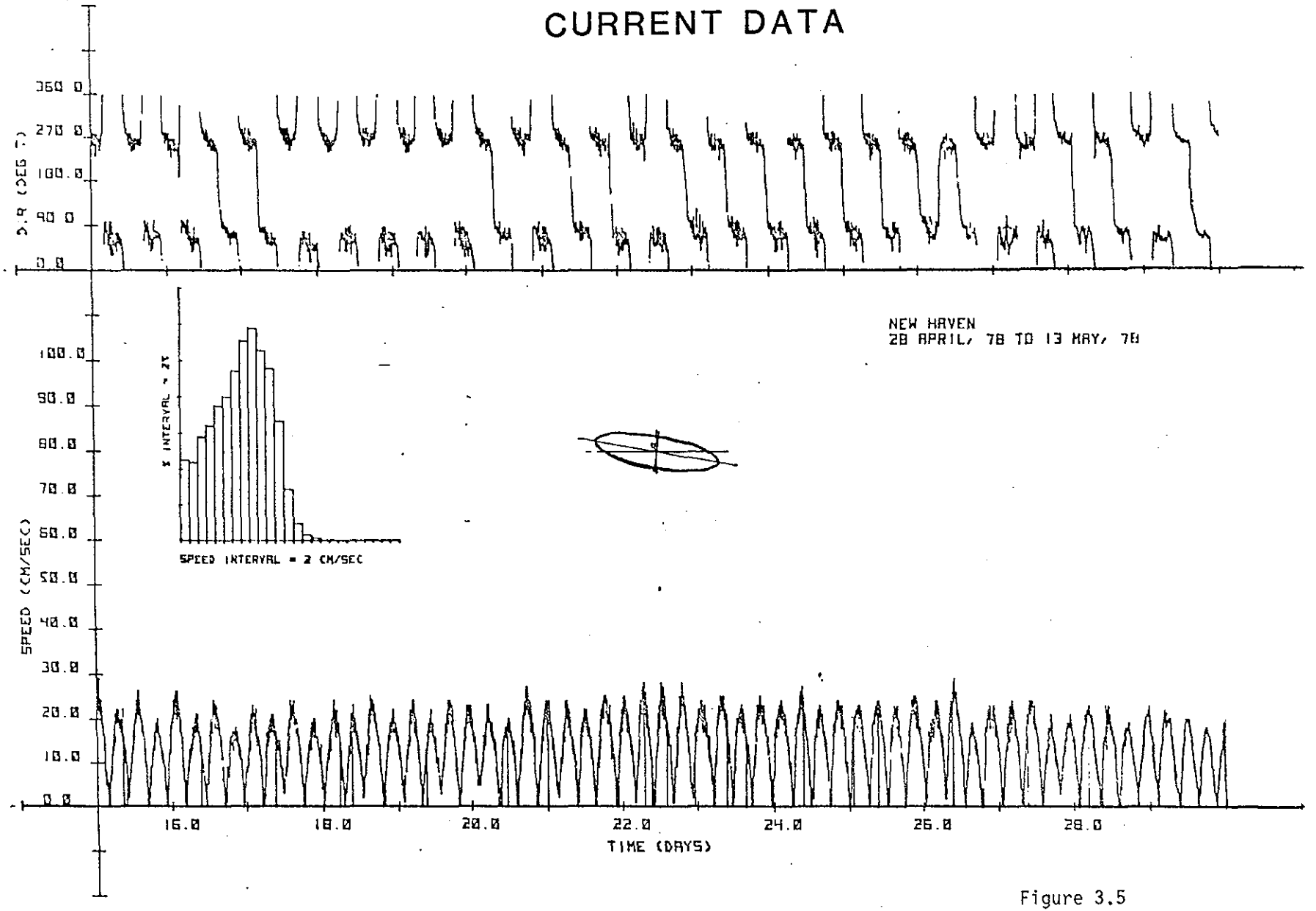

Figure 3.5

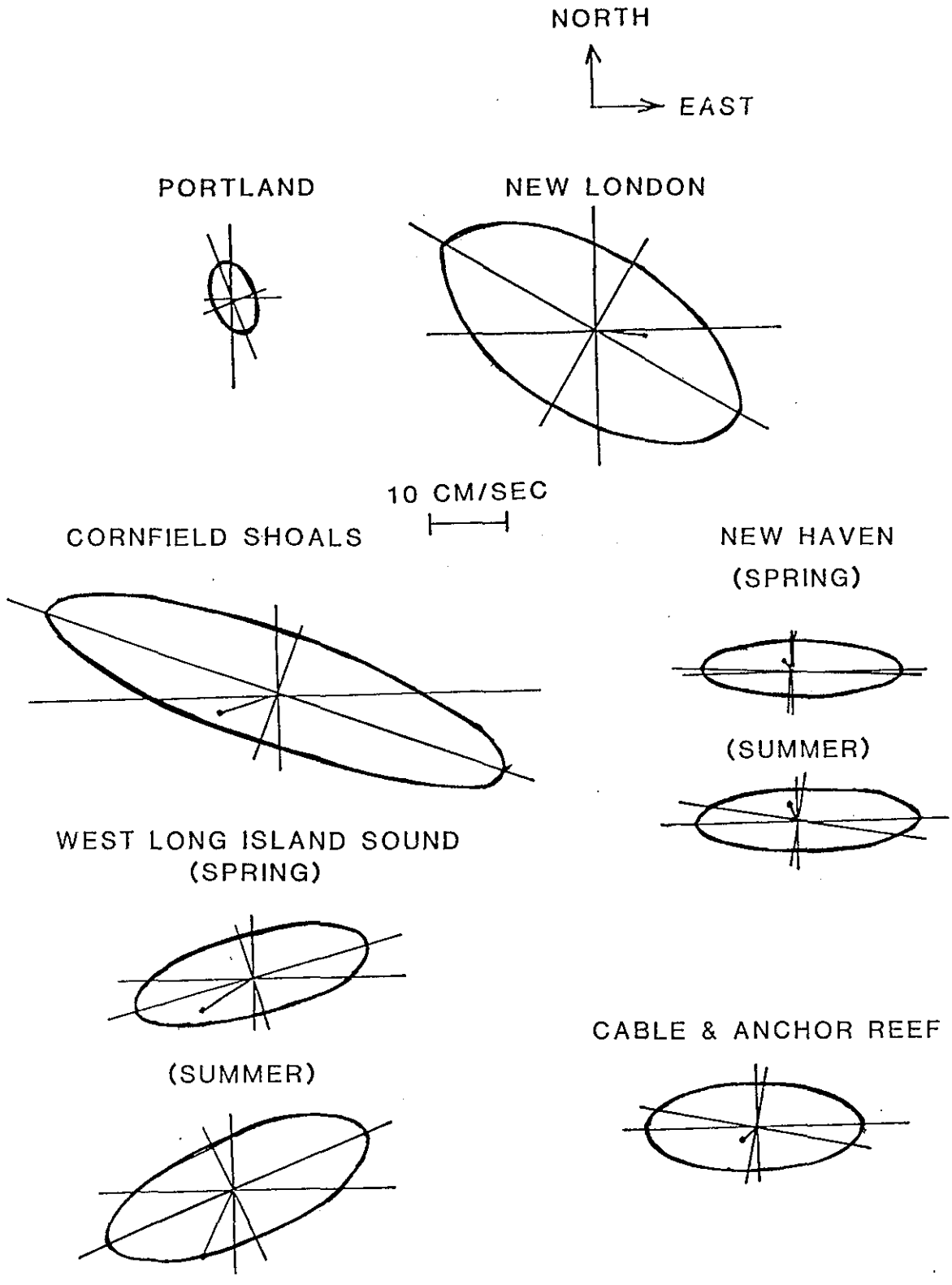

TOTAL MOTION ELLIPSES FOR DAMOS DISPOSAL SITES

Figure 3.6

The distribution of horizontal kinetic energy among frequency components is shown in Table 3.3. The total horizontal KE is partitioned into tidal, residual, and mean components as described above. The most energetic site is Cornfield Shoals and the next most energetic site is New London. However, a large portion of the Cornfield energy is contained in the residual component and may be instrument error. The least energetic site is Portland.

Sites in Long Island Sound derive most of their kinetic energy from the tide. Western Long Island Sound has a high percentage of the total kinetic energy in the mean. This is probably associated with the somewhat constricted nature of this area of Long Island Sound relative to central Long Island Sound.

The Portland site has more kinetic energy in the residual or random component than in the tide. With the exception of western Long Island Sound and Portland, the KE contribution from the mean is less than ten percent. Additional data at the Portland and Boston Foul Ground sites will provide more definition on the energy partition in nonrestricted areas.

Table 3.4 summarizes the results of the elevated speed analysis for the DAMOS sites. The Portland and Boston Foul Ground sites exhibit the lowest overall speeds compared to the Long Island Sound sites. The values in Table 3.4 provide upper limit statistics on current speeds that are encountered at these sites. The significant speeds are the overall maximum values that were actually measured. The peak speed and average maximum speeds are the maximum currents associated with spring tide and maximum currents during individual flood and ebb tides. The analysis summarized in this table does not account for anomalous events such as storm surges or elevated bottom stresses due to meteorological forcing.

Correlation between atmospheric storm conditions and current velocity near the bottom has been observed both in Long Island Sound and at Portland. The contribution of such a forcing function to an increased bottom stress is real but has not been measured in these experiments. It is anticipated that stress measurements made during storm periods by the BOLT system will be correlated with current data at several sites during the coming year.

PARTITION OF TOTAL HORIZONTAL KINETIC ENERGY.

	TOTAL		TIDAL		RESIDUAL		MEAN	
	(DYNES/CM^2)	%	(DYNES/CM^2)	%	(DYNES/CM^2)	%	(DYNES/CM^2)	%
PORTLAND	13	100	5	40	6	48	2	12
NEW LONDON	333	100	244	73	70	21	19	6
CORNFIELD SHOALS[1]	596	100	225	38	336	56		6
NEW HAVEN	126	100	107	85	18	14	2	1
WEST LONG ISLAND SOUND	184	100	126	68	16	9	42	23
CABLE & ANCHOR REEF	135	100	105	78	28	21	2	1

1 QUESTIONABLE DATA.

TABLE 3.3

TABLE 3.4 RANK BY ELEVATED VELOCITIES

SIGNIFICANT SPEED	PEAK SPEED	AVERAGE SPEED
NEW LONDON	CORNFIELD SHOALS	NEW LONDON
WEST LONG ISLAND SOUND	NEW LONDON	CORNFIELD SHOALS
CABLE & ANCHOR REEF	NEW HAVEN	WEST LONG ISLAND SOUND
NEW HAVEN	CABLE & ANCHOR REEF	NEW HAVEN
BRENTON REEF [1]	WEST LONG ISLAND SOUND	CABLE & ANCHOR REEF
BOSTON FOUL GROUND [1]	PORTLAND	PORTLAND
PORTLAND		

1 QUESTIONABLE DATA.

An example of such a correlation is shown in Fig. 3.7 The wind speed increased from 5 to 10 mph to a peak of 30 mph, gradually decreasing over the next 2.5 days to less than 10 mph. Wind direction was northeasterly during this period. Bottom currents responded strongly to the increased wind speed. The flood tidal currents were strongly reinforced by the wind, and the subsequent ebb current was strongly suppressed. The effect is also noted in the current direction trace. A relaxation oscillation is also noted in the current speed record following Day 32.

The bottom stress associated with such phenomena cannot be determined in this manner. Only a system such as the BOLT can adequately measure the stresses involved. In a relative sense, however, a doubling of the current speed such as observed here could result in a fourfold increase in stress.

The possibility of defining accurately the containment potential of disposal sites by current data in the near future appears to be extremely high.

3.5 CONCLUSIONS

The current measurement program is an effective management tool for classification of disposal areas and will continue to be in the foreseeable future. A relative lack of data for the Gulf of Maine DAMOS sites should be corrected. At the present time, there is a backlog of data to be analyzed which will provide additional data for those sites.

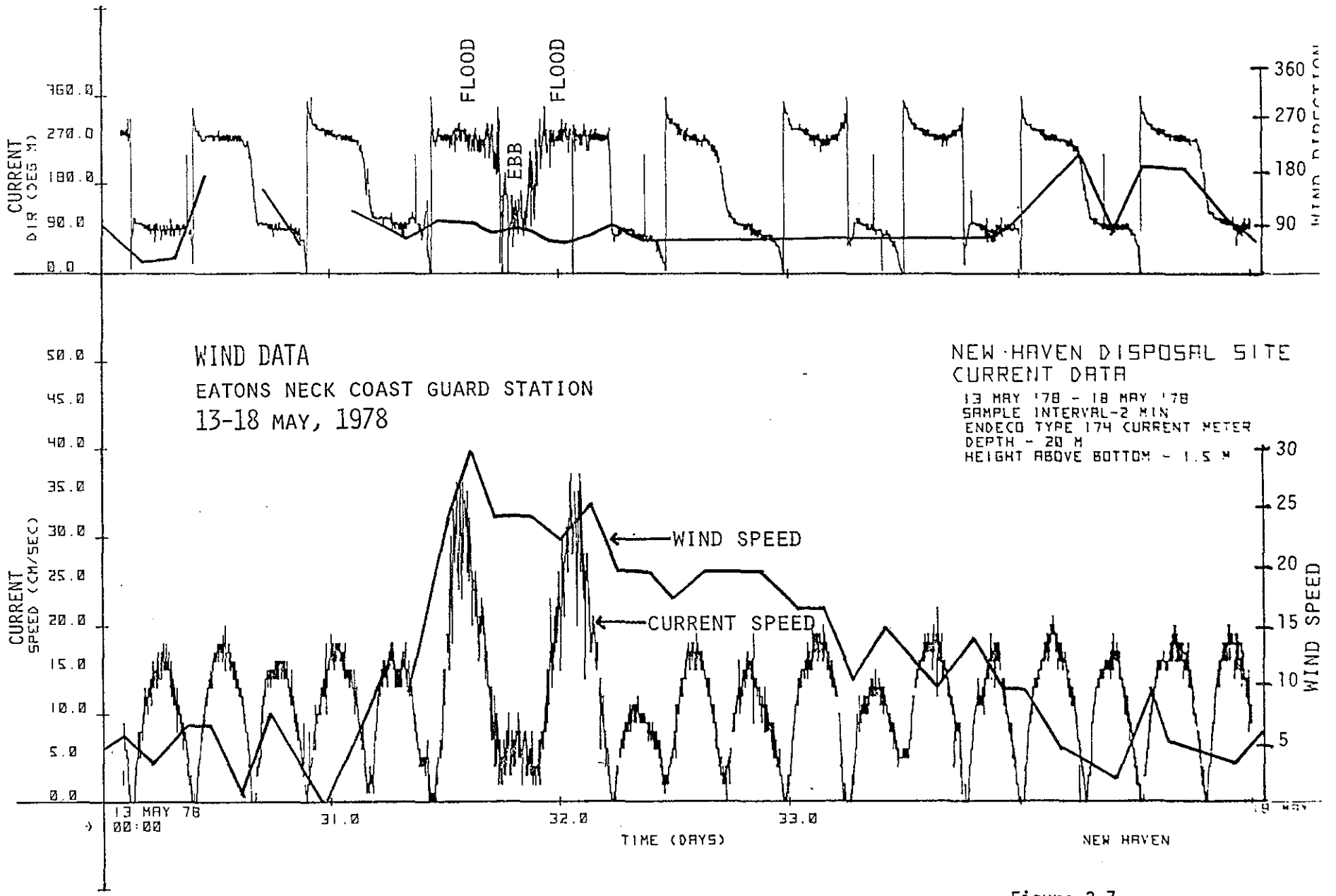
FLOOD
EBB
FLOOD
CURRENT DIR (DEG M)
360.0
270.0
180.0
90.0
0.0
360
270
180
90
WIND DIRECTION
WIND DATA
EATONS NECK COAST GUARD STATION
13-18 MAY, 1978
NEW HAVEN DISPOSAL SITE
CURRENT DATA
13 MAY '78 - 18 MAY '78
SAMPLE INTERVAL-2 MIN
ENDECO TYPE 174 CURRENT METER
DEPTH - 20 M
HEIGHT ABOVE BOTTOM - 1.5 M
WIND SPEED
CURRENT SPEED
CURRENT SPEED (CM/SEC)
50.0
45.0
40.0
35.0
30.0
25.0
20.0
15.0
10.0
5.0
0.0
30
25
20
15
10
5
WIND SPEED
13 MAY 78
00:00
31.0
32.0
33.0
TIME (DAYS)
NEW HAVEN

Figure 3.7

4.0

BOUNDARY LAYER TURBULENCE MEASUREMENTS

JOHN P. IANNIELLO

4.0 BOUNDARY LAYER TURBULENCE MEASUREMENTS

4.1 *INTRODUCTION*

The BOLT (Boundary Layer Turbulence) measurement program is part of the larger DAMOS (Disposal Area Monitoring System) program. DAMOS is responsible for the environmental monitoring of 10 New England regional disposal sites designated for the disposal of dredge spoils. To accomplish this, DAMOS utilizes bathymetric, biological, chemical and physical oceanographic measurements. The BOLT program measures the high-frequency, small-scale fluctuations in velocity near the bottom boundary layer at various disposal sites during both normal and storm conditions. From these measurements the instantaneous shear or Reynolds stress can be calculated. The stress measurements, made above the sea bed, can then be used to infer the bottom stress by extrapolation. The bottom stress is a sensitive indicator of the rate of dredge spoil erosion, whether for a rough (as is most likely) or a smooth bed (Grant and Madsen, 1979; Ariathurai and Krone, 1976); thus, stress measurements, coupled with critical erosion data from both in-situ and laboratory tests, will help to predict if, how, and when dredge material will be eroded.

It is recognized that different erosion mechanisms predominate at different sites. For example, at the northern sites the wave action is probably the dominant erosion mechanism. However, at the southern sites in Long Island Sound, the dominant mechanism is probably tidal current. In both regions, however, storms, with their accompanying large storm waves, may be the most erosive events of all. Thus we must be able to measure and characterize both normal and storm regimes at each site. We note that to attain these goals the BOLT system must be a versatile tool capable of obtaining high quality data for both controlled and monitoring deployments.

Progress in understanding the potential eroding mechanisms requires knowledge of the current structure and stress-producing events near the bottom. This requires three-dimensional, high-frequency, small-scale current measurements. Large rotor and vane current meters of the type used for the long-term measurements are simply not adequate to measure high-frequency turbulence and wave orbital velocities. The BOLT program in the last year has tried to develop a suitable measuring system.

This report documents the progress to date. The major development is complete, although further refinements are planned. Current meter configurations have been selected, the configurations have been calibrated, and preliminary field measurements have been successful. We can now turn to analyzing field data.

4.2 REVIEW OF TURBULENCE SCALES AND CHARACTERISTICS

The BOLT system is capable of high-frequency, small-scale (up to 5 Hz, down to 15-25 cm) three-dimensional velocity measurements. Such sophisticated velocity measurements are clearly needed for determining wave orbital velocities; however, it may not be clear that measurements of this quality are also needed to characterize bottom stress due to large-scale currents, especially since bottom stress is often determined via one-dimensional current meter measurements (see Dyer, 1976a, for a review of methods of obtaining bottom stress). It is important to emphasize that most methods of obtaining bottom stress inherently yield only a time-averaged stress. In some circumstances, however, averages can obscure rather than illuminate the physics of a process (Mollo-Christensen, 1971; Liepmann, 1979). The discussion below will illustrate why the average stress may not be the best indicator of sediment erosion. It will be shown that instantaneous shear stress measurements, requiring the sophistication of the BOLT equipment, are needed to measure both large-scale current generated turbulence as well as wave orbital velocities. These measurements will be particularly important in sorting out the possible nonlinear interactions of waves and currents (Grant and Madsen, 1979).

Instantaneous stress measurements of this type place severe demands on a measurement system. Thus, few measurements of this quality have been made (Wiseman, 1969; Seitz, 1973; William and Tochko, 1977; Tochko, 1978; Smith, 1978).

A conceptual picture of the typical length scales relevant to bottom turbulence is shown in Fig. 4.1. For turbulence due to large-scale currents, not waves, the characteristic regions of the mean velocity profile and the stress profile are shown. Useful reviews of this material can be found in Komar (1976) and Tochko (1978). The viscous sublayer is the region where

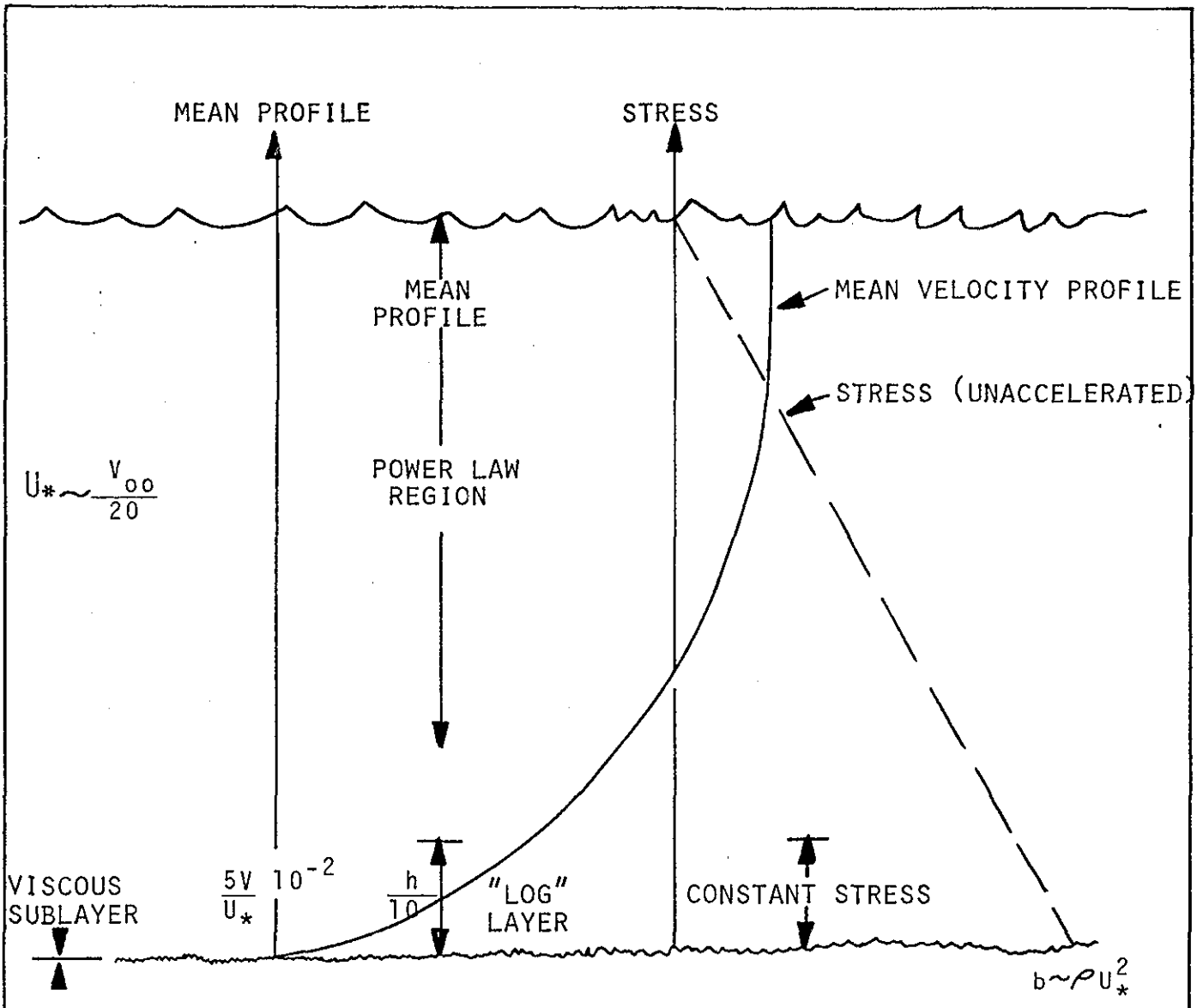

LENGTH SCALE FOR ISOTROPIC LIMIT $\lambda \sim \frac{Z}{2} - \frac{Z}{10}$

LENGTH SCALE FOR APPLICABILITY OF 5/3 LAW $\lambda \sim Z$

WAVE INDUCED TURBULENCE $Z \sim$ 1-5 cm

TURBULENCE LENGTH SCALES

Figure 4.1

molecular viscosity is important. As is indicated in the figure, this region will be on the order of 10^{-2} cm for flows relevant to BOLT; this is much smaller than the roughness elements of the natural bottom, thus a viscous sublayer will not exist.

A second region of the mean velocity profile is the log law region. This is a region, close to the bed, where for an unaccelerated uniform flow, one expects from theoretical considerations that the velocity profile will follow a logarithmic dependence with height. This logarithmic dependence is well documented in laboratory flows and has often been observed in geophysical flows. Whether or not the log profile will be observed at disposal sites depends on the state of the tide, on large-scale roughness characteristics of the bed, and on the averaging time used (Dyer, 1971; Smith, 1978). The final region of the mean velocity profile, that covering the main body of the water column, is best described by a power law dependence (Cartwright, 1961).

The ideal stress profile for unaccelerated, uniform flow is shown on the right-hand side of Fig. 4.1. As is indicated, the ideal stress profile is a linear function of height above the bed, decreasing from a maximum at the bed to zero (given no wind stress) at the surface. Close to the bed there is a region in which the stress does not change appreciably. This region is often referred to as a constant stress region; it corresponds roughly to the region where a log velocity profile would be observed. Theoretically, log profiles should be observed for uniform flow only close enough to the bed so that the stress profile may be taken as constant for engineering purposes. However, the log velocity profile is often observed to give satisfactory results even in the non-constant stress region (Hinze, 1959, p. 469). BOLT sensors will all be placed in this region; bed shear stress must therefore be extrapolated from measurements made in the "constant stress" region. Depending on the bottom topography, some portion of the shear stress measured in the "constant stress" region is required to balance the effective drag caused by turbulent eddies (and the associated pressure gradients) shed from local rough topography. Thus not all of the extrapolated bottom stress is effective in eroding sediment (Smith and McLean, 1977).

The smallest wave length that contributes to the stress is the length scale for the isotropic limit (Monin and Yaglom, 1975, p. 457). One would like to be able to measure fluctuations as small as this scale to be certain that the entire stress-producing region of the spectrum has been observed.

Up to this point we have referred primarily to turbulence due to large-scale currents. In addition, waves are an important potential eroding mechanism; in fact, due to the large velocity gradient near the bottom, a given wave orbital velocity is more erosive by a factor of 10 than an equivalent steady current (Madsen, 1976). Turbulence generated by waves does not extend throughout the water column, as it does for tidal currents, but rather is confined to within 1-10 cm of the bed. Since we are not able to place our sensors in this region, we must measure the wave orbital velocities at 25-100 cm above the bed to infer the stress from wave turbulence (Madsen, 1976; Grant and Madsen, 1979).

A stress is a transfer of momentum across a plane. Imagine two railroad cars, one stationary and one moving. If the sides of the trains rub against each other, the moving train causes the stationary train to move; it imparts momentum to the stationary train--by molecular friction in this case. An equivalent effect would occur if a coal shoveler in the moving train threw shovels of coal into the stationary train. The coal arrives at the stationary train with an excess momentum; thus the coal imparts momentum to the stationary train. In this way a positive plane fluctuation, denoted by w', accompanied by a positive fluctuation parallel to the plane, denoted by u', causes a net transfer of momentum across a plane and hence is a stress. For this reason u'w' may be referred to as an instaneous stress or Reynolds stress, after O. Reynolds, who introduced the concept.

The instantaneous stress (Fig. 4.2) is decidedly non-Gaussian, but is centered around zero with occasional large stress events. This is referred to as intermittency (Gordon, 1974; Heatherstraw, 1974; Gordon, 1975a; Gordon and Witting, 1977). When intermittency occurs, the average may tell very little about the peak stresses, which may cause most of the erosion (Gordon, 1975b). What is needed for a thorough understanding of the erosion mechanism is to establish the relation between the peak values and the mean for various flow conditions.

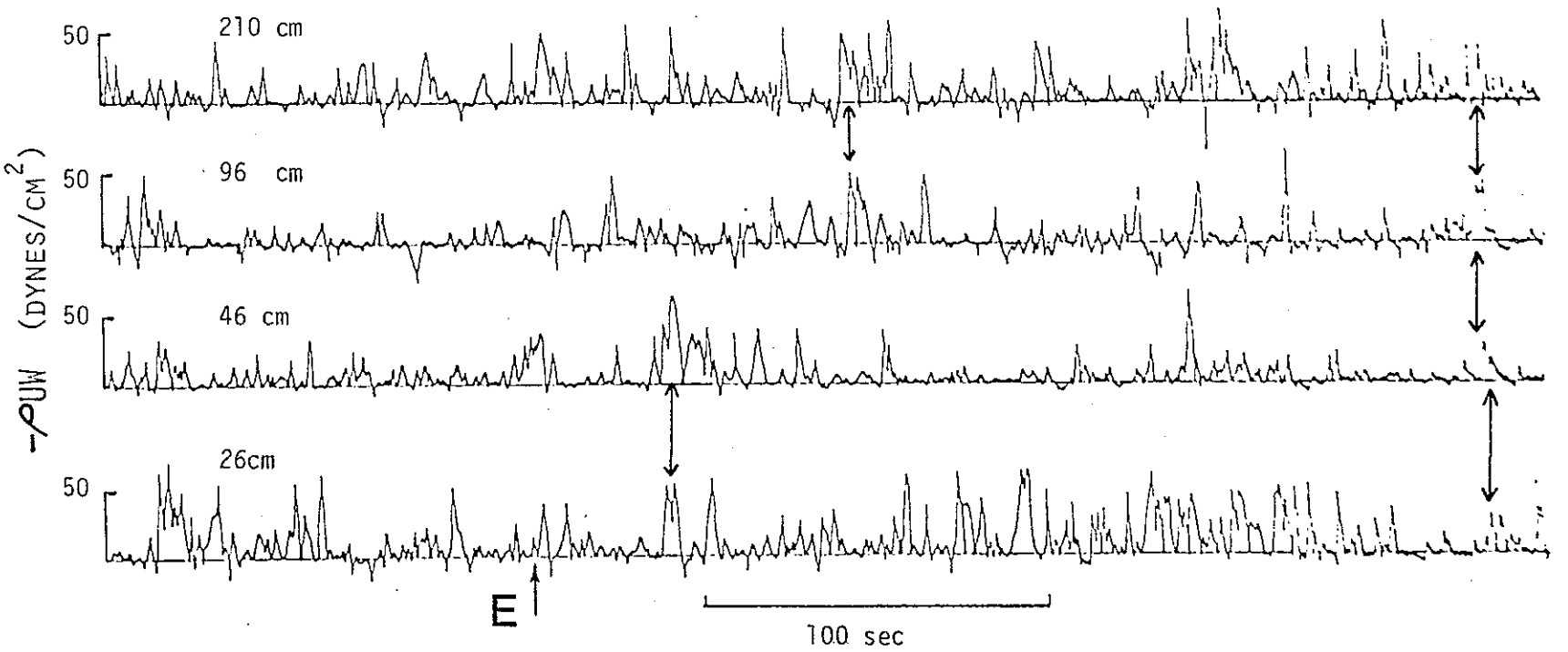

TIME SERIES OF THE $-\rho UW$ PRODUCT AT FOUR POINTS ABOVE THE BOTTOM
(FROM TOCHKO, 1978)

INSTANTANEOUS SHEAR STRESS

FIGURE 4.2

A structural model for visualizing the mechanism of this intermittency has been proposed by Falco (1977) (Fig. 4.3): "typical" eddies, which produce most of the stress, form on the upstream side of large-scale motions. Typical length scales for both features are shown; however, the process is clearly more complex than the simple picture shown in Fig. 4.3. Both the typical eddies and the large-scale motions comprise a wide spectrum of scales. Depending on the characteristics of the flow, the individual eddy types may or may not be distinguishable. Large-scale coherent structures are not required to produce intermittency in the stress time series; the product of two correlated Gaussian variables, without further assumptions about large-scale structure, can be shown to lead to an "intermittent" stress series.

To this point we have been implicitly discussing relatively smooth bottoms. The situation is greatly complicated by large-scale roughness (Fig. 4.4). The large-scale roughness elements shed eddies causing deviations from a linear stress profile or a logarithmic velocity profile (Dyer, 1971; Smith and McLean, 1977; Mulhearn, 1978). Unfortunately, disposal sites are often characterized by regions of large-scale roughness. It is not possible to accurately characterize the stress at a disposal area by measurements at a single location. To obtain a reliable characterization, we need to obtain bottom stress measurements and detailed observations of bottom topography at several locations on the disposal site.

The effects of large-scale roughness on shear stress profiles are further illustrated by the measurements of Smith (1978) (Fig. 4.5). These measurements, made on the upstream side of a gently sloping sinusoidal sandwave, illustrate that, for this type of nonuniform flow, there is not a linear decrease in the stress from the bed to the surface. These results also illustrate the need for making measurements at more than two levels (which is what BOLT is restricted to at present). Similar results and conclusions have been presented by Tochko (1978). Mulhearn (1978) describes interesting observations of the stress profile above a particular type of rough bottom where again the stress increases with height above the bed.

Large Scale Motions - scale with outer flow variables eg h, u

'Typical' eddies - form on upstream side of large scale motions

produce most stress

Reynolds number dependent

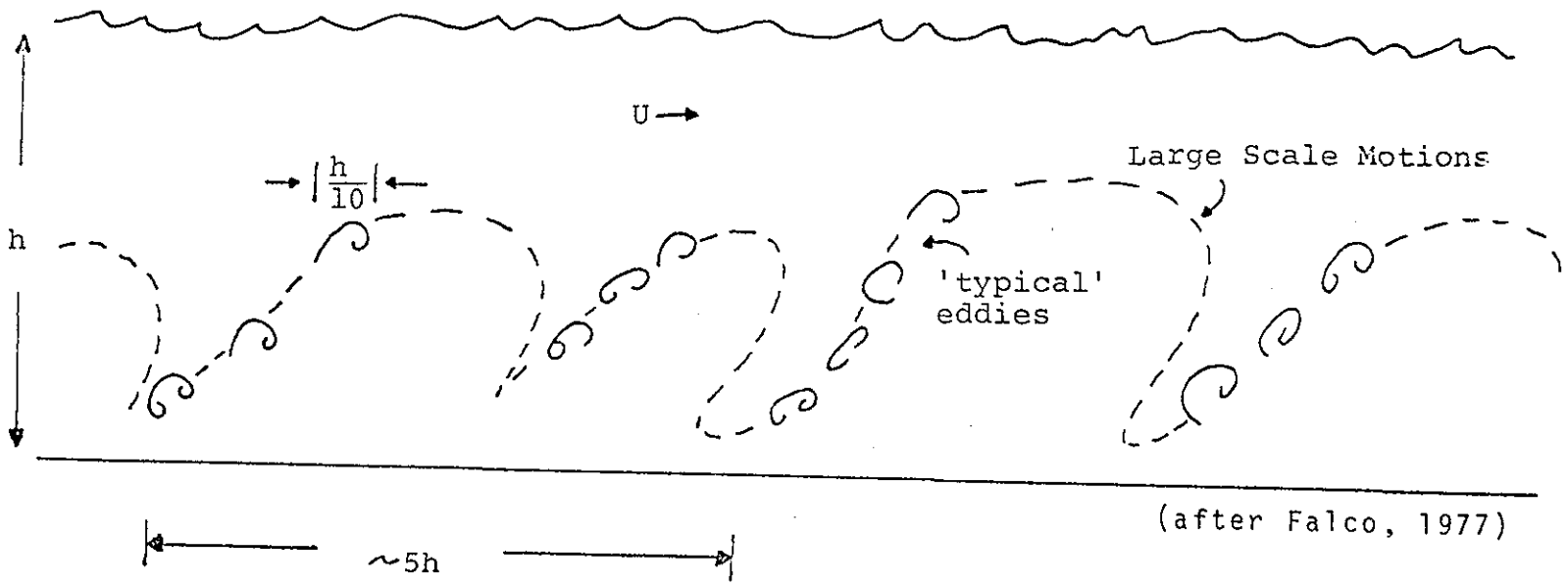

STRUCTURAL MODEL OF OUTER FLOW

Figure 4.3

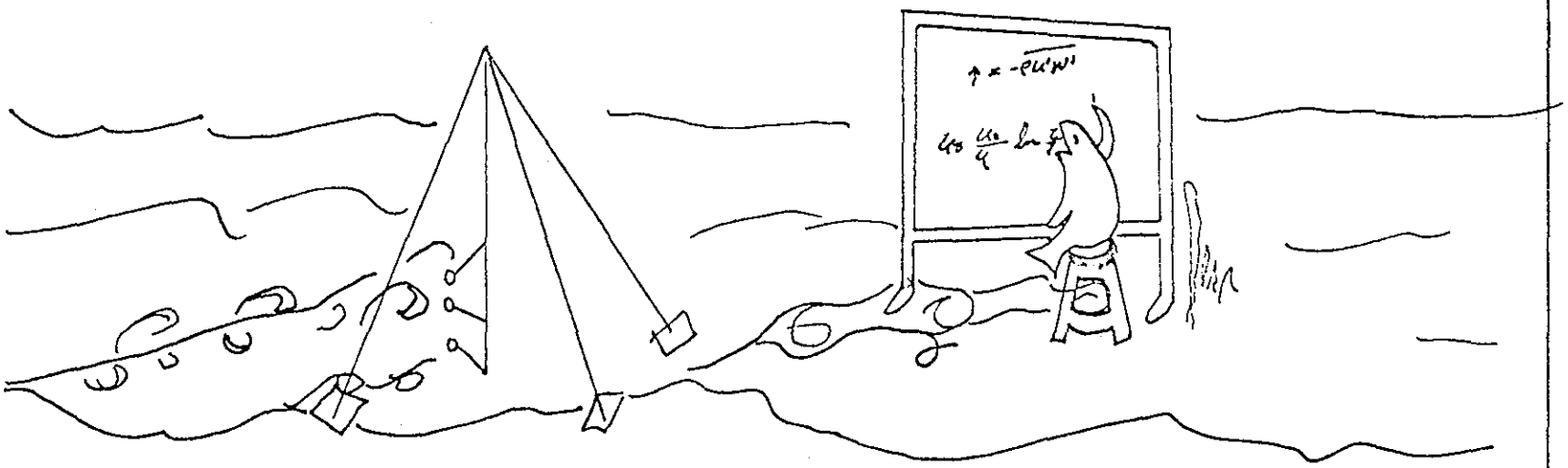

EFFECTS OF LARGE SCALE ROUGHNESS
ON FLOW NEAR THE BED

FIGURE 4.4

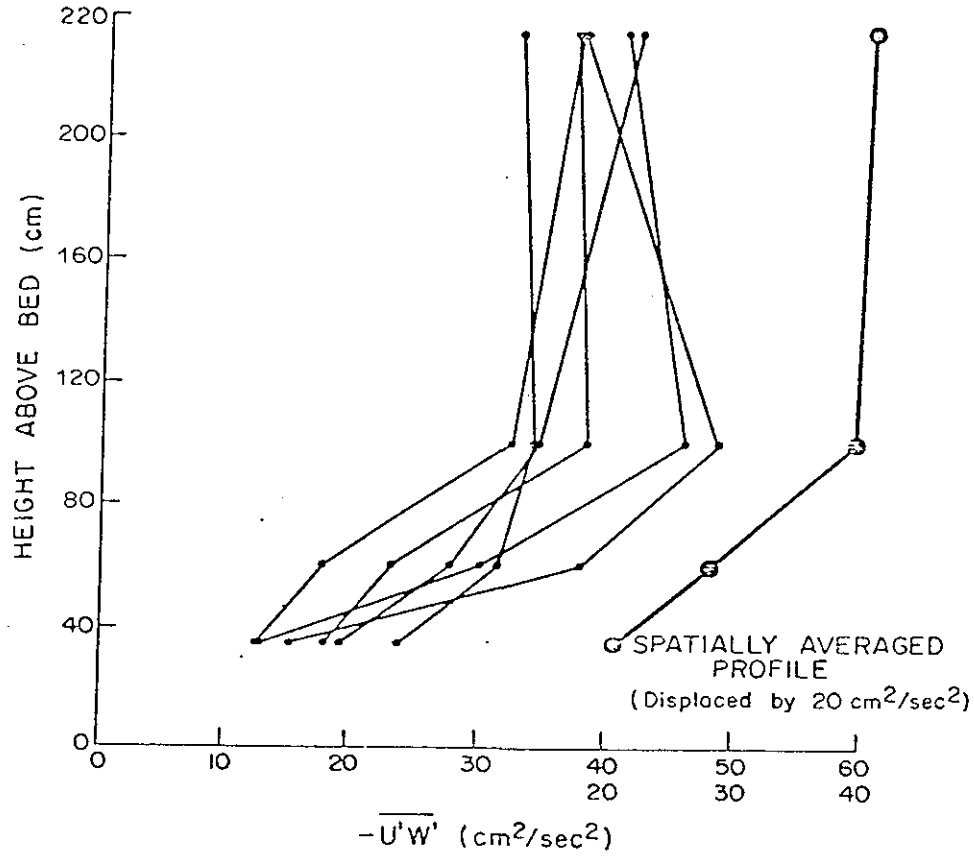

Shear stress profiles for the upstream side of a gently sloping, nearly sinusoidal sand wave 2.1 m in height and 96 m long.

EFFECTS OF LARGE SCALE FEATURES ON STRESS PROFILES

Figure 4.5

4.3 THE BOUNDARY LAYER TURBULENCE (BOLT) MEASURING SYSTEM

To make geophysical turbulence measurements that are adequate to describe sediment erosion mechanisms, small, quickly responding current meters are needed. The meters must be able to sense time scales of 1-10 Hz, depending on flow conditions, and length scales of 10-50 cm. Furthermore, three-dimensional information is required (Smith, 1978). The types of meters used for the long-term current measurements, or those used in an earlier version of BOLT (Cook et al., 1977) are not adequate.

The basic sensor used by BOLT is a ducted impeller current meter developed by Smith (1978) specifically to measure geophysical turbulence. The meter consists of a nearly neutrally buoyant impeller 3.5 cm in diameter by 1.9 cm long mounted in a duct 4.1 cm in diameter by 1.6 cm long. The meter head is mounted on a support rod 26 cm long which contains a Hall effect device. It also houses electronics which generate a pulse each time the magnets, which are imbedded in two of the impeller blades, pass. The meters can respond to frequencies up to and possibly slightly higher than 5 Hz; which is adequate for flows encountered at disposal sites. Details on the performance of the meters can be found in Smith (1978) and in the discussion of our calibration results below.

The current meters are arranged, at present, in one of two configurations of three meters (triads). These current meters can record all three components of the current at the level of the meters. At present a maximum of six velocity sensors (two sets of three) can be recorded by the BOLT electronics. The meters are mounted on a central pole which is supported by a tripod frame 2 m high (Fig. 4.6).

The electronics and power supply are contained in separate pressure cases and are connected to the current meters by a set of cables 15 m long. The electronic processing unit counts the number of pulses in each 0.2-sec interval from each meter and records this on cassette tape. Approximately 6.3 hours of data can be recorded, either continuously or in any burst-sampling scheme (e.g., 15 minutes every 2 hours for 50 hours). The total system is self-contained and can be left unattended in the field indefinitely. This,

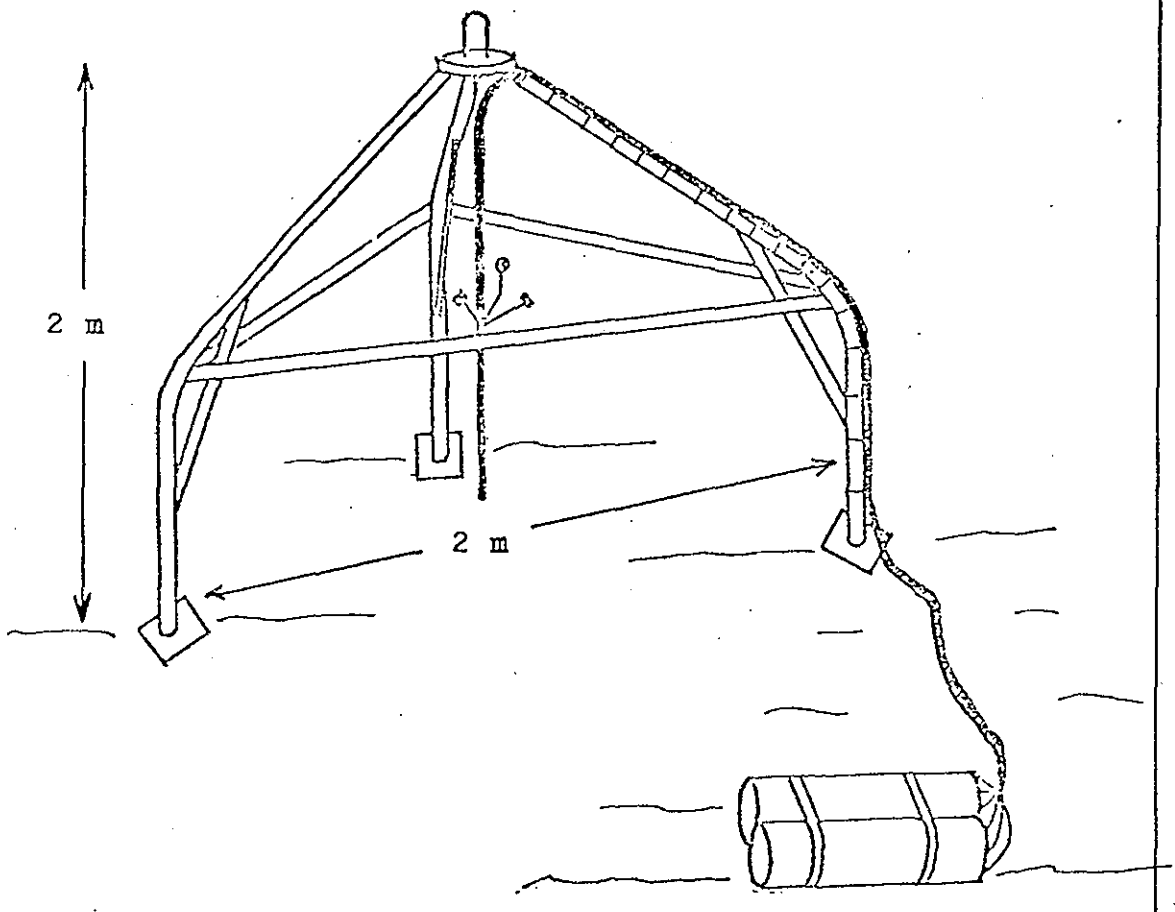

BOLT SYSTEM

REPRESENTATION OF THE BOLT SYSTEM AS DEPLOYED
SHOWING TRIPOD AND ELECTRONICS PACKAGE

FIGURE 4.6

coupled with the selectable start time delays that are available, make the BOLT system quite flexible and especially suited for sampling storm events.

The boundary layer turbulence program has been essentially a development program aimed, first, at checking the electronics, and second, at testing various meter configurations. Since the first deployment in February 1978, we have made several field tests in both tidal and wave regimes using roughly machined meter configurations. Two configurations have been found to be satisfactory. The first, which was used by Smith (1978), is best if the mean flow comes from one direction only (see Fig. 4.7). Approximately 180° of the horizontal plane is in a "shadow" region. If divers can orient and reorient the tripod this would be the best configuration to use since it is least sensitive to errors. Since this is not always possible (either for the deep sites or for storm monitoring), a reversing or bidirectional configuration (Fig. 4.8) is also needed. For this arrangement there will still be a "shadow" region in the sector containing the pole. At many sites, we know the direction of the mean flow (which probably has reversals). Thus, except at deep sites, divers can align the system to place the shadow in an unlikely flow direction. Although omnidirectional configuration would still be desirable, it would require the elimination of the central pole and hence a redesign of the tripod.

It is extremely important to have accurately machined meter mounts for the triads. It can be shown that, to make stress measurements with relative errors of 10 percent, angular placement accuracy must be on the order of 1° (see Appendix 4.2). All the field measurements made to date have been made with roughly machined triads (approximately 5° accuracy). Since December 1978 most of the effort on BOLT has been devoted to designing and calibrating accurately machined meter mounts for both the unidirectional and bidirectional triads. With this improved machining we can achieve angular accuracies of approximately 0.5° for initial setup; bending or other distortions in the field may increase angular uncertainties to about 1°. The bidirectional configuration is more subject to flexing than the unidirectional configuration.

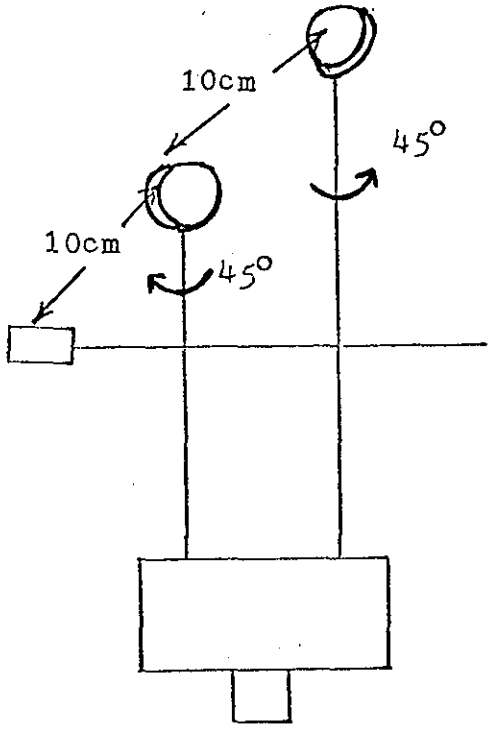

UNIDIRECTIONAL FLOW TRIAD

FIGURE 4.7

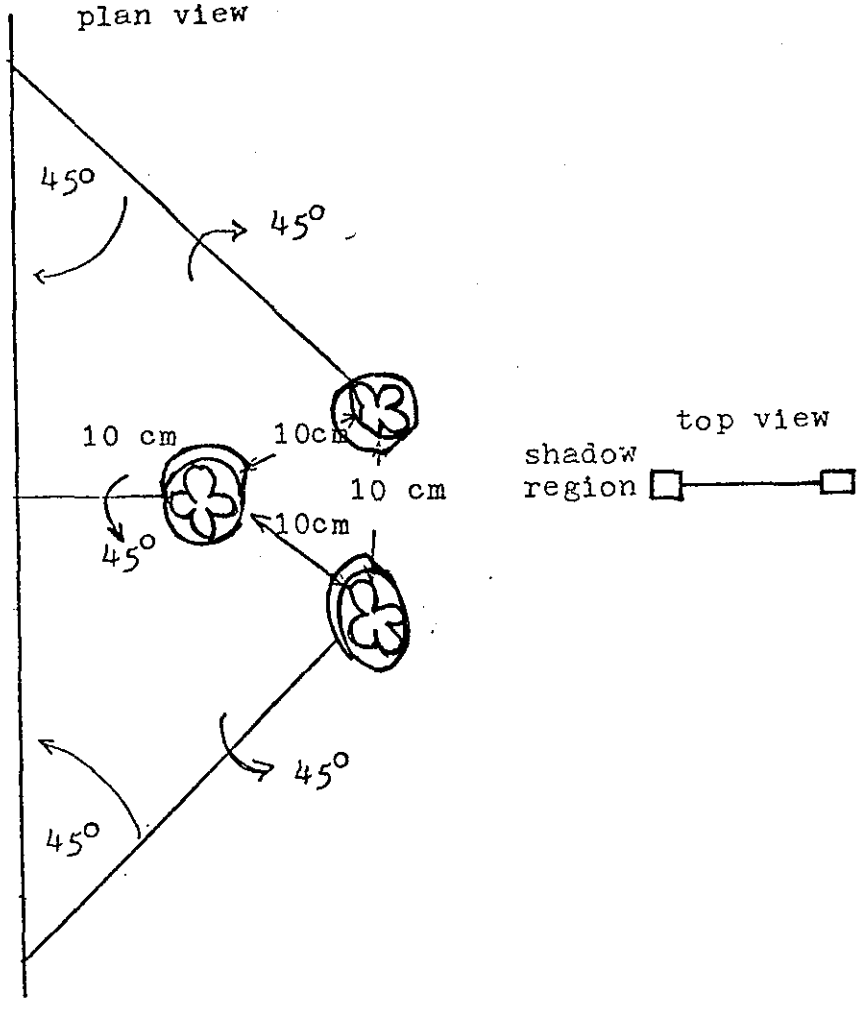

BIDIRECTIONAL TRIAD

FIGURE 4.8

Although we now have a system capable of high-accuracy stress measurements, future improvements are planned. First, a watertight canister containing two inclinometers and a compass has been designed and constructed; this will allow us to determine the orientation of the support pole and will help in analyzing the data. However, software changes to the electronics must be made before this unit can be used. Second, u, v, w measurements are needed at more than two levels. At present we have current meters to make measurements at three levels (nine meters) but the electronics can only sample six meters. To incorporate the additional meters both hardware and software changes must be made. A third improvement is the construction of a new tripod from material of smaller diameter. The frame will be lighter (and hence will settle less into soft mud) and will obstruct the flow less . While wake corrections (for flow obstruction) can be made (Schlichting, 1960, p. 600; Hinze, 1959, p. 396) it is best to minimize the effect of wakes (Smith, 1978). The new tripod will be designed to support an omnidirectional triad. However, for the deep deployments, the ruggedness of the present tripod may still be required.

4.4 FIELD TESTS

The BOLT System has been tested several times in the field using roughly machined triads. These tests have demonstrated that the unidirection and bidirectional configurations were suitable in both tidal- and wave-dominated flows. A complete calibration of all meters and triads has been completed.

The basic data-processing scheme is illustrated in Fig. 4.9. The cassette data are first transferred to a computer-compatible 9-track tape. The raw current meter data are then read, inspected, and converted to velocities using the velocity vs. pulses/sec calibration described below. The velocity data are converted to the velocity components u, v, and w referenced to the triad configuration (see Appendix 4.1), and are then corrected for the non-cosinusoidal angle of attack response of the meters, by the technique described by Smith (1978). The dashes in Fig. 4.9 indicate that this step has not yet been incorporated into the processing as the quality of the data (due to alignment errors) did not warrant it. Finally, the coordinate system is

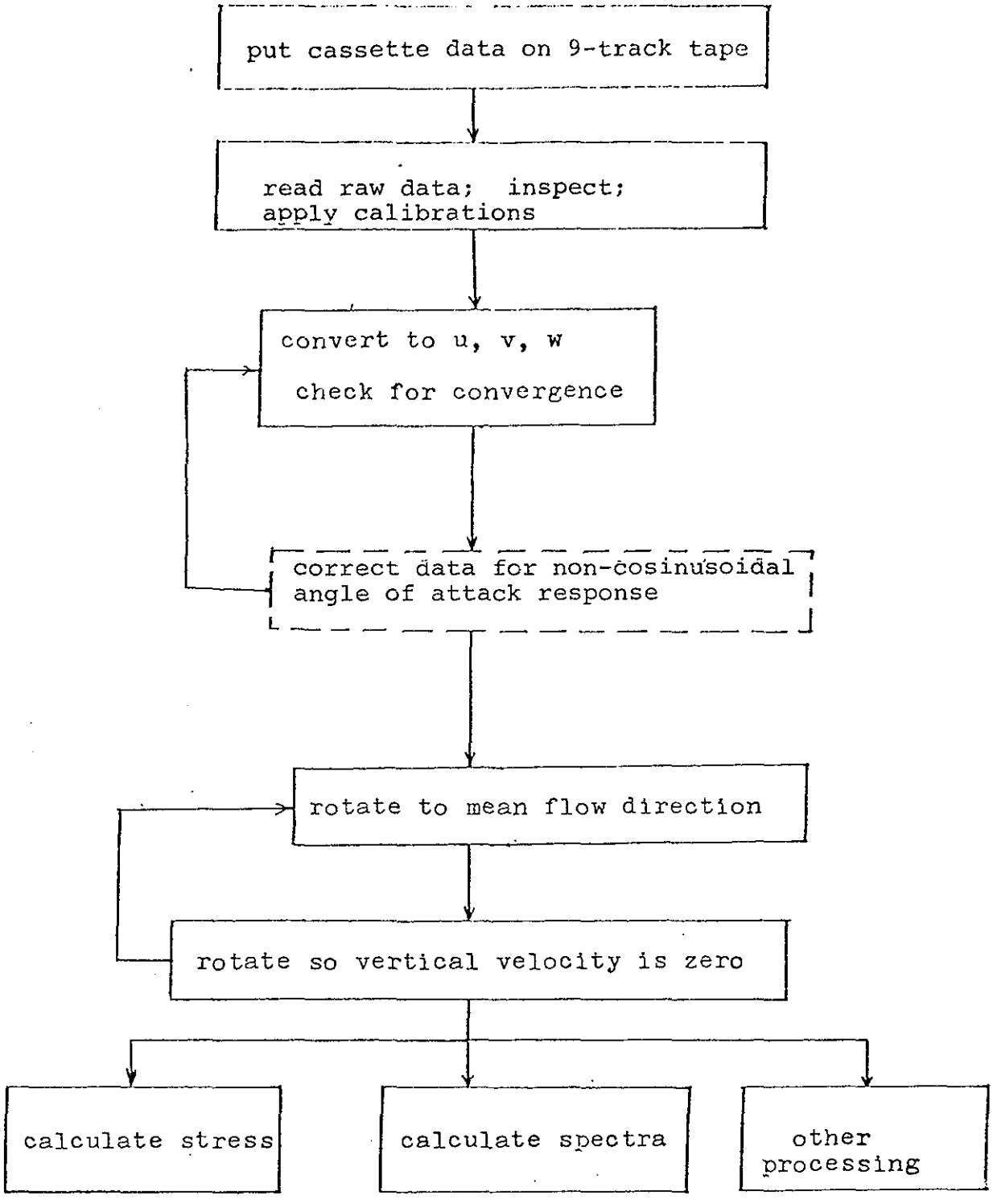

DATA PROCESSING FLOW CHART

FIGURE 4.9

aligned with the mean flow direction and rotated in the vertical so that the average value of w is zero (see discussion in Williams and Tochko, 1977). After these preliminary steps, a variety of final processing procedures are possible.

Tests were made in September 1978 at the New London site to check the bidirectional triad in a tidally dominated current regime. (Since these tests were made with the roughly machined triads, data quality is not as good as we expect it to be in the future.)

The BOLT system was lowered from the ship and oriented by divers so that the expected mean flow would be into the plane of the paper in Fig. 4.10. The bottom of the support pole was just level with the surface of the mud at deployment. The bottom was rough and clumpy, with the clumps about 1 m across. On retrieving the system four days later, the divers reported that the system had settled about 10 cm into the mud. They also observed iron filings on the magnets inset on the impeller blades. Both the settling of the system (which makes it uncertain at which height measurements have been made) and the accumulation of iron filings (which may upset the meter calibrations) are problems to be resolved in the future.

The raw data were transferred from the cassettes to a 9-track tape and then were plotted and examined. The spiking evident in earlier tests, which had been traced to a power supply deficiency, had been eliminated. Only two problems were noted. The first was that the maximum readable current had been set for 50 rather than 100 cm/sec to gain greater resolution. Unfortunately, currents at the meters exceeded 50 cm/sec during the peak of the tidal cycle, causing some of the data to be strongly clipped. Another problem was that meter 3 stopped rotating for about one hour during the middle of the test, possibly because of fouling by seaweed. Foutunately, the meter cleared itself and began rotating again with no apparent deterioration.

Typical plots of the raw data from meters 1, 2, and 3 are shown in Figs. 4.11a and 4.11b. The data shown in Fig. 4.11a were taken during the accelerating portion of the tidal cycle, and those shown in Fig. 4.11b were taken during the decelerating portion. The currents generally exceed the threshold

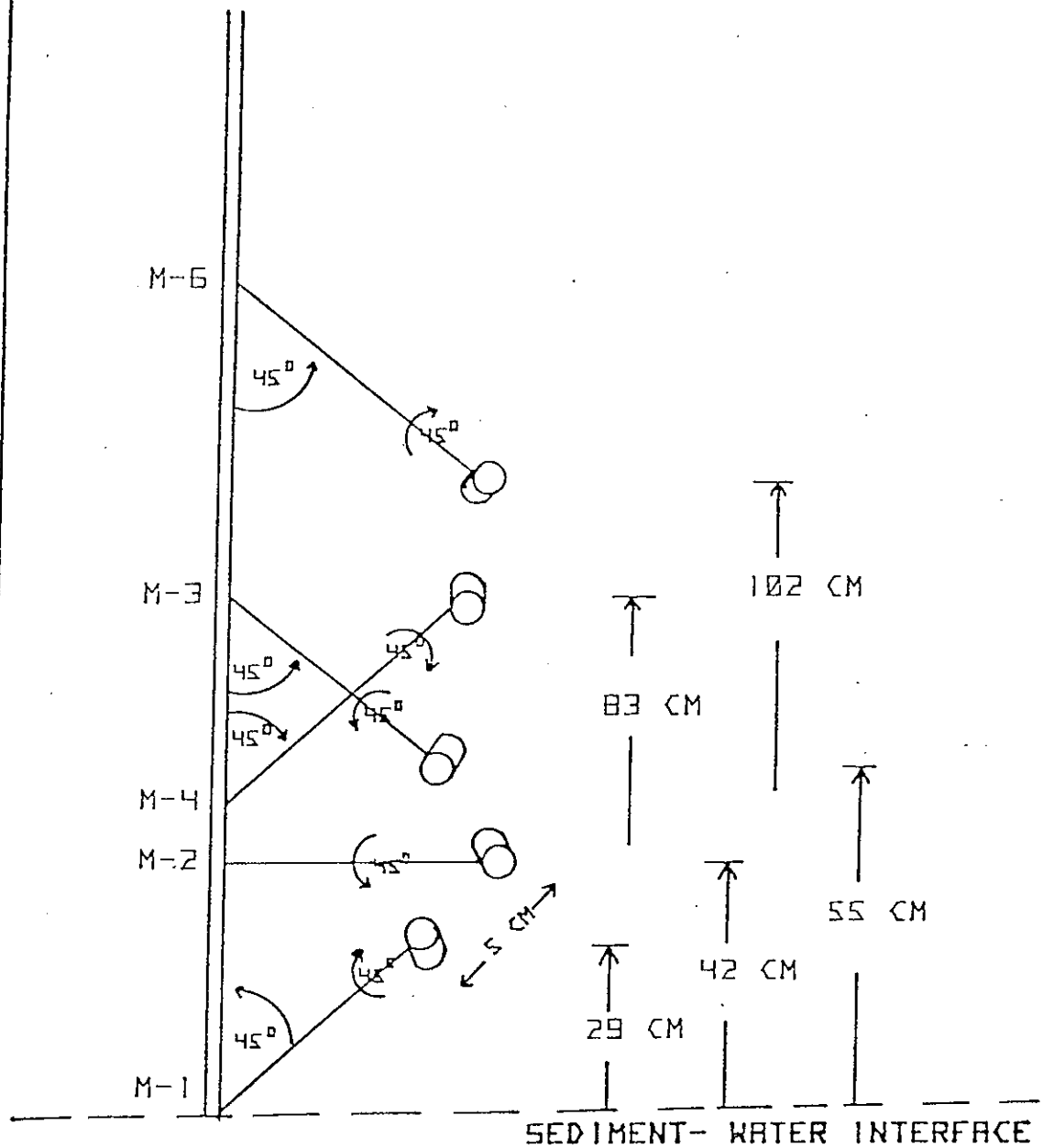

DUCTED METER CONFIGURATION
NEW LONDON DISPOSAL SITE
SEPTEMBER 20, 1978

FIGURE 4.10

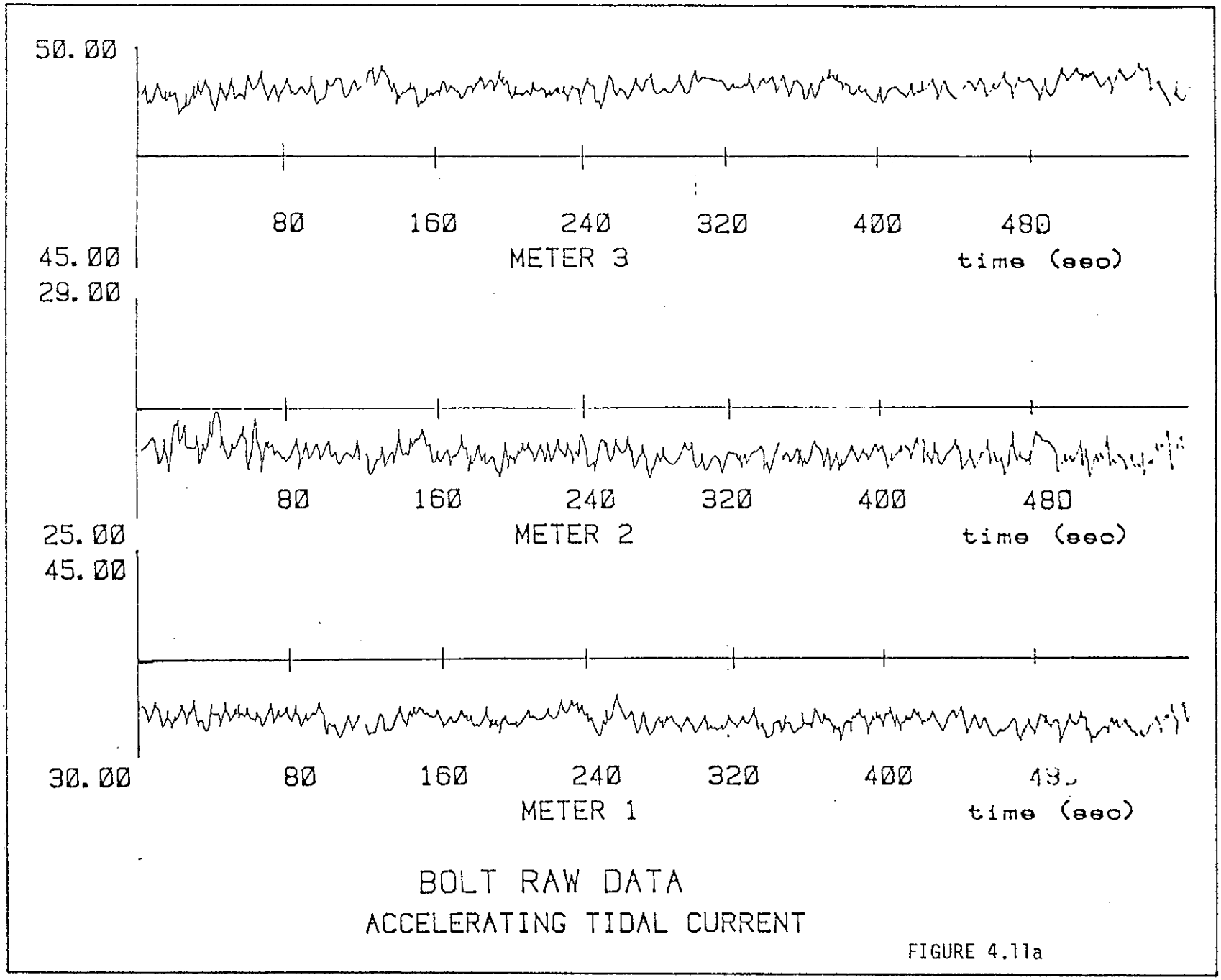

BOLT RAW DATA
ACCELERATING TIDAL CURRENT

FIGURE 4.11a

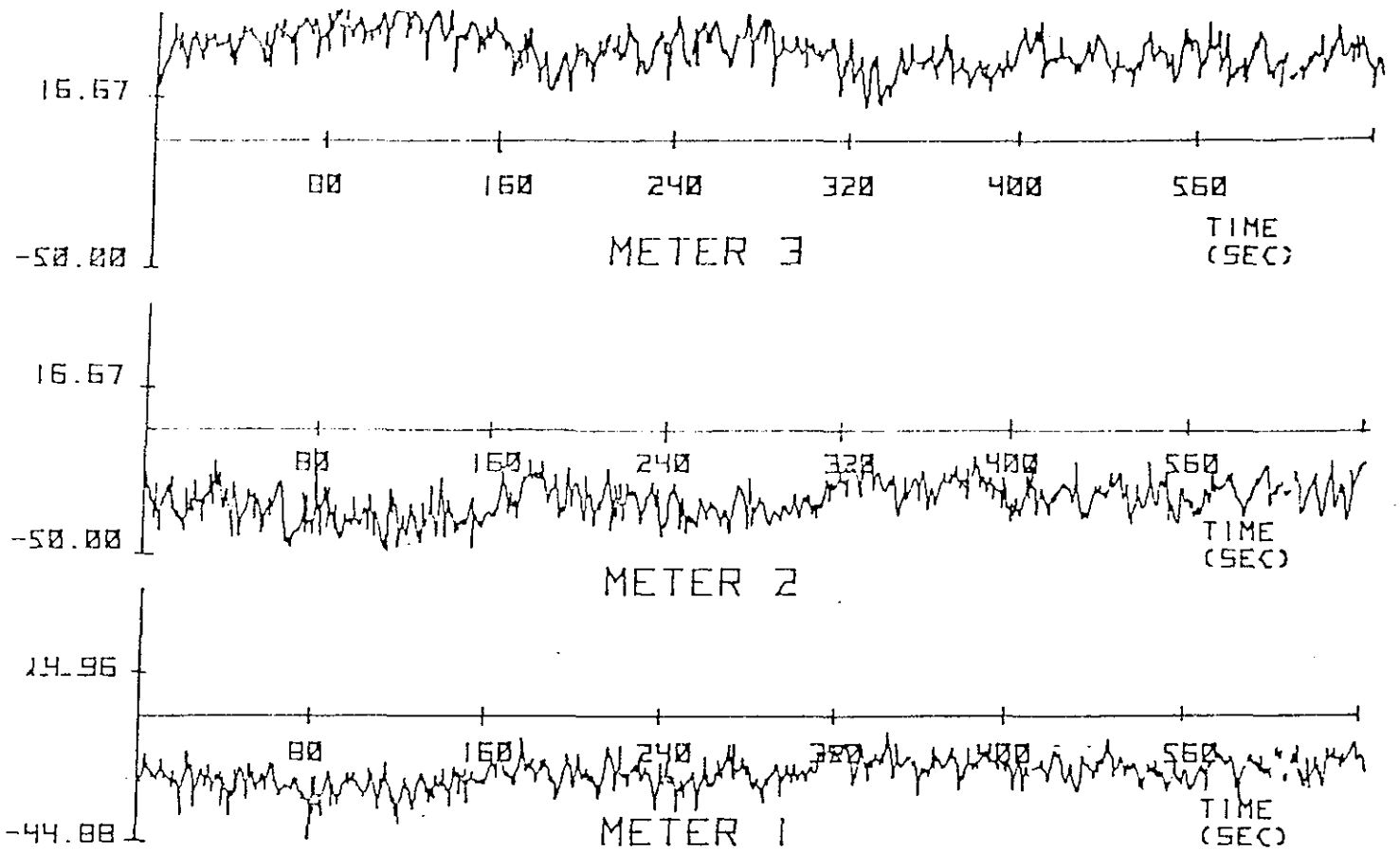

BOLT RAW DATA
DECELERATING TIDAL CURRENT

FIGURE 4.11b

of the meters (about 2 cm/sec). Some clipping at 50 cm/sec can be seen in meter 3 (Fig. 4.11b), between 80 and 100 seconds.

The raw data were converted to u, v, and w components using relationships determined from the geometry of the meter configuration (see Appendix 4.1). The velocity components u, v, and w are instantaneous values of the horizontal and vertical components of the current. They are defined with respect to the vertical plane through the current meters, the u direction being taken as normal to the plane. No correction was made for the noncosinuosidal angle of attack response of the individual meters. Typical data for u, v, and w are shown in the bottom three plots of Figs. 4.12 and 4.12b. The data in Fig. 4.12a are for the accelerating portion of the tidal cycle, whereas those in Fig. 4.12b are for the decelerating portion.

The instantaneous shear stress is given by $-\rho u'w'$, where ρ is the density and u' and w' are the horizontal and vertical turbulent velocity fluctuations. To calculate u' and w', the u axis is aligned with the mean current via two coordinate rotations.

As shown in Figs. 4.12a and 4.12b, the average value of w' over the 10-minute interval shown is not zero. This means that either the bottom was not level, the mounting pole was not precisely vertical, or the current meters were not positioned correctly. Also, the horizontal current is not aligned with the u axis as defined by the perpendicular to the plane of the current meters. To align the u axis with the mean current we must first rotate the horizontal axes so that the new u axis is aligned with the mean flow direction in the horizontal; then we rotate the axes in the vertical so that the average value of w in the new coordinate system is zero. (The process is repeated until convergence to within 1°). This ensures that we have identified the mean flow direction. The turbulent u' fluctuations are then found by subtracting the average value of u in the mean flow direction (or a polynomial fit to the data instead of the average) from the instantaneous value. The turbulent w' fluctuations are given directly by the instantaneous values of w in the rotated coordinate system. Williams and Tochko (1977) discuss these problems and processing techniques.

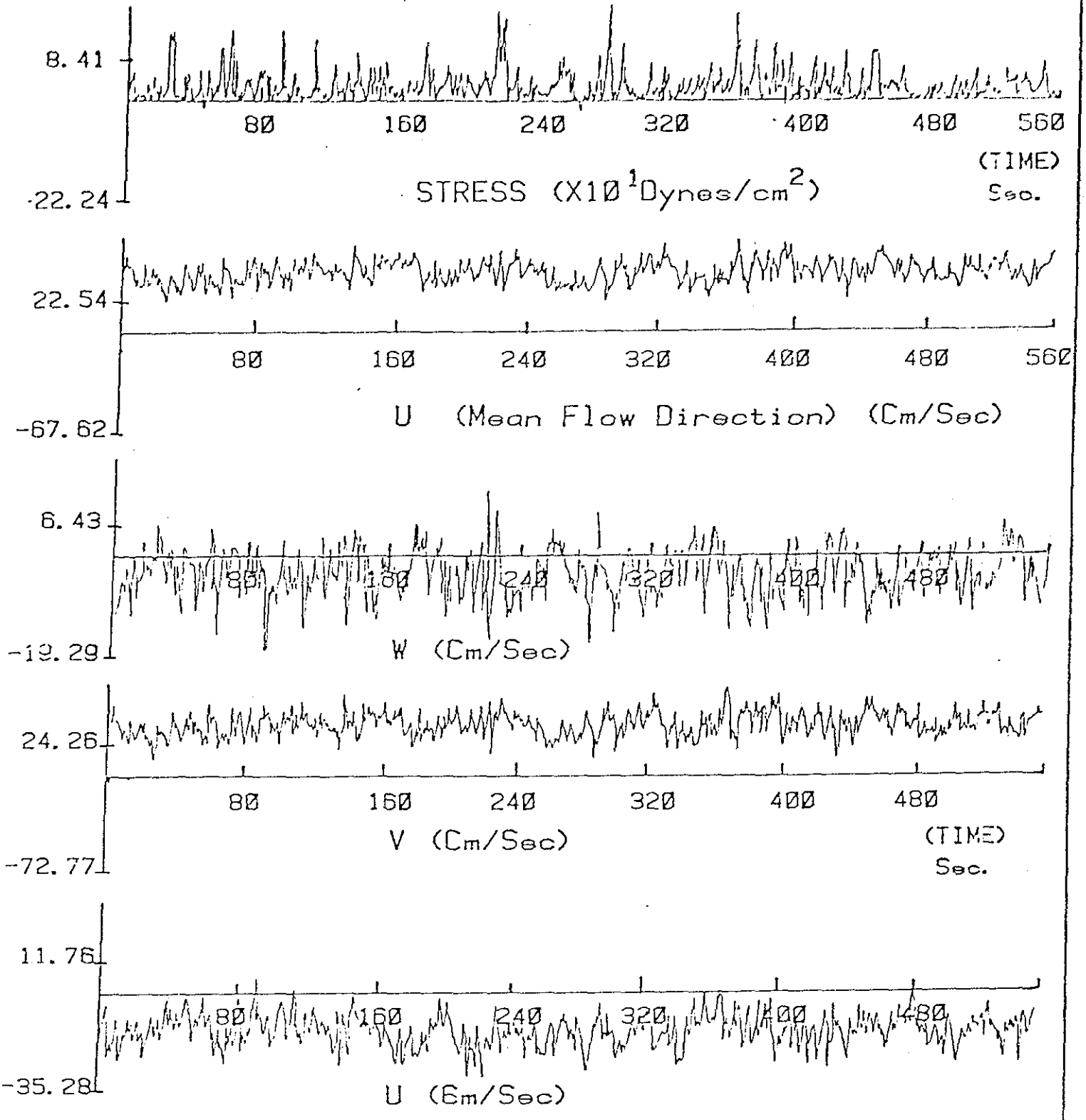

INSTANTANEOUS CURRENT & SHEAR STRESS
ACCELERATING CURRENT

FIGURE 4.12a

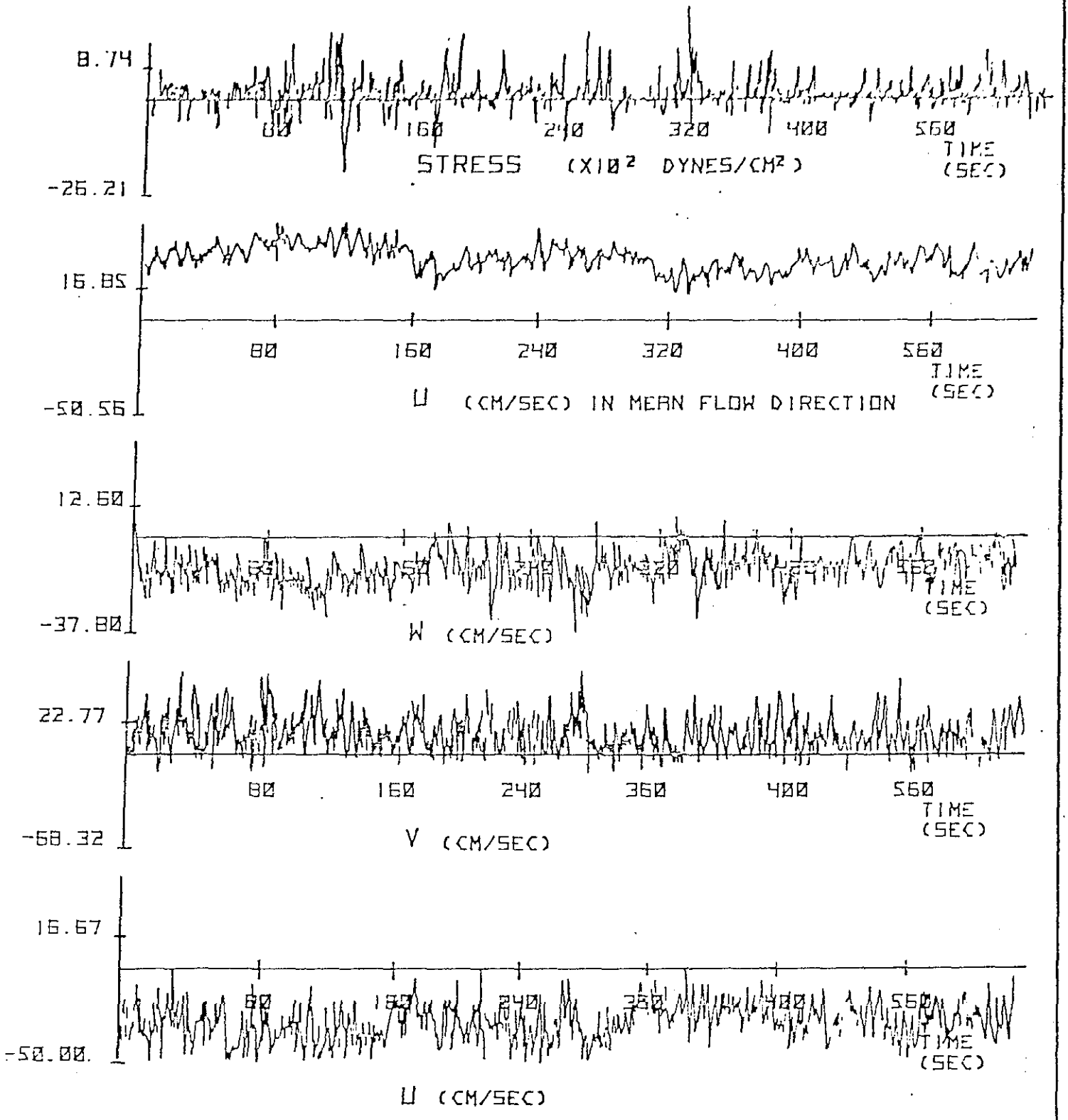

INSTANTANEOUS CURRENT & SHEAR STRESS
DECELERATING CURRENT

FIGURE 4.12b

The averaging time must be selected so that it is long enough to give statistically reliable results (it must include many typical events), but it must be short enough that the process can be considered stationary during the interval. When measuring with tidally induced turbulence an averaging time of about 10 minutes meets these criteria. (See also Heatherstraw and Simpson, 1978.) Thus we have broken the record into 10-minute segments and have performed the coordinate rotations discussed above for each of these segments).

Typical results are shown in the top two panels of Figs. 4.12a and 4.12b, where the instantaneous value of u in the mean flow direction and the instantaneous shear stress are plotted. Note that the shear stress has peak values greatly in excess of its average value, showing some evidence of intermittency.

Table 4.1 shows the average u velocity in the mean flow direction and the average shear stress for a series of continuous 10-minute segments for both the accelerating and the decelerating portions of the tidal cycle. These average values of stress are generally higher than the typical values of about 4 dynes/cm^2 reported earlier (Cook et al., 1977). The earlier values were computed by a different technique (the dissipation method) and used a different instrument. A comparison of results obtained from direct stress measurements and from the dissipation method is given in Table 4.2. In general, the dissipation method yields smaller values. Discrepancies between the methods may be due to the theoretical assumptions underlying the dissipation method not being satisfied., or due to high wave number spectral cutoff, as discussed below. The record-to-record variability in the estimates of the stress shown in Tables 4.1 and 4.2 are to be expected due to the large sampling variability of this quantity (Heatherstraw and Simpson, 1978). Finally, with ± 5° angular accuracy in the placement of the meters, and using the observed values of w' and u' with the results of Appendix 4.2, we estimate relative average stress errors to be about 25 percent.

Additional insight into the performance of the system can be gained by examining the longitudinal velocity spectra (Fig. 4.13) for the New London data. Over a wide range of frequencies the spectrum falls off as $f^{-5/3}$. Such a frequency dependence is to be expected from theoretical considerations. The

Table 4.1 Average current and shear stress over 10-minute intervals

ACCELERATING FLOW		DECELERATING FLOW	
Mean current cm/sec	Mean stress dynes/cm^2	Mean current cm/sec	Mean stress dynes/cm^2
34.1	14.8	26.8	11.1
36.1	16.5	23.9	11.9
36.1	14.5	24.2	7.8
38.9	11.8	24.7	6.8
40.1	16.4	22.7	2.4

Table 4.2 Comparison of two methods of calculating shear stress

$\bar{U}_{44\text{ cm}}$ $\frac{\text{cm}}{\text{sec}}$	E $\frac{\text{cm}}{\text{Sec}^3}$	$\uparrow E$ $\frac{\text{dynes}}{\text{cm}^2}$	$\uparrow_{\text{direct}}$	Previous $\uparrow E$
Accelerating flow				1.2-4.8
26	1.3	8	27	
31	1.5	8	12	
35	1.4	8	15	1. All results from 12.2 minute records
36	1.2	8	17	
38	1.6	9	13	
40	1.3	8	18	2. $E = \frac{\phi(k)}{0.14} K^{5/3}$ $^{3/2}$
Decelerating flow				Assumes: inertial subrange
29	1.0	6	10	3. $\uparrow E = (KZE)^{2/3}$
29	1.0	7	21	
26	0.3	3	12	Assumes: inertial subrange (prod = diss) law of the wall value for K
25	0.3	3	8	
				4. $\uparrow_{\text{direct}} = -12.8$ min $\frac{\text{time average}}{\rho u'w'}$

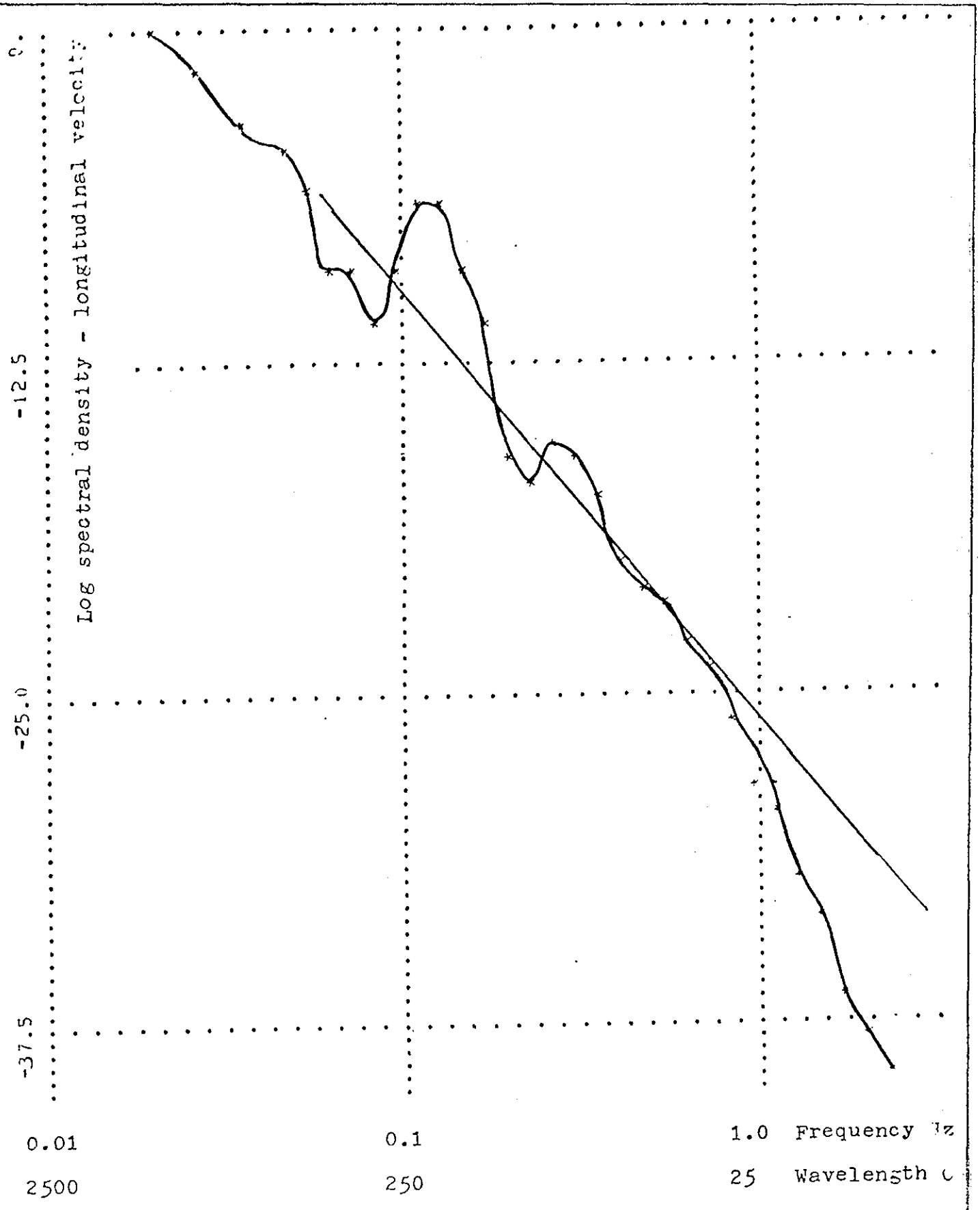

LONGITUDINAL VELOCITY SPECTRUM FOR NEW LONDON DATA

Figure 4-13

conditions under which this falloff might be expected are only marginally satisfied by our data (Cook et al., 1977) but, like with many other investigators, we find a wide range where the $\sim^{5}/_{3}$ law applies.

Note that for frequencies above 1 Hz, or equivalently, for wavelengths less than 25 cm, the spectrum drops below the $f^{-5/3}$ line. This indicates that the smallest wavelength that can be sensed by the bidirectional triad is about 25 cm, as expected.

Figure 4.14 compares the present spectrum with that found using the former BOLT meter (Cook et al., 1977). The new system responds to smaller length scales than the old system. The high-frequency falloff can cause the estimates of stress, using the dissipation method, to be low.

The New London results demonstrate that the bidirectional triad performs well in a tidally dominated regime. The BOLT system has also been deployed successfully in wave-dominated regimes, using both the unidirectional and the bidirectional triads. The unidirectional triad was deployed off Bimini Island on 2 March 1978. Measured orbital particle velocities agreed closely with predictions from estimated wave height and wave length. Also, the ratio of the observed orbital velocities at 100 cm to the observed orbital velocities at 50 cm was compared to the theoretically predicted ratio; these agreed to within 10 percent.

The bidirectional triad was tested in a wave regime at the Portland disposal area. This is a deepwater site (60 m) with low tidal energy. The BOLT system was lowered from the research vessel without diver assistance. The first deepwater BOLT deployment was accomplished with difficulty. The inability to orient the meters exactly or to tell the vertical inclination of the frame once it was on the bottom points to the need for a compass and inclination of the frame once it was on the bottom points to the need for a compass and inclinometers and for an omnidirectional configuration.

The observed currents at Portland had a slowly varying, small-magnitude mean component with relatively large wave orbital velocities superimposed. Portions of the data, however, showed no bottom velocity, indicating that the bottom current was often below the 2 cm/sec threshold of the meters; this

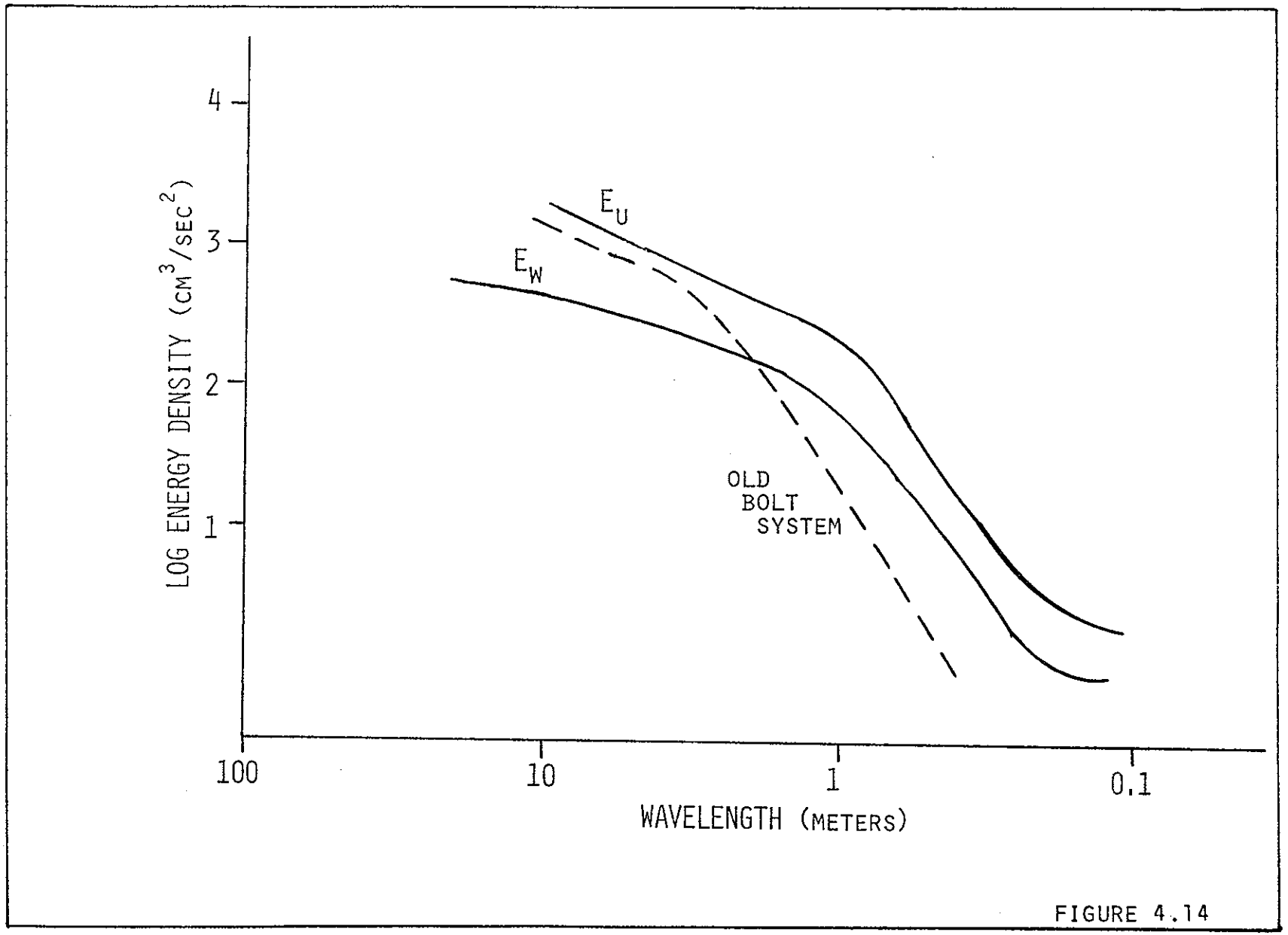

FIGURE 4.14

COMPARISON OF SPECTRA FROM EARLIER AND CURRENT BOLT SYSTEMS

verifies the conclusions of the long-term measurements that Portland is a very low energy site (except possibly during storms). Raw current meter outputs from the bottom set of meters (50 cm above the bottom) are shown in Fig. 4.15. Some deadband occurred at low velocities in all the records. This relatively clean record is representative of 25 percent of the data. The u, v, and w components of the raw data in Fig. 4.15 are shown in Fig. 4.16. The wave direction was (fortuitously) almost exactly along the arbitrarily defined x axis of the meter triad. (If this had not been the case the reference axis would have had to be rotated numerically.) The waves have a period of about 10 sec and appear to arrive in groups. The orbital velocities are about 2-5 cm/sec. Ten-second waves have a deepwater wavelength of 150 m; the depth-to-wavelength ratio is thus 0.4, just below the deep-water limit. With an orbital amplitude of 2.5 cm/sec near the bottom, surface wave amplitudes of 40 cm/sec are predicted. In agreement with the discussion of Madsen (1976), the near-bottom Reynolds number was 3×10^2. If the bottom roughness is arbitrarily assumed to be 2 cm, the relative roughness is about 0.5. From this we estimate a bottom shear stress of roughly 2 dynes/cm^2.

Our field tests demonstrated that the performance of the meter triads was sufficiently well understood to justify constructing accurately machined meter mounts. In the following sections we describe the results of the calibration of these accurately machined triads.

4.5 CALIBRATION RESULTS

A complete calibration of each meter and of the two triad meter configurations was conducted at the MIT Ship Towing Facility on 2-4 April 1979. The towing tank is 33 m long by 2.6 m wide by 1.1 m deep. There is a 16-m test section in the middle of the run. The towing carriage support is leveled to within 0.01"; tow speeds can be measured using a photocell timing unit and were observed to be repeatable to within ± 0.1 cm/sec for tow speeds below 50 cm/sec, and within ± 0.2 cm/sec for tow speeds between 50 and 100 cm/sec. The tank contained filtered fresh water at 27°C.

The meters were mounted on a support pole which in turn was mounted on the towing carriage. All machining was accurate to within ± 0.5°. The

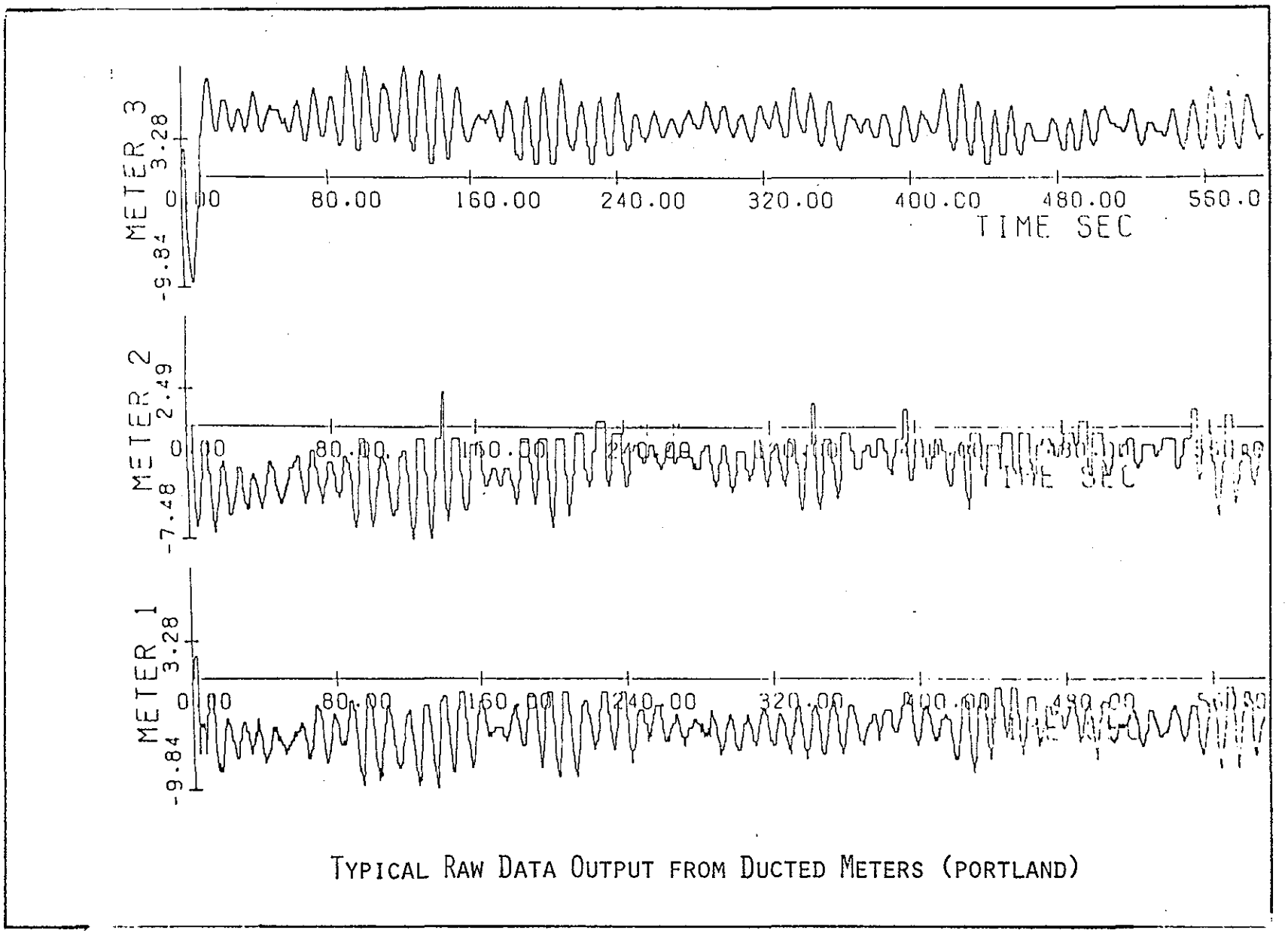

TYPICAL RAW DATA OUTPUT FROM DUCTED METERS (PORTLAND)

FIGURE 4.15

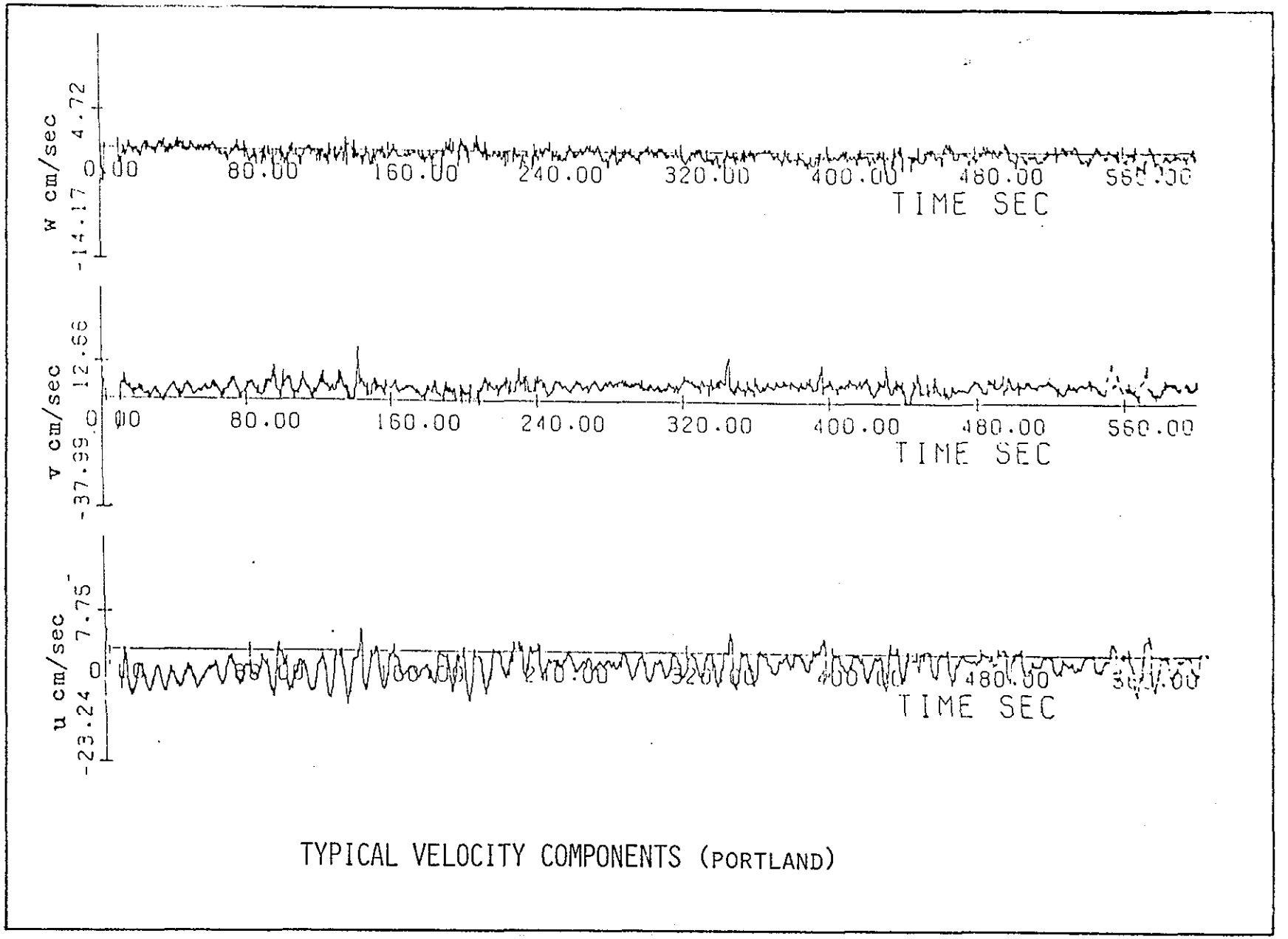

TYPICAL VELOCITY COMPONENTS (PORTLAND)

FIGURE 4.16

support pole was measured (by level) to within ± 0.5° of perpendicular to the water surface when mounted. All angles reported here are within ± 1.0°. Before the calibration all meter bearings were cleaned and inspected; the impeller supports were adjusted to correct small alignment errors.

During "towing" (this term will be used although the meters were not actually towed), the pole vibrated, especially at the higher tow speeds. The amplitude of this vibration at the meters was small and tends to be averaged out in the data processing. Thus these vibrations probably did not noticeably affect the calibration. Most of the test involved an uptank tow followed by a downtank tow. At tow speeds in excess of 20 cm/sec the ambient water was set in motion sufficiently to cause the meters to continue turning after the towing was stopped. Tests were not begun until the meters had stopped rotating.

All 10 of our meters were calibrated individually both for head-on calibration (pulses/sec vs. tow speed) and angle of attack response. Three meters were taken as standards and were calibrated precisely. For the individual calibrations the current meters were mounted three at a time on the support pole. The meters were at 33, 58, and 83 cm below the water surface. Figure 4.17 shows typical raw data output for the uptank and downtank tows.

In processing the data, the first and last 15 seconds of each run were ignored to ensure that start and stop transients were not included in the calibrations. The mean and standard deviation for each run were then computed. The standard deviation of the data about its mean, for each run, was about 0.2 cm/sec for low tow speeds. The quantization level of the electronics is 0.4 cm/sec ($q/(12)^{\frac{1}{2}}$). The standard deviation increased from the minimum of 0.2 cm/sec at low tow speeds to a value roughly 2 percent of the tow speed at high speeds. The estimates of mean value always had at least 100 data points (a minimum of 20 seconds of data). Thus the individual mean value estimates are at least 10 times more precise than the standard deviation of the individual data points, and we judge them to be acceptable.

The results of the head-on calibration of the meters are shown in Fig. 4.18. Here we show the individual data points, our best-fit straight line (labelled DAMOS), and the best-fit straight line as determined by Smith

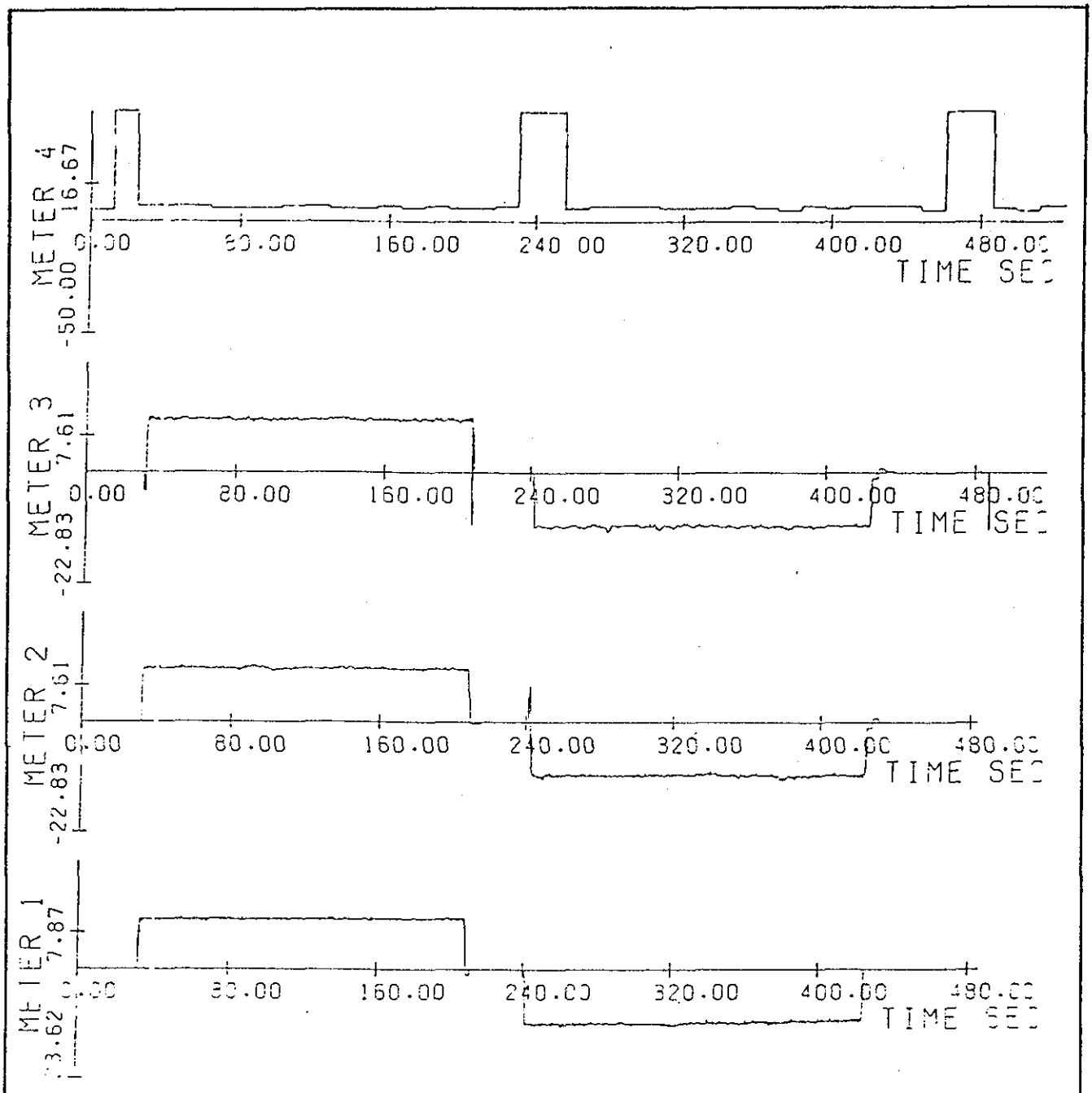

TYPICAL RAW DATA - MIT CALIBRATION TEST

FIGURE 4.17

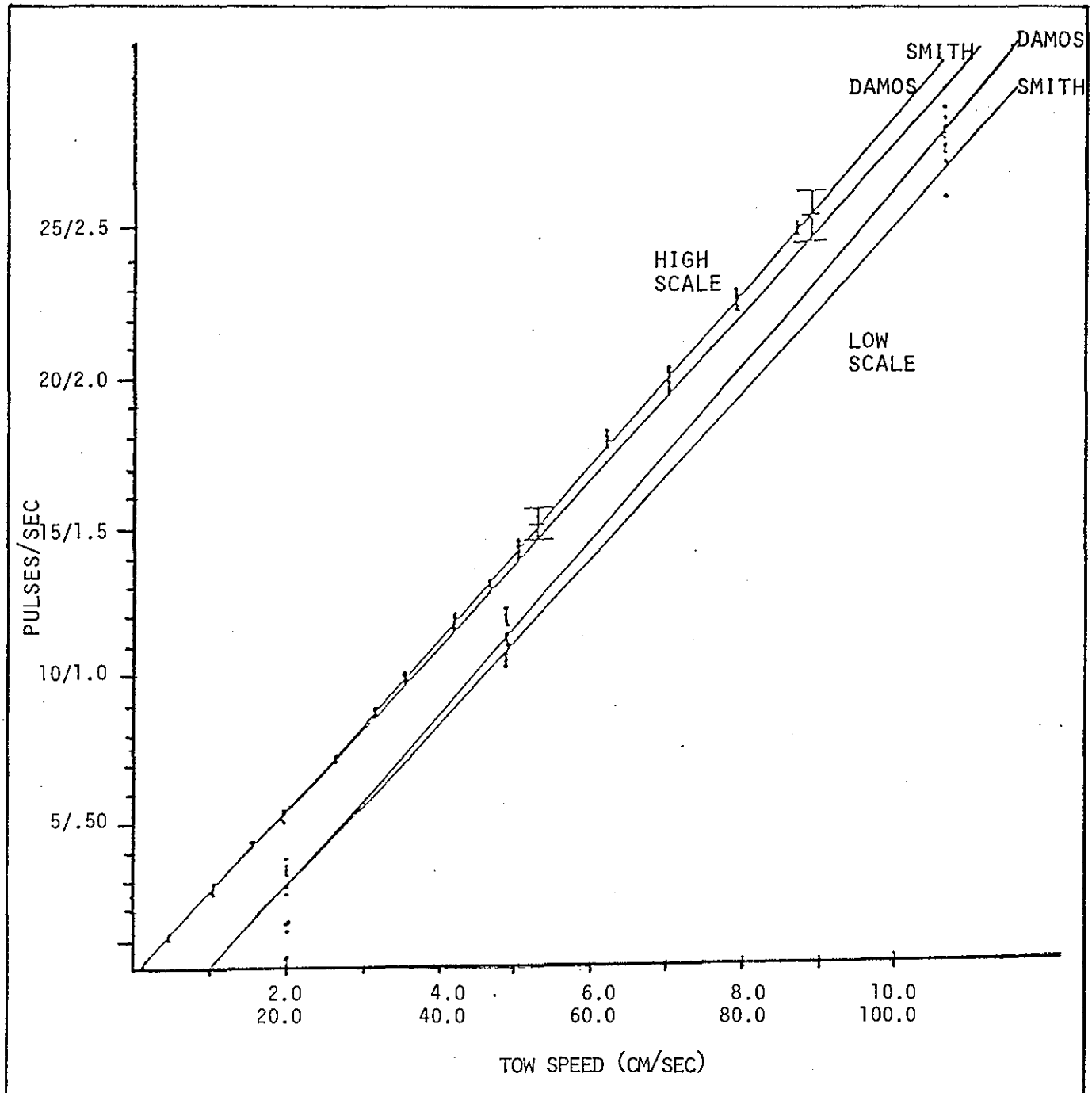

CALIBRATION OF CURRENT SPEED AT ZERO ANGLE OF ATTACK

FIGURE 4.18

(1978). The straight line is the best fit to all the data (all speeds, forward and backward). We have not yet investigated whether a higher-order polynomial, or different straight lines for different regions would better fit the data. McPhee (1975), using similar meters, found that his calibrations were best fit by straight-line segments.

The calibration appears to be linear. (This is not important as long as it is repeatable.) For the meters as a group, the calibration gives a precision of ± 0.3 cm/sec or 1 percent of the measured value, whichever is larger. This agrees with Smith's results. The repeatability of measurements for identical meters was examined at speeds of 10.7, 26.1, and 42 cm/sec. The average difference between measurements with the same meter was 0.2 cm/sec with no speed dependence noted; thus individual meters could be calibrated to a precision of ± 0.2 cm/sec.

The equation for the straight line we have plotted is: $V + 3.519f + 0.897$, where f is the tow speed (in cm/sec). Smith obtained $V = 3.601f + 1.089$. A more thorough curve-fitting analysis will be performed to see if this difference is statistically significant.

The error bars (Fig.4.18) are ± 5 percent of the actual value; this is the maximum allowable error for achieving stress measurements with relative errors of 10 percent. The DAMOS calibration is in agreement with Smith's calibration to within 5 percent. An earlier attempt to calibrate the meters on 5 March 1979, which was aborted because of electronics problems, did yield useful data. The data from that test exactly duplicate the data of Fig. 4.18, demonstrating that the experimental precision is good.

The data were examined to see if meter location affected the calibration. The difference between the middle meter and the other two meters is plotted in Fig. 4.19 as a function of tow speed for three separate tests. The top plot shows that meter 9 (the middle meter) was consistently slower than meters 1 and 3. This indicates that, while there are consistent differences between meters, there is no consistent effect due to meter location.

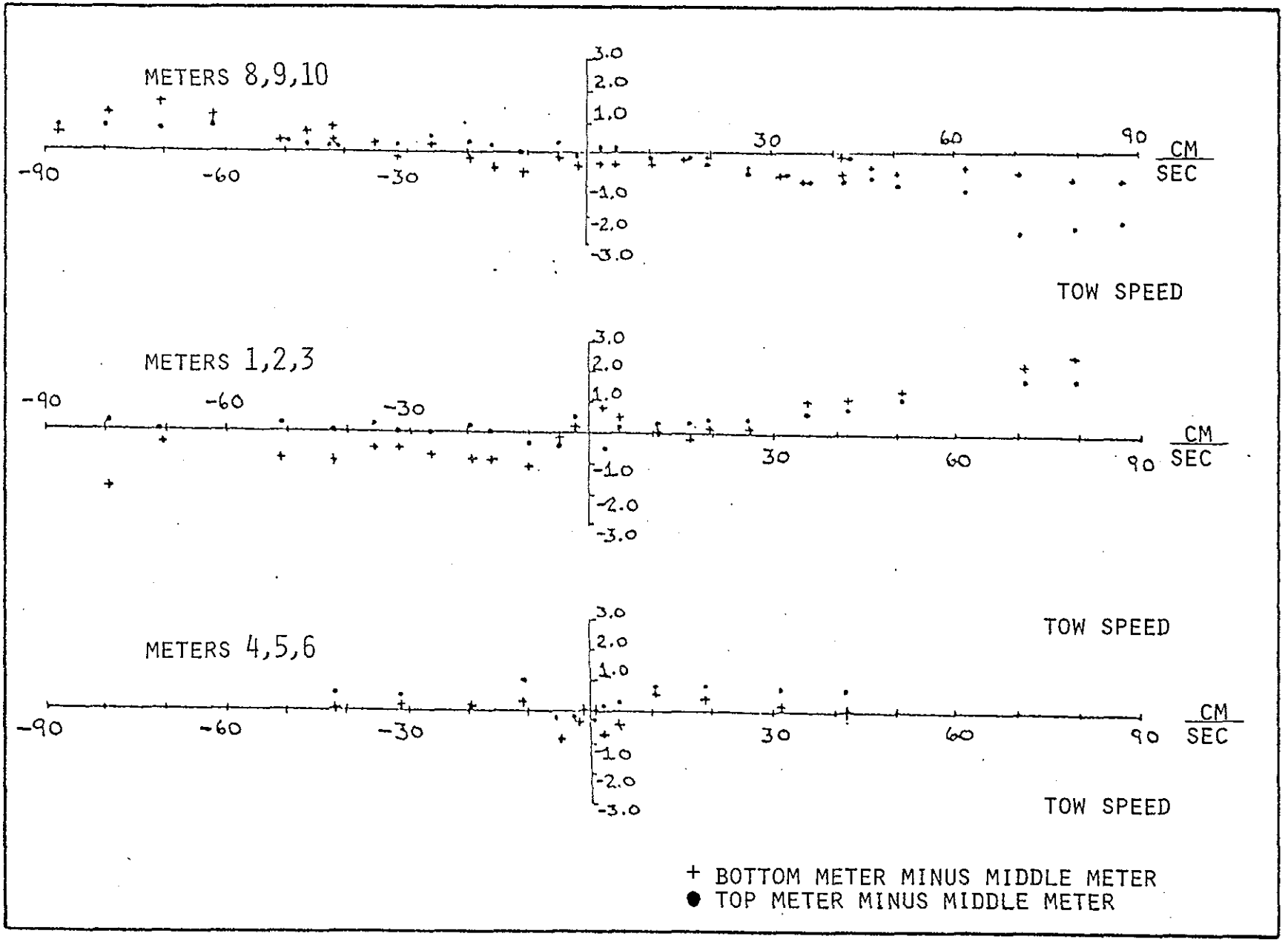

DIFFERENCE BETWEEN CURRENT METER OUTPUTS

FIGURE 4.19

The minimum or threshold velocity for reliable rotation was also investigated. All but two of the meters rotated reliably at 2 cm/sec. Below 2 cm/sec none of the meters rotated reliably. The threshold for steady rotation of the group of meters is estimated to be slightly greater than 2 cm/sec.

The spacing between the tip of current meter rod and the impeller blade is variable, thus it is of interest to know how sensitive the calibration is to this spacing. It was found that if the spacing was greater than 2.0 mm the calibration was not noticeably affected. At a spacing of 1.0 mm the recorded speed increased by 1 percent of the actual speed. This was a very brief test and the result may be spurious; it does indicate, however, that the calibration is not particularly sensitive to spacing. The meters were calibrated at a spacing of 2.0 mm.

Ideally, the response of the meters should decrease proportionally to the cosine of the angle of attack. This difficult design goal cannot be achieved exactly; thus a correction for angle of attack is required. This correction is shown in Fig. 4.20 and 4.21 as a multiplicative function (Smith, 1978). If the correction function is less than unity for a given angle, that meter reads higher than it would for a perfect cosine response. Different corrections are required for rotations in the plane of the support rod (Θ) and for rotations about the support rod ($\emptyset$).

In Fig. 4.20 and 4.21 we have plotted the angle of attack correction for Θ and $\emptyset$ for the DAMOS calibration and the Smith (1978) calibration, along with the 7th-order polynomial fitted by Smith to the data. The results are similar, with the exception of the several obviously high values at large angles of attack. Most of these high values came from the same set of three meters which, incidentally, were our newest meters and had never been used in the field. There is no obvious difference in construction between these newest meters and the earlier ones to account for this discrepancy. Smith concludes that for flow speeds above 7 cm/sec, the angle of attack correction is good to $\pm$ 0.3 cm/sec or 2 percent of the actual value, whichever is larger. Note that the error becomes larger as the angle of attack increases.

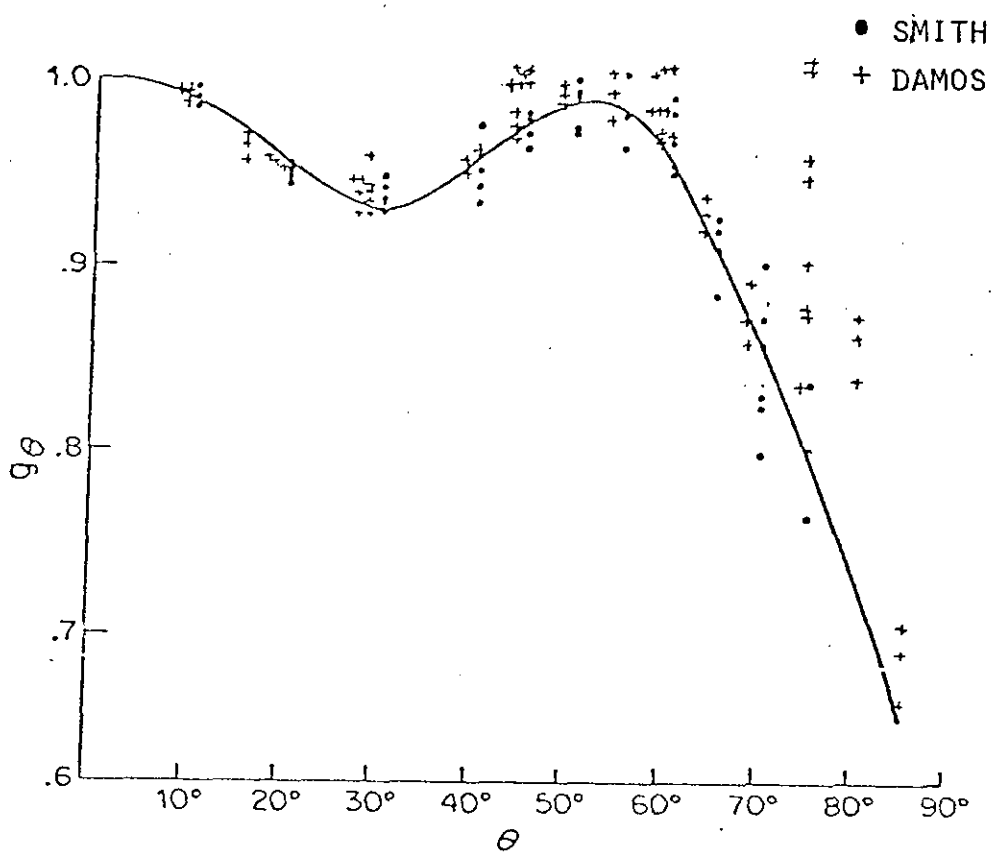

ANGLE OF ATTACK CORRECTION - FOR ALL PULSE CURRENT METERS CONSIDERED TOGETHER, WHEN THEY ARE ROTATED IN THE UPSTREAM DIRECTION IN THE PLANE OF THEIR SUPPORT RODS

FIGURE 4.20

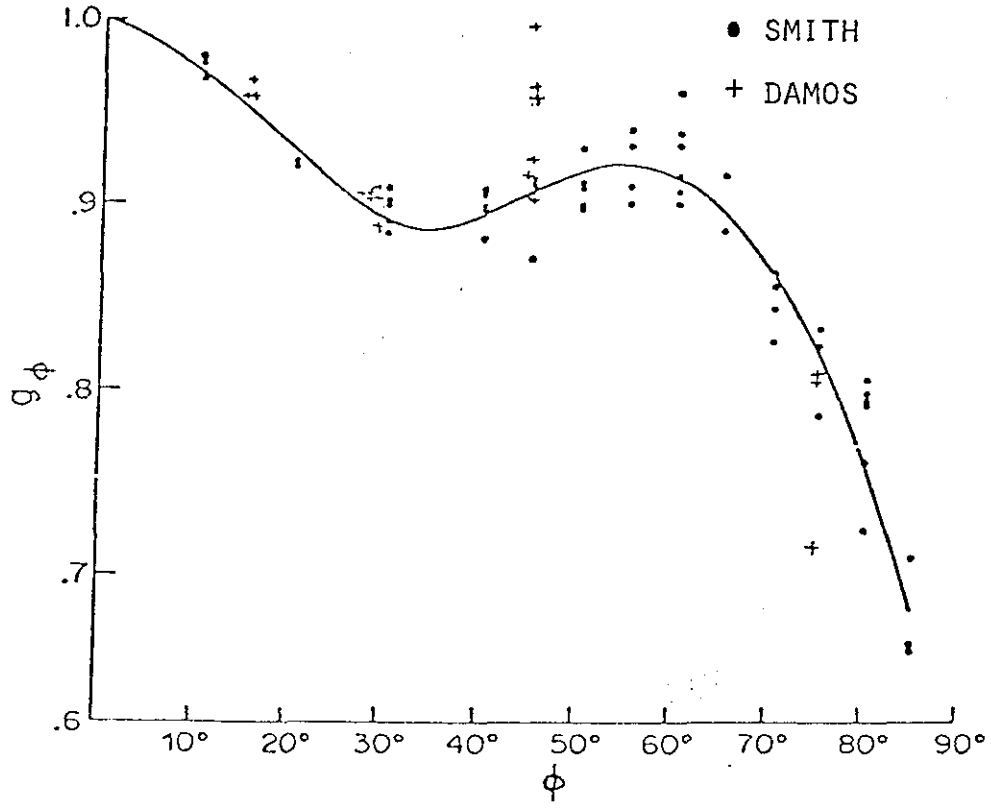

ANGLE OF ATTACK CORRECTION - FOR ALL PULSE CURRENT METERS CONSIDERED TOGETHER, WHEN THEY ARE ROTATED AROUND THE AXES OF THEIR SUPPORT RODS

FIGURE 4.21

The meter triads were also calibrated as a function of horizontal angle and speed. The results of this calibration are shown in Figs. 4.22 and 4.23 for the unidirectional and the bidirectional triads, respectively. The raw data for each meter were corrected for angle of attack using the interpolation procedure described by Smith (1978); u, v, and w were then calculated from the geometry of the triad. We have plotted the magnitude of the response normalized by the average calibration of the three meters used and the horizontal and vertical angular errors as a function of horizontal angle. The normalized magnitude would be unity for all angles, and the horizontal and vertical angular errors would be zero if the triad had no effect on the flow. Error bars based on the accuracy of the meter calibration and the geometry of the configuration are indicated. Results are shown for tow speeds of 26.1 and 10.7 cm/sec.

The unidirectional configuration has a flat response with a reduction in magnitude of 5 percent between ± 50°. There is slight evidence of asymmetry (therefore a trend) in the angular errors, possibly due to misplacement of the meters, but the observed errors are within the error bars. The bidirectional triad is unaffected for normal incidence but undergoes a 10 percent reduction at 90°. No significant effect due to speed is noted. One set of data (the rectangles in Fig. 4.23) was taken with the meters almost touching. No significant effect was noted (for angles less than 30°), indicating that these calibrations are not overly sensitive to configuration spacing. (The spacing can, of course, be tightly controlled.)

These tests were conducted using just one set of meters. It would be useful to repeat them with several different sets of meters to obtain a larger data base. This will be done when and if there is a calibration of the proposed omnidirectional configuration.

A preliminary check of current meter frequency response was made by towing the meters through the wave field generated by the towing facility wave generator. Results are shown in Fig. 4.24. The downtank tow (away from the waves) has a frequency of 0.58 Hz, whereas the uptank tow has a frequency of 0.73 Hz. A future frequency response calibration might be based on this method.

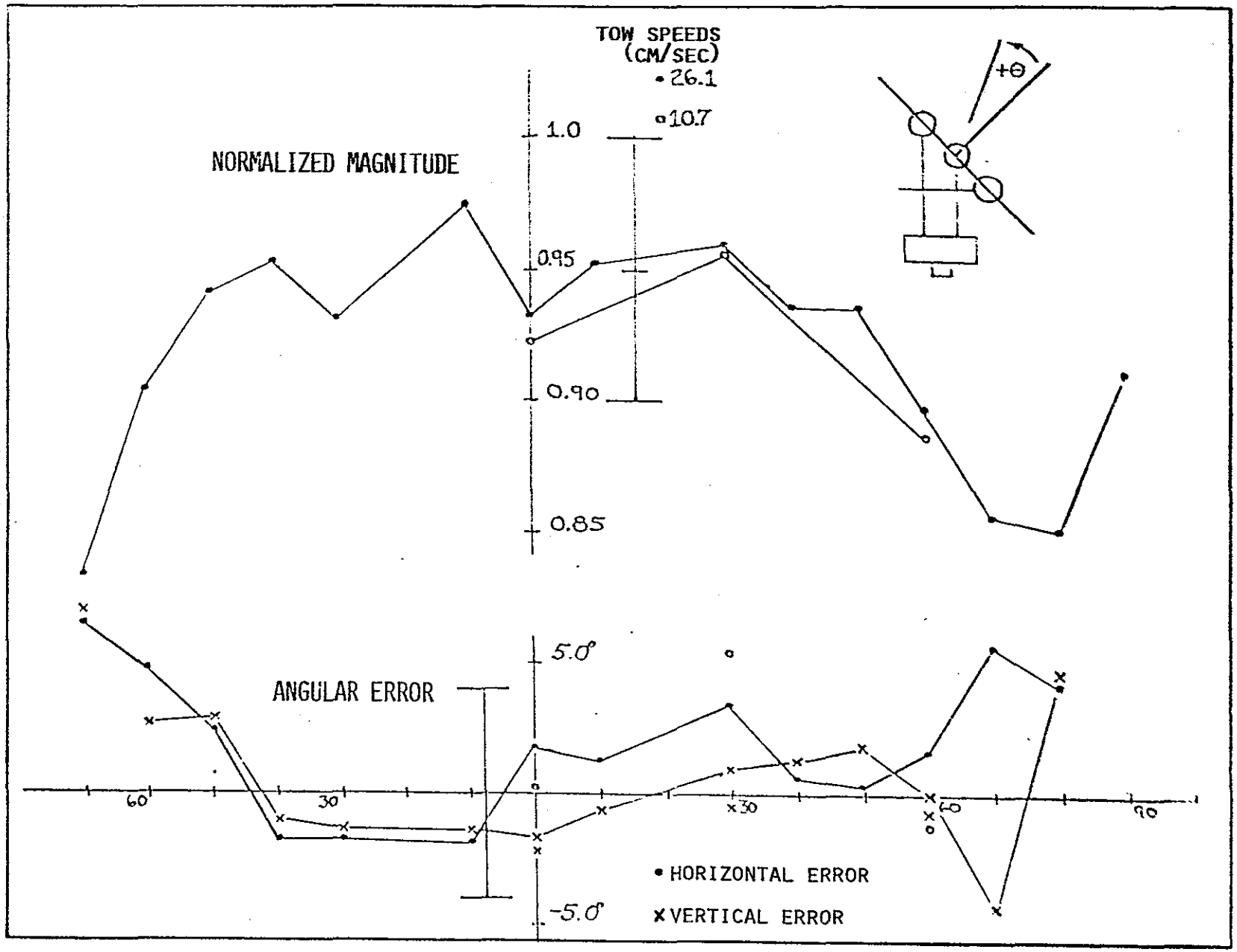

CALIBRATION OF UNIDIRECTIONAL TRIAD

FIGURE 4.22

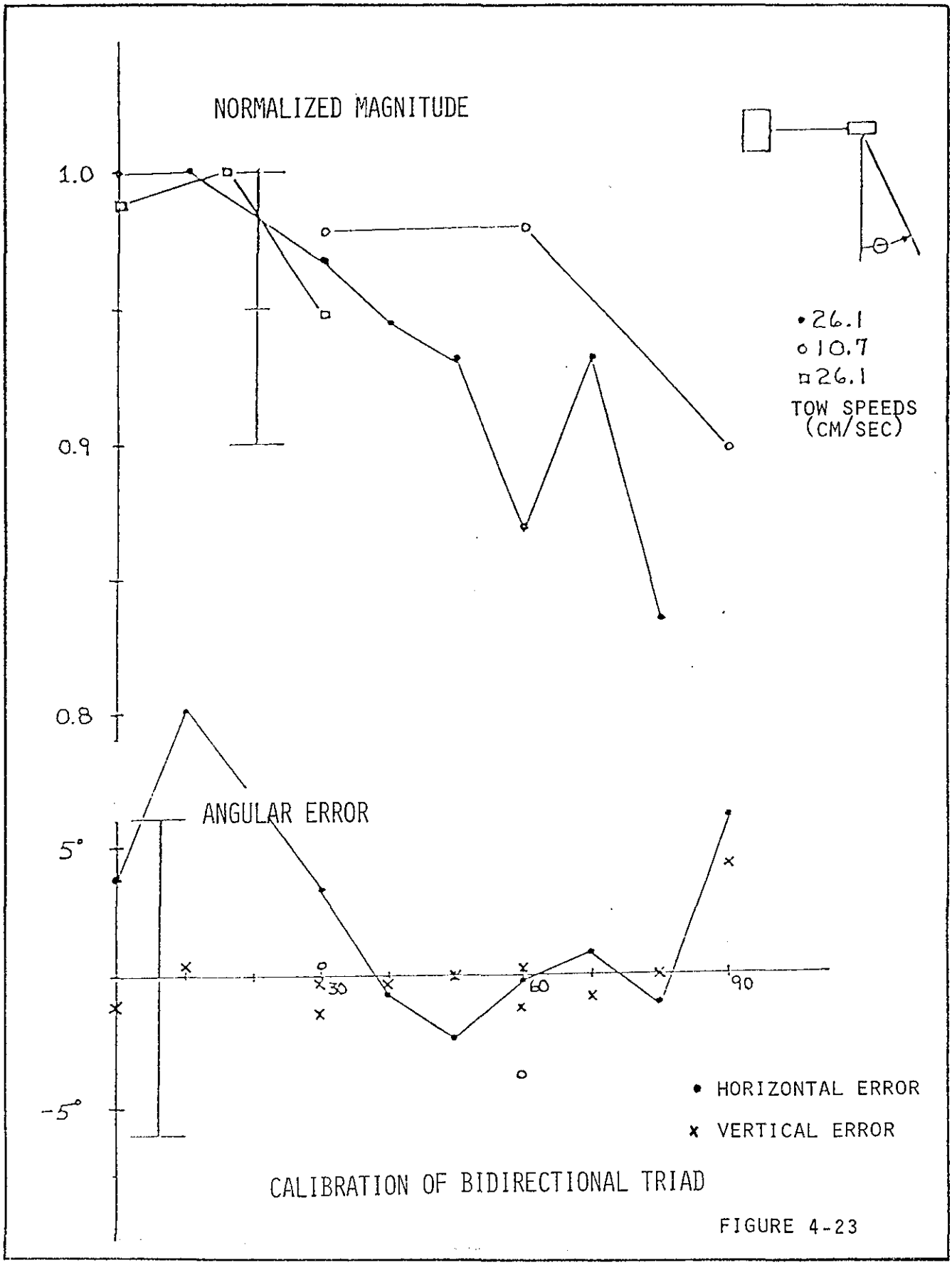

CALIBRATION OF BIDIRECTIONAL TRIAD

FIGURE 4-23

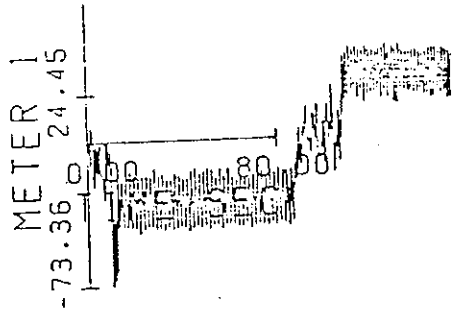

OUTPUT OF CURRENT METER WHEN TOWED THROUGH
A WAVE FIELD

FIGURE 4.24

4.6 ACKNOWLEDGMENT

Tony Petrillo (URI) assisted in all BOLT tests and assumed major responsibility for field deployments; John Roklan (NUSC) designed the BOLT electronics and is responsible for hardware and software modifications.

4.7 REFERENCES

Ariathurai, R., and R. B. Krone. 1976. Finite element model for cohesive sediment transport. J. Hyd. 102: 323-38.

Cartwright, D. E. 1961. A study of currents in the Strait of Dover. J. Inst. Nav. 14: 130-51.

Cook, G. S., R. W. Morton, and A. T. Massey. 1977. A teport on environmental studies of dredge spoils disposal sites. In: Bottom turbulence, J. Nihoul (ed.), Elsevier, Amsterdam.

Dyer, K. R. 1976a. Current velocity profiles in a tidal channel. Geophys. J. Roy. Astr. Soc. 22: 143-61.

Dyer, K. R. 1976b. The measurement of bed shear stresses and bedload transport rates. In: Estuarine processes. M. Wiley (ed.), Academic Press, N.Y.

Falco, R. E. 1977. Coherent motions in the outer regions of turbulent boundary layers. Phys. Fluids 20: 393-4.

Gordon, C. M. 1974. Intermittent

Gordon, C. M. 1975a. Period between bursts at high Reynolds number. Phys. Fluids 18: 141-3.

Gordon, C. M. 1975b. Sediment entrainment and suspension in a turbulent tidal flow. Mar. Geol. 18: M57-M64.

Gordon, C. M., and J. Witting. 1977. Turbulent structure in a benthic boundary layer. In: Bottom turbulence. J. Nihoul (ed.), Elsevier, Amsterdam.

Grant, W. D., and O. S. Madsen. 1979. Combined wave and current interaction with a rough bottom. J. Geophys. Res. 84: 1797-1808.

Heatherstraw, A. D. 1974. Bursting phenomena in the sea. Nature 248: 393-5.

Heatherstraw, A. D., and J. Simpson. 1978. The sampling variability of the Reynolds stress. Est. Coast. Mar. Sci. 6: 263-74.

Hinze, J. O. 1959. Turbulence. McGraw-Hill, N.Y.

Kaimal, J. C., and D. A. Haugen. 1969. Some errors in the measurement of Reynolds stress. Jour. App. Met. 8: 460-462.

Jinarm, O. D. (1976). Boundary layer flow under steady unidirectional currents. In: Marine sediment transport and environmental management, D. J. Stanley and D. Swift (eds.), Wiley, N.Y.

Liepmann, H. W. 1979. The rise and fall of ideas in turbulence. Amer. Sci. 67: 221-8.

Madsen, O. S. 1976. Wave climate of the continental margin: elements of its mathematical description. In: D. J. Stanley and D. Swift, (eds.), Marine sediment transport and environmental management, Wiley, N.Y.

McPhee, M. G. 1975. An experimental investigation of the boundary layer under pack ice. Dep. Oceanogr., Univ. Washington, Seattle. Tech. Rep. M74-14.

Mollo-Christensen, E. 1971. Physics of turbulent flow. AIAA J. 9: 1217-1228.

Monin, A. S., and A. M. Yaglom. 1975. Statistical fluid mechanics. II. MIT Press, Cambridge, Mass.

Mulhearn, P. J. 1978. Turbulent flow over a periodic rough surface. Phys. Fluids 21: 1113-5.

Schlichting, H. 1960. Boundary layer theory. McGraw-Hill, N.Y.

Seitz, R. C. 1973. Observations of intermediate and small scale turbulent water motion in a stratified estuary. Chesapeake Bay Inst., Johns Hopkins Univ. Tech. Rep. 79.

Smith, J. D. 1978. Measurement of turbulence in ocean boundary layers. Proc. of a Working Conference on Current Measurements, Coll. Mar. Stud., Univ. Delaware, Newark. Tech. Rep. DEL-SG-3-78.

Smith, J. D., and S. R. McLean. 1977. Spatially averaged flow over a wavy surface. J. Geophys. Res. 82: 1775-1746.

Tochko, J. S. 1978. Study of the velocity structure in a marine boundary layer; instrumentation and observation. Unpublished Dissertation. MIT/WHOI Joint Prog. Oceanogr., Woods Hole, Mass.

Williams, A. J., and J. S. Tochko. 1977. An acoustic sensor of velocity for benthic boundary layer studies. In: Bottom turbulence, J. Nihoul (ed.), Elsevier, Amsterdam.

Wiseman, W. J. 1969. On the structure of high-frequency turbulence in a tidal estuary. Chesapeake Bay Inst., Johns Hopkins Univ. Tech. Rep. 59.

APPENDIX 4.1

Conversion of raw meter output to u, v, w velocity components

Assuming that the current meters have a perfect cosinusoidal angle of attack response, the relation between the raw meter outputs u_1, u_2, and u_3 and the x, y, z components of the current u, v, w, is

$$u_i = \cos \Theta_{xi} + v \cos \Theta_{yi} + w \cos \Theta_{yi} + \cos \Theta_{zi},$$

where Θ_{xi} is the angle between the positive x axis (u direction) and the positive (zero angle of attack) axis of the i^{th} meter, where i = 1, 2, 3. Thus u, v, w can be found in terms of the raw meter outputs as long as the direction angles are known. These angles must be determined separately for the individual configurations.

Unidirectional configuration

Using the geometry shown in Fig. A.1, direction angles are determined as shown in Table A.1. Then we have

$$u_1 = \tfrac{1}{2}u + \tfrac{1}{2}v - \tfrac{1}{2}w$$
$$u_2 = \tfrac{1}{2}u + \tfrac{1}{2}v + \tfrac{1}{2}w$$
$$u_3 = \tfrac{1}{2}u - \tfrac{1}{2}w$$

and

$$u = \tfrac{1}{2}(u_1 + u_2) + \tfrac{1}{2}u_3 \qquad (A.1)$$
$$v = \tfrac{1}{2}(u_1 + u_2) - \tfrac{1}{2}u_3$$
$$w = \tfrac{1}{2}(u_2 - u_1)$$

Bidirectional configuration

Using the geometry shown in Fig. A.2, direction angles are determined as shown in Table A.1. Then we have

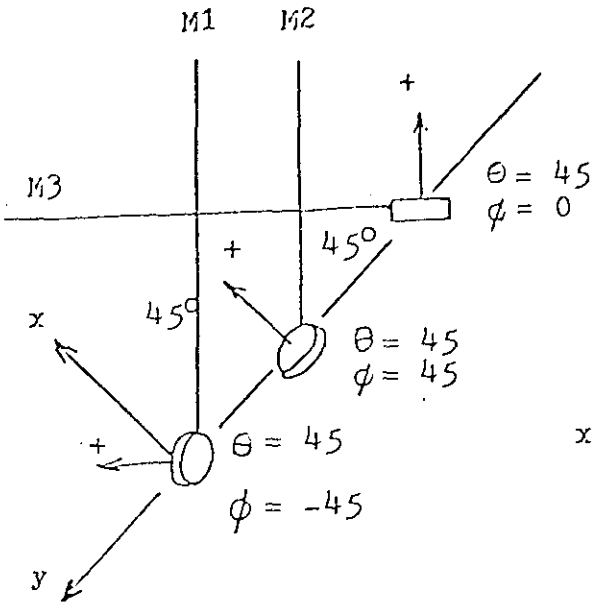

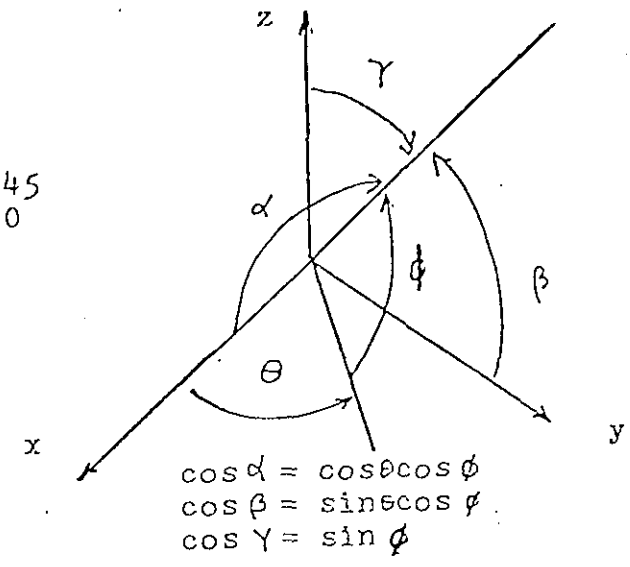

GEOMETRY FOR UNIDIRECTIONAL TRIAD FIGURE A.1

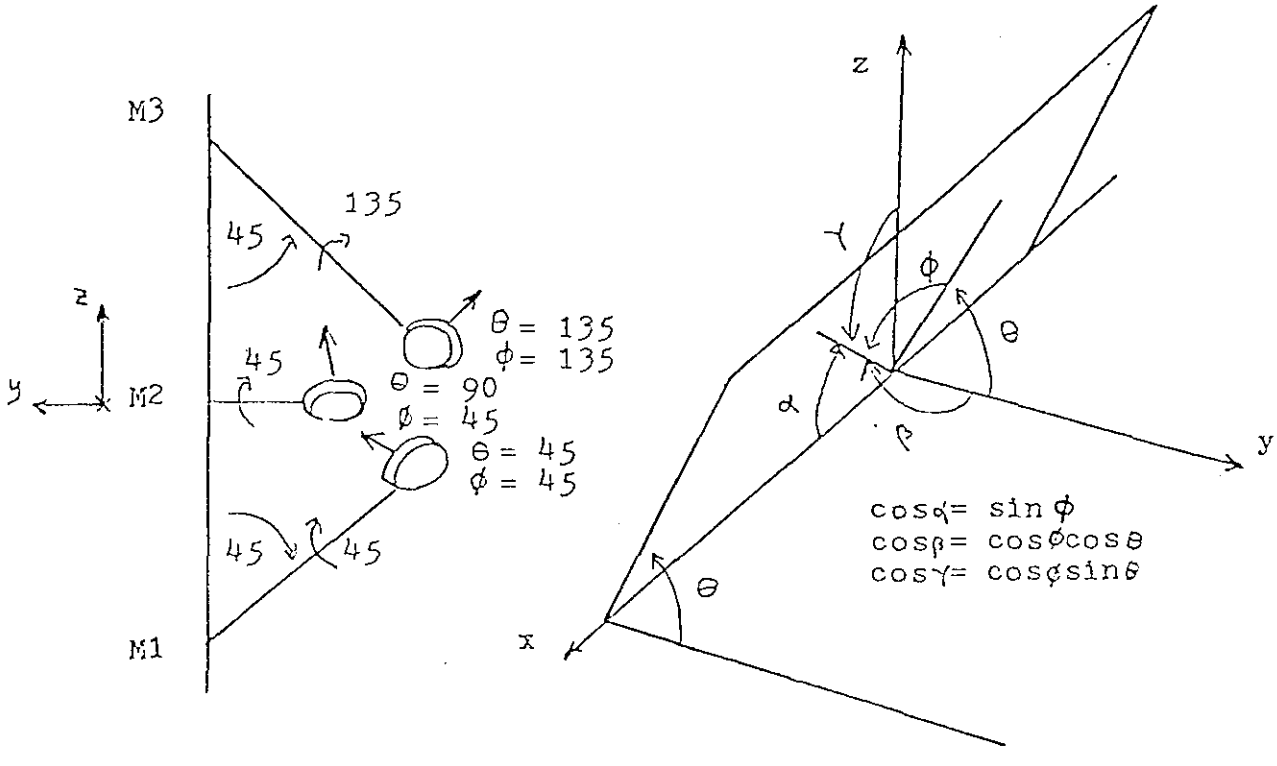

GEOMETRY FOR BIDIRECTIONAL TRIAD FIGURE A.2

$$u_1 = \tfrac{1}{2}u + \tfrac{1}{2}v + \tfrac{1}{2}w$$
$$u_2 = \tfrac{1}{2}u + \tfrac{1}{2}w$$
$$u_3 = \tfrac{1}{2}u + \tfrac{1}{2}v - \tfrac{1}{2}w$$

and (A-2)

$$u = 2u_2 - u_1 + u_3$$
$$v = 2(u_1 - u_3) + u_1 + u_3 - 2u_2$$
$$w = 2(u_1 - u_3).$$

Table A.1 Direction angle for unidirectional and bidirectional configurations

Configuration	Θ_{x1}	Θ_{y1}	Θ_{z1}	Θ_{x2}	Θ_{y2}	Θ_{z2}	Θ_{x3}	Θ_{y3}	Θ_{z3}
unidirectional	60	60	135	60	60	45	45	135	0
bidirectional	45	60	60	45	90	45	45	60	120

APPENDIX 4.2

Error analysis

The precision in measurement required to make accurate velocity and stress measurements is considered. First, consider the accuracy with which measurements of u, v, and w can be made using the different triads. Assume that the uncorrelated measurement errors for the individual meter outputs are $\pm e_i$. Then, for example, from Equations A.1, the worst case error in the u measurement, using the unidirectional configuration is

$$e_{u_{wc}} = \pm \tfrac{1}{2}(e_1 + e_2) + \tfrac{1}{2} e_3.$$

The RMS error (ensemble averaged over the set of meters) is

$$e_{uRMS} = [\tfrac{1}{4}(e_1^{\,2} + e_2^{\,2}) + \tfrac{1}{2} e_3^{\,2}]^{\frac{1}{2}}.$$

Assuming the e_i are equal, and taking $e_i^{\,2} = \overline{e_i}^{\,2}$, we have $e_{uwc} = \pm 1.7e$ and $e_{uRMS} = \pm e$. Similar results are given in Table A.2 for u, v, and w for both the unidirectional and the bidirectional configurations.

Table A.2 Velocity measurement errors

	$\frac{e_{uwc}}{1.7e}$	$\frac{e_{urms}}{e}$	$\frac{e_{vwc}}{1.7e}$	$\frac{e_{vrms}}{e}$	$\frac{e_{wwc}}{1.4e}$	$\frac{e_{wrms}}{e}$
unidirectional						
percent of V		3		3		3
quantization error		0.1,0.2		0.1,0.2		0.1,0.2
bidirectional	3.4e	2e	4.8e	3.2e	2e	2e
percent of V		6		10		4
quantization error		0.2,0.4		0.3,0.6		0.2,0.4

The unidirectional configuration is inherently more precise than the bidirectional configuration since its internal angles are orthogonal. We can

conservatively estimate e by combining the precision of the head-on calibration (± 0.3 cm/sec or 1 percent of speed) with that of the angle of attack correction (± 0.3 cm/sec or 2 percent of speed, but actually variable with angle of attack). The RMS error due to these two factors is 0.4 cm/sec or 3 percent of the actual speed. The quantization increments for the BOLT electronics are either 0.2 or 0.4 cm/sec (rms error of 0.1 or 0.2 cm/sec), which are on the order of the inherent accuracy of the meters. The percentage error for the various velocities are written in the RMS error column in Table A.2. These indicate the precision of individual u, v, and w data points. The error due to quantization noise is also shown.

We now determine the errors in instantaneous stress measurements due to errors in u and w. Thus, let u_m (the measurement) = u (the actual value) ± e_u (the error). Then

$$u'w' = (u_m-\bar{u}_m)(w_m-\bar{w}_m) = (u-\bar{u}+e_u-\bar{e}_u)(w+e_w-\bar{e}_w).$$

The relative error for individual data points is

$$\frac{u'w'-(u-\bar{u})w}{(u-\bar{u})w} = \frac{e_u-\bar{e}_u}{u-\bar{u}} + \frac{e_w-\bar{e}_w}{w} + \frac{(e_u-\bar{e}_u)(e_w-\bar{e}_w)}{(u-\bar{u})w}$$

The overbar represents a long-term time average sufficient to establish a valid mean for u, etc. $e_u-\bar{e}_u$ represents the error after any trends (due for example to the actual calibration of the individual meters being different from the group calibration) have been subtracted out. Thus $e_u-\bar{e}_u$ depend on the precision of individual current meters; we estimate this as either 0.5 percent of the true speed (Smith, 1978) or as the quantization noise floor. Thus we see that for individual points the relative stress error can become large, especially if u or w is small.

The error in the average stress is

$$\overline{u'w'} - (\overline{u'\bar{u}})w - \overline{(e_u-\bar{e}_u)(e_w-\bar{e}_w)}.$$

For the unidirectional configuration this is

$$\overline{u'w'} - \overline{(u-\bar{u})w} = \frac{1}{2\sqrt{2}}\overline{(e_1 - \bar{e}_1)^2} - \overline{(e_2 - \bar{e}_2)^2}$$

Since the variances of the errors of the meters are likely to be similar, this error will be small.

For the bidirectional configuration the error in the average stress is

$$\overline{u'w'} - \overline{(u-\bar{u})w} = -\left[\overline{(e_1 - \bar{e}_1)^2} + \overline{(e_3 - \bar{e}_3)^2}\right]$$

Ordering $e_i - e_i$ as U/100 and (u-u)w as $3\times10^{-3}U2$, we find relative stress errors of about 10 percent; for low speeds the relative errors would be greater, since the meter error would then be dominated by the quantization noise.

To this point we have considered errors due only to meter calibration errors; we now consider errors due to angular inaccuracies in the placement of the meters within the triads. Kaimal and Haugen (1969) review the meteorological literature on this subject.

For the error resulting from a complete axis rotation (referred to as levelling error in the meteorological literature), as in Fig. A.3, the measured components of velocity will be

$$u_m = u \cos + w \sin$$
$$w_m = u \sin + w \cos.$$

We will usually rotate the axes numerically so that w = 0. If this is done perfectly there will be no error. If there is a residual angular error, the error in the instantaneous stress will be

$$u_m'w_m' - u'w' + (w'^2 - u'^2).$$

Roughly ordering w' as u/20 and u' as u/10 we find instantaneous errors of about $10^{-2}u^2$. With u + 20 cm/sec, $\Delta\theta$ = 5°, this leads to errors of ± 0.3 dynes/cm², or a relative error of about 15 percent.

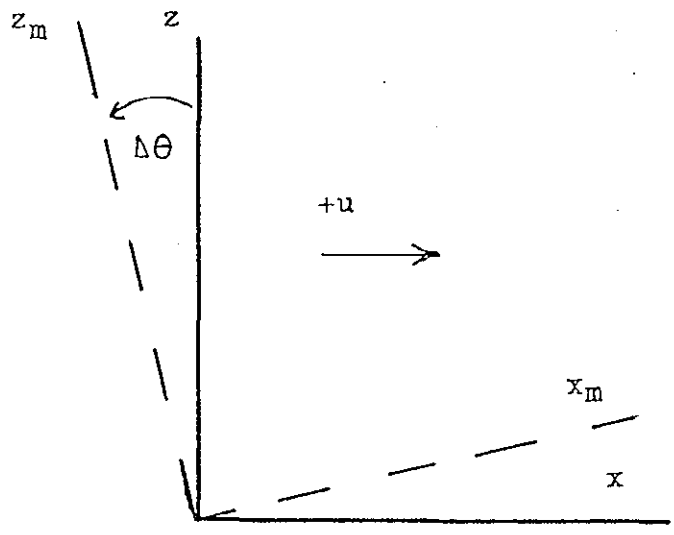

GEOMETRY FOR AXIS ROTATION ERRORS

FIGURE A.3

The relative error in the average stress is

$$\frac{u_m' w_m' - u'w'}{u'^2} \quad \frac{w'^2 - u'^2}{u'^2}.$$

With $w'/u_* + 2.5$ (Kaimal and Haugen, 1969) we require $\Delta\theta$ less than 1/25° to obtain relative average stress measurements of 10 percent.

We can also assume that instead of a rotation of axes there is a misalignment of one axis. After rotating so that $w_m = 0$, this leads to relative stress errors of the order

$$\frac{w^{12}}{u^{12}}.$$

This requires $\Delta\theta$ of 4° to obtain relative stress errors of 10 percent. We note that the accuracy requirements on the actual placement of the meters will be more stringent than given here, since the results here represent the errors due to errors in the effective coordinate systems of the triads. The errors in velocity and stress measurements due to angular uncertainties within the triads will be worked out in detail and presented in a future report.

5.0

SEDIMENT CRITICAL STRESS PARAMETERS

RICHARD M. HEAVERS & VITO A. NACCI

5.0 SEDIMENT CRITICAL STRESS DETERMINATION

5.1 INTRODUCTION

Materials dredged from the bottoms of harbors and waterways are presently being deposited at selected offshore locations. The resulting dredged spoil deposits often consist largely of clay- and silt-size materials which have a high organic content. As these sediments may also contain heavy metals, pesticides, and nutrients, there is concern about future erosion and transport of sediment from dredged spoil mounds.

For cohesive sediments, interparticle bonds must be broken before entrainment in a flow can take place. That a critical fluid shear stress on the bed must be exceeded before surface erosion of the bed can begin is well-documented in the literature.

According to Ariathurai and Krone (1976):

> The resistance of a cohesive bed to erosion by flowing water depends on the following: (1) types of clay minerals that constitute the bed; (2) structure of the bed (which in turn depends on the environment in which the aggregates that formed the bed were deposited), time, temperature, and the rate of formation; (3) chemical compositions of the pore and eroding fluids; (4) stress history, i.e., the maximum overburden pressure the bed has experienced and the time at various stress levels; and (5) organic matter and its state of oxidation.

Krone (1962) observed that settled aggregates are crushed by those settling above, resulting in an increased number of interparticle bonds. This in turn causes an increase in resistance to fluid shear stress occurring in layers of about 2.5-cm thickness, until the overburden is sufficient to crush the aggregates to primary particles. It is therefore apparent that an undisturbed (unremolded) sediment sample is required if in-situ critical shear stress is to be obtained from laboratory flume measurements. Undisturbed samples should be several times 2.5 cm in thickness.

Turbulence measurements made in the benthic boundary layer by other investigators will provide estimates of the magnitude and direction of the horizontal stress τ exerted on the ocean bottom. Predictive knowledge of the stress τ, together with critical erosion stress τ_c and erosion rate $\dot{\varepsilon}$ for $\tau > \tau_c$ must be available for numerical models of long-term stability of dredged spoil mounds.

5.2 SAMPLER

The undisturbed surface sediment sampler (USSS) is shown assembled in Fig. 5.1. The USSS consists of a frame with weighted feet to support the sampler subassembly (lower center of Fig. 5.1) on the ocean bottom. The subassembly contains a plastic sample box which is open at top and bottom, and has inside dimensions of 1 m in length, 13 cm in width, and 15 cm in height. Sample thicknesses must be less than 15 cm.

After the sampler frame has stabilized on the ocean bottom, the subassembly and sample box sink into the bottom sediment to a depth limited by an adjustable horizontal bearing plate on each side of the subassembly. An undisturbed sediment sample is then sliced at the level of the box bottom by 0.03-cm-thick stainless steel sheets (closures) which travel in slots milled in the sides of the subassembly. The closures are activated by falling lead cylinders located on each end of the subassembly. The cutting ends of the closures are fitted with knife edges which butt together following slicing to eliminate winnowing of sediment as the USSS is retrieved. The top of the sample box is covered by a plate fitted with flapper valves for exhausting water from the inside of the sample box and to prevent winnowing.

A sample retrieval and transport system for use with the USSS is nearly complete. The sample in the sample box will be deposited directly from the subassembly into a transport caddy. Closed-cell foam rubber will be used to insulate the sample in the caddy from mechanical and thermal shock during transport. To eliminate erosion of the sediment sample by waves in the caddy, there will be no free surface bounding the fluid above the sample.

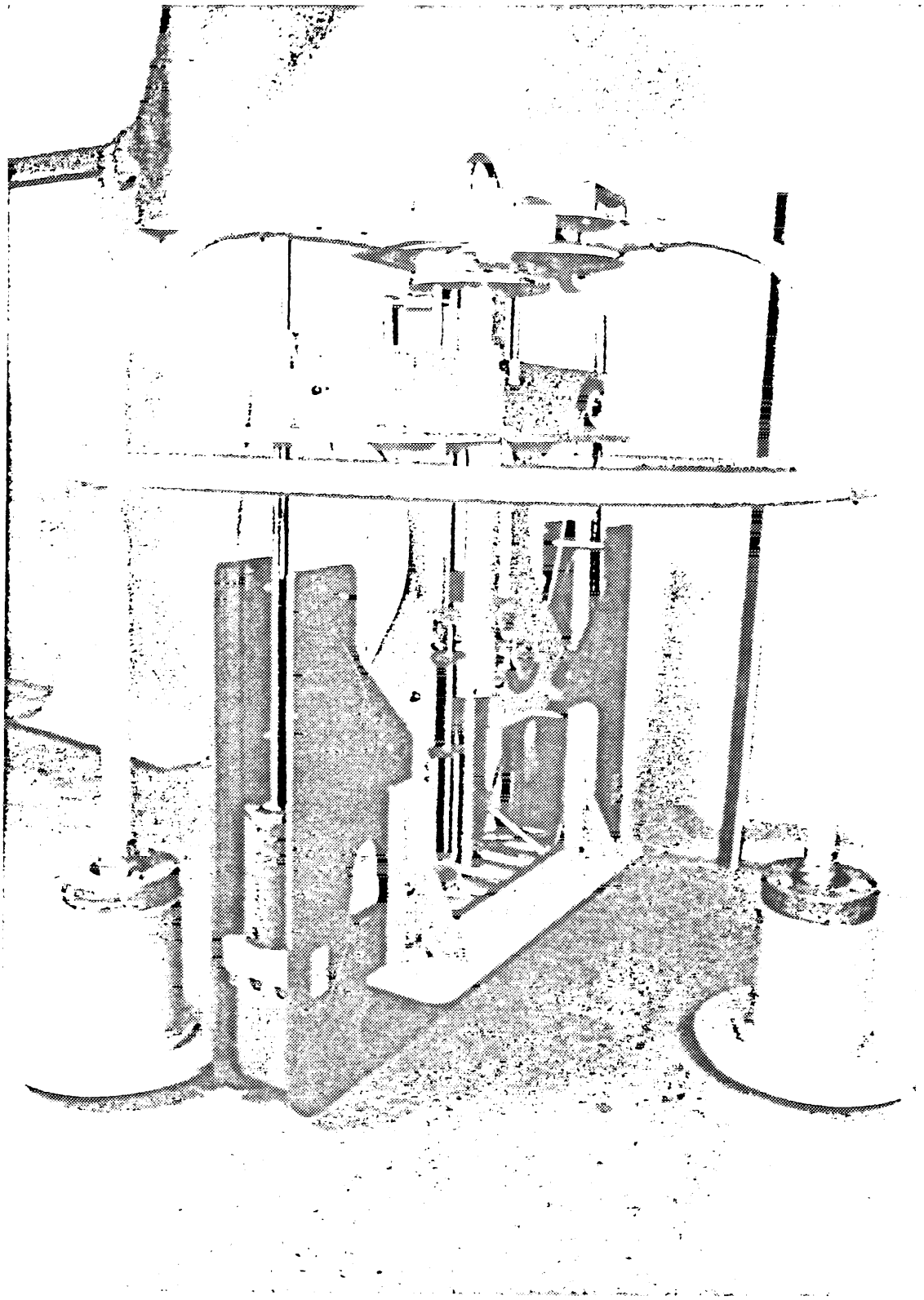

UNDISTURBED SURFACE SEDIMENT SAMPLER (USSS)
(NOTE 2 METER SCALE IN BACKGROUND)

FIGURE 5.1

The USSS has been field tested on three occasions, but is not yet fully operational.

5.3 FLUME MEASUREMENTS

Water flowing in the recirculating flume (Fig. 5.2) follows an oval path about 10 m in length. A sample to be examined is placed in the instrumented section (Fig. 5.3) which has a 15.2 cm^2 cross section. The mean horizontal speed $\bar{U}_{max}$ at the center of this cross section may be varied from 0 to 1 m/sec by use of a valve and/or by changing the propeller pitch. Water temperature in the flume may be controlled to within $\pm$ 0.2°C and increased or decreased at about 0.5°C/min.

The center line speed $\bar{U}_{max}$ is measured with a small ducted impeller current meter. Suspended sediment concentration is measured with a laser-photocell system calibrated for each sediment sample. The average horizontal shear stress τ on the bottom as a function of $\bar{U}_{max}$ (Fig. 5.4) was measured by Gularte (1978) using a shear tray mounted on strain gauges. The shear tray contained a smoothed clay bed.

The vertical variation of the average horizontal speed $\bar{U}_{max}$ above the smoothed bed (Fig. 5.5) was measured with a DISA 55R61 hot film probe in conjunction with a DISA 55D01 constant temperature anemometer. The root mean square velocity fluctuation (standard deviation, σ) was measured with a DISA 55D30 rms voltmeter. At 7.6 cm above the bed, the ratio $\sigma/\bar{U}_{max}$ was 0.13 for $\bar{U}_{max}$ between 15 and 45 cm/sec.

In a typical flume experiment, flow speed is increased in steps. A plot of suspended sediment concentration versus time (Fig. 5.6) is used to construct a plot of erosion rate $\dot{\varepsilon}$ versus speed $\bar{U}_{max}$ (Fig. 5.7). Critical erosion speed V_c is obtained by extrapolation, as shown in Fig. 5.7. The critical erosion stress τ_c corresponding to V_c is obtained from Fig. 5.4.

In the present flume, Nacci et al. (1975) reported V_c = 53 cm/sec for material from the bottom of the Thames River, New London, Connecticut. For Thames River sediments Nacci et al. (1976) found the relationship between erosion rate and fluid shear stress on the bed to be:

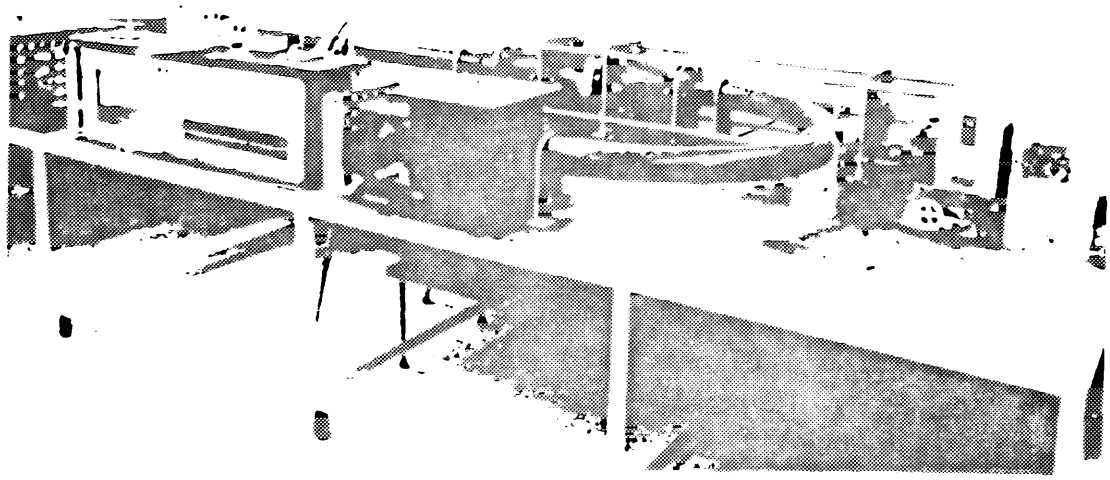

RECIRCULATING REFRIGERATING WATER TUNNEL

FIGURE 5.2

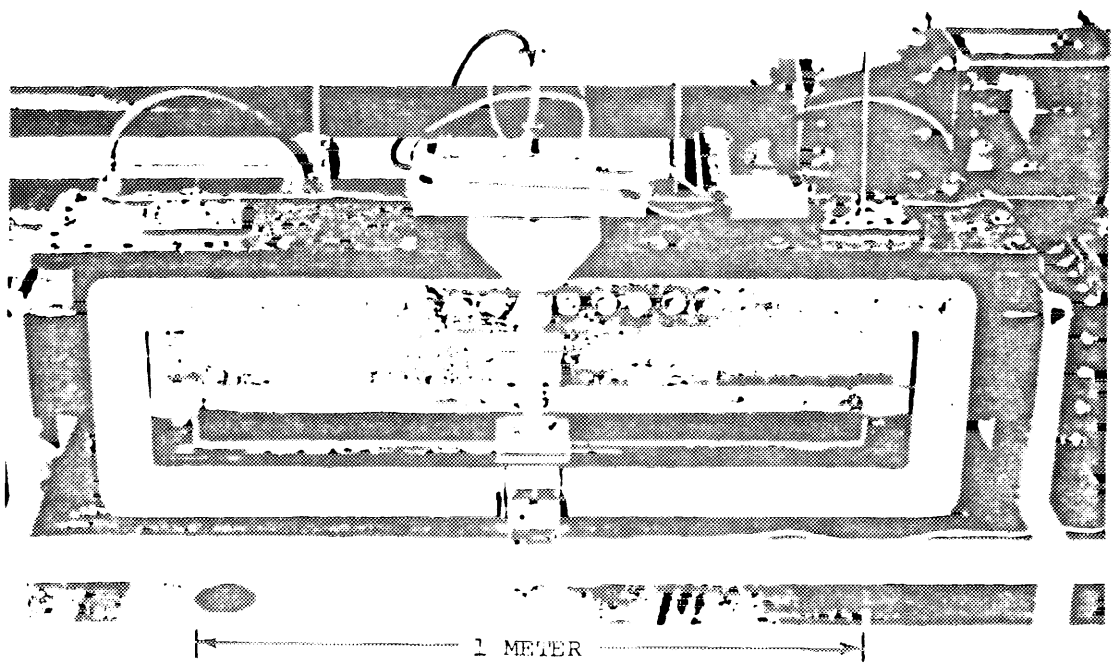

INSTRUMENTED SHEAR TRAY

FIGURE 5.3

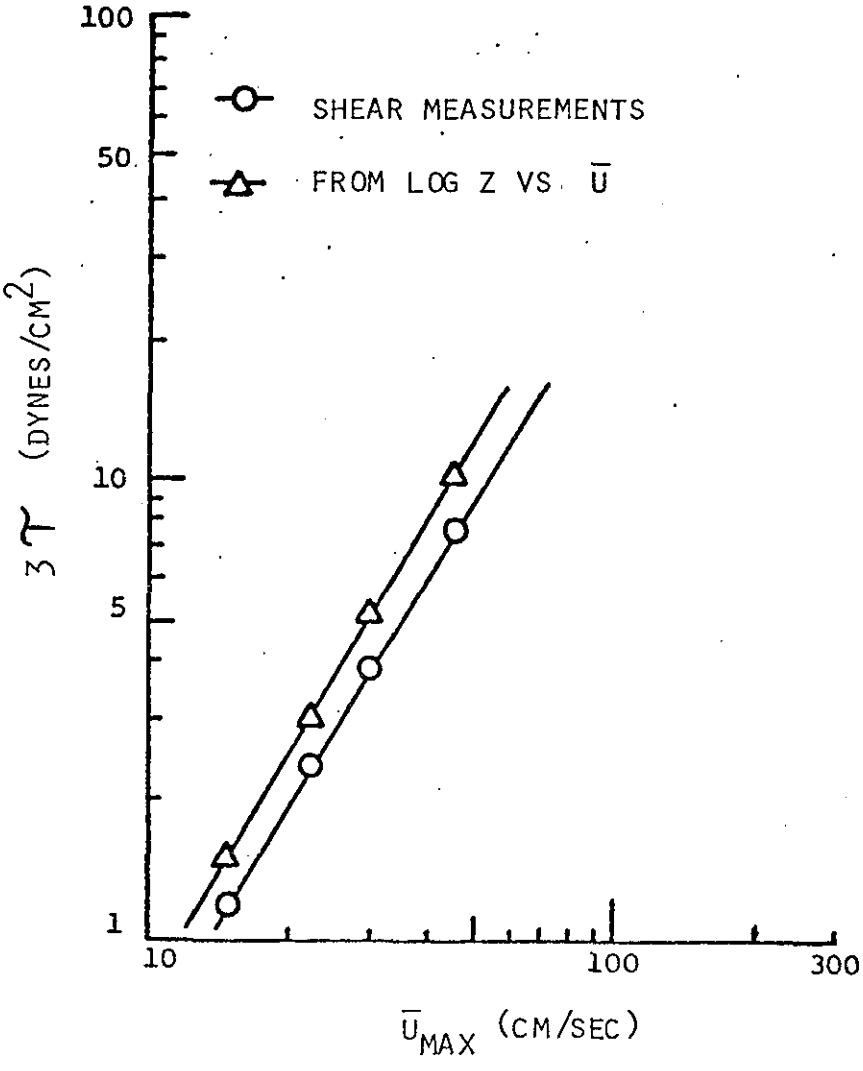

BED SHEAR STRESS τ VERSUS
FLUME FLOW SPEED $\bar{U}_{MAX}$
(AFTER GULARTE, 1978)

FIGURE 5.4

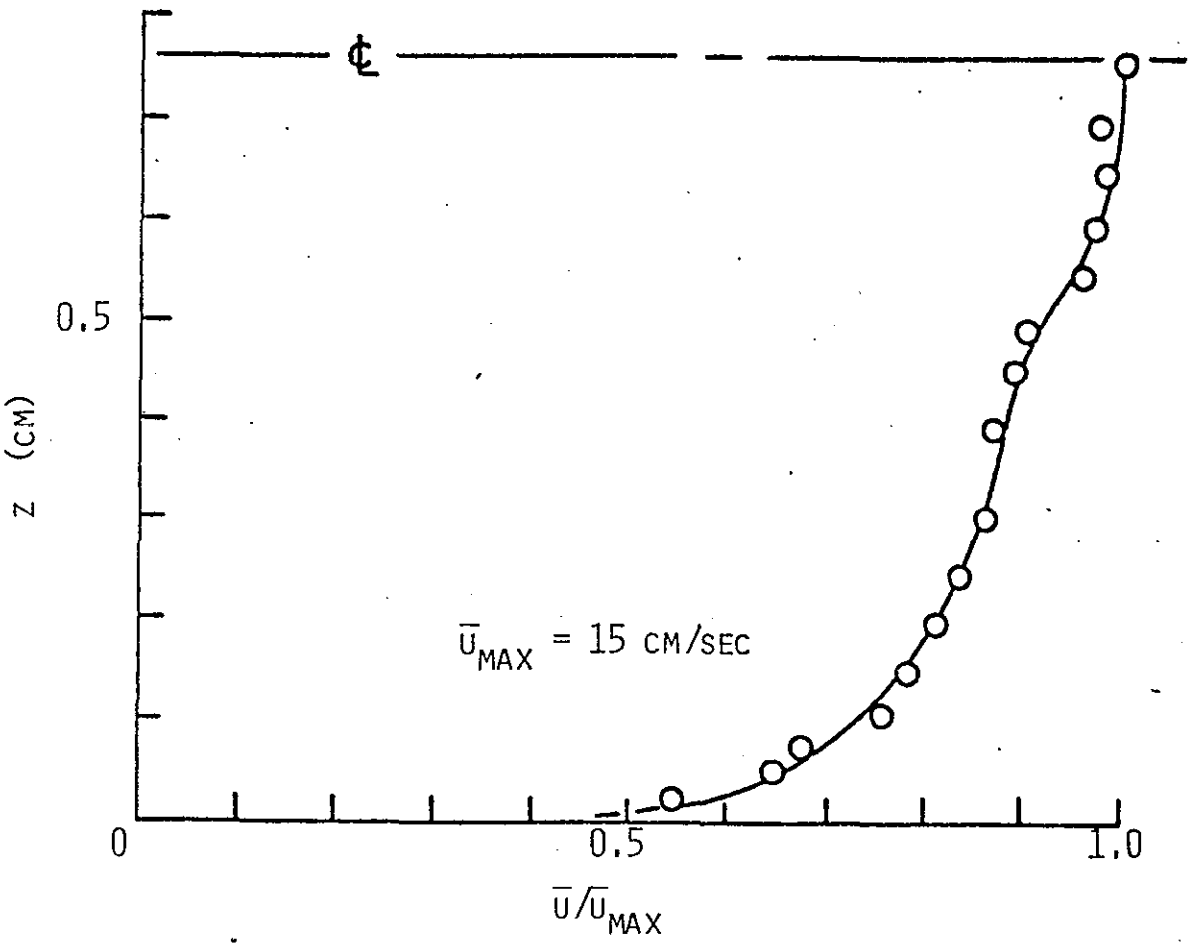

DISTANCE Z ABOVE BED VERSUS NORMALIZED HORIZONTAL SPEED,
(AFTER GULARTE, 1978)

FIGURE 5.5

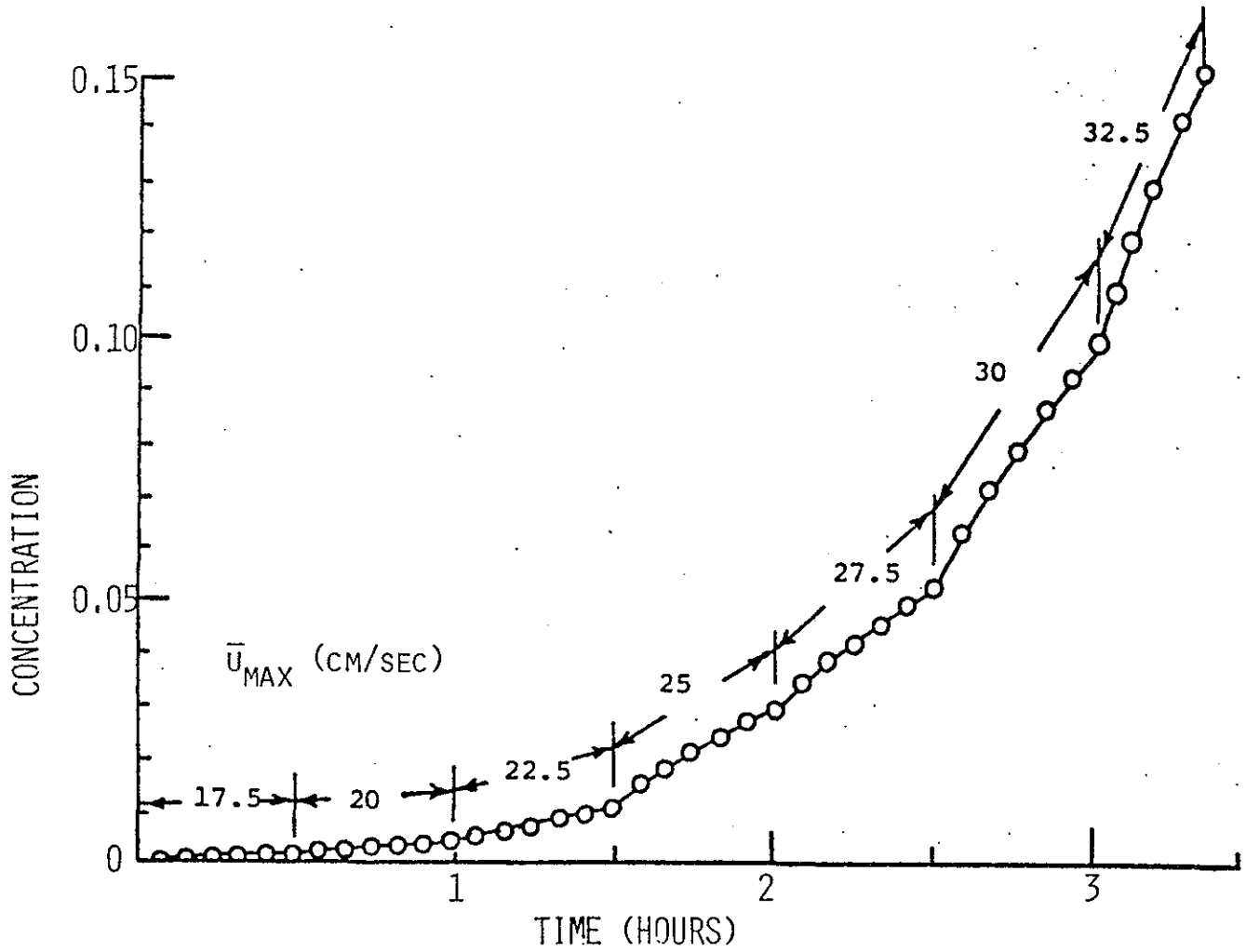

SUSPENDED SEDIMENT CONCENTRATION VERSUS TIME FOR VARIOUS FLUME FLOW SPEEDS $\bar{U}_{MAX}$ (AFTER GULARTE, 1978)

FIGURE 5.6

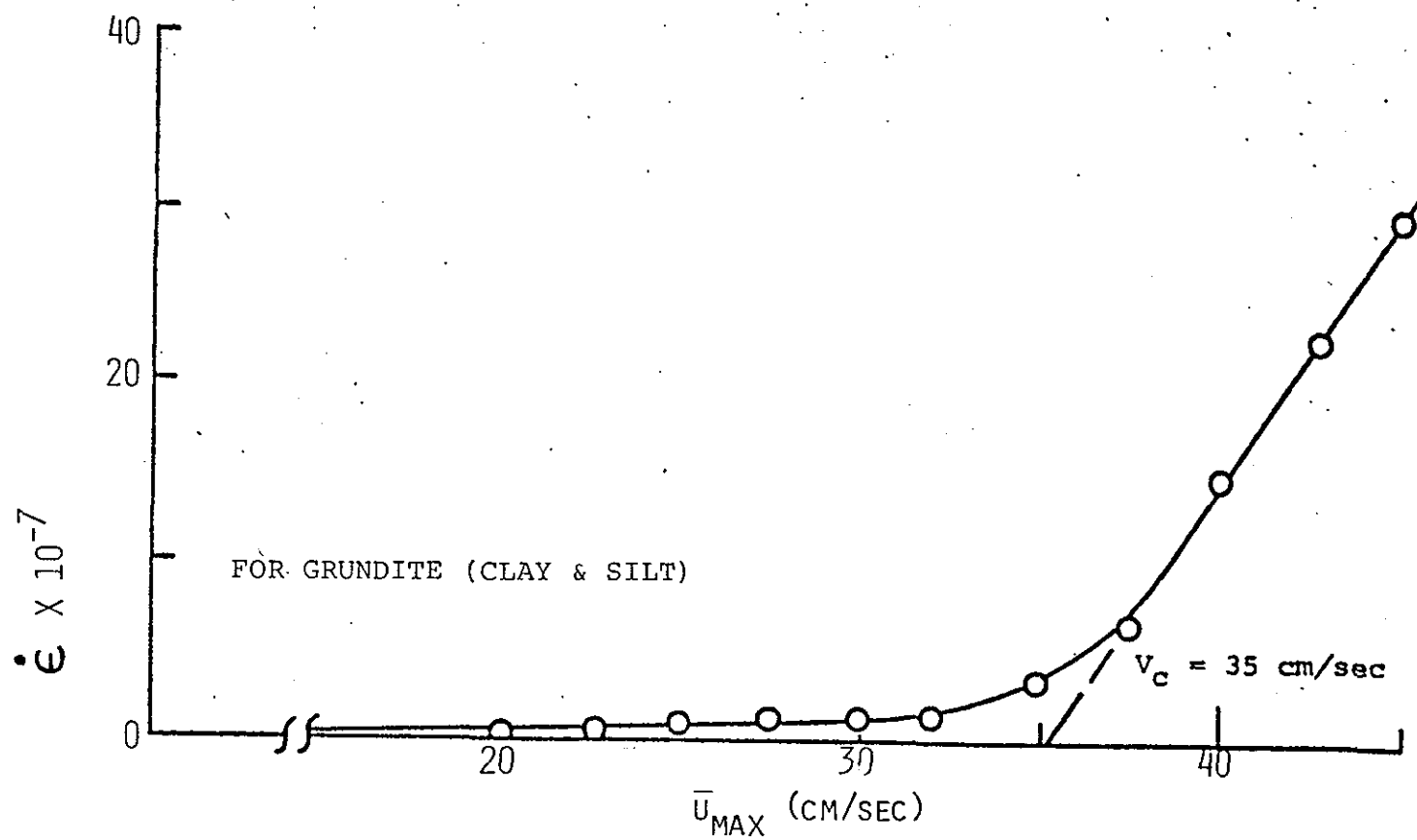

EROSION RATE $\dot{\epsilon}$ VERSUS FLUME SPEED $\bar{U}_{MAX}$ (AFTER GULARTE, 1978)

FIGURE 5.7

$$\dot{\varepsilon} = (1.63 \times 10^{-6} \text{ sec/cm})\ \tau,$$

where the coefficient of proportionality is two orders of magnitude greater than that reported by Partheniades (1965) and one order less than those reported by Sargunam (1975) and Arulanandan et al. (1975).

5.4 DISCUSSION

This discussion will examine how well the measured bed stress represents the stress actually entraining the sediment particles and whether measured stresses are comparable to those found at dredged spoil disposal sites.

The vertical variation of mean horizontal speed $\bar{U}$ is assumed to have a logarithmic variation of the form

$$\bar{U} = \frac{U_*}{k_o} \ln \frac{Z}{Z_o}, \qquad (1)$$

where $k_o = 0.4$ is von Karman's constant, and Z_o is the roughness length. The vertical coordinate Z is positive upwards with origin at the ocean or flume bed. The friction velocity U_*, the scaling speed for the boundary layer, is defined in terms of the water density ρ and horizontal shear stress τ on the bottom by

$$U_* \equiv (\tau/\rho)^{\frac{1}{2}}. \qquad (2)$$

The plot of Z versus $\bar{U}$ given in Fig. 5.8 has been constructed from the data in Fig. 5.5. The variation in $\bar{U}$ with distance above the bed is logarithmic to at least within 0.2 cm above the bed. From Equations (1) and (2), $U_* = 0.74$ cm/sec and $\tau = 0.55$ dynes/cm^2 for the data in Fig. 5.8. For $\bar{U}_{max} = 15$ cm/sec, $U_* = 0.74$ cm/sec, and $Z = 7.6$ cm, the roughness length, $Z_o = 0.0023$ cm, which is the distance above the bottom at which the mean speed $\bar{U} = 0$.

From Fig. 5.4 for $\bar{U}_{max} = 15$ cm/sec, $3\ \tau = 2.5$ dynes/cm^2, so $\tau \pm 0.5$ dynes/cm^2. Gularte (1978) used the "law of the wall," an equation similar to Equation (1), to determine bottom shear stresse from vertical speed profiles

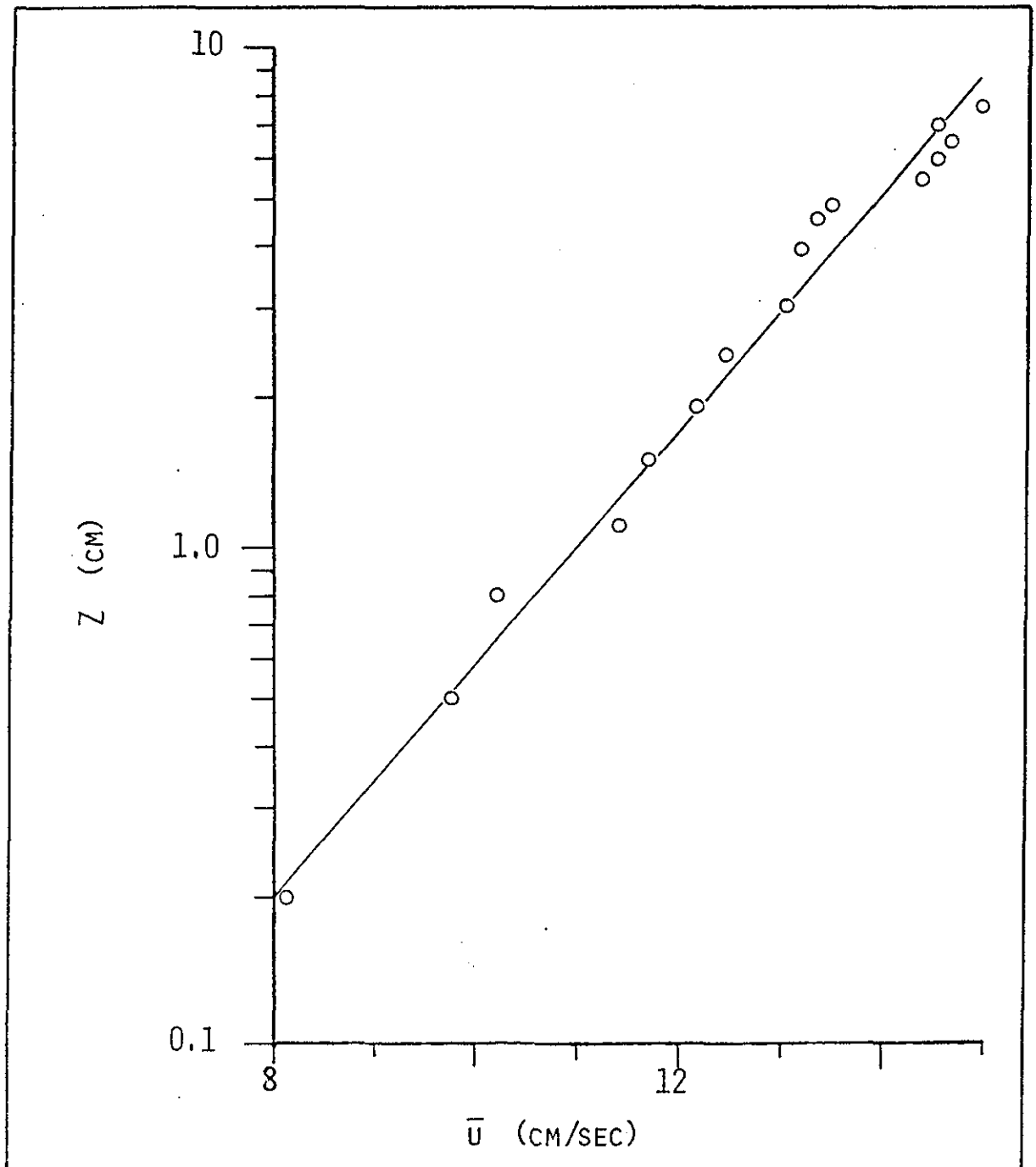

DISTANCE Z ABOVE BED VERSUS HORIZONTAL SPEED $\bar{U}$.
DATA TAKEN FROM FIG. 5.5

FIGURE 5.8

measured at four different values of $\bar{U}_{max}$ (Fig. 5.4). At anticipated values of critical shear stress, there is about a 30 percent difference between the spatially averaged bottom shear stresses measured with the shear tray and time averaged values inferred from the speed profiles at the center of the shear tray. There has been some uncertainty about this point since the flume length is insufficient for a fully developed turbulent boundary layer.

Schlichting (1960) indicates that a parabolic velocity profile develops in a channel with flat upper and lower walls in a length:

$$l_E = 0.16a\ (U_o\ a/v), \tag{3}$$

where U_o is the uniform velocity at the inlet, 2a is the channel height, and $v \doteq 0.01\ cm^2/sec$ is the kinematic viscosity of the fluid. For a = 7.6 cm and U_o = 15 cm/sec, l_E = 100 m, which is over 20 times the present half-flume length. At critical erosion speeds, the flume length required for a fully developed boundary layer may even be two or three times 100 m.

The thickness of the viscous sublayer (if it exists) below the logarithmic layer is

$$\delta \sim 12\ v/U_* = 12(0.01/0.74\ cm = 0.16\ cm$$

(see Wimbush and Munk, 1970). Viscous effects dominate in this layer if the roughness elements have characteristic dimension $d < \delta/4 = 0.04$, which is certainly true for a maximum sediment grain diameter,

$$d_o = 10\mu = 0.001\ cm.$$

According to Wimbush and Munk (1970), for

$$d_o < \delta/4,\ Z_o \doteq 0.1\ v/U_* = 0.1(0.02/0.74\ cm = 0.0014,$$

which is about 0.6 times the value of Z_o obtained from Equation (1). It is concluded that the magnitudes of both U_* and Z_o obtained from Equation (1) and the magnitude of d_o are consistent with the existence of a viscous sublayer.

The roughness Reynolds number

$$U_* d_o / \nu \quad 0.74(0.001/0.01)\ \text{cm} = 0.074 < 5$$

also indicates that flow near the bed should be hydraulically smooth (see Yalin, 1977, p. 97). *The hydraulic shear at the bed is an accurate measure of* the entrainment force since no velocity fluctuations are present at the roughness height.

Cook et al. (1976) used ducted impeller current meters to make boundary layer turbulence measurements at the New London dredged spoil disposal site 5 km south of the Thames River entrance and at East Hole, a proposed disposal site 15 km southeast of New London on the continental shelf. At the New London and East Hole sites, the water depths are 20 m and 30 m, respectively. Root mean square velocity fluctuations (standard deviation) reported by Cook et al. (1976) for 25 cm above the ocean bottom are typically 15 to 30 percent of the mean horizontal speed. These are close to the 13 percent values measured in the flume at 7.6 cm above the bed, although the length scales associated with these fluctuations may be quite different.

Values of friction velocity U_* reported by Cook et al. (1976) are less than 2 cm/sec. Heavers (1978) reported a maximum U_* value of 2.9 cm/sec for data taken during two three-week periods with an electromagnetic current meter array at Brown's Ledge off the Rhode Island coast. Brown's Ledge is a proposed dredged spoil disposal site exposed to the open sea; the water depth is 30 m. Heavers (1978) also reported instantaneous horizontal speeds of 54 cm/sec at 0.5 m above the bottom during a hurricane.

It appears that events for which U_* exceeds 3 cm/sec are unlikely at coastal locations with depths greater than 20-30 m. The corresponding shear stress on the bottom, $\tau = \rho U_*^2 = 9$ dynes/cm^2, is readily obtained in the flume at flow speed $\bar{U}_{max} = 50$ cm/sec.

5.5 FUTURE WORK

As part of the effort to assess long-term stability of dredged spoil materials, future activities should include the following:

1. Perfect the USSS, develop sampling technique, and establish criteria for assessing whether a sample is undisturbed.

2. Measure critical erosion stress and erosion rate versus applied bottom stress for priority disposal areas.

3. Use USSS during in-situ turbulence (J. Ianniello, NUSC) and sediment resuspension (F. Bohlen, University of Connecticut) experiments.

4. In the flume, measure all three components of fluctuating velocity, Reynolds stress, bottom stress at the sediment surface with a miniature sensor, and possibly pore pressure just below the sediment surface.

5. Modify flume as indicated by 4.

6. Continue attempts to relate erosion parameters to various geotechnical properties of sediments.

    a. Critical erosion stress has already been observed to vary in a general way with sediment water content (Gularte, 1978), although Partheniades (1965) found no correlation between critical stress and sediment shear strength. Surface erosion is possibly best characterized by a viscoelastic parameter such as Bingham yield stress.

    b. The phenomenon of bulk erosion will be examined and possibly be related to sediment shear strength, if the appropriate bed stresses can be attained in the flume. Definitive bulk erosion experiments should include measurements of sediment pore pressure, particle arrangement, clay mineralogy, and degree of compaction.

5.6 SUMMARY

This paper describes apparatus, developed and fabricated at the University of Rhode Island, for obtaining an undisturbed sample of the uppermost sediment layers on the ocean bottom. The sampling apparatus has been field tested on three occasions but is not yet fully operational. The sample obtained will be placed in a 10-m recirculating flume where critical erosion stress τ_c and erosion rate $\dot{\varepsilon}$ at in-situ temperature, salinity, and pH will be determined. Only cohesive sediments will be analyzed.

In the flume, when flow speed $\bar{U}_{max}$ = 15 cm/sec, the vertical velocity profile measured above a smoothed bed with a hot film probe is logarithmic at levels greater than 0.2 cm above the bed and possibly closer. The friction velocity U_* = 0.74 cm/sec, roughness length Z_o = 0.0023 cm/sec, and maximum sediment diameter d_o = 0.001 cm are consistent with the existence of the viscous sublayer of thickness δ = 0.16 cm. Also the roughness Reynolds number $U_* d_o/\nu$ = 0.074 is less than the critical value of 5, so the bed is hydraulically smooth. The hydraulic shear at the bed is therefore an accurate measure of the entrainment force, since no velocity fluctuations are present at the roughness height.

Agreement within 30 percent between average bottom shear stresses measured with a shear tray and those inferred from velocity profiles indicate that critical stress determinations may be reliable even though the flume is shorter than that required for fully developed turbulent flow. The flume can produce bottom stresses corresponding to maximum friction velocities of U_* = 3 cm/sec occurring in offshore areas. The standard deviation of speed is 13 percent of the mean speed in the flume and is similar to those measured at dredged spoil disposal sites.

5.7 REFERENCES

Ariathurai, R., and R. B. Krone. 1976. Finite element model for cohesive sediment transport. J. Hydraulics 102: 323-38.

Arulanandan, K., P. Loganathan, and R. B. Krone. 1975. Pore and eroding fluid influences on surface erosion of soil. J. Geotech. Engng. 101: 51-66.

Cook, G. S., R. W. Morton, and A. T. Massey. 1976. A report on environmental studies of dredge spoil disposal sites: Part I: An investigation of a dredge spoil disposal site; Part II: Development and use of a bottom boundary layer probe. Internal report, Naval Underwater Systems Center, Newport, R.I.

Gularte, R. C. 1978. Erosion of cohesive marine sediments as a rate process. Ph.D. Dissertation, University of Rhode Island, Kingston.

Heavers, R. M. 1978. On the vertical distribution of turbidity at a location off Rhode Island. Ph.D. Dissertation, University of Rhode Island, Kingston.

Krone, R. B. 1962. Flume studies of the transport of sediment in estuarial shoaling processes, Final Report, Hydraulic Engineering Laboratory and Sanitary Engineering Research Laboratory, University of California, Berkeley.

Nacci, V. A., W. E. Kelly, and R. C. Gularte. 1975. The erosional behavior of Thames River sediment, Report to New England Division Army Corps of Engineers, University of Rhode Island, Kingston.

Nacci, V. A., W. E. Kelly, and R. C. Gularte. 1976. The influence of spoil texture and salinity eroding fluid on threshold erosional velocities, Report to New England Division Army Corps of Engineers, University of Rhode Island, Kingston.

Partheniades, E. 1965. Erosion and deposition of cohesive soils. J. Hydraulics, 105-138.

Sargunam, A., P. Riley, and K. Arulanandan. 1973. Physicochemical factors in erosion of cohesive soils. J. Hydraulics 99: 555-58.

Schlichting, H. 1960. Boundary Layer Theory, McGraw-Hill, N.Y.

Wimbush, M., and W. Munk. 1970. The benthic boundary layer, 4: 731-58. In: The sea, A. E. Maxwell, (ed.), Wiley-Interscience, N.Y.

Yalin, M. S. 1977. Mechanics of sediment transport, Pergamon Press, N.Y.

6.0

DAMOS SUSPENDED SEDIMENT TRANSPORT STUDIES

W. F. BOHLEN

6.0 DAMOS SUSPENDED SEDIMENT TRANSPORT STUDIES

6.1 INTRODUCTION

The study of suspended material transport in the vicinity of selected dredge spoil disposal sites within the DAMOS study area was initiated in January 1979. The first three months were primarily a period of project organization, with particular emphasis being placed on personnel assignments, data reviews, specification, and design of an in-situ monitoring array and procurement of the required components for this system. This report details the objectives of the studies and describes the initial array configuration, its assembly status, and its projected test and deployment schedules.

The major fraction of sediment dredged from within New England coastal embayments and estuaries consists of fine-grained sand, silt, and clay. When eroded by a high energy flow, the transport of these cohesive materials occurs primarily as a free particulate suspension. The percentage of sediment moving as bedload, adjacent to or in contact with the sediment/water interface, is relatively small and is addressed using visual observations.

A quantitative determination of the mass of material moved in suspension requires detailed measurements in both space and time. In most coastal areas the latter factor is especially important. A variety of observations have shown that suspended material distribution is best represented by the combination of an average background level and a series of large-amplitude, aperiodic perturbations. In eastern Long Island Sound, for example, typical storm-induced perturbations can increase the concentration of suspended material by more than a factor of four (Fig. 6.1). Given sufficient duration and frequency of occurrence, these events will serve to significantly increase the total mass of sediment being transported.

Because of the above characteristics, prediction of suspended material transport in coastal waters requires special analytical procedures which can be satisfied using an in-situ sampling program. The time variability of transport is of special importance. This intermittent character, along with the inherent difficulty of scheduling and executing shipboard sampling during

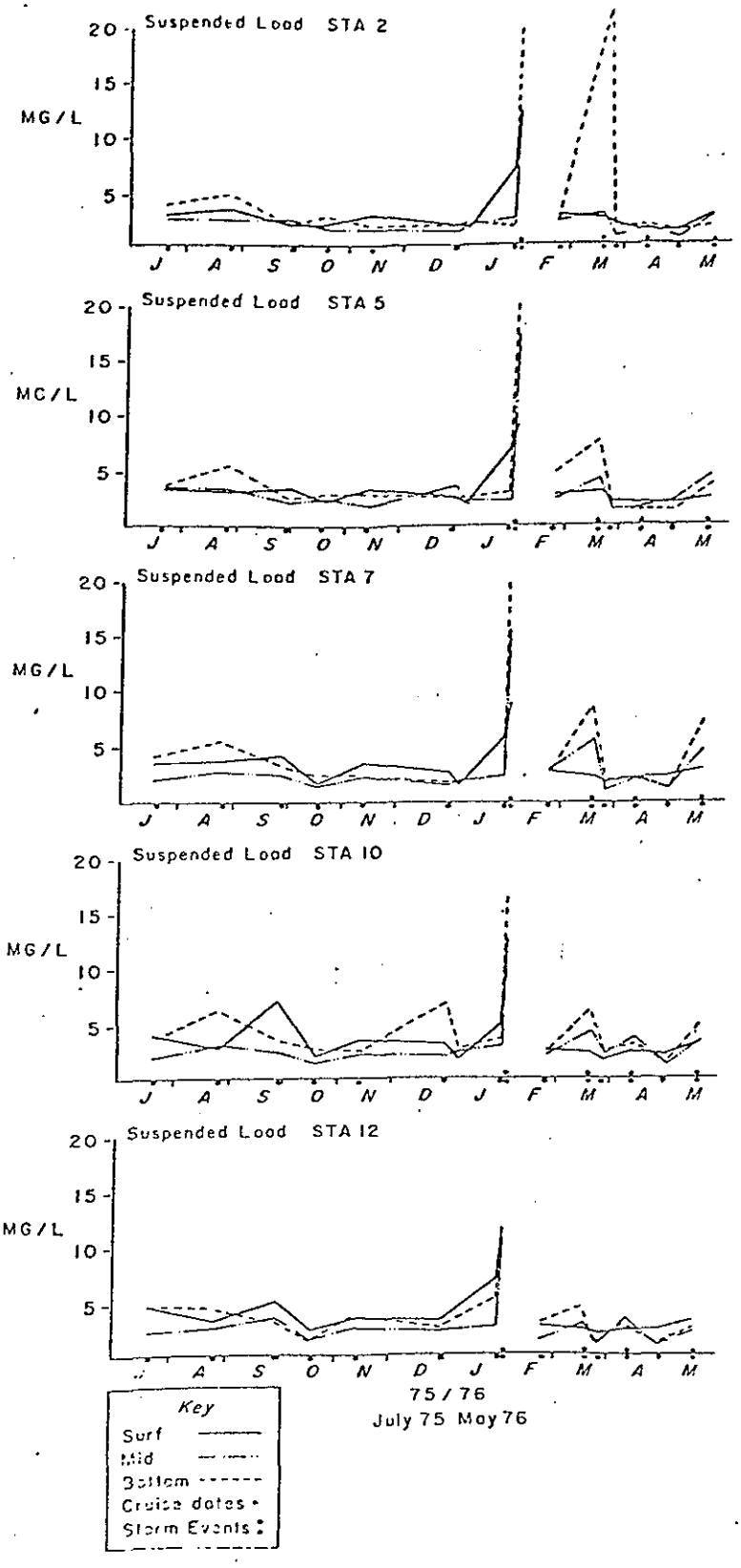

THAMES RIVER SUSPENDED MATERIAL CONCENTRATION

FIGURE 6.1

storms, favors the use of in-situ instrumentation that will provide long-term observations of suspended material concentration and composition at fixed locations. These arrays, in turn, must be designed to permit sampling of high-frequency, short-term events as well as lower-frequency, seasonal variations that affect material concentrations. When properly designed, the system should provide not only the required direct observations, but also a means to verify transport predictions. Such predictions are being developed as part of DAMOS, using the combination of field velocity measurements (Boundary Layer Turbulence or BOLT) and laboratory observations of critical erosion velocity. These studies are described in detail in other sections of this report.

6.2 PROGRAM OBJECTIVES

The investigation of suspended material transport in the vicinity of selected dredge spoils disposal areas was designed to accommodate the above considerations. The primary objectives of this program are to:

- Design and construct a series of instrumentation arrays capable of providing long-term, quantitative observations of suspended material in coastal waters.
- Use these arrays in combination with shipboard sampling to quantitatively evaluate suspended material in the vicinity of dredge spoil disposal areas. Observations will be sufficiently detailed to provide information on both material concentrations and composition.
- Verify transport predictions developed using field velocity measurements and laboratory observations of critical erosion velocities.

6.3 SYSTEM DESCRIPTION

The required long-term monitoring of coastal suspended material is best realized using a combination of direct and indirect sampling techniques. The system designed to satisfy these rquirements is shown schematically in Fig. 6.2. This instrument array consists of a control module and four subsystems:

(1) System control - Primary control for each of the array subsystems is centered in the digital data logger. In addition, this programmable

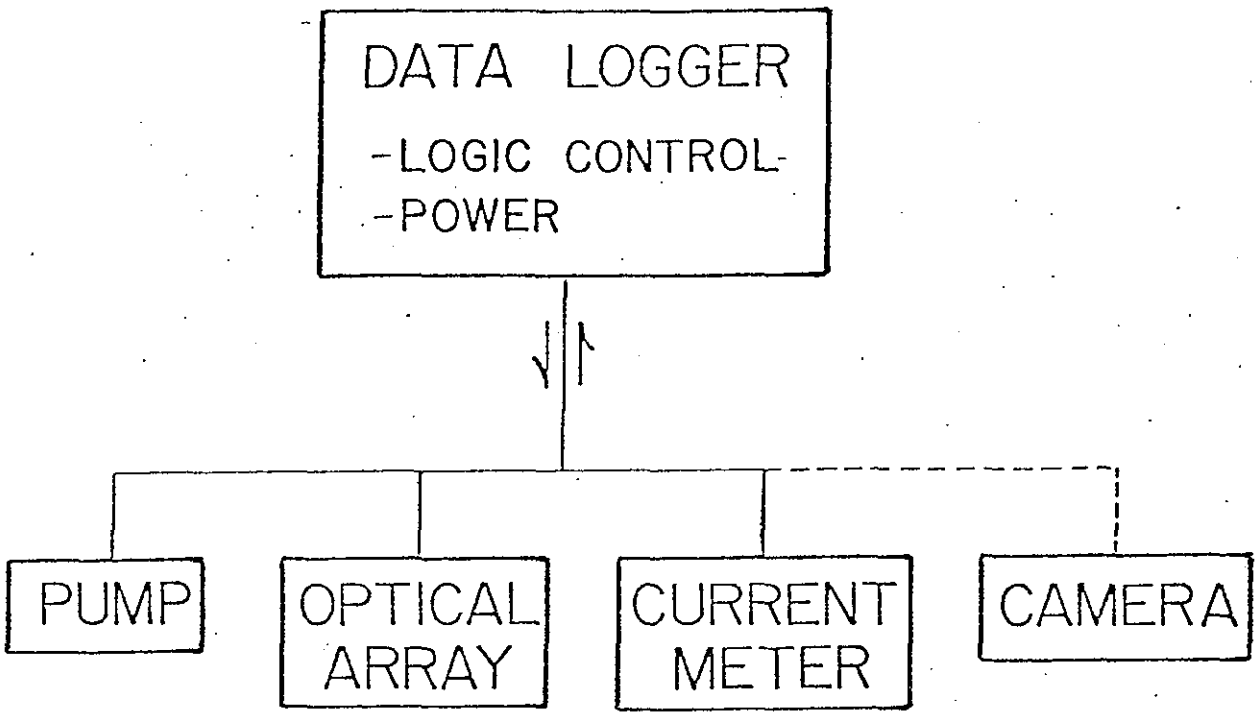

MONITORING ARRAY CONFIGURATION

FIGURE 6.2

unit records the analog outputs from the transmissometers and current meter, and provides the system time standard and power supply. As initially designed, the logger can receive output from eight sensors and has sufficient recording capacity to permit 36 days of untended operation. All data are recorded on magnetic tape cassettes in a format that can be readily converted to computer-compatible code.

(2) Pump/filtration unit - Designed to provide direct samples of the materials in suspension, this system consists of a variable-volume positive displacement pump and a series of 36 inline filtration units, each containing a 47-mm diameter, 0.4-μ pore size Nuclepore filter. The filters are attached to a central manifold containing a sliding piston which in turn is attached to the intake line of the pump. As the piston is slowly driven along the length of the manifold, filters are sequentially placed into the intake line. Piston position and excursion rate determine the filter being sampled and the sampling duration, respectively. In the initial configuration, a relatively low sampling rate has been selected which allows one filter per day at a pumping volume of one liter per day.

In addition to the 47-mm primary filter, each inline unit also contains a 25-mm filter holder intended to accept a K-V Associates Metrodisk. This filtration disk is used to measure selected dissolved heavy metal concentrations associated with the individual samples. Such measurements complement analyses being conducted within other elements of DAMOS which are concerned with metal concentrations within shellfish and the local sediment column.

(3) Optical array - Indirect measurement of suspended material concentration will be obtained using a series of small, red-light transmissometers. Each of these units provides an analog output which is proportional to the concentration of suspended sediments. The instruments have a fixed path length and are designed to be relatively insensitive to dissolved materials and water matrix variations. Optical path lengths are to be specified following

evaluation of the ambient suspended material concentrations and the characteristic variations to be expected at the particular study area. Typical path lengths range from 4 cm to 100 cm.

A minimum of two transmissometers will be deployed on each array. The units will be spaced vertically so as to provide measurements immediately adjacent to, and approximately 2 m above, the sediment/water interface. Each unit will be sampled sequentially at rates to be determined following the initial calibration phase. A maximum rate of two samples per second is provided by the data acquisition system.

To complement the optical measurements, simultaneous water temperature and salinity observations will be obtained during each sampling interval. Sensors for each parameter will be located immediately adjacent to each of the transmissometers. Sampling rates will be identical for all sensors.

(4) Current meter - To provide a measure of the mean velocity conditions prevailing during each deployment, the instrument array will contain a simple mechanical current meter. This meter is not intended to provide detailed observations of the velocity field. Such data will be obtained using the BOLT system. The mechanical meter is included primarily to measure gross variations produced by major storm events. In principle, it is analogous to the standard anemometer used in routine meteorological surveys.

(5) Lapsed-time camera - As originally designed, the instrumentation array contained only the above four components. During the past several months it has become apparent that verification of the laboratory predictions of critical erosion velocity requires direct observations of the stability of the sediment/water interface under a variety of flow conditions. To satisfy this requirement, a lapsed-time camera is being added to the original array configuration. This camera is intended for use primarily during periods when the array is deployed jointly with the BOLT system. The remainder

of the time it is expected to provide only qualitative information on near-bottom conditions.

The lapsed-time system consists of a modified Super 8 mm motion picture camera, control electronics, and a strobe light. Sampling rate can be internally programmed or governed by an external control system. The combination permits the unit to be used either as an integral part of the array or independently.

6.4 PROGRAM STATUS AND SCHEDULES

During April 1979, the initial system design considerations were completed. Component specifications for each of the subsystems were established and all commercially available units were ordered. Two transmissometers were constructed, field tested, and calibrated. These operations were completed in mid-July 1979, and permitted the units to be deployed with the BOLT system in early August.

Construction of the instrument array was completed by mid-August 1979. The system has been deployed and tested for a period of approximately six weeks. If those tests provide satisfactory results the unit will be deployed for its initial survey period in mid-October. Plans call for initial deployments in two areas--one north of Cape Cod in a wave-dominated region (e.g., east of Portland, Maine) and the second south of Cape Cod in a tidally dominated area (e.g., eastern Long Island Sound). If additional engineering is required, the initial survey period will be delayed until late January 1980.

7.0

CHEMISTRY OF SURFACE SEDIMENTS

EVERETT L. JONES

7.0 CHEMISTRY OF SURFACE SEDIMENTS

7.1 INTRODUCTION

The chemical analysis of surface sediments taken from harbors and proposed disposal sites is part of the overall DAMOS program which assesses the impact or potential impact of dredged spoils on the disposal site environment.

The determination of chemical constituents of the sediments provides a means of characterizing and tracing sediments of different sources. Thus, if significant differences exist between the spoil and the natural sediments of the disposal site, a sediment characteristic of harbor spoil may be traced near the disposal site after dumping. If the physical properties of the spoil and natural sediments are similar, the chemical differences may provide a means of estimating the spread of spoil away from the point of dumping. The chemical composition of sediments in the area of the disposal site help interpret trends of metal uptake in the tissues of animals sampled during studies of the effect of spoil on the biomass. Sediment chemical information also helps in selection of a suitable material for capping the site. By choosing a sediment that has significantly different chemical characteristics from those of the primary spoil, the success of the cap can be monitored chemically.

7.2 DATA

The DAMOS program encompasses sites from western Long Island Sound to Rockland, Maine (Table 7.1) with diverse chemical properties. Sites range from pristine regions to highly contaminated ones. Samples are most variable at sites where old spoils exist and least variable in virgin areas. Harbors have the highest sample-to-sample variation. The high variability of the most contaminated harbors has been attributed to "hot spots." Samples from highly contaminated harbors are inherently heterogeneous and therefore difficult to sample. Our analysis of the surface sediments for the last year and a half has included nine metals, oil/grease, and volatile solids. While most of the heavy metals analyzed were strongly site-specific, other metals were not. Iron and cobalt were found at many sites. Iron, understandably, is more widespread than heavy metals associated with man-made pollution and is a major constituent of all sediments. Why cobalt is ubiquitous is not clear.

Table 7.1 STATION IDENTIFICATION AND PLOTTING LEGEND

Station	Point Code	Date
ROCKLAND, MAINE (1-9)		
Harbor between can #1 and nun #2, can #1 off shore on opposite side of harbor from Coast Guard station	1H	May 78; Nov. 78
Reference 1	2R	May 78
Reference 2	3R	May 78
Reference 3	4R	May 78
Rockland dump site; immediate vicinity of mussel cage	5D	May 78; Nov. 78
Rockland dump site canyon - dredge 1	6D	Nov. 78
Rockland harbor - buoy #2, 3-400 yards off C.G. sta.	7H	Nov. 78
PORTLAND, MAINE (10-19)		
Portland dump site (proposed); drag #2	10D	May 78; Nov. 78
Portland Harbor - turning basin inner harbor	11H	May 78
Portland Harbor off C.G. sta. buoy #4	12H	May 78
Portland Harbor - Pomroy Rock at can #1	13H	May 78
Portland Harbor - channel dog leg buoy #2	14H	May 78
Portland Harbor - red nun #6	15H	Nov. 78
Portland Harbor - red nun #6 between House and Cushing Islands	16H	Nov. 78
Portland Harbor - halfway between Fish Point and Old Portland Breakwater Lighthouse (N.E. Aquarium sta. #GEB-3-78)	17H	Nov. 78
Portland Harbor - 180-270 m inside harbor bridge in middle of channel (N.E. Aquarium sta. #GEB-1-78)	18H	Nov. 78
ISLE OF SHOALS & PISCATAQUA RIVER (20-29)		
Isle of Shoals site - dredge 1	20	May 78
Isle of Shoals site - dredge 2	21	May 78
Isle of Shoals site - dredge 3	22	May 78
Piscataqua River (harbor) - Navy Yard between berth 5-6; Navy Yard between pier 5-6	23H	May 78; Dec. 78
Piscataqua River (harbor) - off C.G. sta. light buoy #5; at black buoy #5 off C.G. sta.	24H	May 78; Dec. 78
Piscataqua River (harbor) - between bridges at tug pier	25H	May 78
Piscataqua River (harbor) - Navy berth #12 north of pier	26H	May 78

Table 7.1 (cont.)

Station	Point Code	Date
Isle of Shoals dump site - drag #1 (New sta. location from previous sample dates)	27	Dec. 78
Piscataqua River (harbor) - off pier 2 at Navy Yard (This is most landward area of pier sections.)	27H	Dec. 78
Isle of Shoals dump site - drag #3 (New sta. location - this drag is identical with location of drag #1)	28	Dec. 78
BOSTON, MASSACHUSETTS		
Boston Foul Ground - dredge 1; drag 2	30	May 78; Dec. 78
Boston Foul Ground (dump) - dredge 3	31D	May 78; Dec. 78
Boston Lightship site - dredge 1	32	May 78
Boston Lightship site (dump) - dredge 2; drag 1	33D	May 78; Dec. 78
BRENTON REEF, RHODE ISLAND (40-49)		
Brenton Reef reference	40R	Apr. 78; Aug. 78
Brenton Reef reference - drag 1	40R	Dec. 78
Brenton Reef - drag 1	41	Apr. 78; Aug. 78; Dec. 78
Brenton Reef - drag 2	42	Apr. 78
CORNFIELD SHOALS, CONNECTICUT (50-59)		
Cornfield Shoals control site - drag 1	50	Mar./Apr. 78; July. 78
Cornfield Shoals dump site - drag 1	51	Mar./Apr. 78
Cornfield Shoals dump site - drag 2	52D	Mar./Apr. 78; Jul. 78
Cornfield Shoals dump site - drag 3	53	Mar./Apr. 78
Cornfield Shoals north of marker - drag 2	54	Mar./Apr. 78
Cornfield Shoals south of marker - drag 4	55	Mar./Apr. 78
Cornfield Shoals west of marker - drag 5	56	Mar./Apr. 78
Cornfield Shoals reference 1	57R	Jul. 78
CABLE AND ANCHOR REEF, CONNECTICUT (60-69)		
Cable and Anchor Reef reference (3)	60R	Apr. 78
Cable and Anchor Reef - drag 1	61	Apr. 78; Jul. 78
Cable and Anchor Reef - drag 2	62	Jul. 78
Cable and Anchor Reef - drag 3	63	Apr. 78; Jul. 78
Cable and Anchor Reef - western L.I. Sound reference 1	64R	Jul. 78

Table 7.1 (cont.)

Station	Point Code	Date
WESTERN LONG ISLAND SOUND (70-79)		
Western L.I. Sound - drag 1	70	Apr. 78; Jul. 78
Western L.I. Sound - drag 2	71	Apr. 78
Western L.I. Sound - drag 3	72	Apr. 78
Western L.I. Sound reference 1	73R	Apr. 78
NEW HAVEN, CONNECTICUT (80-89)		
New Haven reference	80R	Apr. 78; Jul. 78
New Haven - drag 1	81	Apr. 78; Jul. 78
New Haven - drag 2	82	Apr. 78
New Haven - drag 3	83	Apr. 78
NEW LONDON, CONNECTICUT (90-99)		
Dump site grid station A-10-3	90	Sep. 78
Station C-1	91	Sep. 78
Station C-3	92	Sep. 78
Station C-4	93	Sep. 78
Station C-6 (dump)	94D	Sep. 78
Station C-8 (dump)	95D	Sep. 78
Station C-9 from 2nd Smith-McIntyre grab	96	Sep. 78
Station F-4	97	Sep. 78
Station F-8	98D	Sep. 78
NOTES: The letters R, H, and D refer to reference, harbor, and dump, respectively.		
NEW HAVEN NETWORK PREDISPOSAL SOUTH SITE		
Center of grid	800	Jan. 79
500 m east	801	
500 m north	802	
500 m west	803	
500 m south	804	
1000 m east	805	
1000 m west	806	
HARBOR SAMPLES		
Inner Harbor, New Haven	81H 84H 82H 85H 83H	
Outer Harbor, New Haven	86H	
Inner Harbor, Stamford	110 112 111 113	
Inner Harbor, Norwalk	120 123 121 122	
Outer Harbor, Norwalk	124	

Since iron exhibits the least variability compared to the other elements, it is used as a basis against which the other elements are compared. All the sediment chemistry has been represented by plots of iron vs. the other element. Iron plots in many cases have demonstrated regional differences.

7.3 RESULTS AND DISCUSSION

Each study site has been considered separately. A comparison of the sediment characteristics at the disposal sites, in the harbors, and in pristine areas adjacent to the disposal site will be made. Charts presented in this section are representative of most metals at each site.

7.3.1 Northern Region

Sites in the northern region include Rockland and Portland, Maine, and Portsmouth, New Hampshire (the Isle of Shoals disposal site). The proposed or existing disposal sites in these areas have few, if any, heavy metals in the surface sediments.

7.3.1.1 Rockland, Maine

The samples from the Rockland disposal site show a higher metal concentration than some of the Rockland Harbor samples (Fig. 7.1). Historical data show that this site has been spoiled on in the past. Rockland Harbor samples vary in concentration according to the distance from the inner harbor. The available data suggest that it would be very difficult to distinguish sediments from Rockland harbor from those from Rockland dump site.

7.3.1.2 Portland, Maine

The proposed dump site for Portland has been changed during the two years. Now the site consists of a small valley 60 m deep between rocky outcrops. Sediment is either rock or sand. The site appears pristine. Portland harbor sediments are characteristically high in metals in the inner harbor, while outer harbor stations show lower concentrations of metals (Fig. 7.2). Inner harbor sediments could be distinguished easily at the present dump site.

, a physical differentiation by observations of mud layers on top of

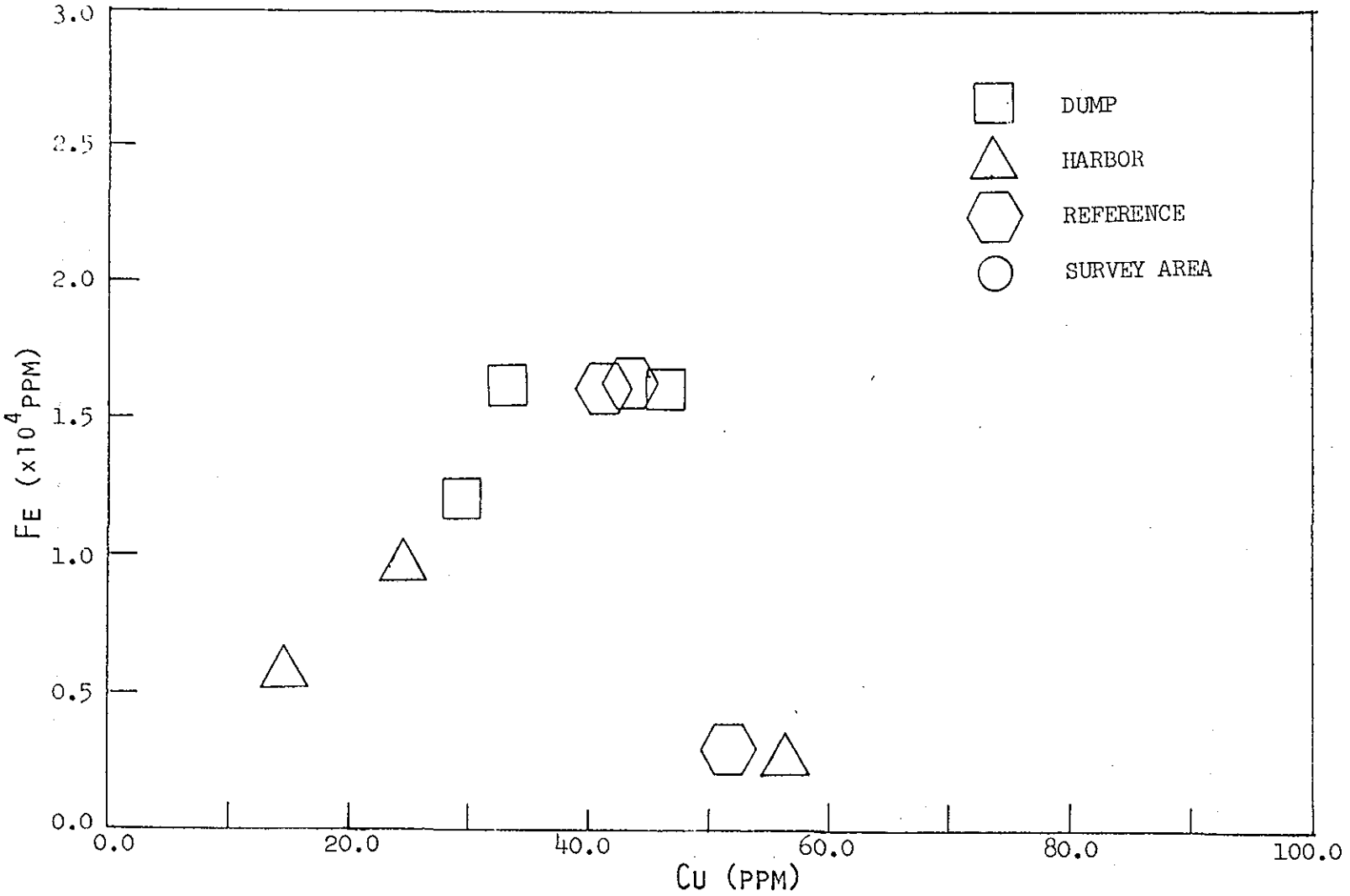

COPPER CONCENTRATION
ROCKLAND, ME

FIGURE 7.1

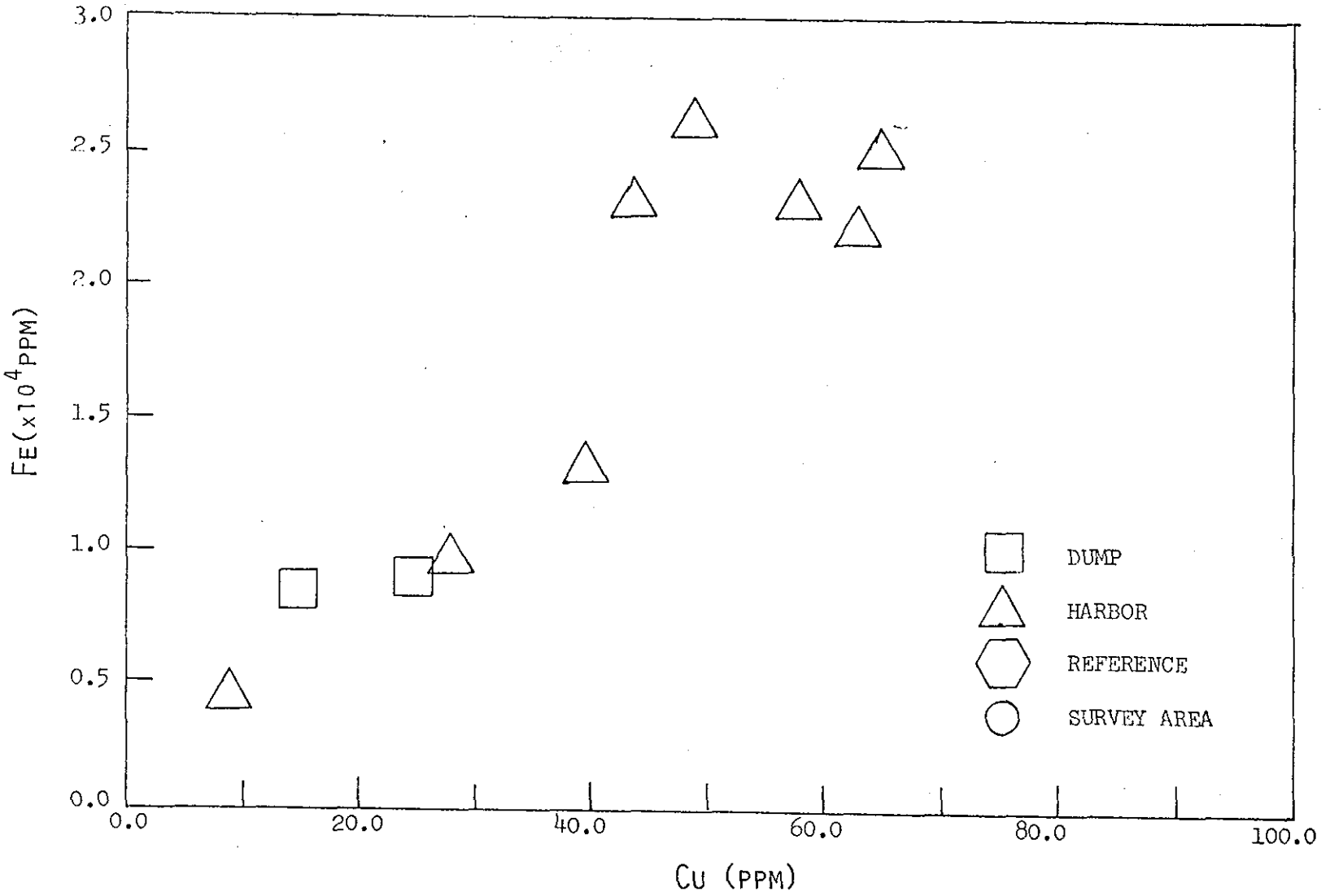

COPPER CONCENTRATION
PORTLAND, ME

FIGURE 7.2

sand might be possible. If Portland harbor spoils are dumped here, the usual fingerprinting technique may be useful when sediments having significantly different heavy metal composition are dumped over Portland spoils.

7.3.1.3 Portsmouth/Isle of Shoals, New Hampshire

The proposed dumping site near the Isle of Shoals is a pristine area. In contrast, Portsmouth harbor has some highly contaminated sediments (Fig. 7.3). The inner harbor sediments are extremely enriched. Thus, there would be no difficulty in identifying Portsmouth harbor spoil at the proposed dump site.

7.3.2 Boston Sites

Both Boston sites are in use. Boston Foul Ground sediments are higher in heavy metals than any of the northern sites discussed above (Fig. 7.4). Boston dump site sediments differ from other contaminated sites in that the iron/metal ratio is constant with increasing concentration.

To date we have not sampled harbor sediments, and therefore cannot speculate whether spoil can be distinguished from existing dump sediments.

7.3.3 Brenton Reef, Rhode Island

The dump site at Brenton Reef has been capped with a fine sand since dumping in 1974. The site is stable and biologically productive. Heavy metal concentrations are very low and similar to the levels at a nearby control station (Fig. 7.5). The introduction of spoil of almost any type except sand should be readily detectable, either physically or chemically.

7.3.4 Long Island Region

7.3.4.1 New London, Connecticut

The New London dump site was used extensively from 1971 to 1977. Most of the spoil came from the Thames River as a result of several U.S. Navy projects

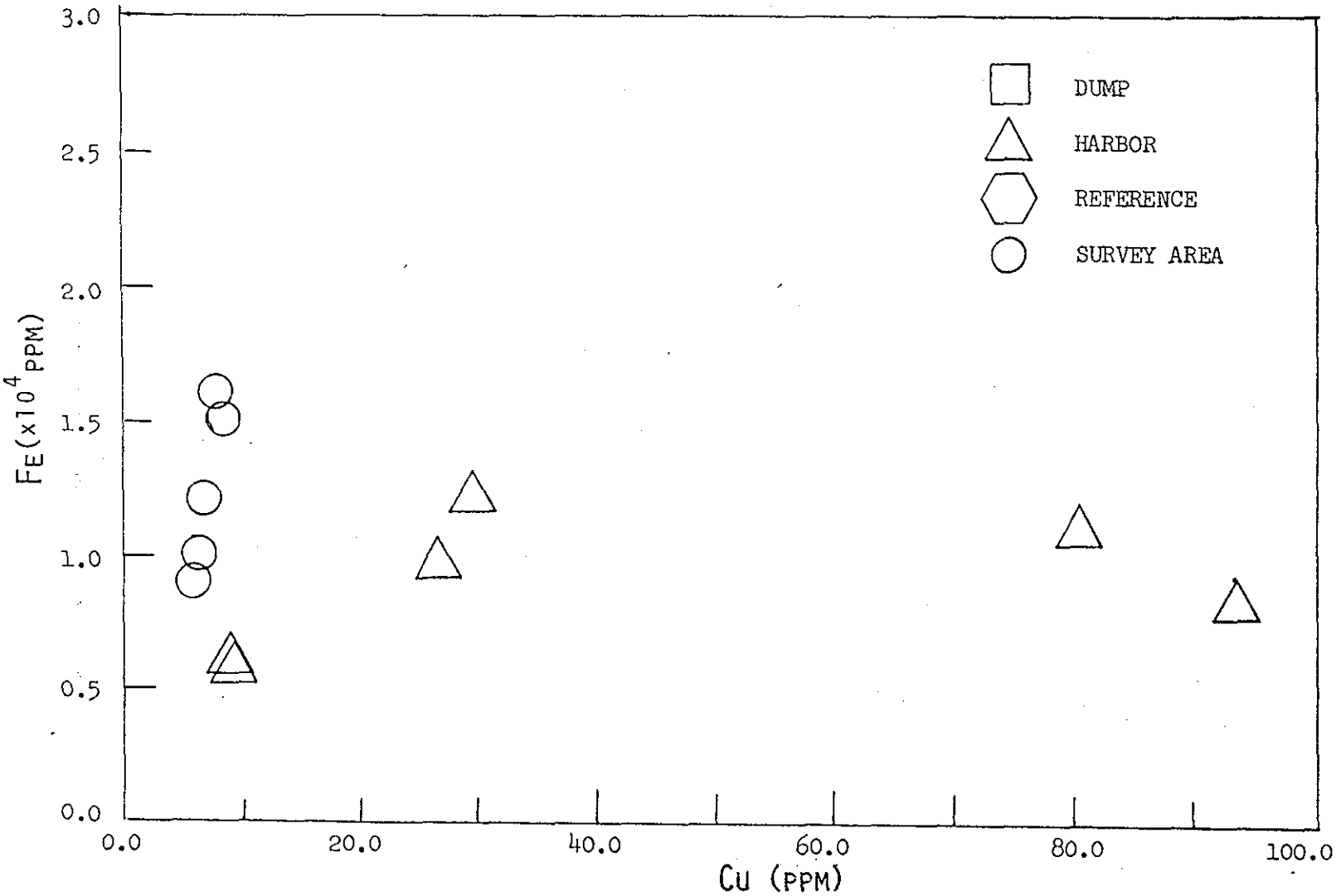

COPPER CONCENTRATION
ISLE OF SHOALS

FIGURE 7.3

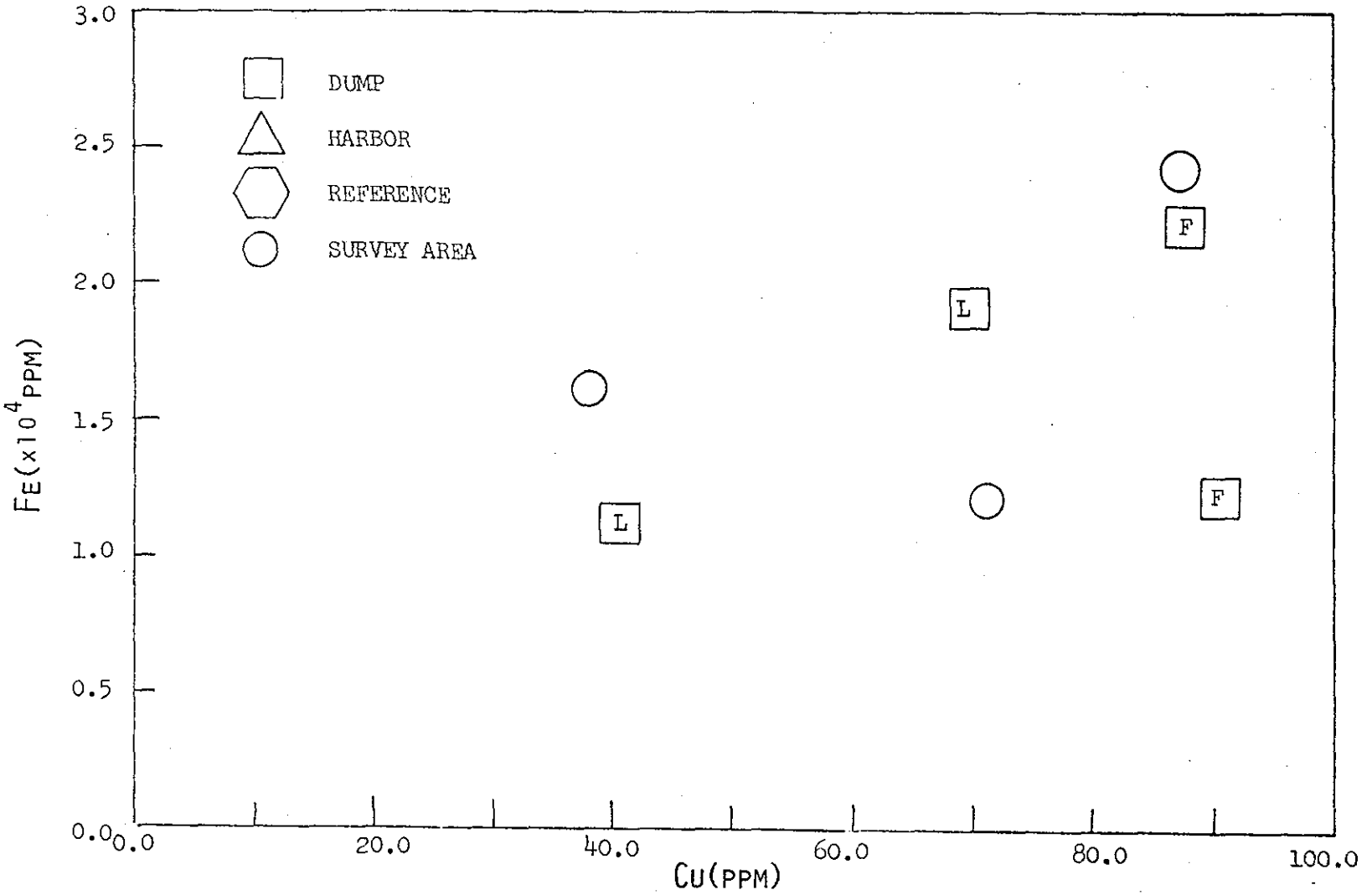

COPPER CONCENTRATION
MASSACHUSETTS BAY

FIGURE 7.4

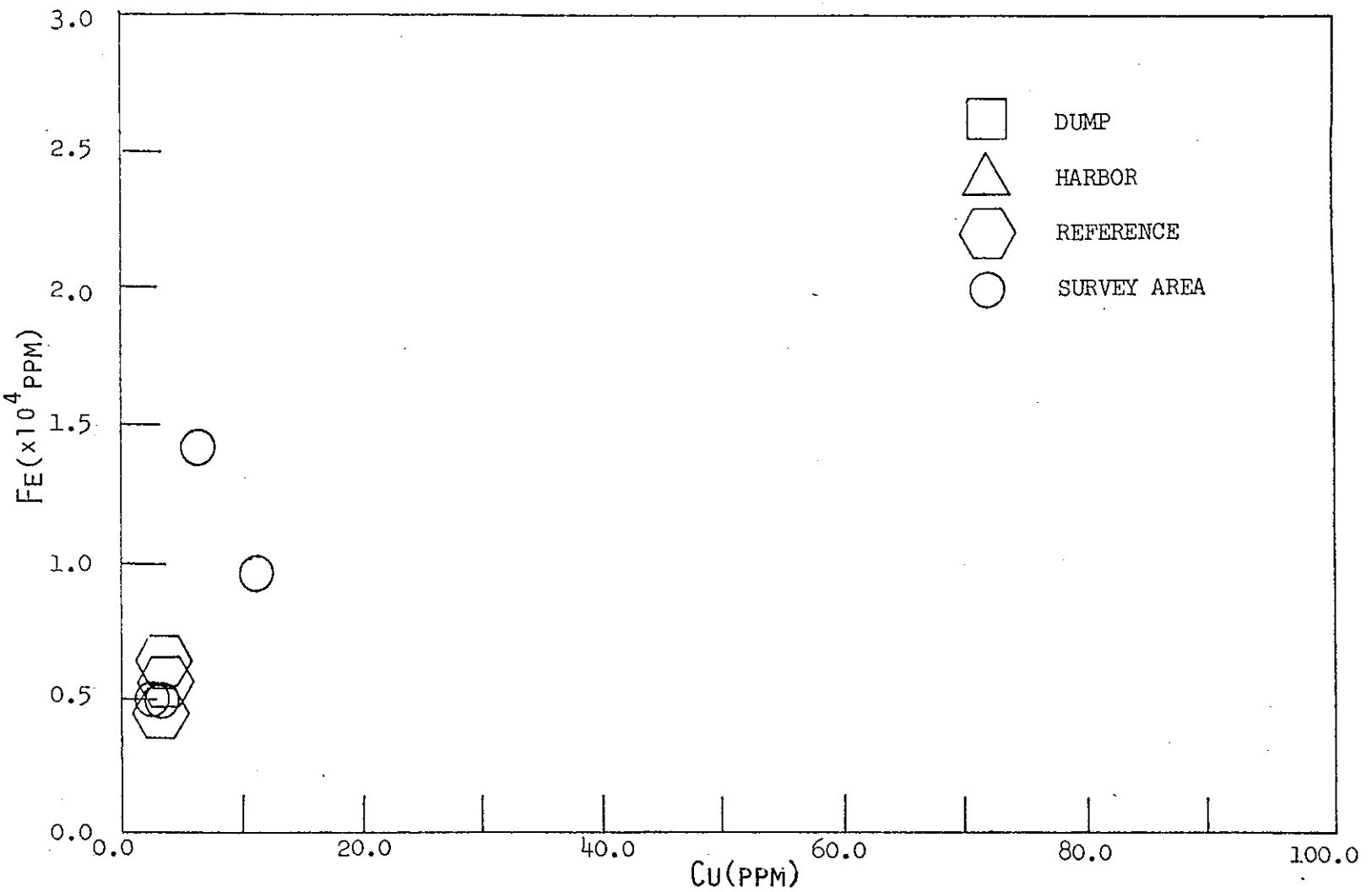

COPPER CONCENTRATION
BRENTON REEF

FIGURE 7.5

to deepen the river from its mouth to just north of the U.S. Submarine Base. Although there is no dumping now, additional dredging of the Thames River is planned for the near future.

An extensive chemical survey of the sediments in and around the New London site has been made since 1975 by the Navy and DAMOS. Our results draw on the data of both programs. Additional data on this site can be obtained from the Final Report, Phase II Environmental Monitoring Program published by the Naval Underwater Systems Center.

As New London is midway between the northern and Long Island sites, so the concentration of heavy metals in New London dump site sediments is intermediate between the northern and Long Island sites: higher than those at the northern sites excluding Boston and lower than those at New Haven and the sites off Norwalk, Connecticut.

Surface sediments from the large New London spoil heap are easily differentiated from outer station sediments. The spoil appears to be well contained. Heavy metal concentrations within the dump vary greatly between stations. Concentrations appear to depend on the origin of the spoil dredged from the Thames River and the repositioning of the dumping buoy. It is apparent that the spoil of the New London site is not homogeneous. Since it is already so diverse, the introduction of additional Thames River sediment will probably be impossible to distinguish from older sediments by chemical methods alone.

7.3.4.2 Cornfield Shoals, Connecticut

The Cornfield site, unlike the others considered here, is a dispersal site. The sea bottom surface is composed of sand and gravel and is chemically uncontaminated. A small amount of spoil from Old Saybrook Harbor was dumped here in 1977 just prior to our sampling. Spoil was identified by observation and was shown to be high in heavy metals (Fig. 7.6). This spoil is therefore easily identifiable when present at the site. In our latest sampling of the area (about six months after first locating the spoil), we were unable to find any spoil. It apparently had been dispersed.

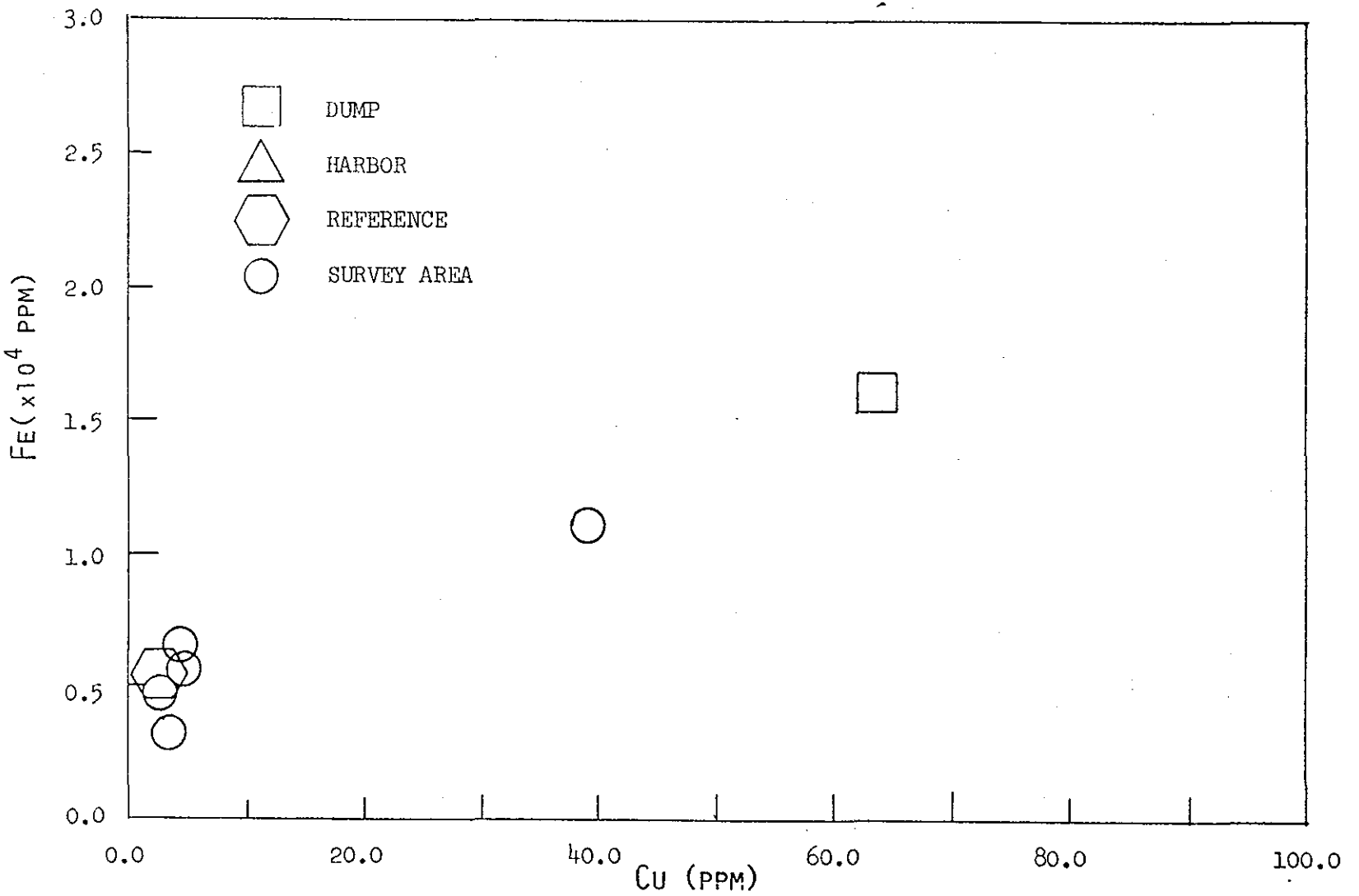

COPPER CONCENTRATION
CORNFIELD SHOALS

FIGURE 7.6

7.3.4.3 New Haven, Connecticut

An intensified monitoring program was set up by DAMOS to evaluate the dumping of Stamford harbor sediments and the subsequent capping with New Haven harbor spoil and sand at the New Haven dump site.

Chemical analysis (Table 7.2) showed significant differences between sediments from Stamford Harbor and those from New Haven Harbor, and between sediments from Norwalk Harbor and those from the New Haven dump site. In fact, the only pair of sediments that could not be distinguished at the $\geq$ 90 percent confidence level were those from Norwalk Harbor and New Haven Harbor (Table 7.3). Thus, capping Norwalk Harbor sediments with New Haven Harbor sediments would be unwise in that these two sediments are not chemically distinguishable.

At the New Haven dump site prior to spoiling, a cruciform sampling network was set up (Fig. 7.7). The results from baseline sampling showed excellent agreement between replicate samples (two standard deviations comprising no more than plus or minus 10 percent of the mean levels for most metals) and uniformity among metal levels within the sampling network. In contrast, replicate samples of harbor sediments showed higher variability with increasing metal levels, such that:

$$\frac{\text{sigma } A}{X_A} > \frac{\text{sigma } B}{X_B},$$

where A and B are the same metal but A is more concentrated than B.

Metal concentrations were highly variable between stations, even between harbor stations. These effects are to be anticipated in highly polluted harbors because of inhomogeneity. Oil traps metal-containing particles before or soon after introduction into the harbor waters. The globules sink but retain their identity, leading to metal hot spots. Stamford Harbor sediments were particularly high in oil globules.

Assessing the extent of spoil dispersion at the New Haven dump site was not difficult. Stamford spoil can be easily distinguished visually and chemically from the baseline of the New Haven site (Fig. 7.8). Farther from the disposal

Table 7.2 COMPARISON OF HARBOR AND DISPOSAL SITE

MEAN VALUES

STATION #	CODE	Cd	Co	Cr	Cu	Fe (x10⁴)	Hg	Ni	Pb	Zn	%Vol Sol	O/G x10³ ppm
SH 1	110	14	8.8	171	431	1.9	1.1	60	414	741	14	13
SH 2	111	35	9.4	374	919	4.1	1.9	116	1008	1957	30	41
SH 3	112	25	8.5	258	683	2.4	2.5	89	646	1125	19	24
SH 4	113	18	8.8	273	825	3.0	2.1	39	244	803	14	8.7
NWH 0	120	2.4	9.5	53	115	2.1	.89	34	214	254	16	5.9
NWH 1	121	3.1	9.4	106	315	2.8	1.1	47	194	317	21	10
NWH 2	122	1.7	9.5	87	169	2.6	.56	32	98	175	17	3.7
NWH 3	123	.95	8.3	73	122	2.2	.43	25	72	96	16	3.4
NWH 4	124	.35	4.5	27	22	.99	.08	9.8	16	44	2.9	.47
NH 1	80H	3.9	8.7	120	267	2.4	.47	37	187	312	21	6.0
NH 2	81H	2.2	9.0	96	186	2.4	.50	28	112	225	16	6.8
NH 3	82H	1.7	8.4	91	146	2.2	.48	24	83	206	11	4.8
NH 4	83H	1.4	7.5	64	96	1.8	.47	20	60	145	10	3.6
NH 5	84H	1.6	8.5	48	82	1.7	.33	20	57	143	12	2.4
NH 6	85H	1.1	9.3	97	115	2.6	.44	29	78	137	18	2.6
NH 7	86H	.61	3.4	13	9.8	.40	.05	8.6	14	23	4.8	.63
NH 1-A	800	.58	7.9	48	54	1.5	.33	16	43	149	12	.73
NH 2-A	801	.46	8.0	41	43	1.6	.34	15	44	130	17	.31
NH 3-A	802	1.1	7.3	52	92	1.6	.39	17	51	177	14	2.1
NH 4-A	803	.58	8.5	38	47	1.7	.23	19	43	135	14	1.1
NH 5-A	804	.46	10	40	46	2.4	.23	25	50	150	13	1.6
NH 6-A	805	.25	9.8	39	46	2.6	.22	23	47	146	16	3.3
NH D	81D	.54	4.3	18	28	.78	.11	8.3	37	57	4.4	.09
NH REF	80R	.54	7.0	52	58	1.8	.27	19	40	127	16	.63
NH 7-A	806	.41	9.4	39	47	2.0	.22	20	45	141	16	1.0

SH = Stamford Harbor
NWH = Norwalk Harbor
NH = New Haven Harbor
NH #-A = New Haven south dump site network before dumping
NH D = Old New Haven dump site
NH REF = Northwest control site New Haven

Table 7.3 DIFFERENCE IN SURFACE SEDIMENTS

AREA	Cd	Co	Cr	Cu	Fe	Hg	Ni	Pb	Zn
Stamford Harbor + New Haven Harbor	**	NS	**	**	*	**	**	**	**
Stamford Harbor + Norwalk Harbor	**	NS	**	**	NS	**	**	**	**
Stamford Harbor + New Haven site	**	NS	**	**	*	**	**	**	**
Norwalk Harbor + New Haven Harbor	NS	NS	NS	NS	NS	NS	NS	NS	NS
Norwalk Harbor + New Haven site	**	NS	**	**	NS	**	**	**	NS
New Haven Harbor + New Haven site	**	NS	**	**	NS	*	NS	**	NS

NS Not a significant difference
** Significant difference at 95% confidence level
* Significant difference at 90% confidence level

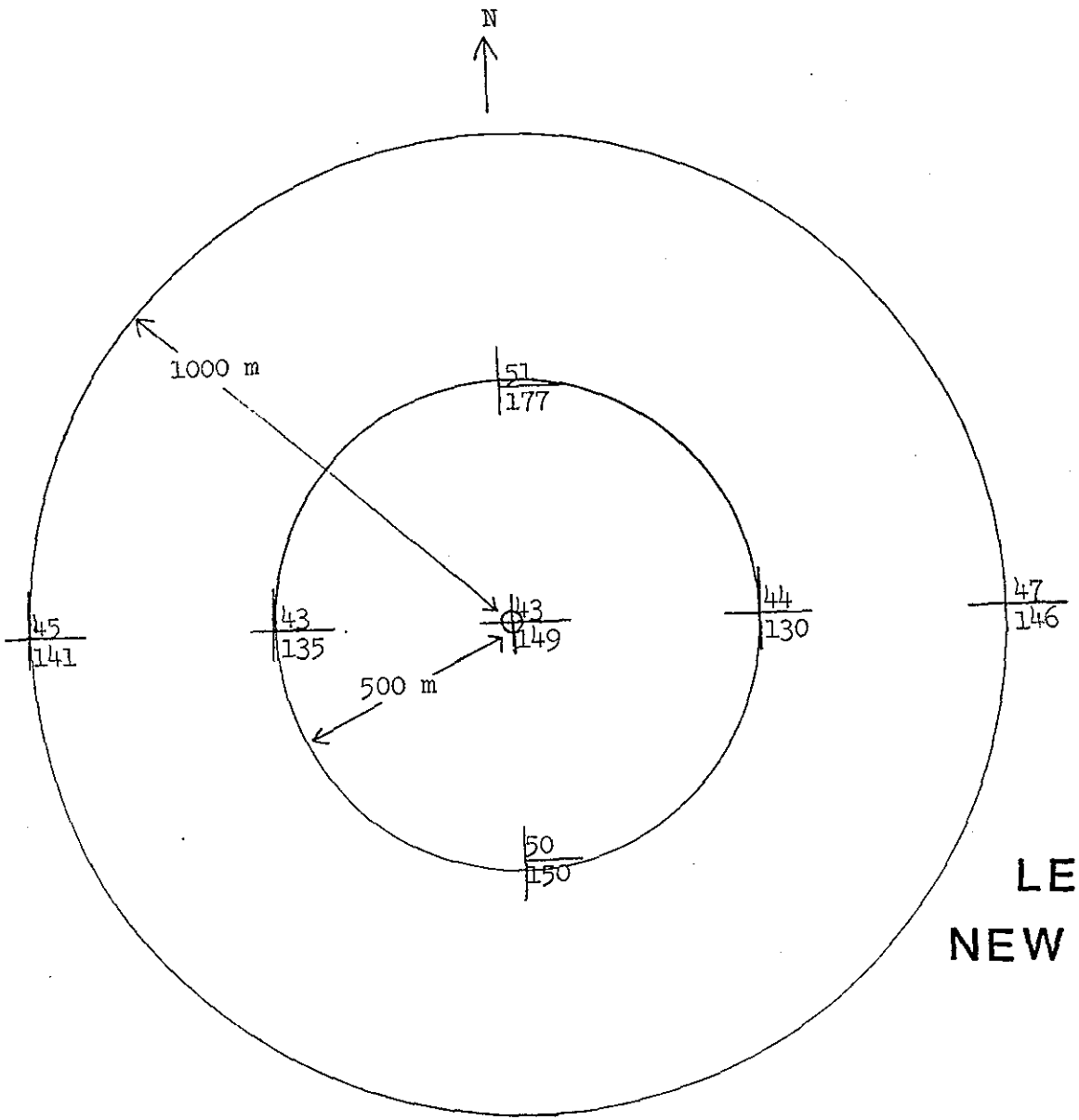

INNER HARBOR SEDIMENTS

	Pb	Zn	
Stamford	1008	1957	(ppm)
Norwalk	214	254	(ppm)
New Haven	187	312	(ppm)

Pb
Zn

Mean Values

LEAD/ZINC DISTRIBUTION NEW HAVEN DISPOSAL SITE

FIGURE 7.7

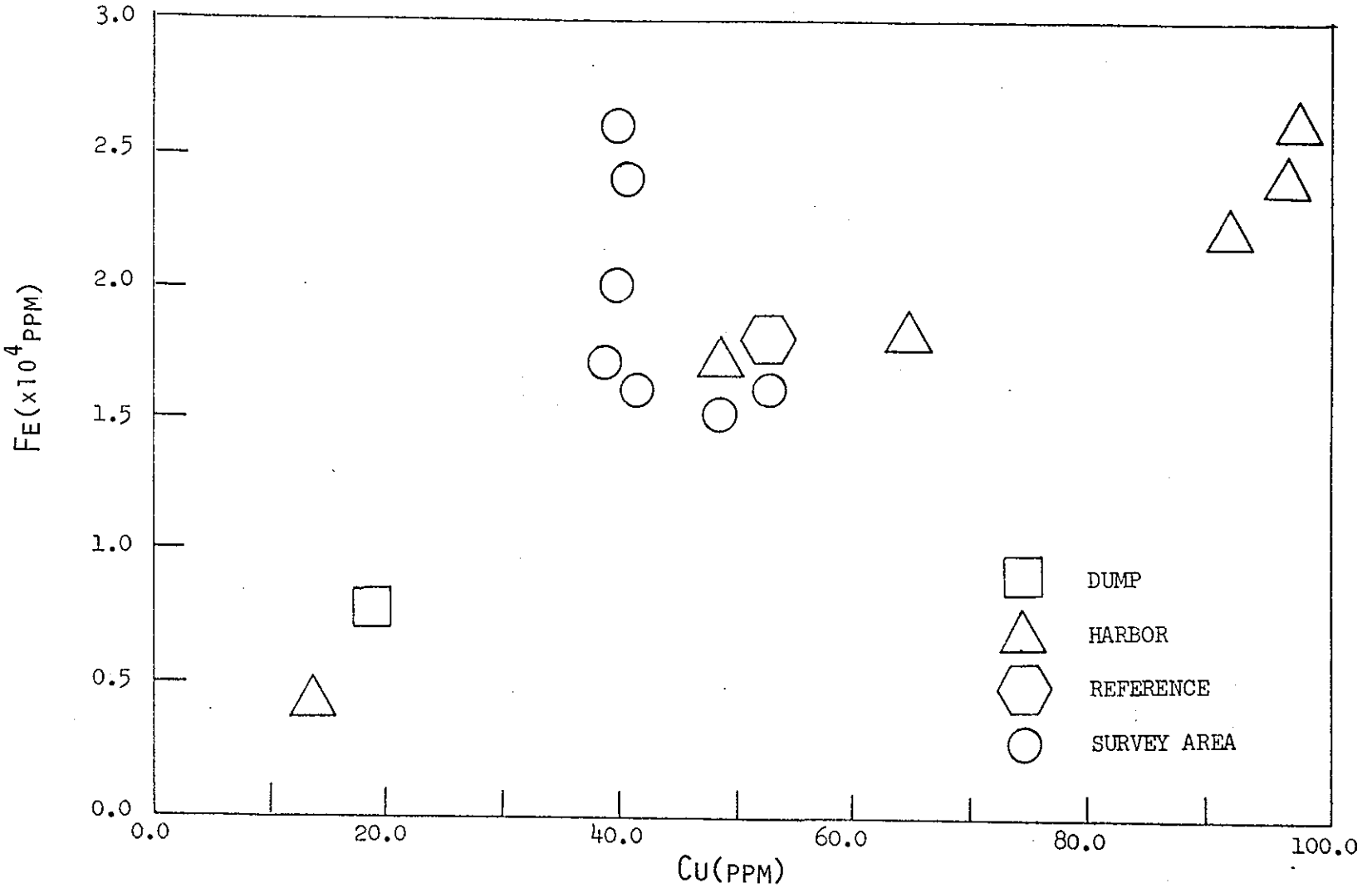

COPPER CONCENTRATION
NEW HAVEN

FIGURE 7.8

pile, we began to detect surface layers of black oily spoil over normal sediments. The farther the sample site from the disposal point, the thinner the veneer of spoil. At 100 m from the dump the spoil layer was only several millimeters thick. Layers this thin are not easily sampled for chemical analysis. It is clear that in this case visual examination can tell us more than chemical analysis. How does the chemical composition change between flank areas and the point of dumping? Except for the absence of the interstitial solutions, the spoil on the flanks of the pile ought to resemble closely the bulk spoil at the dump which has not migrated. Only after a period of reworking between veneered spoil and the underlying sediments, whether by physical or biological means, can the expected exponential concentration decay as a function of distance. We have no data available to determine how long a period is necessary for reworking.

Samples for chemical analysis were collected at the south and north New Haven dump sites before dumping of Stamford spoil, during dumping of Stamford spoil, and after capping with New Haven spoil (at the south site) and New Haven Outer Harbor sand (at the north site). Sixteen stations were occupied at each site; samples in triplicate were taken at each station. The results of the chemical analyses from all these samples are not available to us at this time. The interpretation of these data will not be difficult. Not only do we have Stamford harbor-spoil veneer on the flanks of two dump piles, but also, as a result of the capping, another thin layer of New Haven capping material. Fortunately, we recorded the thickness of the various layers discovered while sampling: estimates of the distribution of Stamford spoil and New Haven capping material will be made visually.

7.3.4.4 Western Long Island Sound and Cable and Anchor Reef

Both proposed dump site areas are inactive. Surface sediments are characterized by enrichment in almost all heavy metals with respect to iron (Figs. 7.9, 7.10). These sites are among the most highly enriched, although no recent dumping has occurred here. The sediments are more enriched than the sediments at the New London site. The western Long Island Sound and Cable and Anchor Reef sites are farthest west and most removed from the northern New England site. That they are richest in metals in the absence of dumping

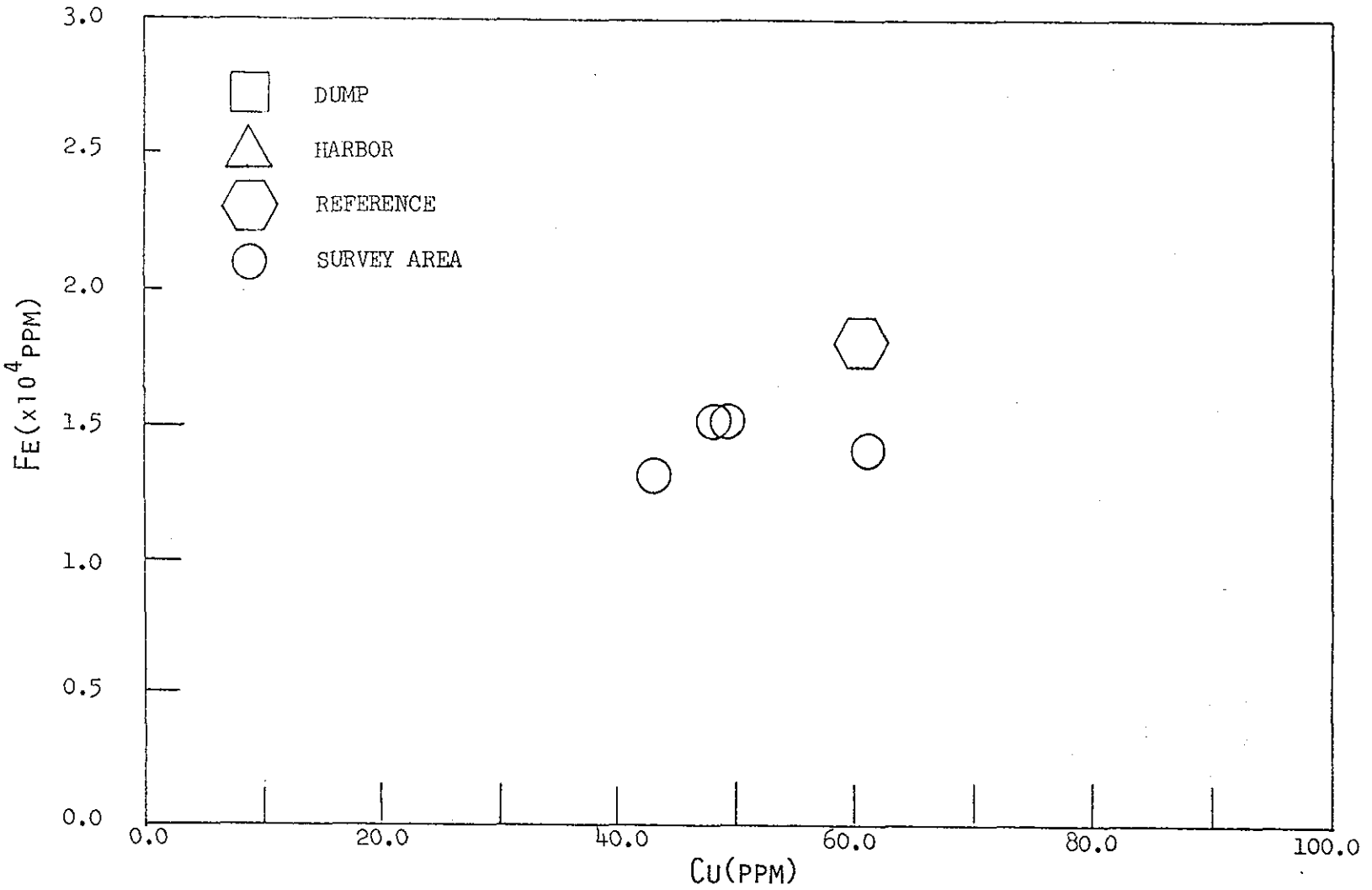

COPPER CONCENTRATION
WESTERN LONG ISLAND SOUND

FIGURE 7.9

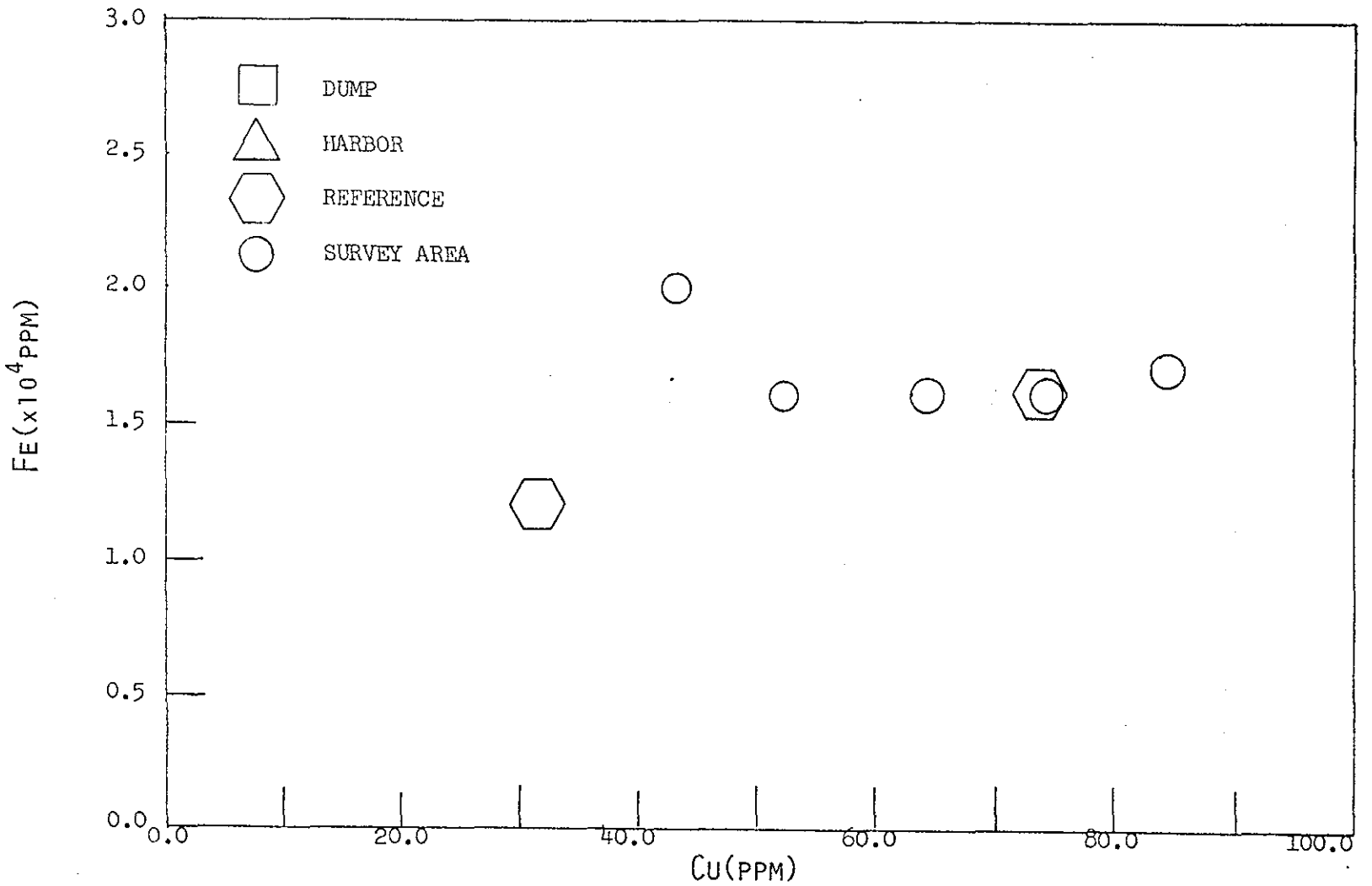

COPPER CONCENTRATION
CABLE & ANCHOR REEF

FIGURE 7.10

follows the trend exemplified by other sites: chemical contamination of sediments worsens as one moves from northern New England towards New York City (Figs. 7.11, 7.12).

7.4 CONCLUSIONS

The chemical analysis of sediments from disposal sites, proposed disposal sites, and harbors has demonstrated significant regional differences in sediments. Although sample-to-sample variability is high in highly contaminated sediments, such as those from harbors, statistical analysis of samples from natural open-water locations show low variability and spatial uniformity. It is possible in many cases to use chemical data to trace the distribution of spoil at a disposal site. With sufficient baseline information, longer-term deposition of spoil away from a dump site may well be determined.

High-intensity, short-term chemical data derived from surface sediments, such as we obtained from New Haven in 1979, are wasteful. Spoil on a dump pile and spoil on the flanks of a pile have about the same metals composition; there is no exponential decay in concentration as a function of distance from the pile in the short term. In the case of Stamford spoiling at the New Haven dump site, chemical analysis verified that the black oily material. overlying the natural bottom was a result of dumping Stamford Harbor dredge material. It is clearly simpler to examine these samples from the network visually than to make interpretation from chemical data, especially when sampling is further complicated by the introduction of a capping material.

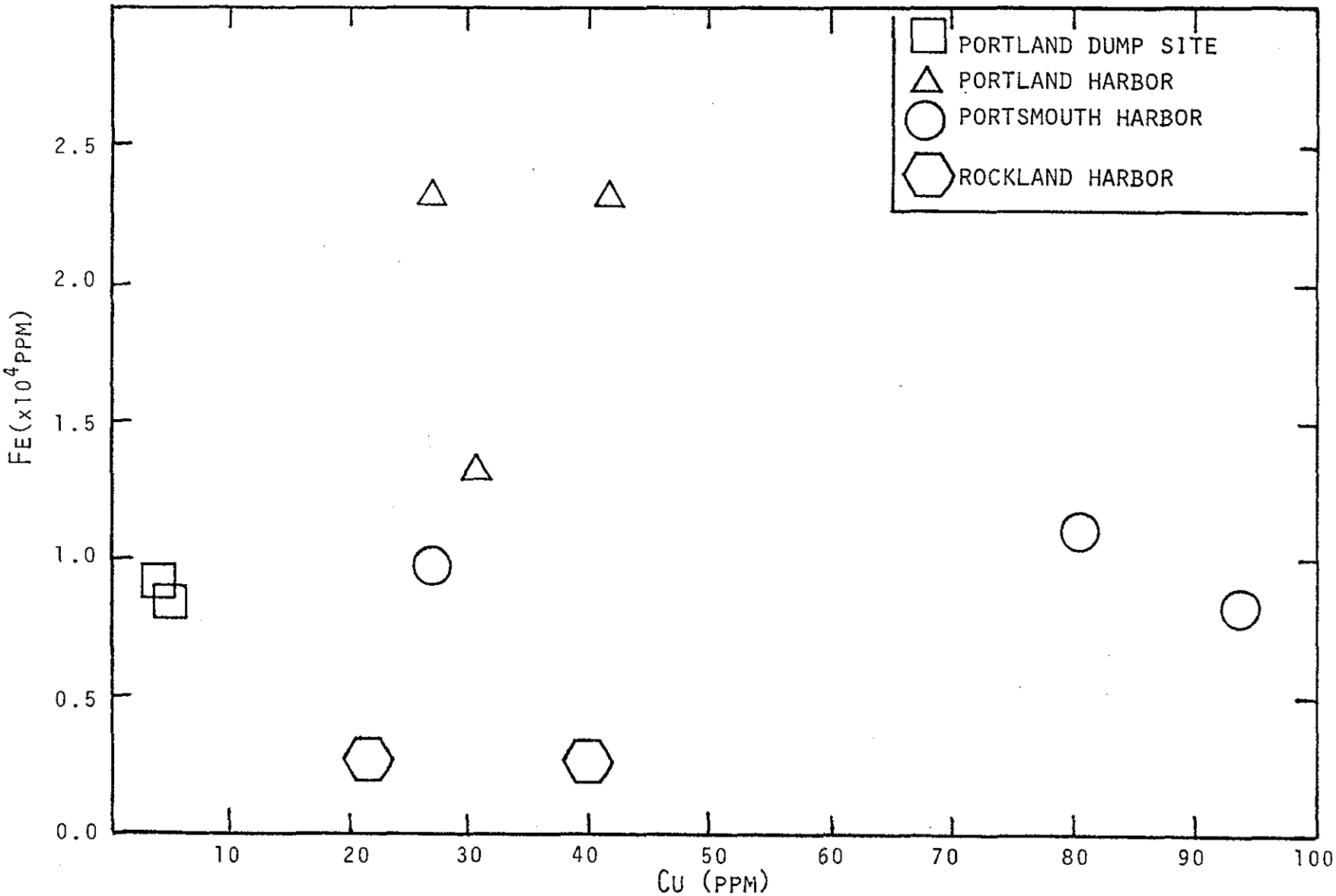

REGIONAL DISTRIBUTION OF COPPER CONCENTRATION
ROCKLAND TO BOSTON

FIGURE 7.11

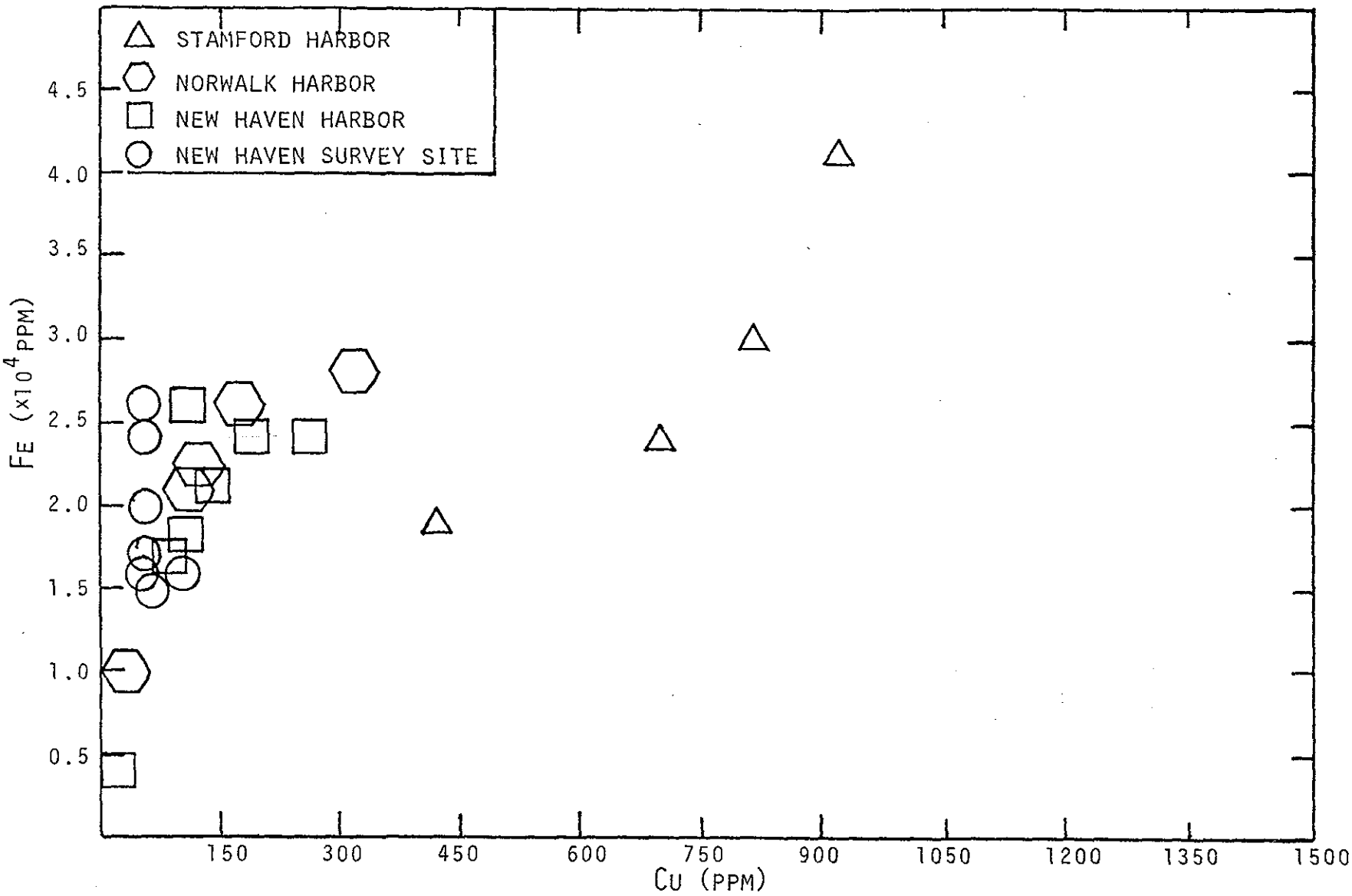

REGIONAL DISTRIBUTION OF COPPER CONCENTRATION
STAMFORD TO NEW HAVEN

FIGURE 7.12